# ESI

**Note after first publication:** This supplementary information replaces that previously published on 24/11/2025, the molecular formulae of a couple of compounds have been revised to include the counter ions.

**Heterolytic Cleavage of the B–H Bond in $H_3B{\cdot}L$ (L = THF, $NMe_2H$) by an Electrophilic Ir(III) Pincer Complex [Ir(H)($PMe_3$)($^{tBu4}$POCOP)][$BAr^F{}_4$]**

Mitarani Pradhan,[a] Zeel Y. Surati,[b] Apurba K. Pal,[a] Kumar Vanka,[b]* Balaji R. Jagirdar[a]*

[a] Department of Inorganic and Physical Chemistry, Indian Institute of Science, Bengaluru 560012, India

[b] Physical and Materials Chemistry Division, CSIR-National Chemical Laboratory, Pune 411 008, India

&

Academy of Scientific and Innovative Research (AcSIR), Ghaziabad 201 002, India

## Table of Contents

1. Reaction of [Ir(H)Cl($^{tBu4}$POCOP)] (**1**) with $PMe_3$: formation of [Ir(H)Cl($PMe_3$)($^{tBu4}$POCOP)] (**2**).

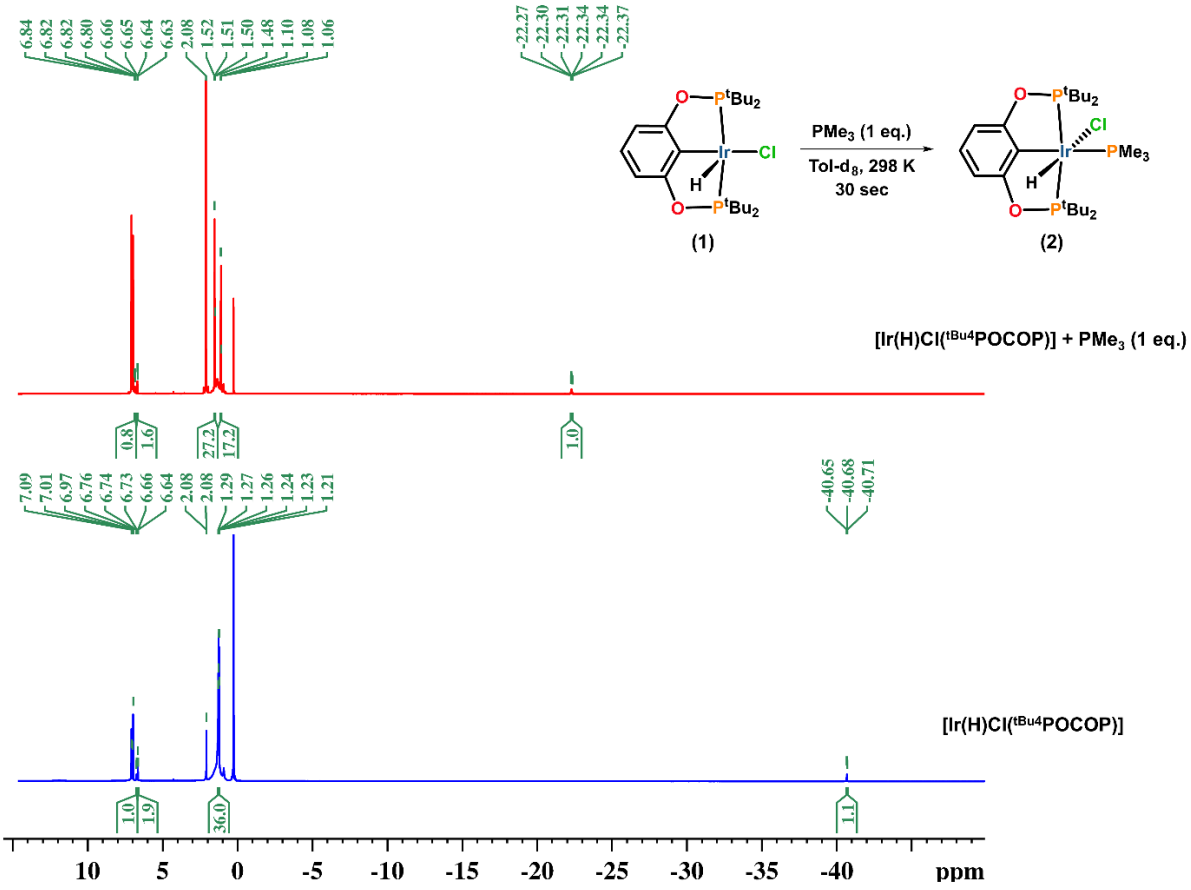


**Figure S1.** $^1$H NMR (400.0 MHz, Tol-$d_8$, 298 K) spectral stack plot of the reaction of [Ir(H)Cl($^{tBu4}$POCOP)] (**1**) (spectrum shown in blue color is before adding $PMe_3$) with 1.0 equiv of $PMe_3$: formation of [Ir(H)Cl($PMe_3$)($^{tBu4}$POCOP)] (**2**) (spectrum shown in red color).

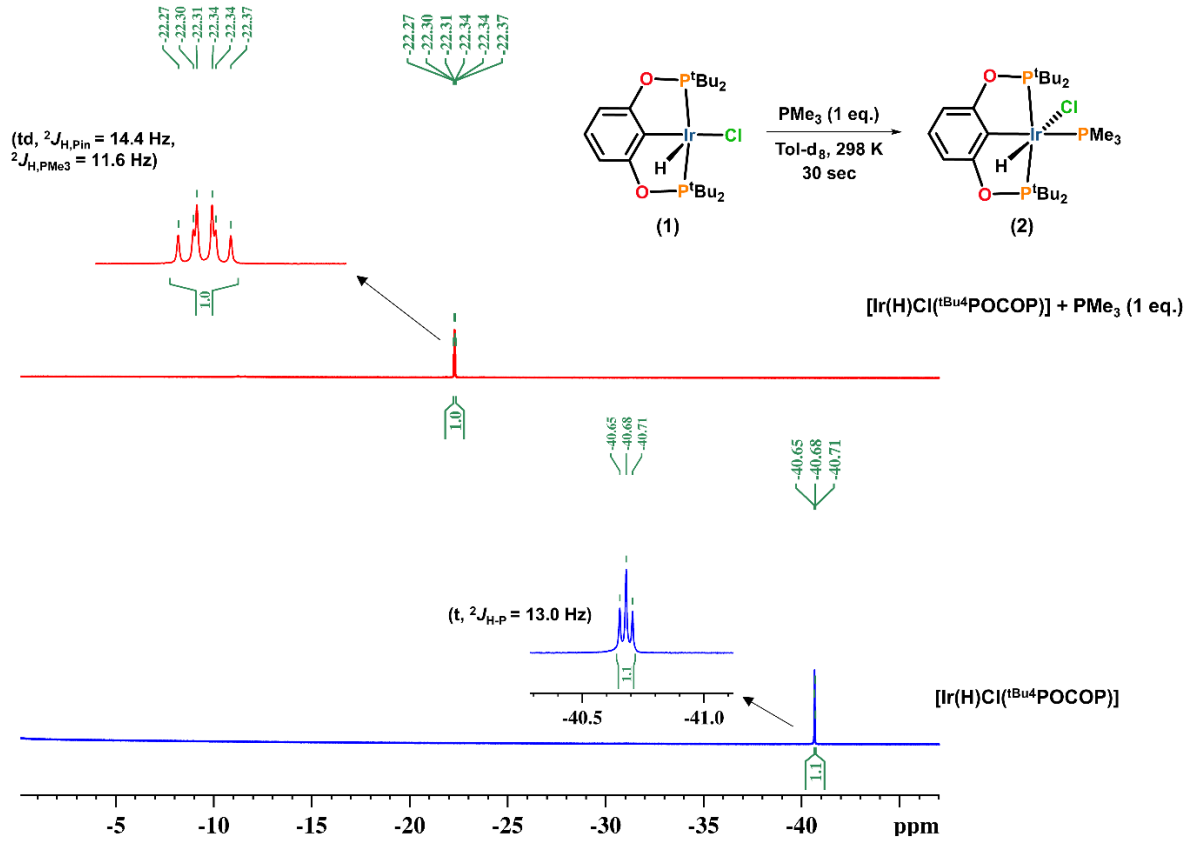


**Figure S2.** Partial $^1$H NMR (400.0 MHz, Tol-d$_8$, 298 K) spectral stack plot (hydride region) of the reaction of [Ir(H)Cl($^{tBu4}$POCOP)] (**1**) (spectrum shown in blue color is before adding PMe$_3$) with 1.0 equiv of PMe$_3$: formation of [Ir(H)Cl(PMe$_3$)($^{tBu4}$POCOP)] (**2**) (spectrum shown in red color).

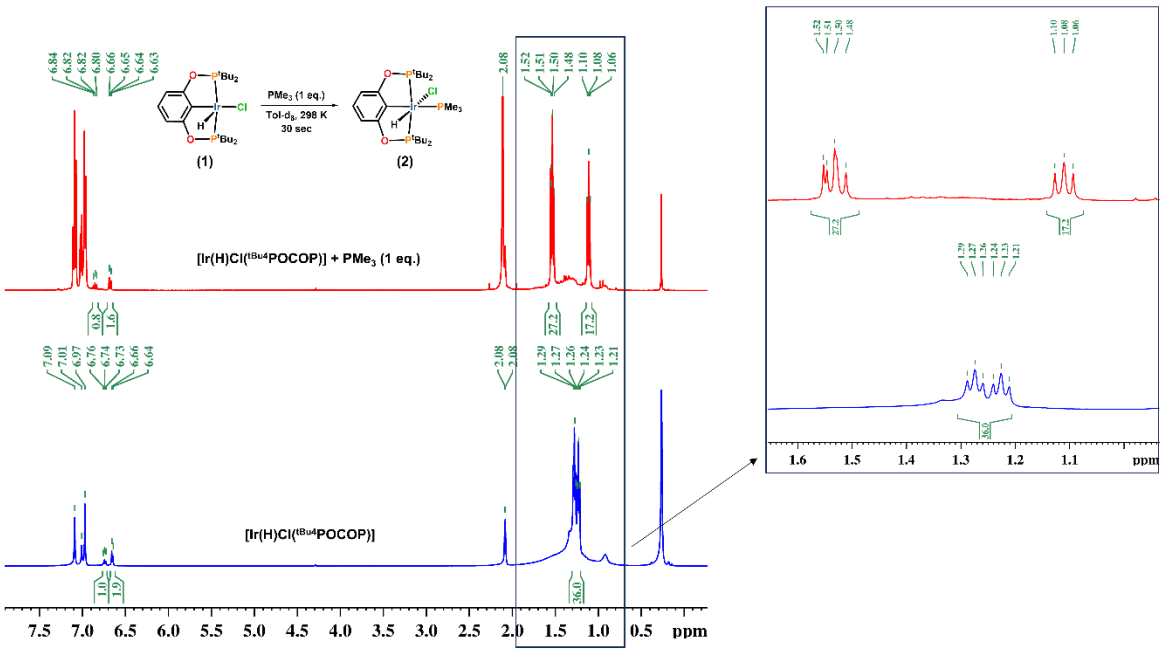


**Figure S3.** Partial $^1$H NMR (400.0 MHz, Tol-d$_8$, 298 K) spectral stack plot (downfield region) of the reaction of [Ir(H)Cl($^{tBu4}$POCOP)] (**1**) (spectrum shown in blue color is before adding PMe$_3$) with 1.0 equiv of PMe$_3$: formation of [Ir(H)Cl(PMe$_3$)($^{tBu4}$POCOP)] (**2**) (spectrum shown in red color).

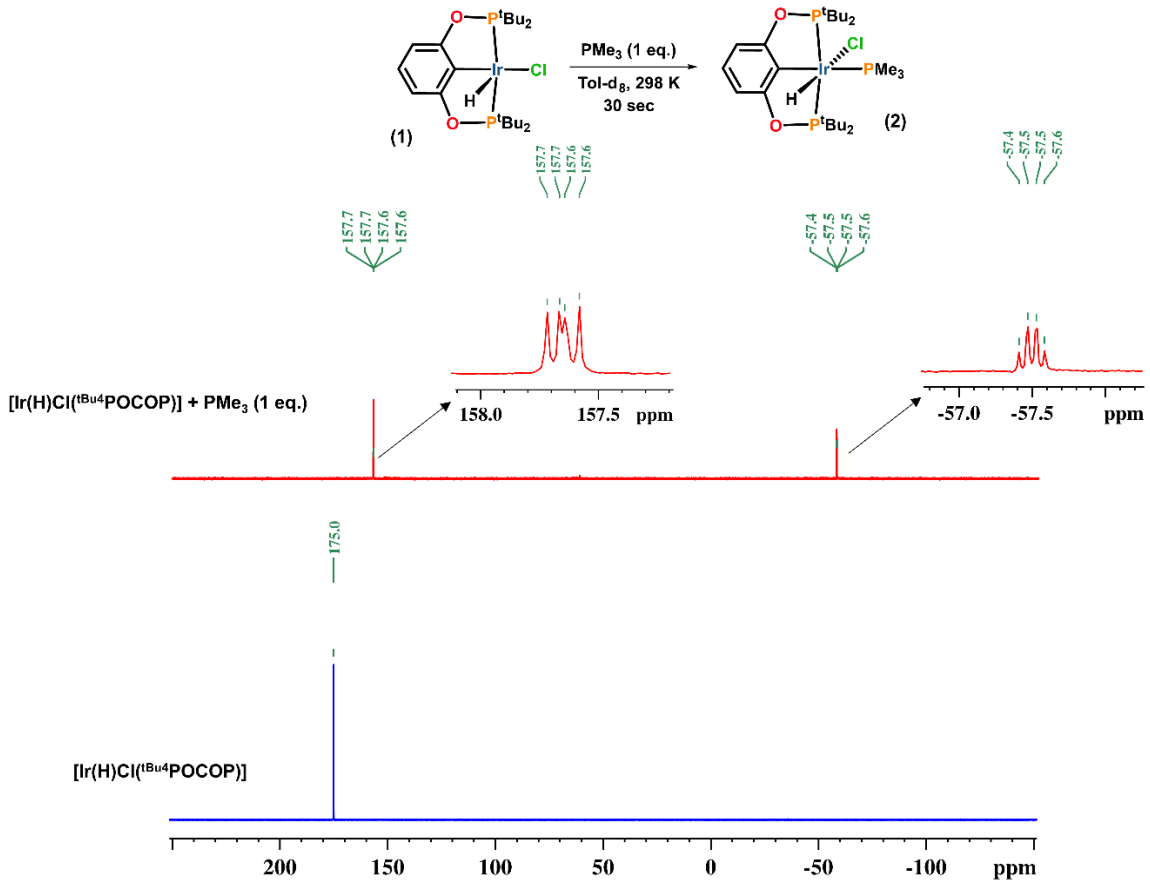


**Figure S4.** $^{31}P\{^{1}H\}$ NMR (161.9 MHz, Tol-$d_8$, 298 K) spectral stack plot of the reaction of [Ir(H)Cl($^{tBu4}$POCOP)] (**1**) (spectrum shown in blue color is before adding $PMe_3$) with 1.0 equiv of $PMe_3$: formation of [Ir(H)Cl($PMe_3$)($^{tBu4}$POCOP)] (**2**) (spectrum shown in red color).

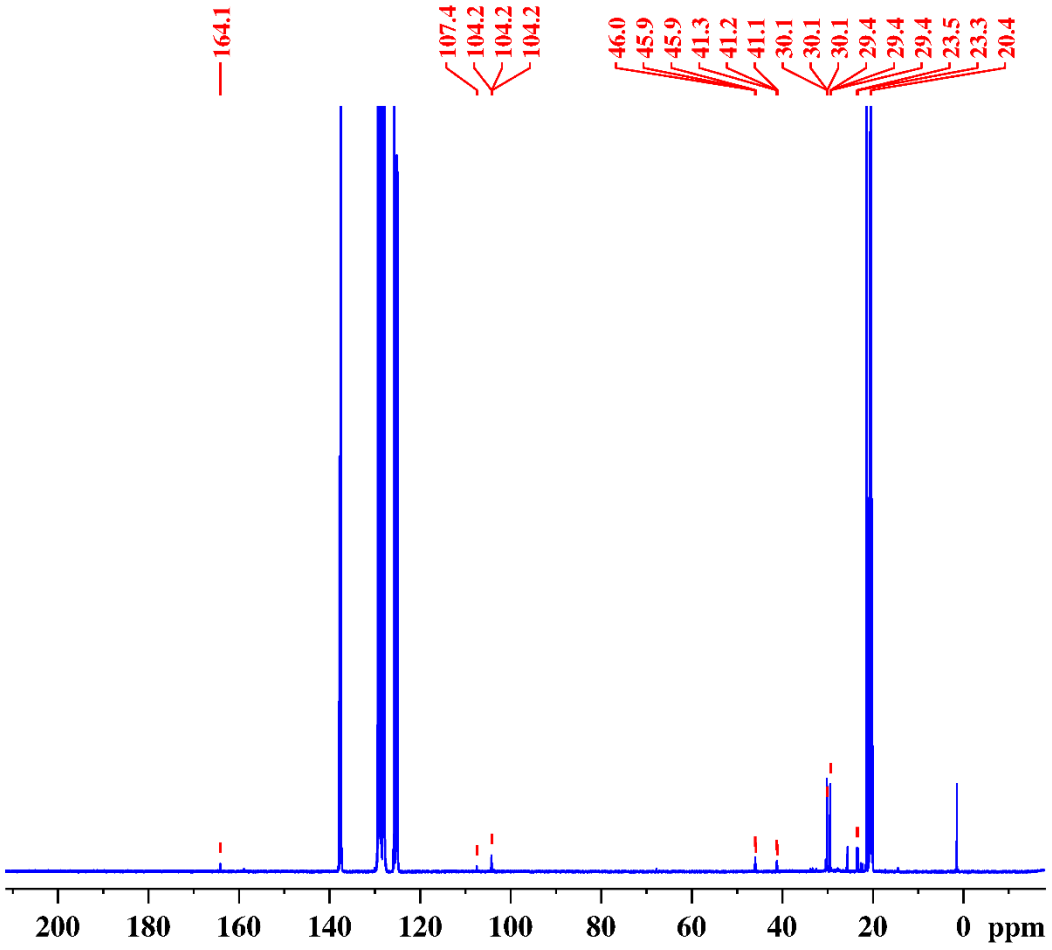


**Figure S5.** $^{13}C\{^{1}H\}$ NMR (125.0 MHz, Tol-$d_8$, 298 K) spectrum of [Ir(H)Cl(PMe$_3$)($^{tBu4}$POCOP)] (**2**).

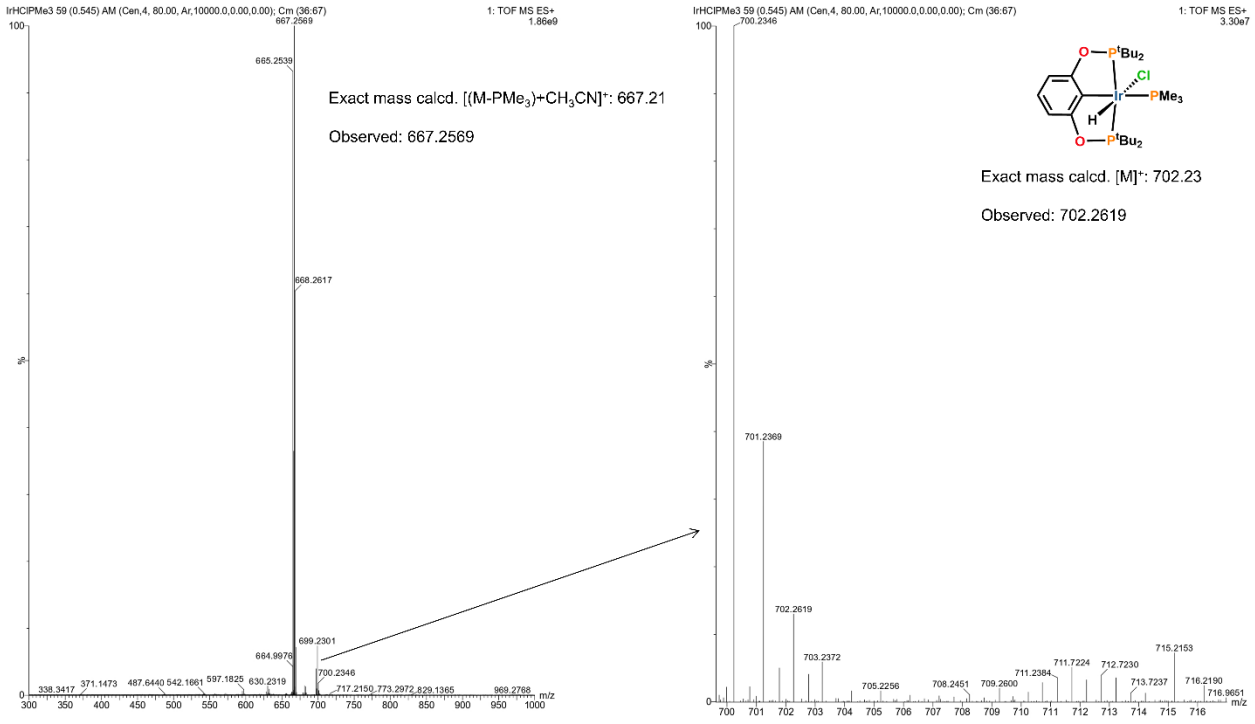


**Figure S6**. HRMS spectrograph of [Ir(H)Cl(PMe$_3$)($^{tBu4}$POCOP)] (**2**).

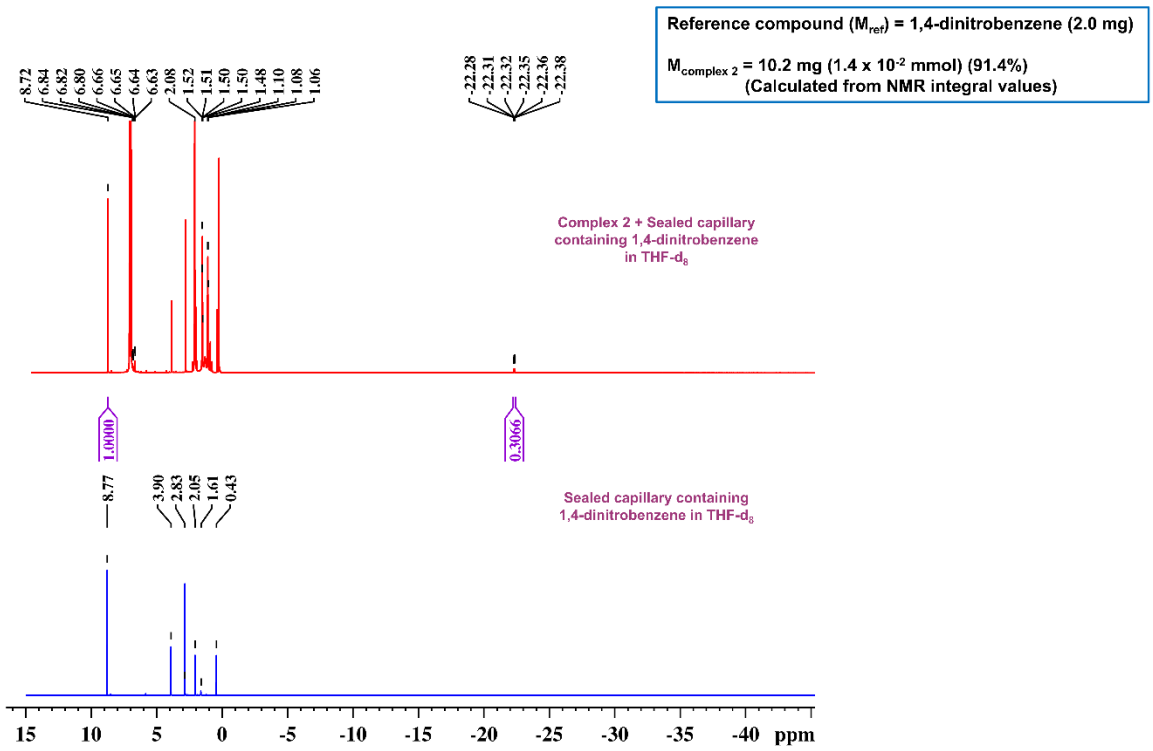


**Figure S7.** $^{1}$H NMR (400.0 MHz, Tol-$d_8$, 298 K) spectral stack plot of 1,4-dinitrobenzene in THF-$d_8$ (spectrum shown in blue color) and complex **2** + 1,4-dinitrobenzene (spectrum shown in red color).

The box at the top right shows the calculation of the % of complex **2** present in the sample, as shown in the red-colored spectrum.

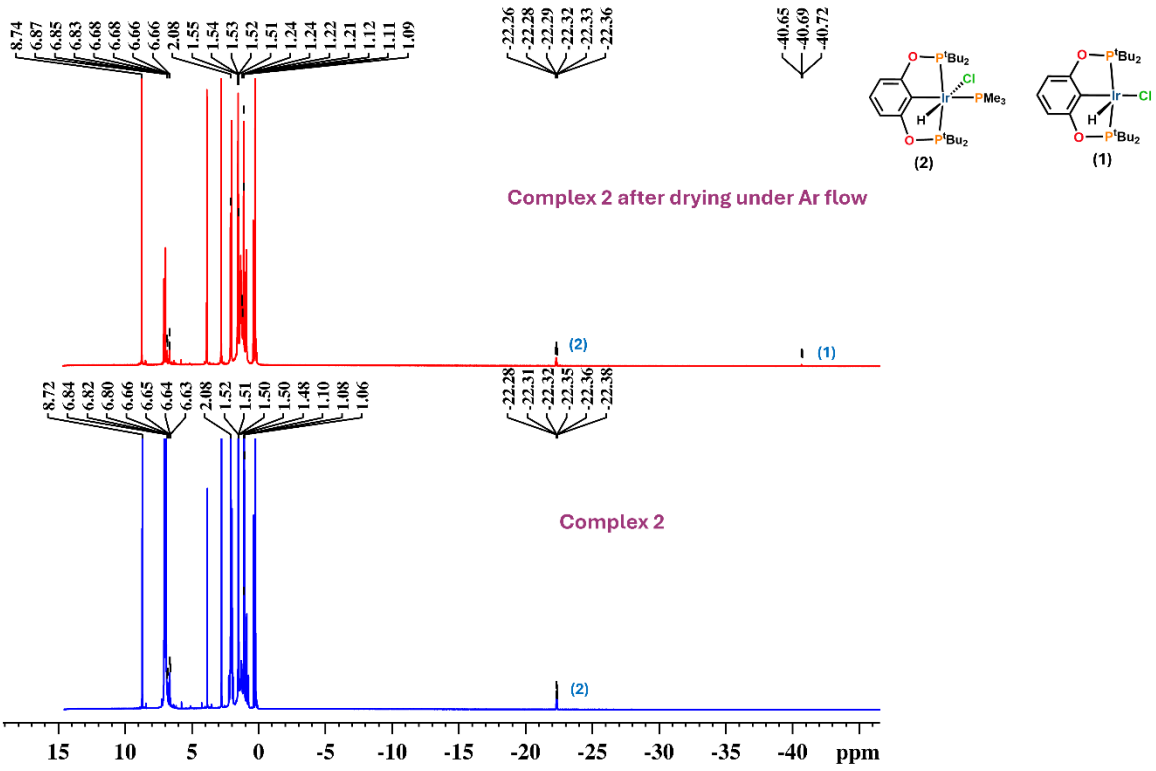


**Figure S8.** $^{1}$H NMR (400.0 MHz, Tol-$d_8$, 298 K) spectral stack plot of [Ir(H)Cl($PMe_3$)($^{tBu4}$POCOP)] (**2**) (spectrum shown in blue color) and complex **2** after drying under an Ar flow (spectrum shown in red color).

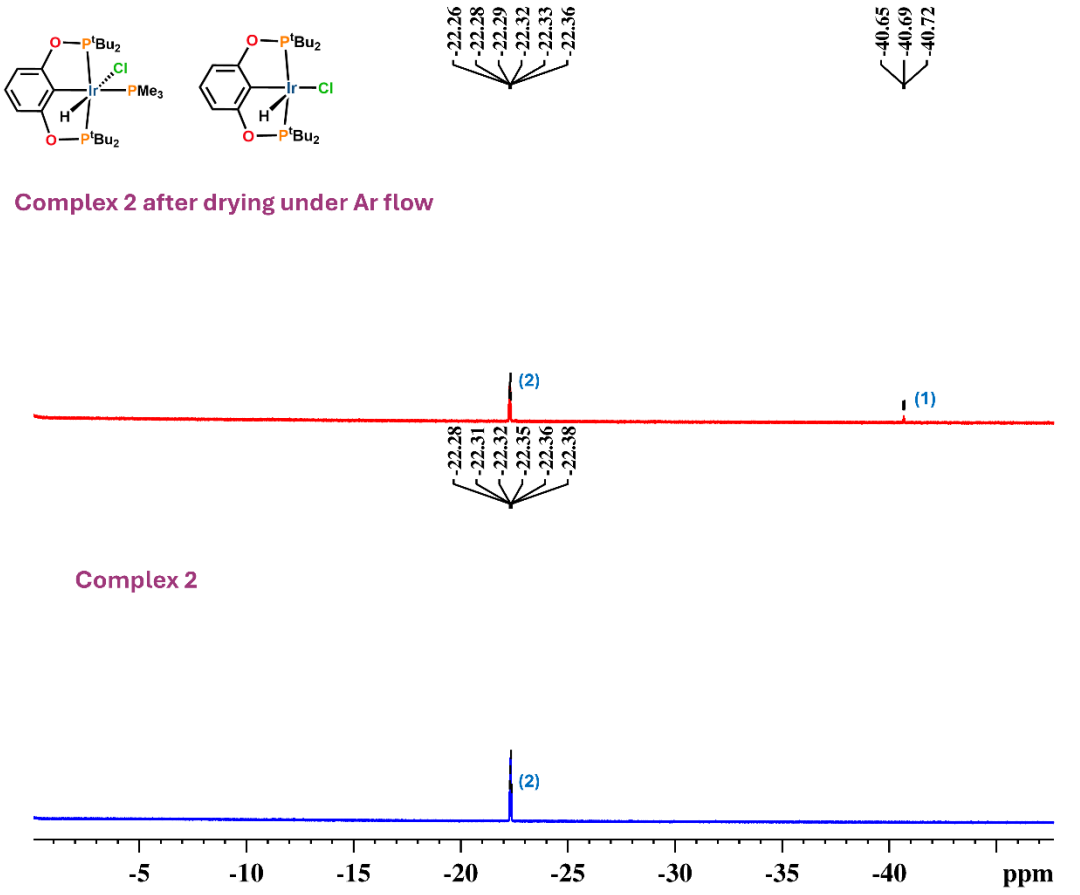


**Figure S9.** Partial $^{1}$H NMR (400.0 MHz, Tol-$d_8$, 298 K) spectral stack plot (hydride region) of [Ir(H)Cl(PMe$_3$)($^{tBu4}$POCOP)] (**2**) (spectrum shown in blue color) and complex **2** after drying under an Ar flow (spectrum shown in red color).

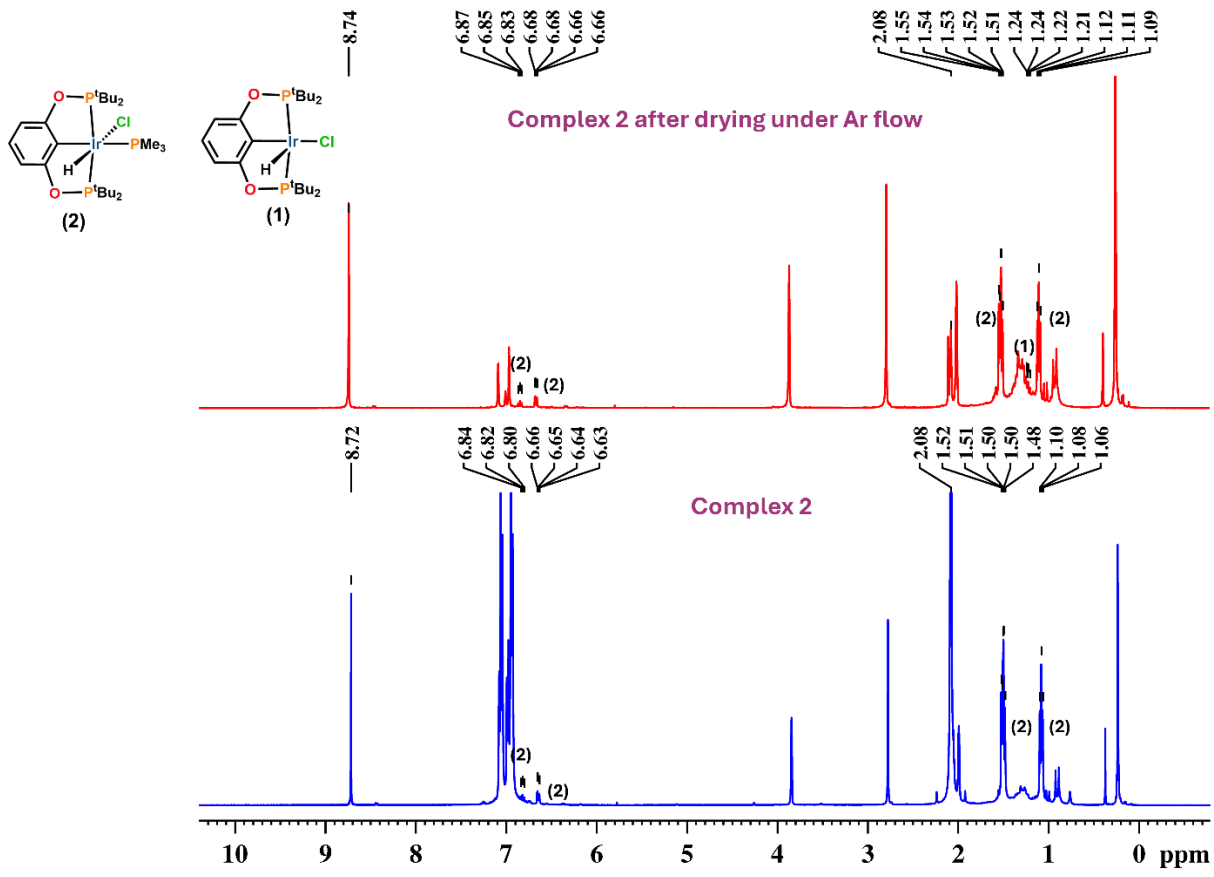


**Figure S10.** Partial $^{1}$H NMR (400.0 MHz, Tol-$d_8$, 298 K) spectral stack plot (downfield region) of [Ir(H)Cl($PMe_3$)($^{tBu4}$POCOP)] (**2**) (spectrum shown in blue color) and complex **2** after drying under an Ar flow (spectrum shown in red color).

The aryl peaks corresponding to complex **1** could not be assigned due to overlap with the aryl signals of complex **2**.

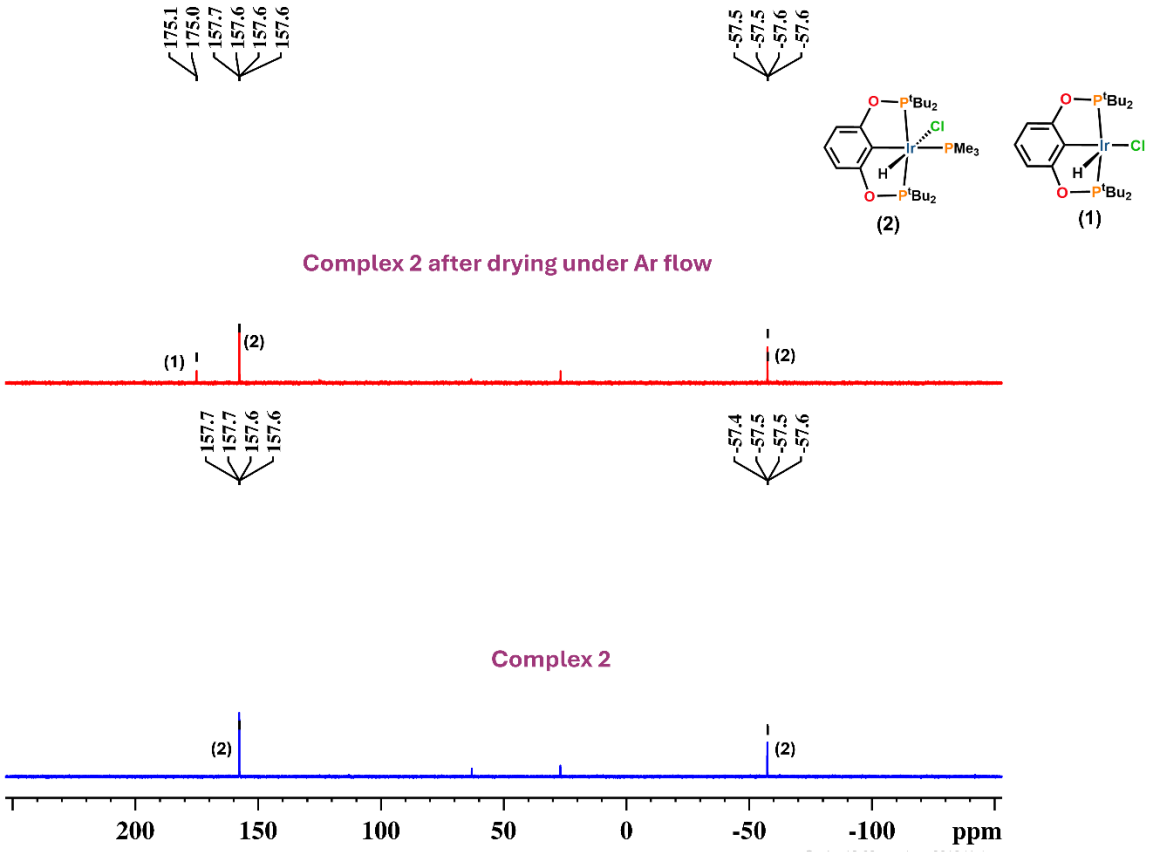


**Figure S11.** $^{31}P\{^{1}H\}$ NMR (161.9 MHz, Tol-$d_8$, 298 K) spectral stack plot of [Ir(H)Cl($PMe_3$)($^{tBu4}$POCOP)] (**2**) (spectrum shown in blue color) and complex **2** after drying under an Ar flow (spectrum shown in red color).

## 2. Characterization of [Ir(H)(PMe$_3$)($^{tBu4}$POCOP)][BAr$^F_4$] (**3**).

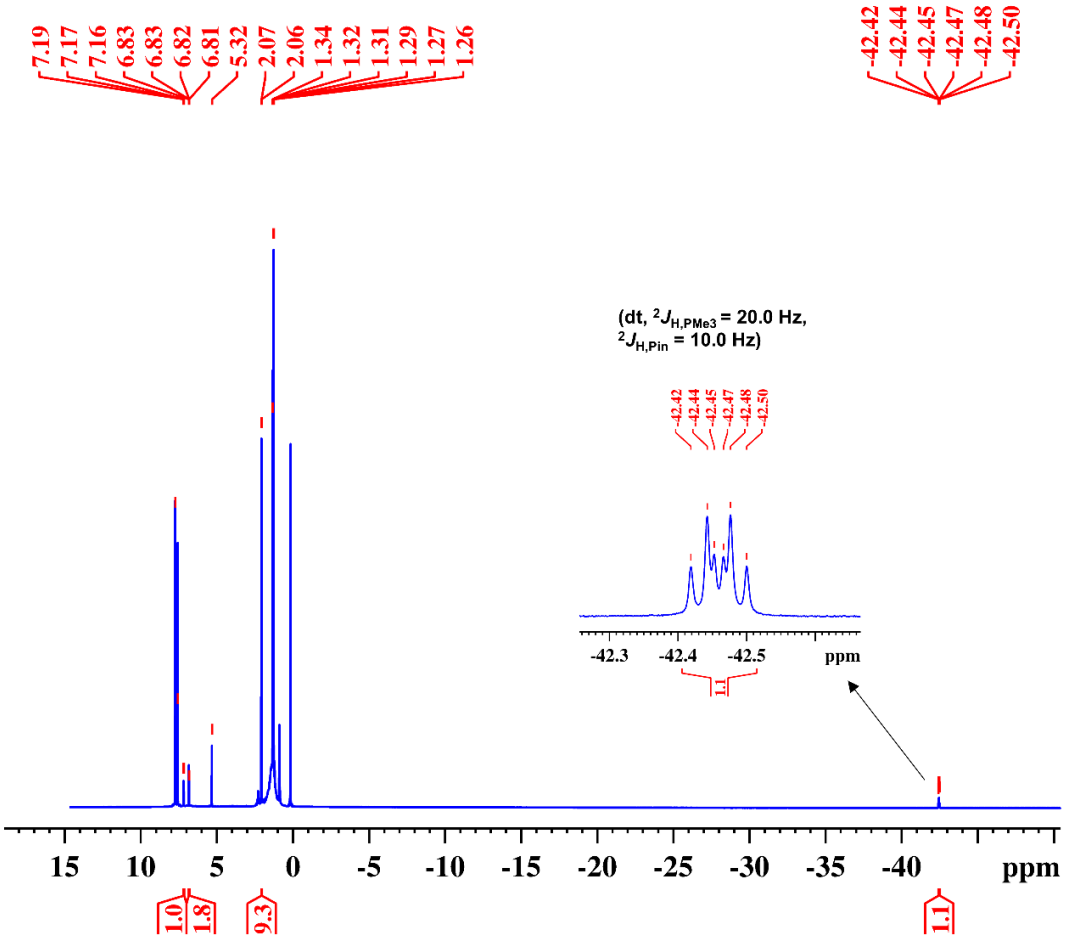


**Figure S12.** $^1$H NMR (500.0 MHz, $CD_2Cl_2$, 298 K) spectrum of [Ir(H)(PMe$_3$)($^{tBu4}$POCOP)][BAr$^F_4$] (**3**).

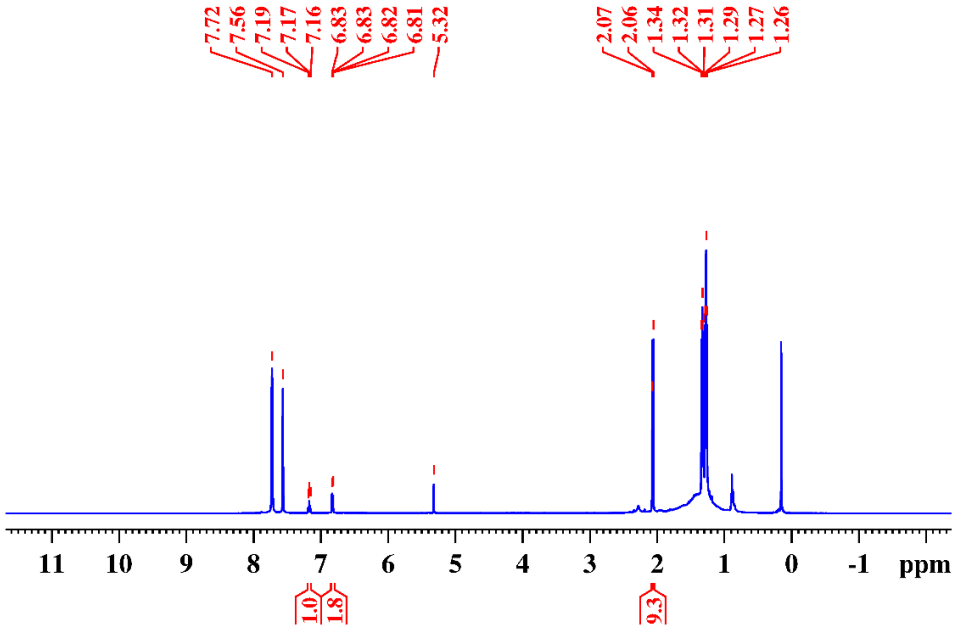


**Figure S13.** Partial $^1$H NMR (500.0 MHz, $CD_2Cl_2$, 298 K) spectrum of [Ir(H)(PMe$_3$)($^{tBu4}$POCOP)][BAr$^F_4$] (**3**).

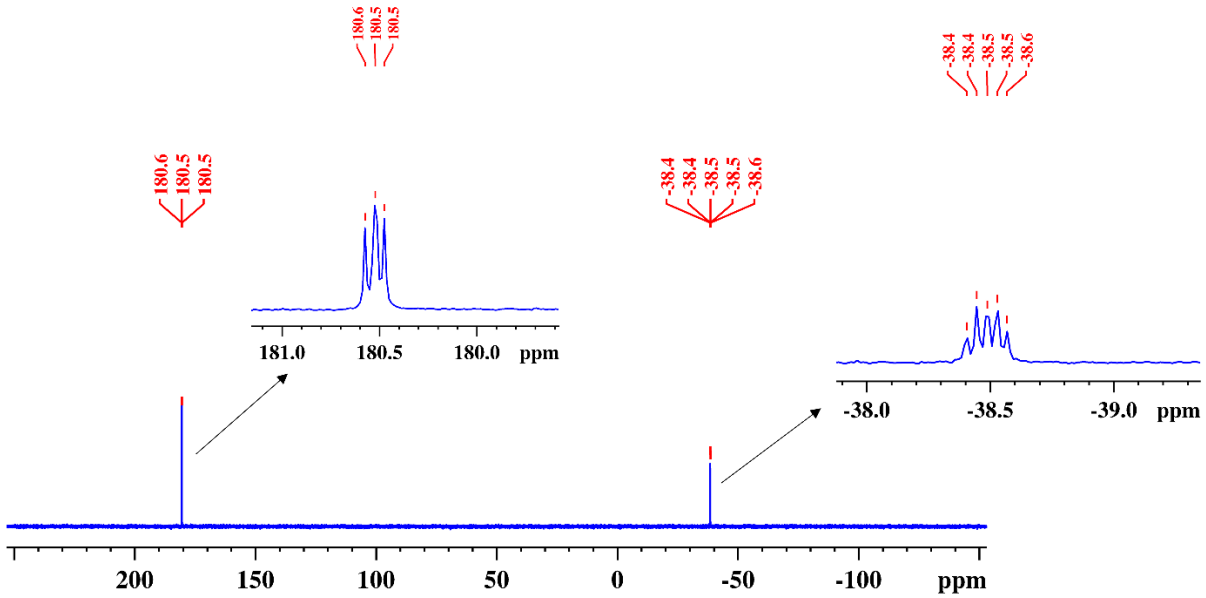


**Figure S14.** $^{31}P\{^{1}H\}$ NMR (161.9 MHz, $CD_2Cl_2$, 298 K) spectrum of [Ir(H)($PMe_3$)($^{tBu4}$POCOP)][$BAr^F_4$] (**3**).

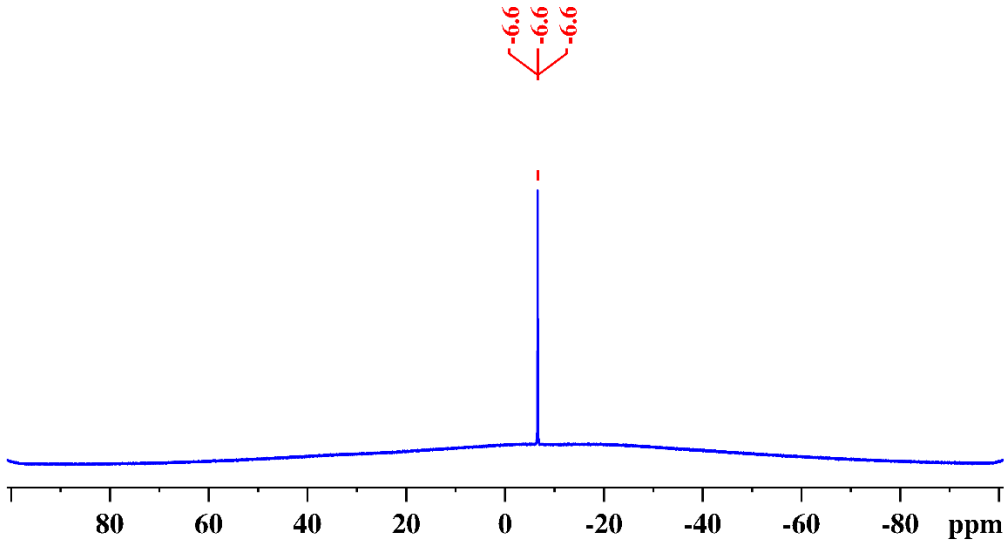


**Figure S15.** $^{11}B$ NMR (128.3 MHz, $CD_2Cl_2$, 298 K) spectrum of [Ir(H)($PMe_3$)($^{tBu4}$POCOP)][$BAr^F_4$] (**3**).

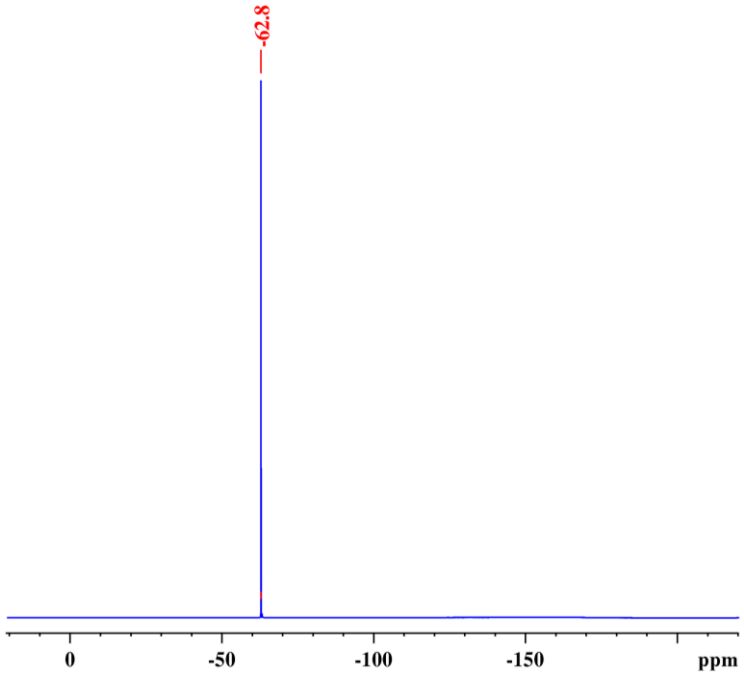


**Figure S16.** $^{19}F\{^{1}H\}$ NMR (376.5 MHz, $CD_2Cl_2$, 298 K) spectrum of [Ir(H)($PMe_3$)($^{tBu4}$POCOP)][$BAr^F_4$] (**3**).

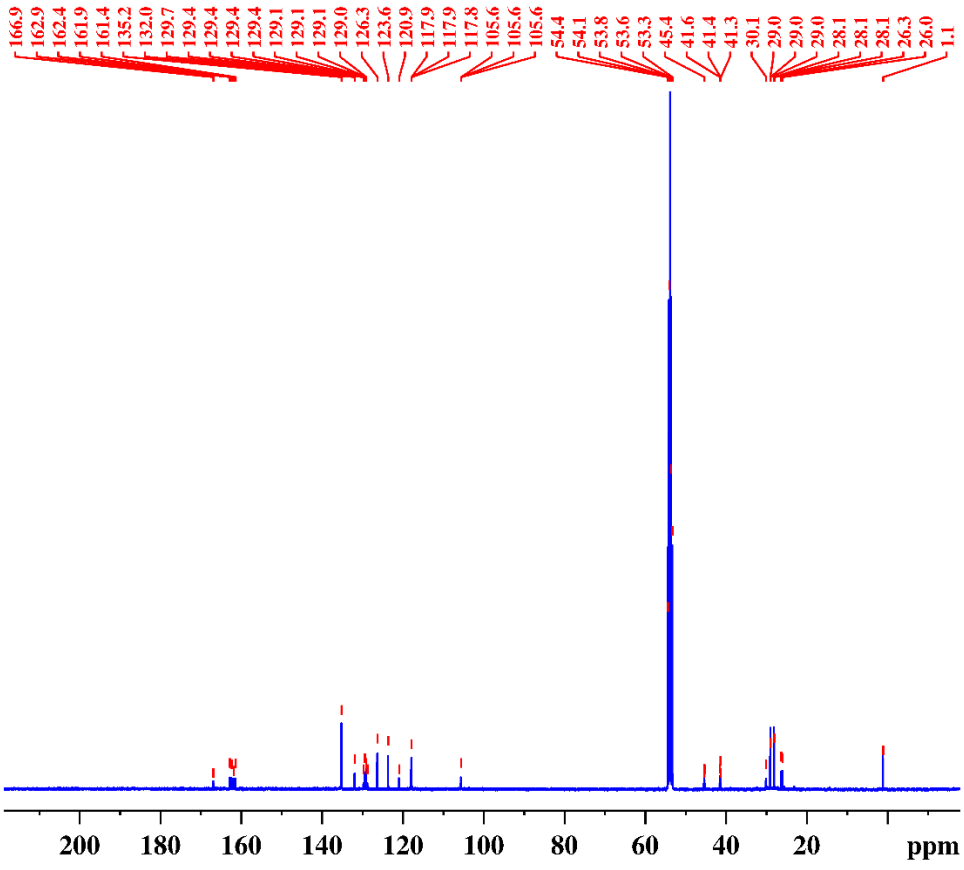


**Figure S17.** $^{13}C\{^{1}H\}$ NMR (100.0 MHz, $CD_2Cl_2$, 298 K) spectrum of [Ir(H)($PMe_3$)($^{tBu4}$POCOP)][$BAr^F_4$] (**3**).

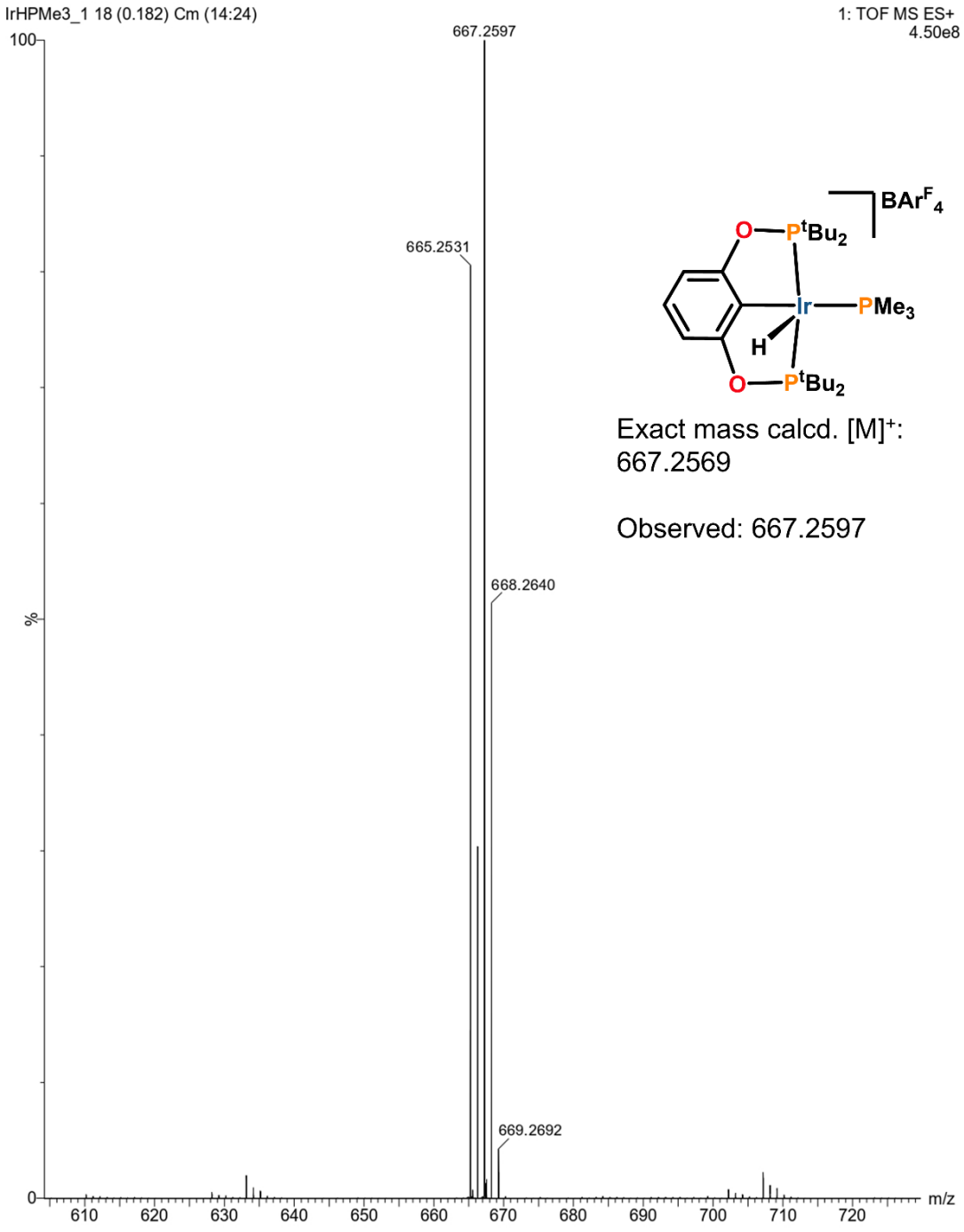


**Figure S18**. HRMS spectrograph of [Ir(H)(PMe$_3$)($^{tBu4}$POCOP)][BAr$^F_4$] (**3**).

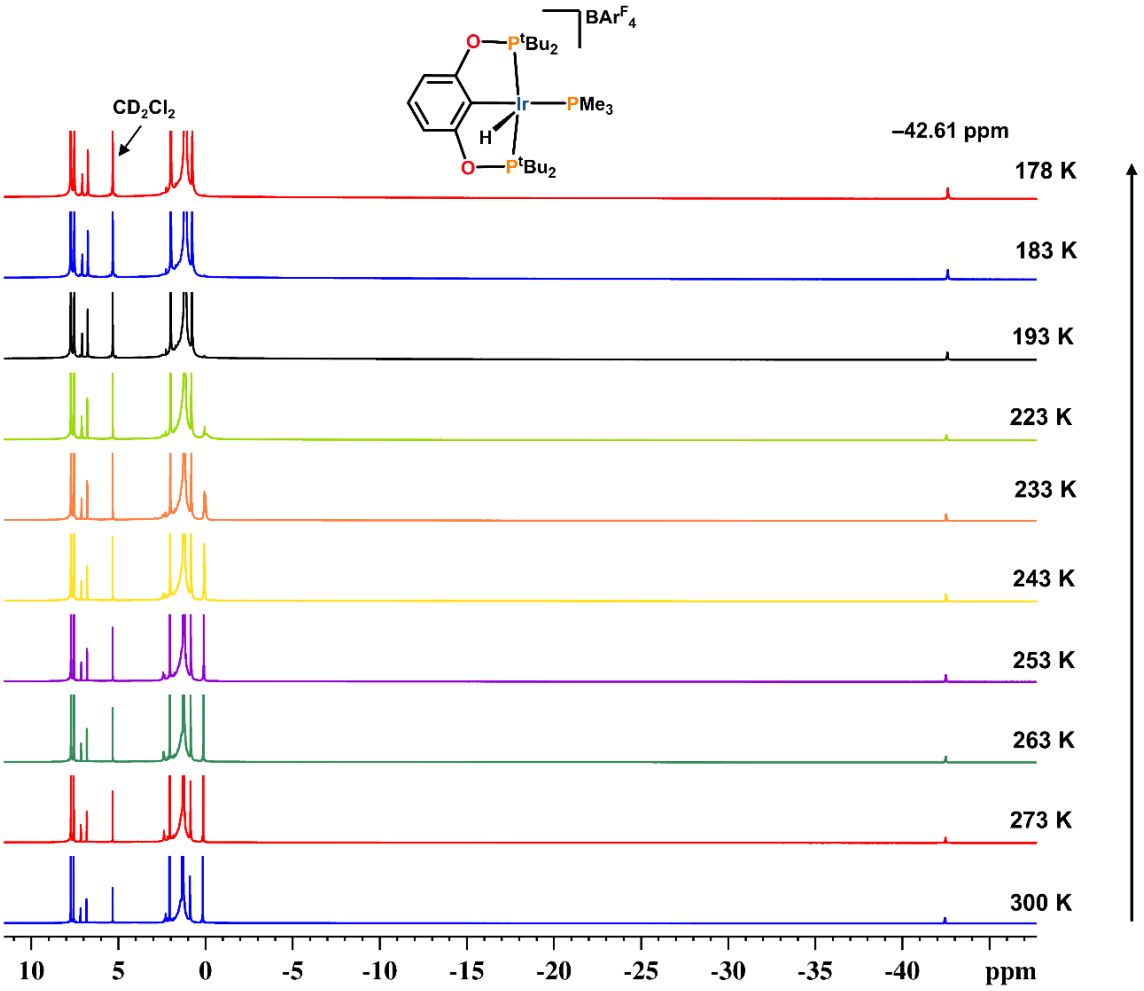


**Figure S19.** VT $^1$H NMR (500.0 MHz, $CD_2Cl_2$) spectral stack plot of [Ir(H)($PMe_3$)($^{tBu4}$POCOP)][$BAr^F_4$] (**3**).

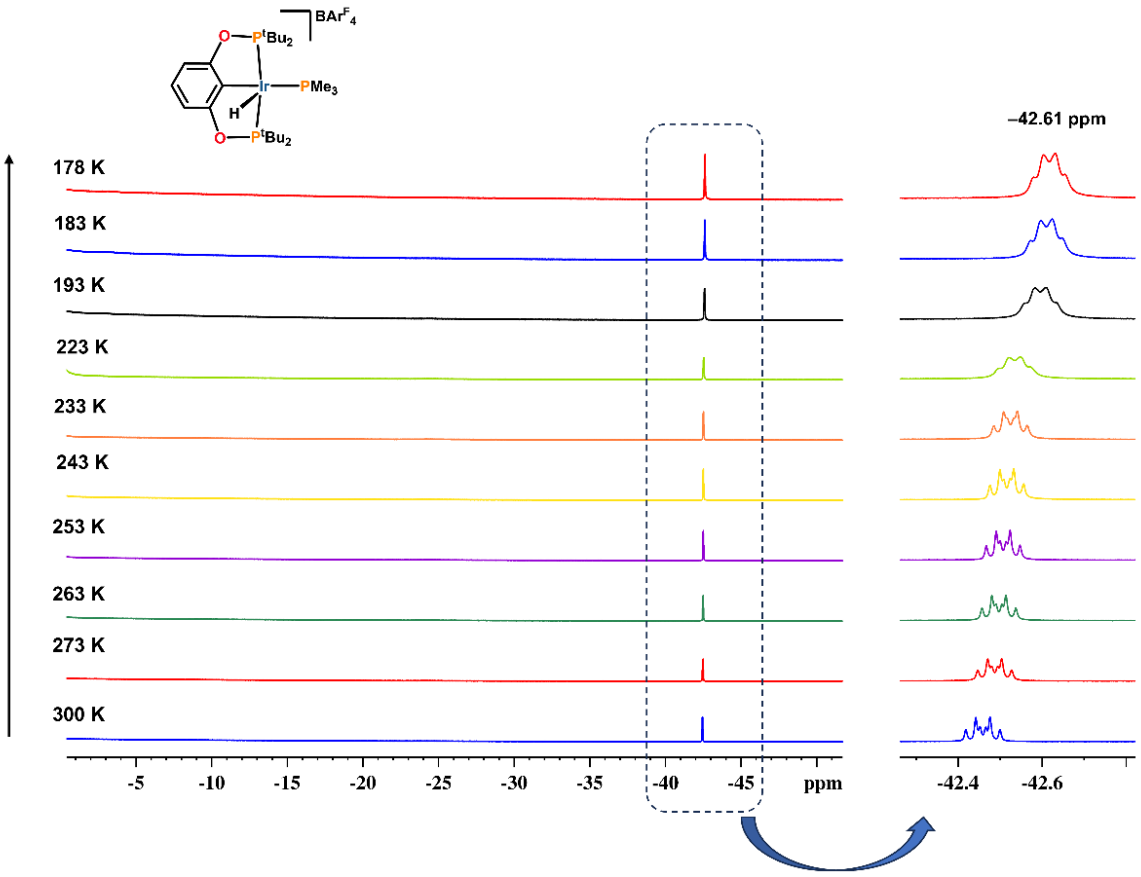


**Figure S20.** Partial VT $^1$H NMR (500.0 MHz, $CD_2Cl_2$) spectral stack plot (hydride region) of [Ir(H)(PMe$_3$)($^{tBu4}$POCOP)][BAr$^F_4$] (**3**).

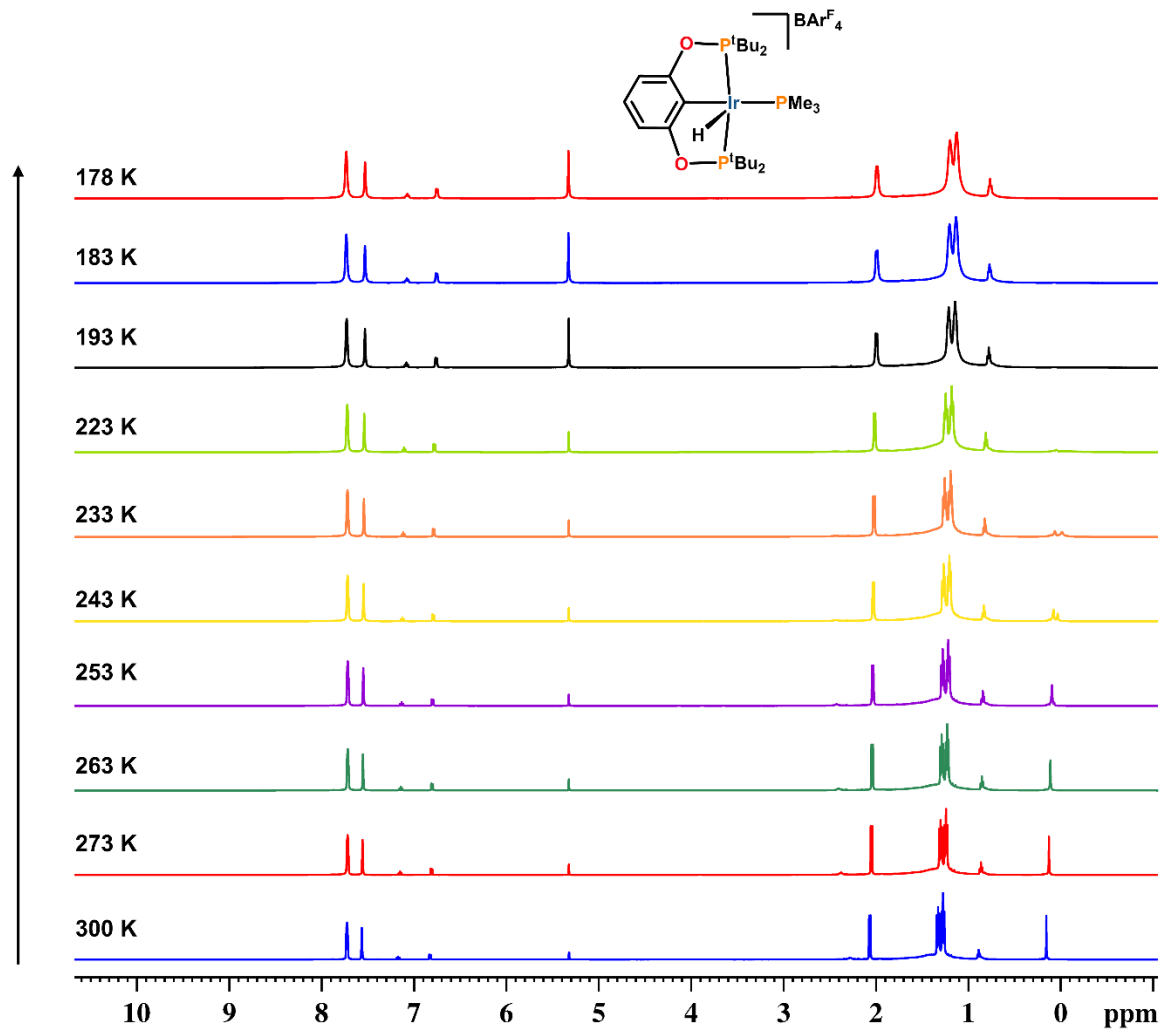


**Figure S21.** Partial VT $^1$H NMR (500.0 MHz, $CD_2Cl_2$) spectral stack plot (downfield region) of [Ir(H)($PMe_3$)($^{tBu4}$POCOP)][$BAr^F_4$] (**3**).

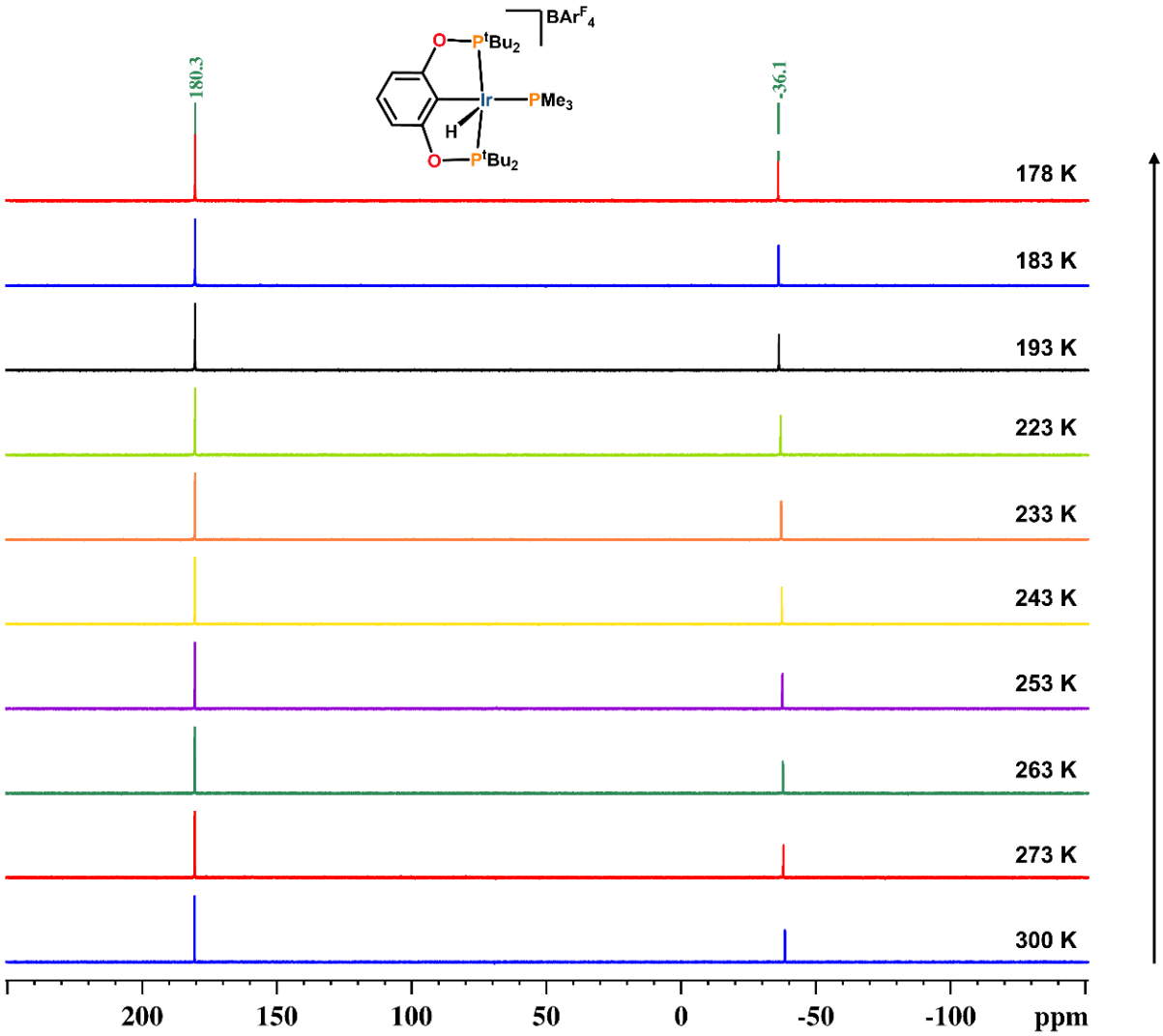


**Figure S22.** VT $^{31}P\{^1H\}$ NMR (202.4 MHz, $CD_2Cl_2$) spectral stack plot of [Ir(H)($PMe_3$)($^{tBu4}$POCOP)][$BAr^F_4$] (**3**).

## 3. Reactivity of [Ir(H)(PMe$_3$)($^{tBu4}$POCOP)][BAr$^F_4$] (**3**) with $CD_2Cl_2$ and THF-$d_8$.

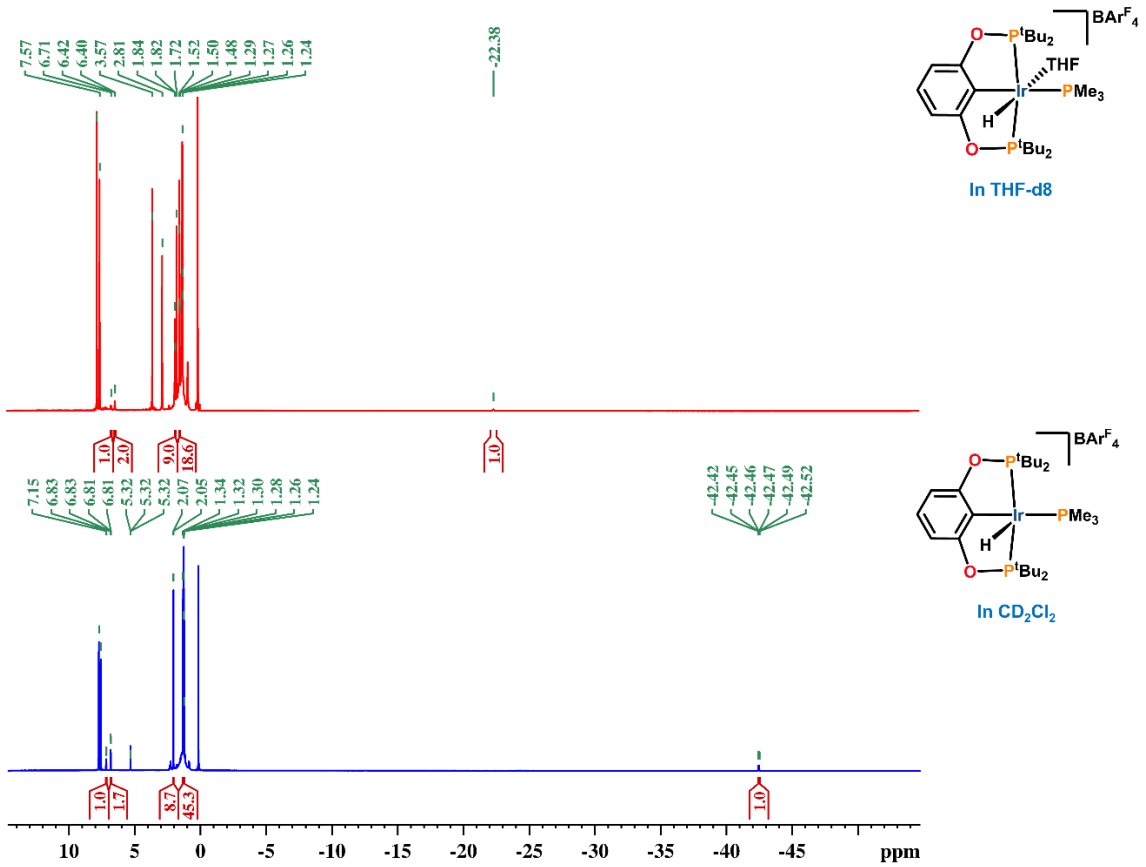


**Figure S23.** $^1$H NMR (400.0 MHz, 298 K) spectral stack plot of [Ir(H)(PMe$_3$)($^{tBu4}$POCOP)][BAr$^F_4$] (**3**) in $CD_2Cl_2$ (spectrum shown in blue color) and [Ir(H)(THF)(PMe$_3$)($^{tBu4}$POCOP)][BAr$^F_4$] (**4**) in THF-$d_8$ (spectrum shown in red color).

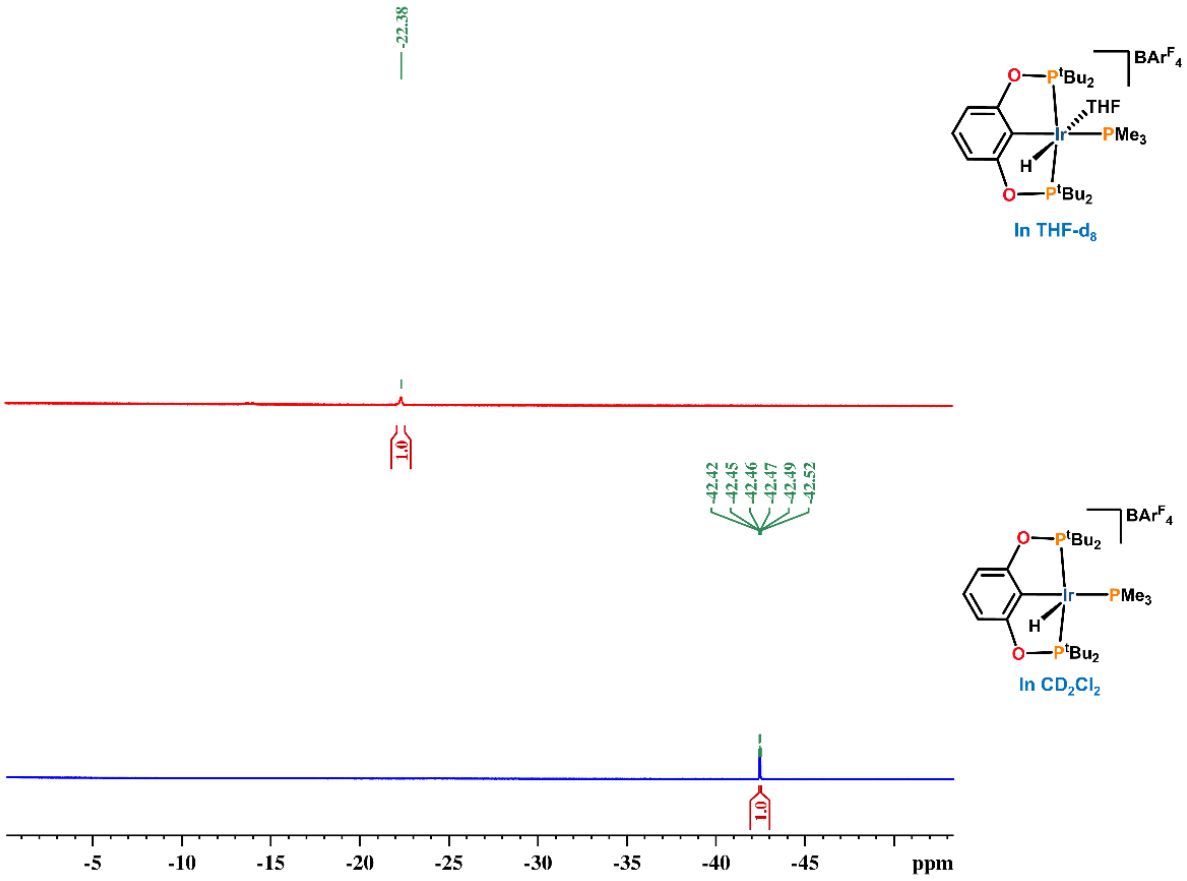


**Figure S24.** Partial $^1$H NMR (400.0 MHz, 298 K) spectral stack plot (hydride region) of [Ir(H)(PMe$_3$)($^{tBu4}$POCOP)][BAr$^F_4$] (**3**) in $CD_2Cl_2$ (spectrum shown in blue color) and [Ir(H)(THF)(PMe$_3$)($^{tBu4}$POCOP)][BAr$^F_4$] (**4**) in THF-d$_8$ (spectrum shown in red color).

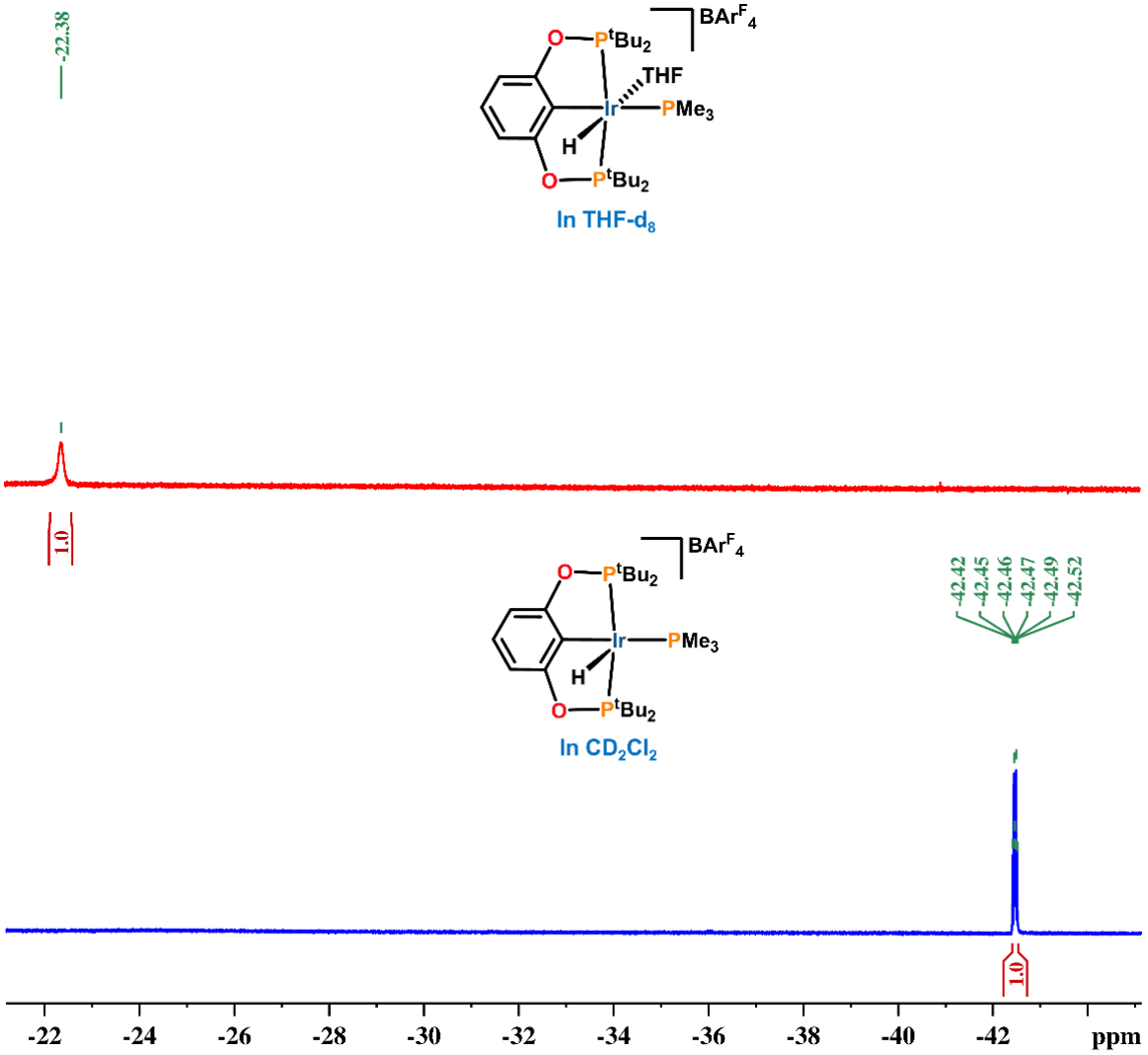


**Figure S25.** Partial $^1$H NMR (400.0 MHz, 298 K) spectral stack plot (expanded hydride region) of [Ir(H)(PMe$_3$)($^{tBu4}$POCOP)][BAr$^F_4$] (**3**) in $CD_2Cl_2$ (spectrum shown in blue color) and [Ir(H)(THF)(PMe$_3$)($^{tBu4}$POCOP)][BAr$^F_4$] (**4**) in THF-d$_8$ (spectrum shown in red color).

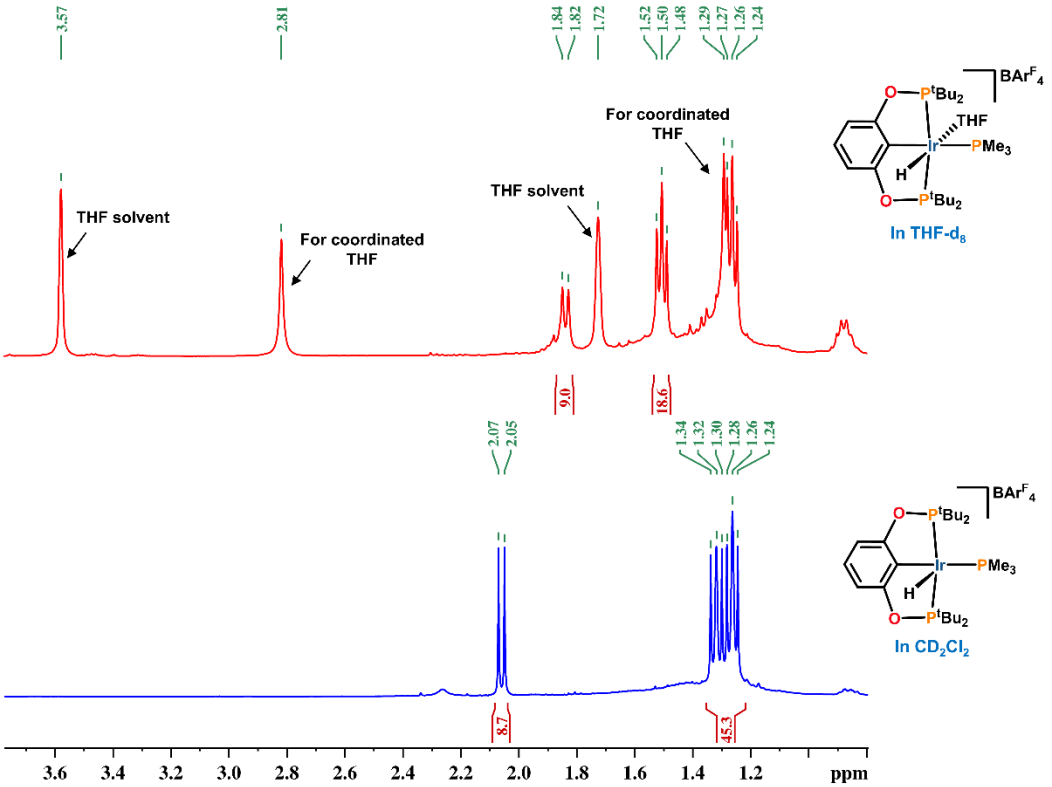


**Figure S26.** Partial $^{1}$H NMR (400.0 MHz, 298 K) spectral stack plot (downfield region) of [Ir(H)(PMe$_3$)($^{tBu4}$POCOP)][BAr$^F_4$] (**3**) in $CD_2Cl_2$ (spectrum shown in blue color) and [Ir(H)(THF)(PMe$_3$)($^{tBu4}$POCOP)][BAr$^F_4$] (**4**) in THF-d$_8$ (spectrum shown in red color).

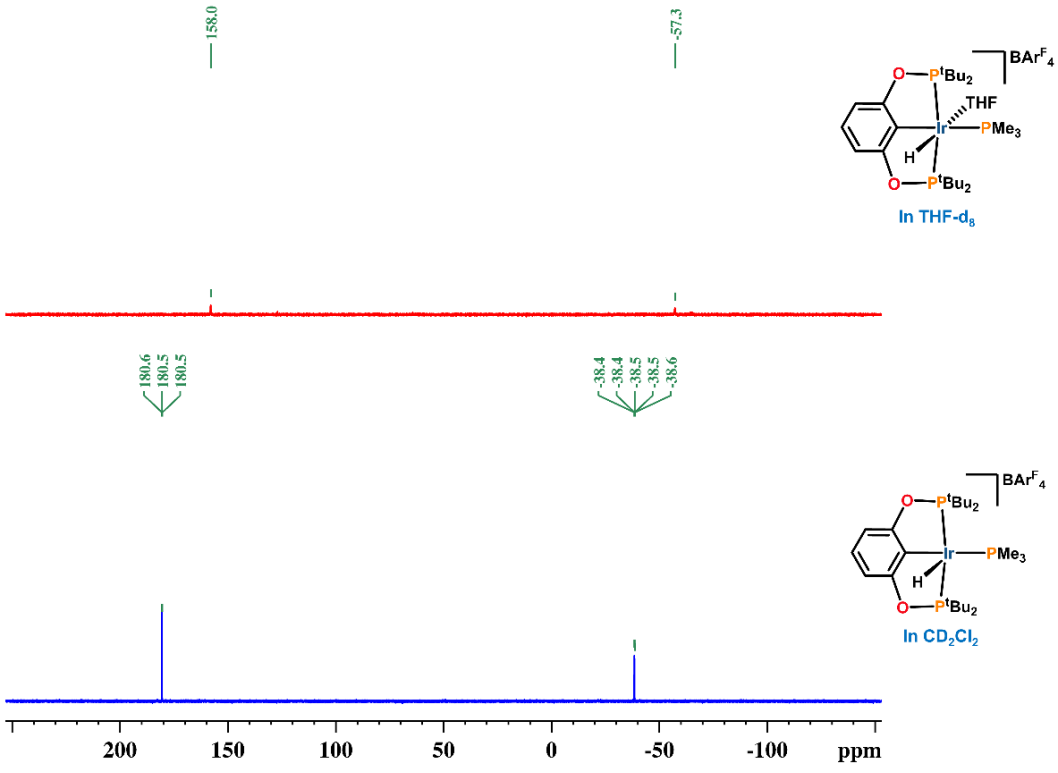

**Figure S27.** $^{31}P\{^{1}H\}$ NMR (161.9 MHz, 298 K) spectral stack plot of [Ir(H)($PMe_3$)($^{tBu4}$POCOP)][$BAr^F_4$] (**3**) in $CD_2Cl_2$ (spectrum shown in blue color) and [Ir(H)(THF)($PMe_3$)($^{tBu4}$POCOP)][$BAr^F_4$] (**4**) in THF-$d_8$ (spectrum shown in red color).

## 4. Conversion of [Ir(H)(THF)($PMe_3$)($^{tBu4}$POCOP)][$BAr^F_4$] (**4**) into [Ir(H)(THF)($^{tBu4}$POCOP)][$BAr^F_4$] (**4a**) over time.

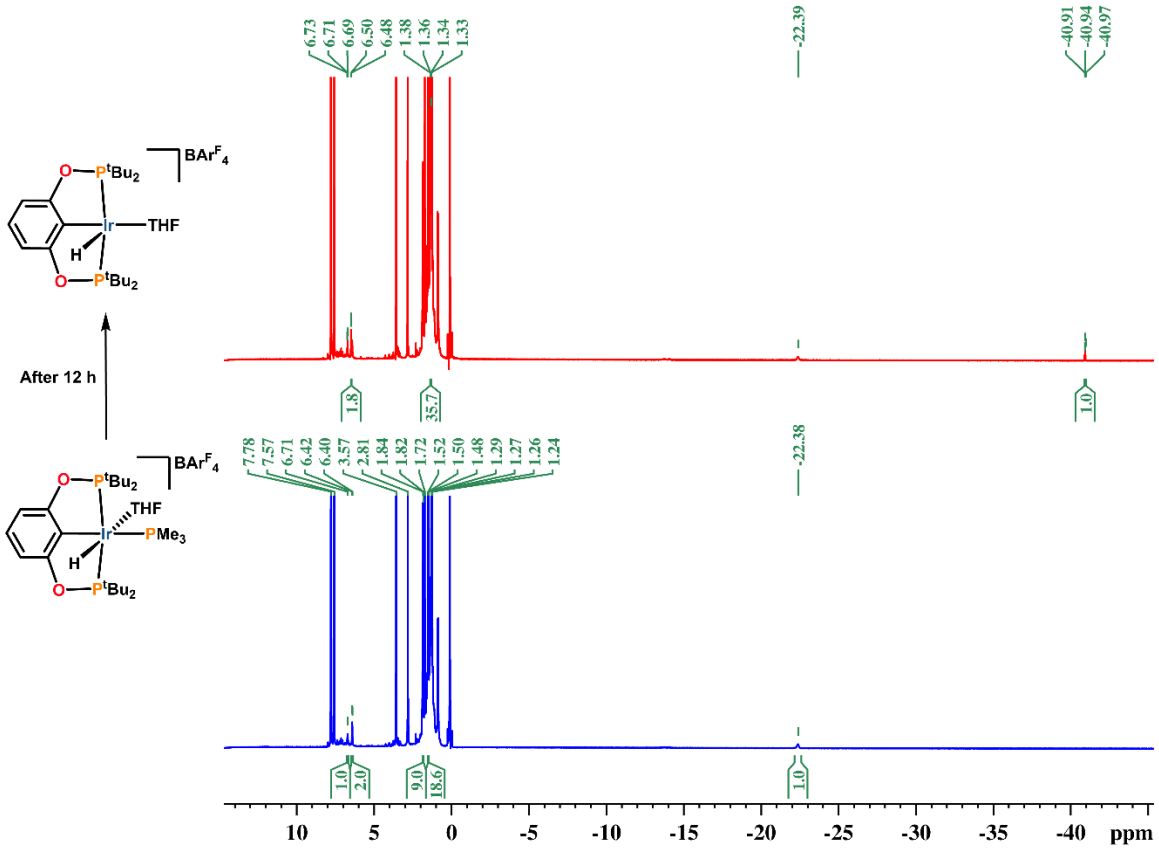


**Figure S28.** $^{1}H$ NMR (400.0 MHz, THF-$d_8$, 298 K) spectral stack plot of the gradual conversion of [Ir(H)(THF)($PMe_3$)($^{tBu4}$POCOP)][$BAr^F_4$] (**4**) (spectrum shown in blue color) to [Ir(H)(THF)($^{tBu4}$POCOP)][$BAr^F_4$] (**4a**) (spectrum shown in red color) over 12 h.

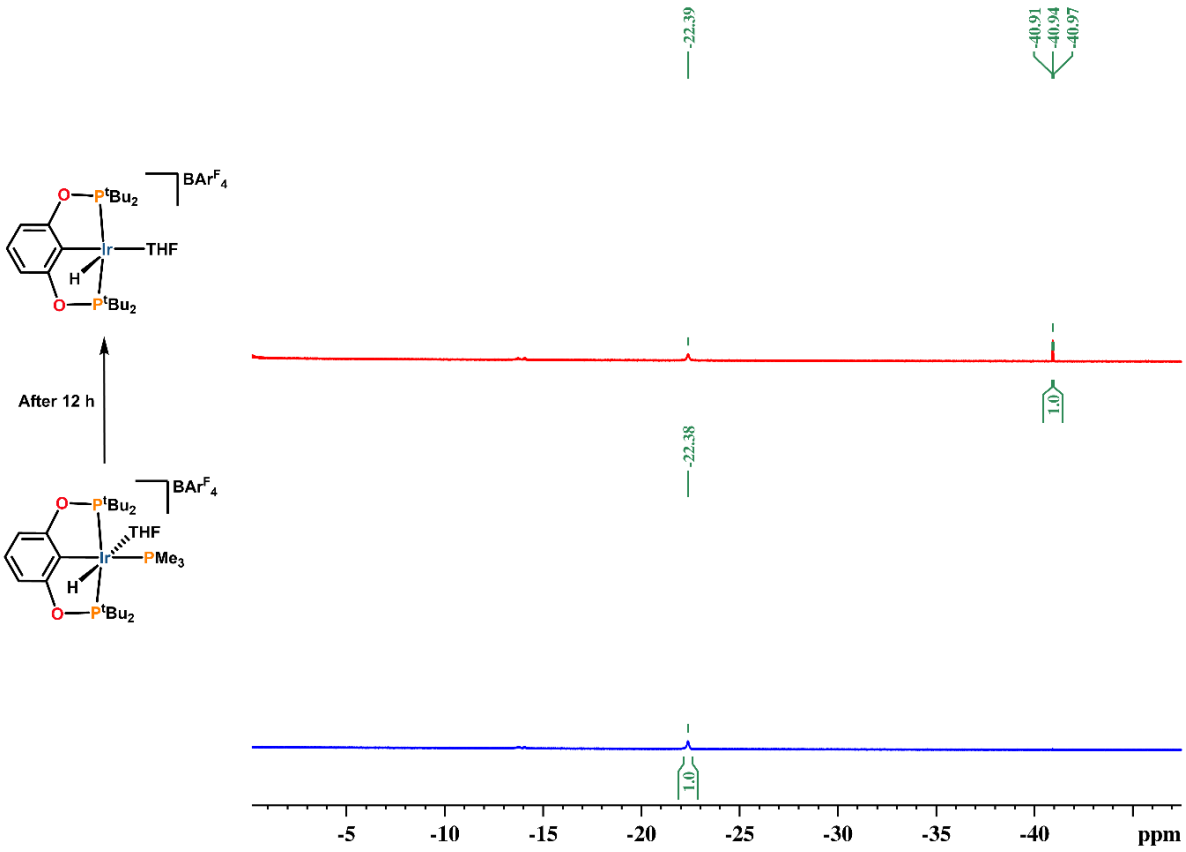


**Figure S29.** Partial $^1$H NMR (400.0 MHz, THF-$d_8$, 298 K) spectral stack plot (hydride region) of the gradual conversion of [Ir(H)(THF)(PMe$_3$)($^{tBu4}$POCOP)][BAr$^F_4$] (**4**) (spectrum shown in blue color) to [Ir(H)(THF)($^{tBu4}$POCOP)][BAr$^F_4$] (**4a**) (spectrum shown in red color) over 12 h.

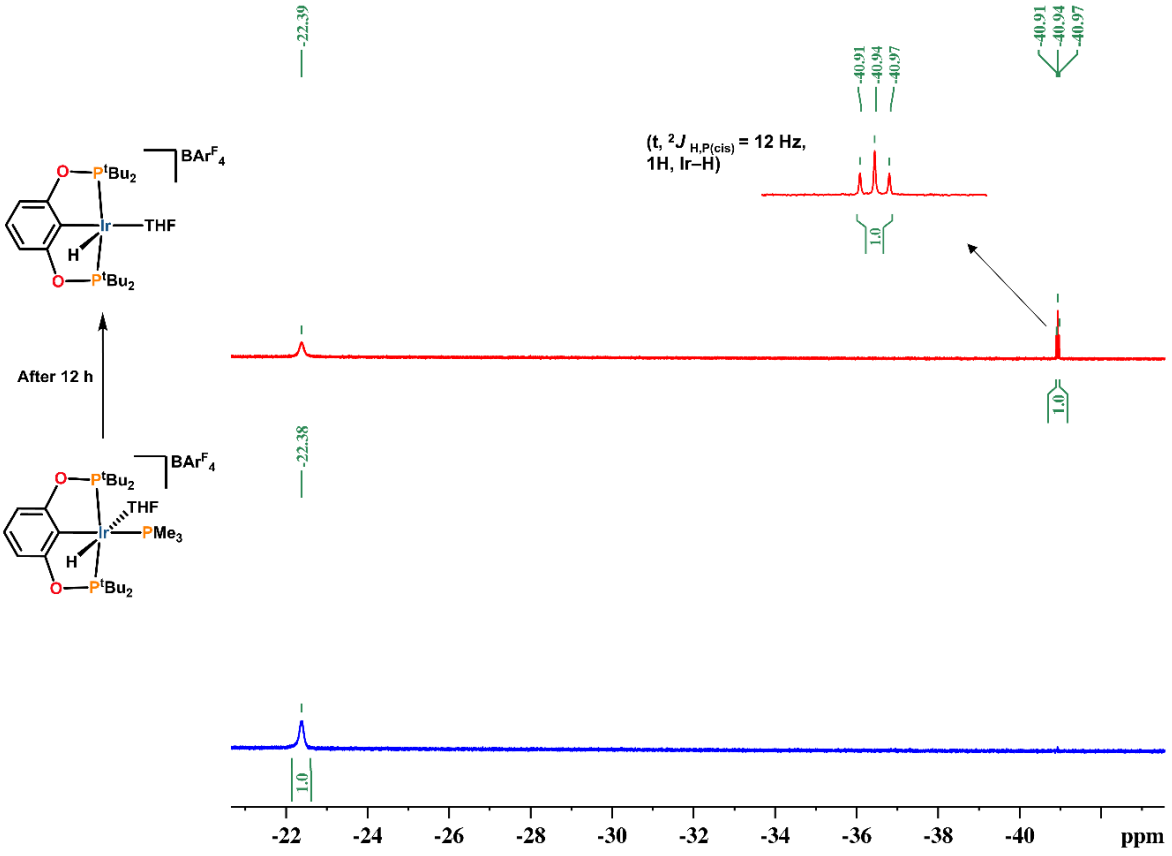


**Figure S30.** Partial $^1$H NMR (400.0 MHz, THF-d$_8$, 298 K) spectral stack plot (expanded hydride region) of the gradual conversion of [Ir(H)(THF)(PMe$_3$)($^{tBu4}$POCOP)][BAr$^F_4$] (**4**) (spectrum shown in blue color) to [Ir(H)(THF)($^{tBu4}$POCOP)][BAr$^F_4$] (**4a**) (spectrum shown in red color) over 12 h.

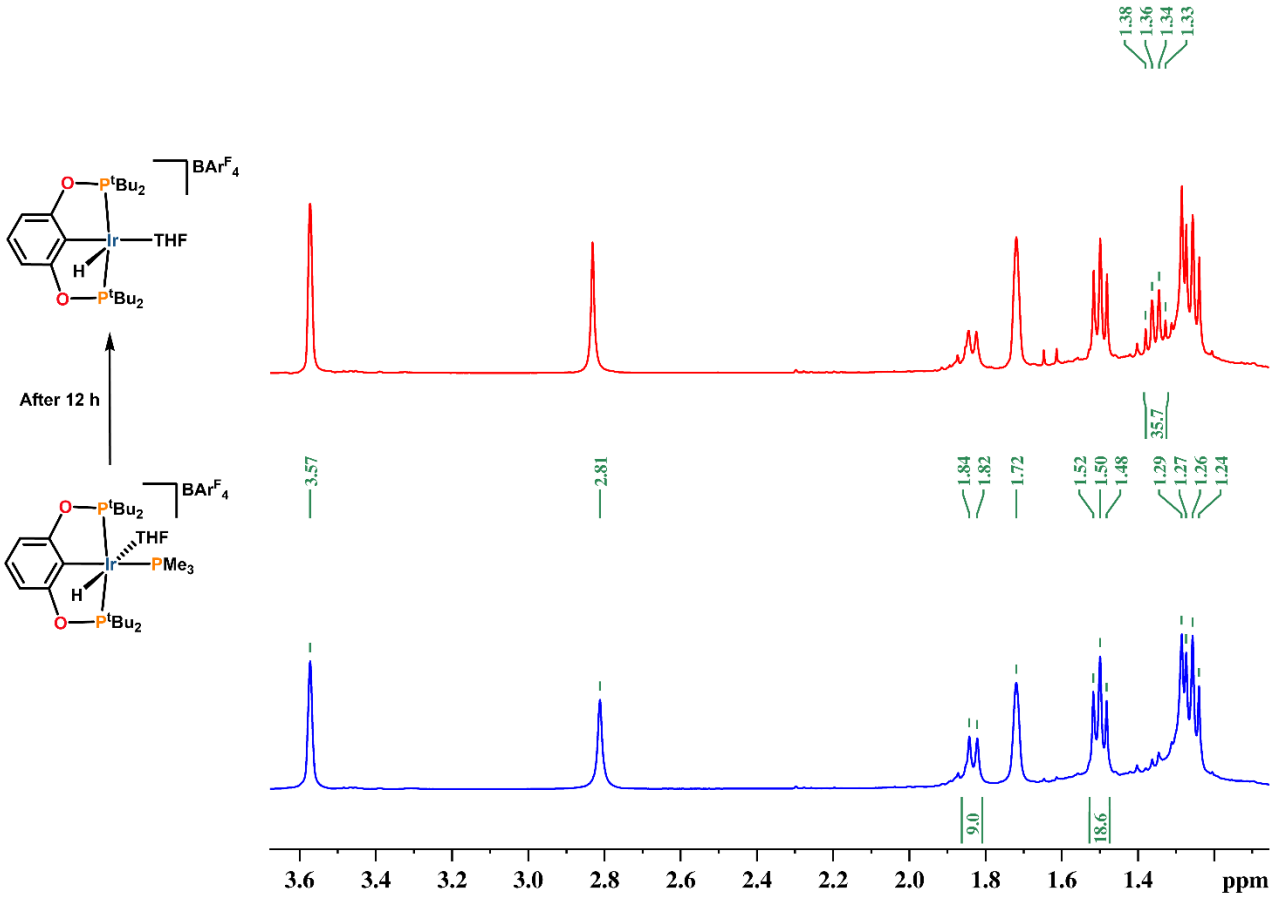


**Figure S31.** Partial $^1$H NMR (400.0 MHz, THF-$d_8$, 298 K) spectral stack plot (expanded alkyl region) of the gradual conversion of [Ir(H)(THF)(PMe$_3$)($^{tBu4}$POCOP)][BAr$^F_4$] (**4**) (spectrum shown in blue color) to [Ir(H)(THF)($^{tBu4}$POCOP)][BAr$^F_4$] (**4a**) (spectrum shown in red color) over 12 h.

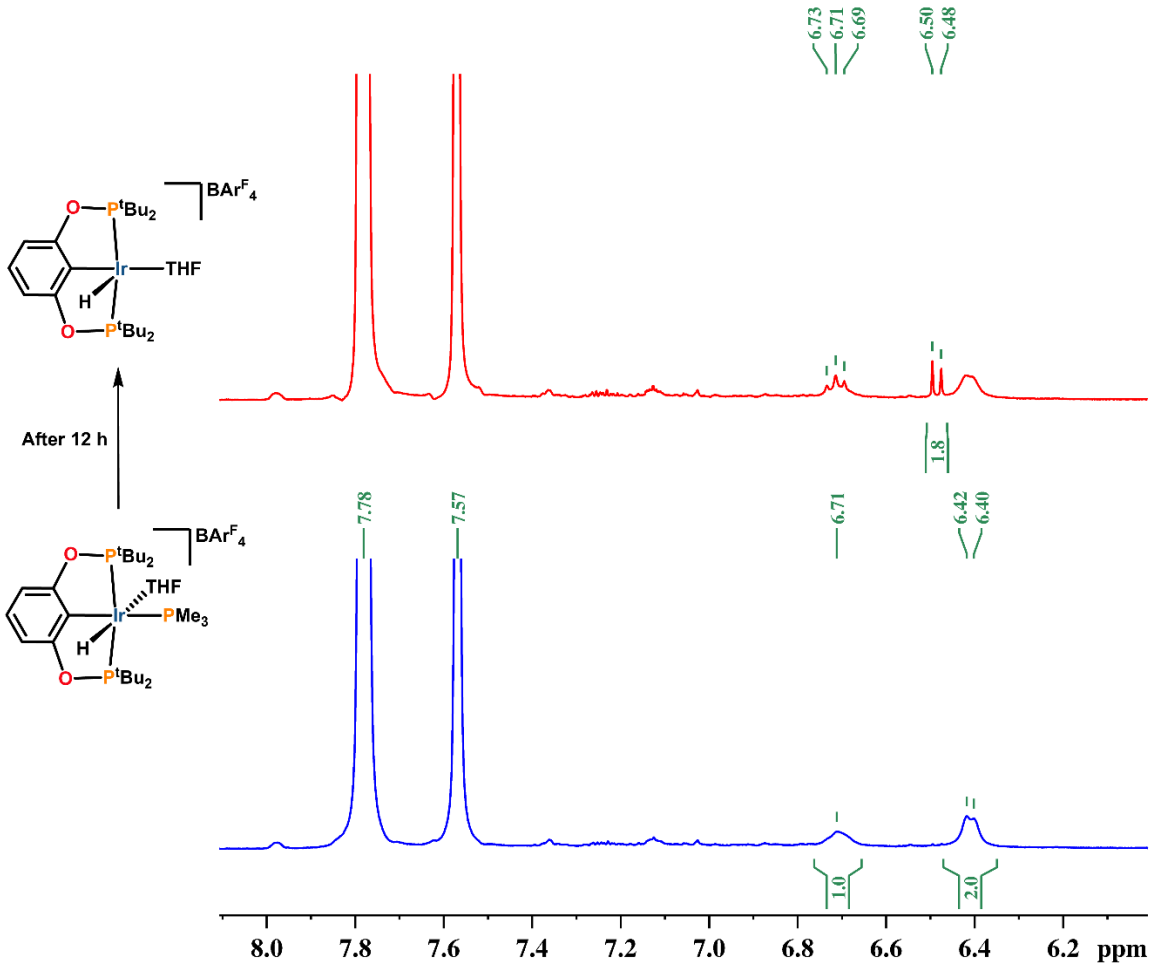


**Figure S32.** Partial $^1$H NMR (400.0 MHz, THF-d$_8$, 298 K) spectral stack plot (expanded aryl region) of the gradual conversion of [Ir(H)(THF)(PMe$_3$)($^{tBu4}$POCOP)][BAr$^F_4$] (**4**) (spectrum shown in blue color) to [Ir(H)(THF)($^{tBu4}$POCOP)][BAr$^F_4$] (**4a**) (spectrum shown in red color) over 12 h.

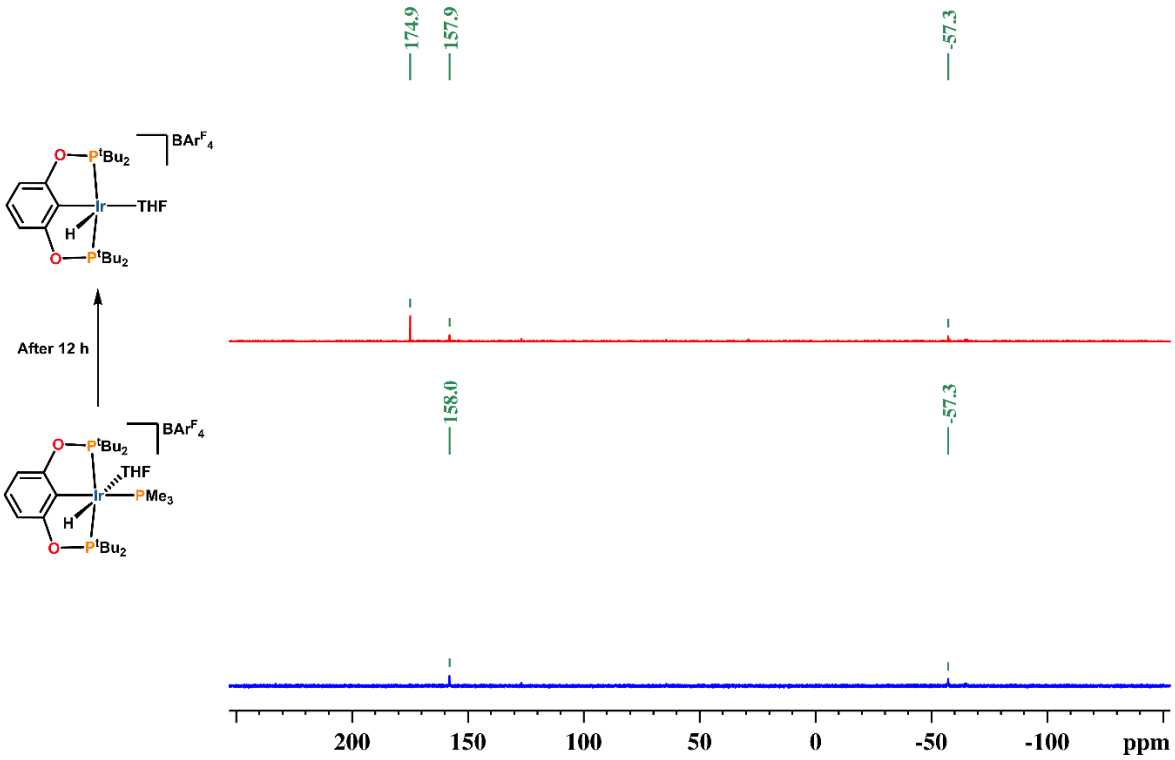


**Figure S33.** $^{31}P\{^1H\}$ NMR (161.9 MHz, THF-$d_8$, 298 K) spectral stack plot of the gradual conversion of [Ir(H)(THF)(PMe$_3$)($^{tBu4}$POCOP)][BAr$^F_4$] (**4**) (spectrum shown in blue color) to [Ir(H)(THF)($^{tBu4}$POCOP)][BAr$^F_4$] (**4a**) (spectrum shown in red color) over 12 h.

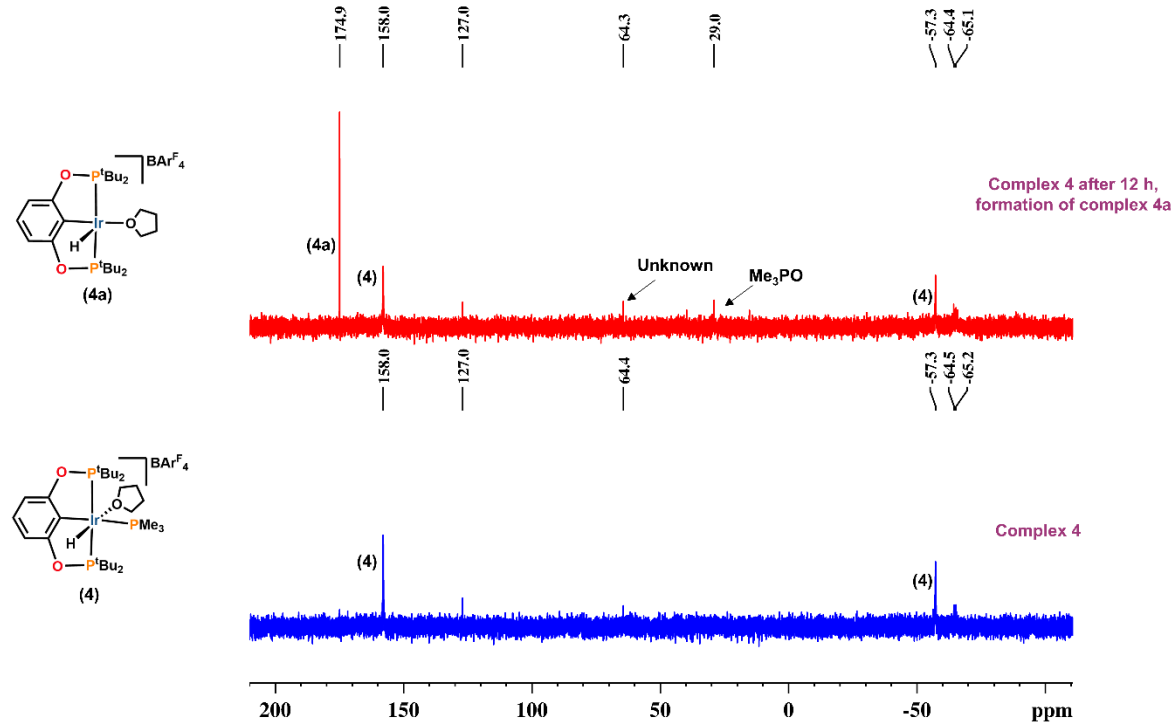


**Figure S34.** $^{31}P\{^1H\}$ NMR (161.9 MHz, THF-$d_8$, 298 K) spectral stack plot (enlarged region) of the gradual conversion of [Ir(H)(THF)(PMe$_3$)($^{tBu4}$POCOP)][BAr$^F_4$] (**4**) (spectrum shown in blue color) to [Ir(H)(THF)($^{tBu4}$POCOP)][BAr$^F_4$] (**4a**) (spectrum shown in red color) over 12 h.

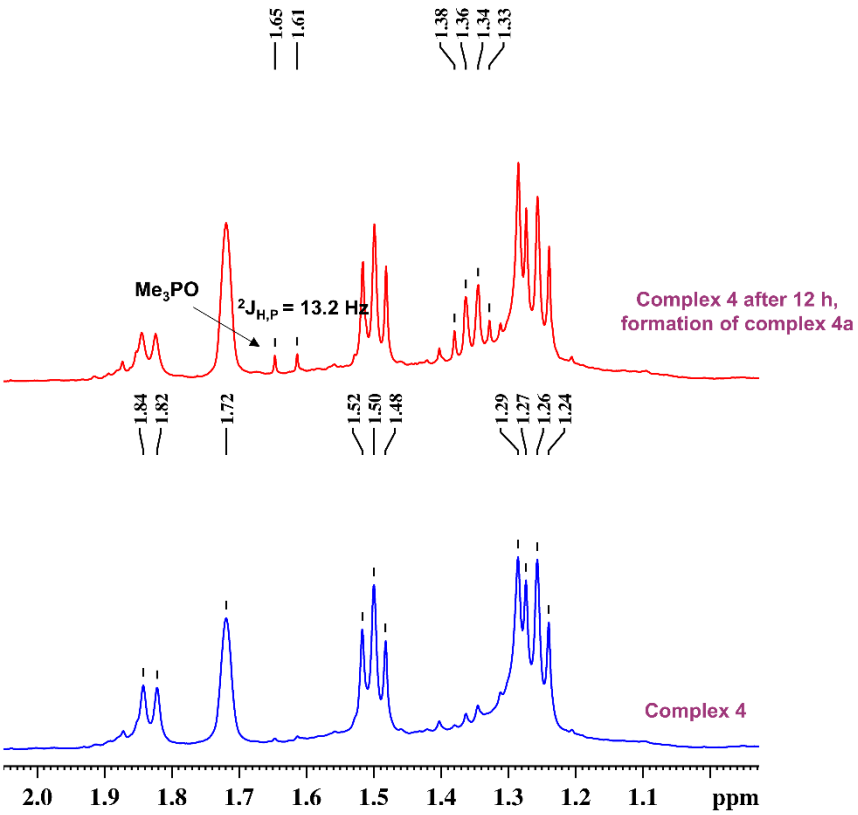


**Figure S35.** Partial $^{1}$H NMR (400.0 MHz, THF-$d_8$, 298 K) spectral stack plot (enlarged alkyl region) of the gradual conversion of [Ir(H)(THF)($PMe_3$)($^{tBu4}$POCOP)][$BAr^F_4$] (**4**) (spectrum shown in blue color) to [Ir(H)(THF)($^{tBu4}$POCOP)][$BAr^F_4$] (**4a**) (spectrum shown in red color) over 12 h.

## 5. Reaction of [Ir(H)(PMe$_3$)($^{tBu4}$POCOP)][BAr$^F_4$] (**3**) with $H_2$.

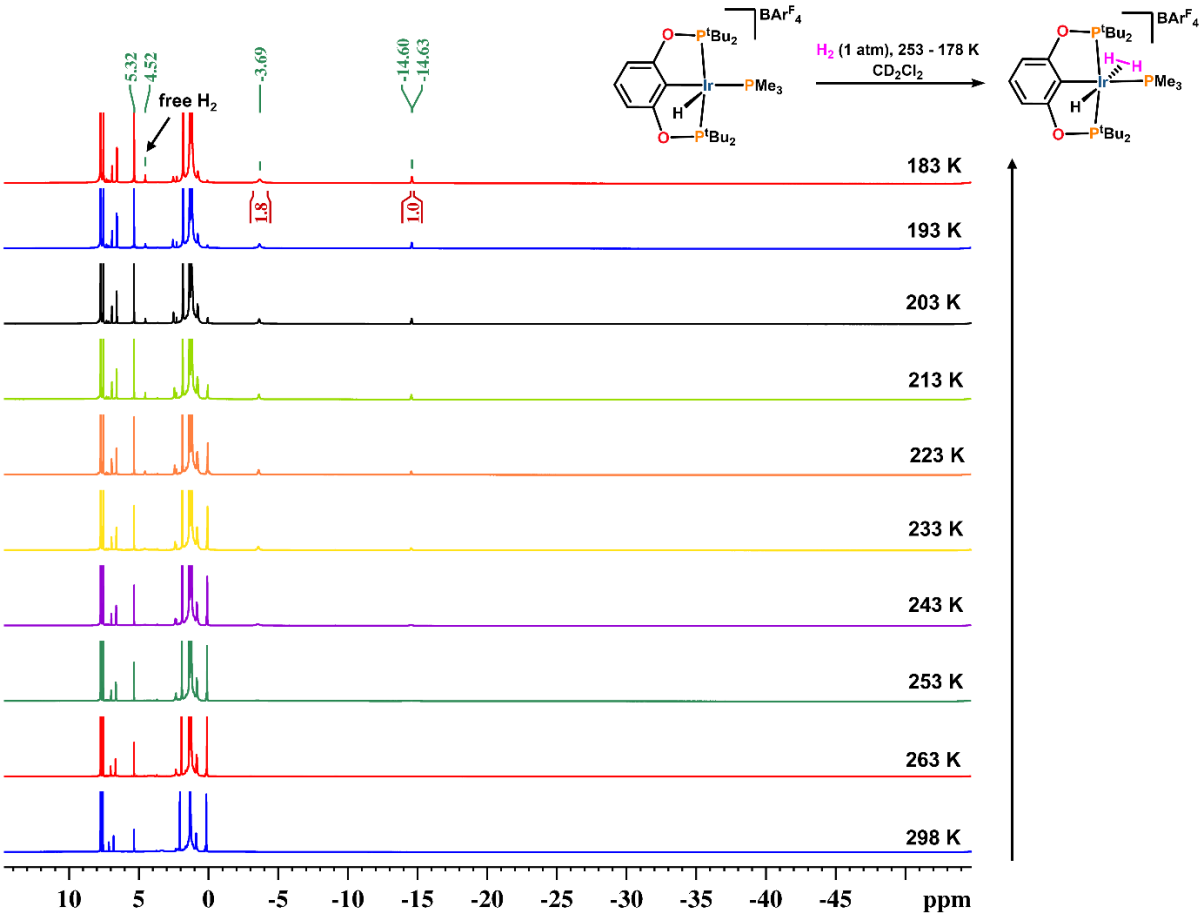


**Figure S36.** VT $^1$H NMR (500.0 MHz, $CD_2Cl_2$) spectral stack plot of the reaction of [Ir(H)(PMe$_3$)($^{tBu4}$POCOP)][BAr$^F_4$] (**3**) with $H_2$: formation of [Ir(H)($\eta^2$-$H_2$)(PMe$_3$)($^{tBu4}$POCOP)][BAr$^F_4$] (**5**).

The peaks of complex **5** resolved over a temperature range of 253-178 K.

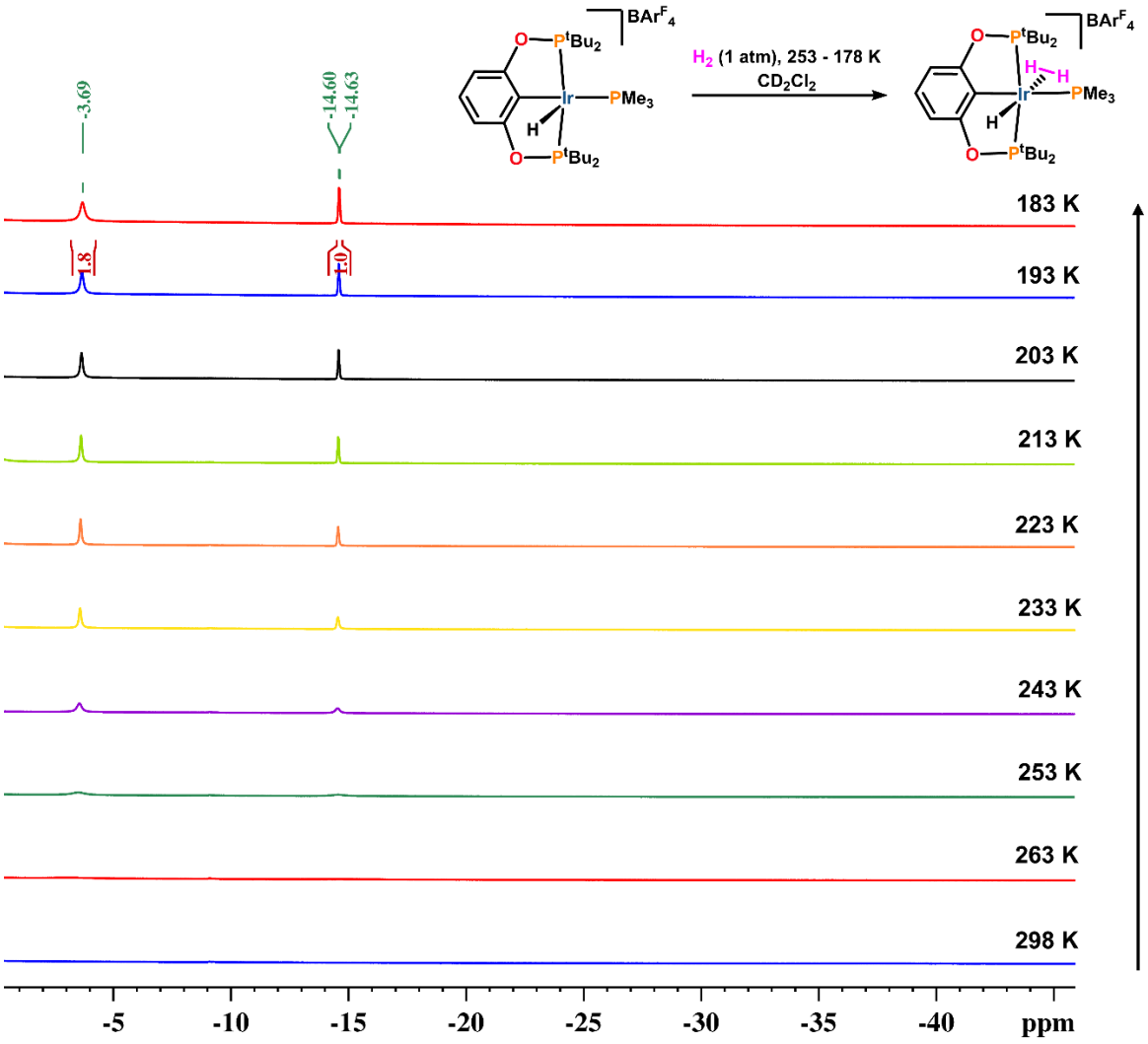


**Figure S37.** Partial VT $^1$H NMR (500.0 MHz, $CD_2Cl_2$) spectral stack plot (hydride region) of the reaction of [Ir(H)($PMe_3$)($^{tBu4}$POCOP)][$BAr^F_4$] (**3**) with $H_2$: formation of [Ir(H)($\eta^2$-$H_2$)($PMe_3$)($^{tBu4}$POCOP)][$BAr^F_4$] (**5**).

The peaks of complex **5** resolved over a temperature range of 253-178 K.

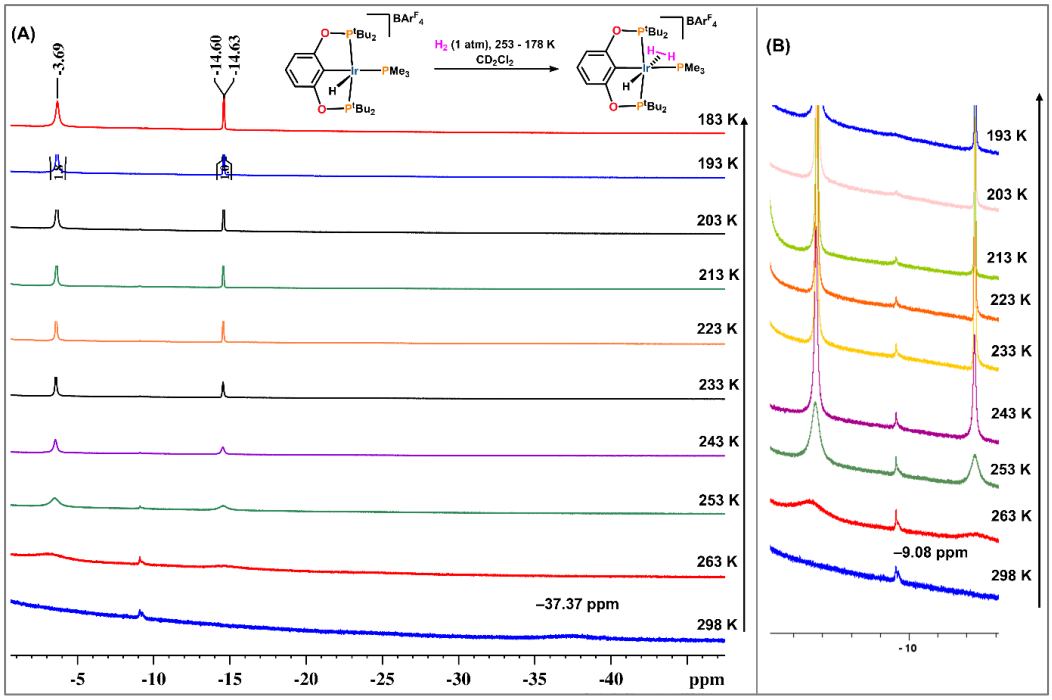


**Figure S38. (A)** Partial VT $^{1}$H NMR (500.0 MHz, $CD_2Cl_2$) spectral stack plot (enlarged hydride region) of the reaction of [Ir(H)(PMe$_3$)($^{tBu4}$POCOP)][BAr$^F_4$] (**3**) with $H_2$: formation of [Ir(H)($\eta^2$-$H_2$)(PMe$_3$)($^{tBu4}$POCOP)][BAr$^F_4$] (**5**). The peaks of complex **5** resolved over a temperature range of 253-178 K. **(B)** Expanded region for the peak at –9.08 ppm. This peak is for an unidentified compound and not associated with the other peaks for the reaction of complex **3** with $H_2$.

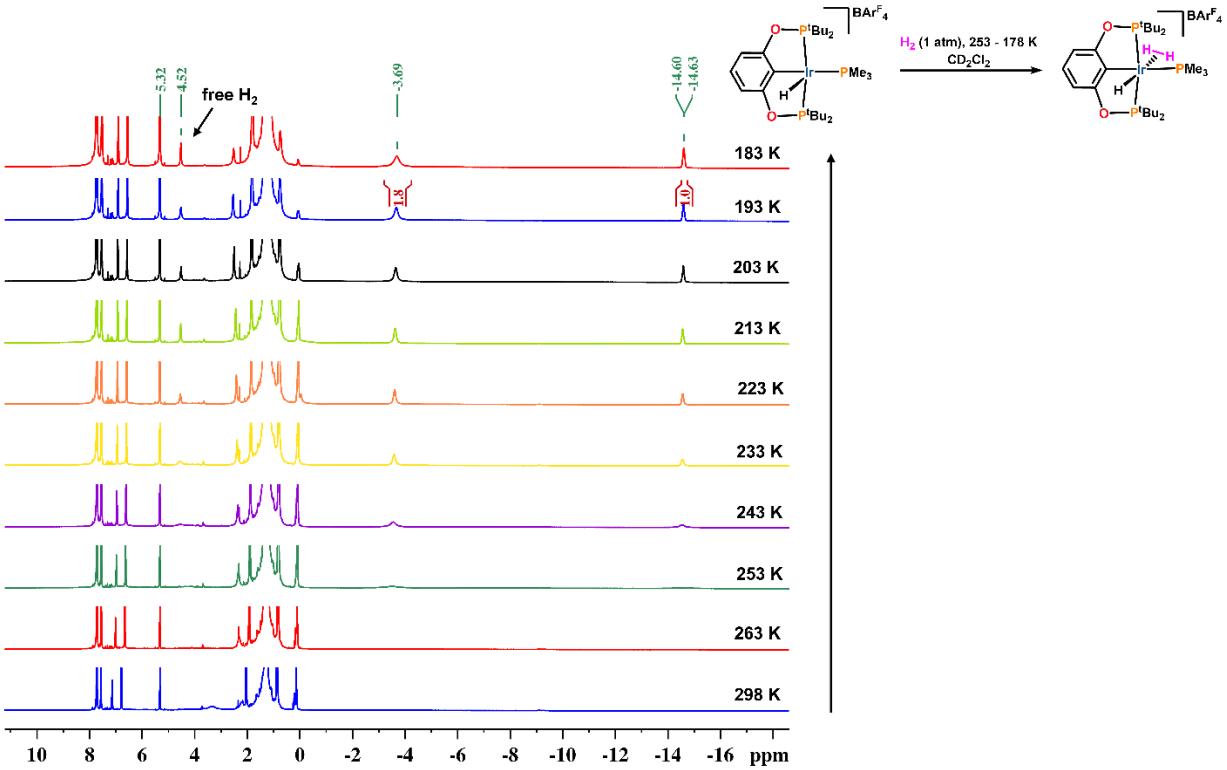


**Figure S39.** Partial VT $^{1}$H NMR (500.0 MHz, $CD_2Cl_2$) spectral stack plot of the reaction of [Ir(H)(PMe$_3$)($^{tBu4}$POCOP)][BAr$^F_4$] (**3**) with $H_2$: formation of [Ir(H)($\eta^2$-$H_2$)(PMe$_3$)($^{tBu4}$POCOP)][BAr$^F_4$] (**5**).

The peaks of complex **5** resolved over a temperature range of 253-178 K.

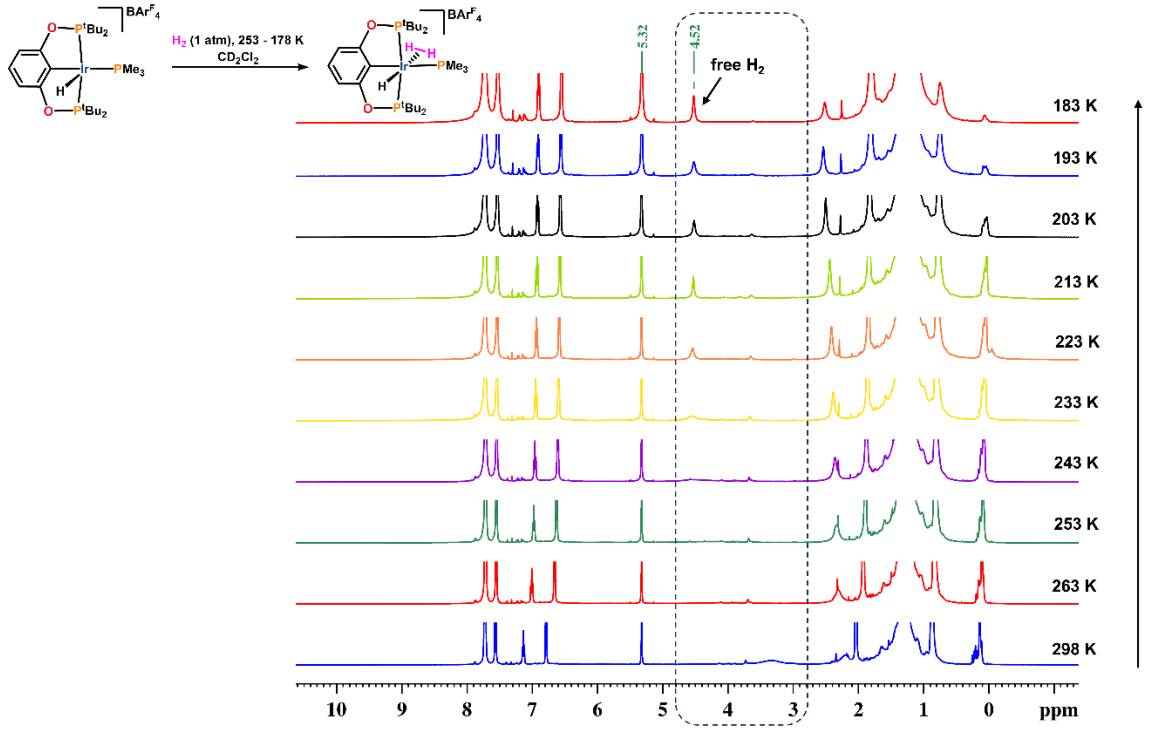


**Figure S40.** Partial VT $^{1}H$ NMR (500.0 MHz, $CD_2Cl_2$) spectral stack plot (downfield region) of the reaction of [Ir(H)($PMe_3$)($^{tBu4}$POCOP)][$BAr^F_4$] (**3**) with $H_2$: formation of [Ir(H)($\eta^2$-$H_2$)($PMe_3$)($^{tBu4}$POCOP)][$BAr^F_4$] (**5**).

The peaks of complex **5** resolved over a temperature range of 253-178 K.

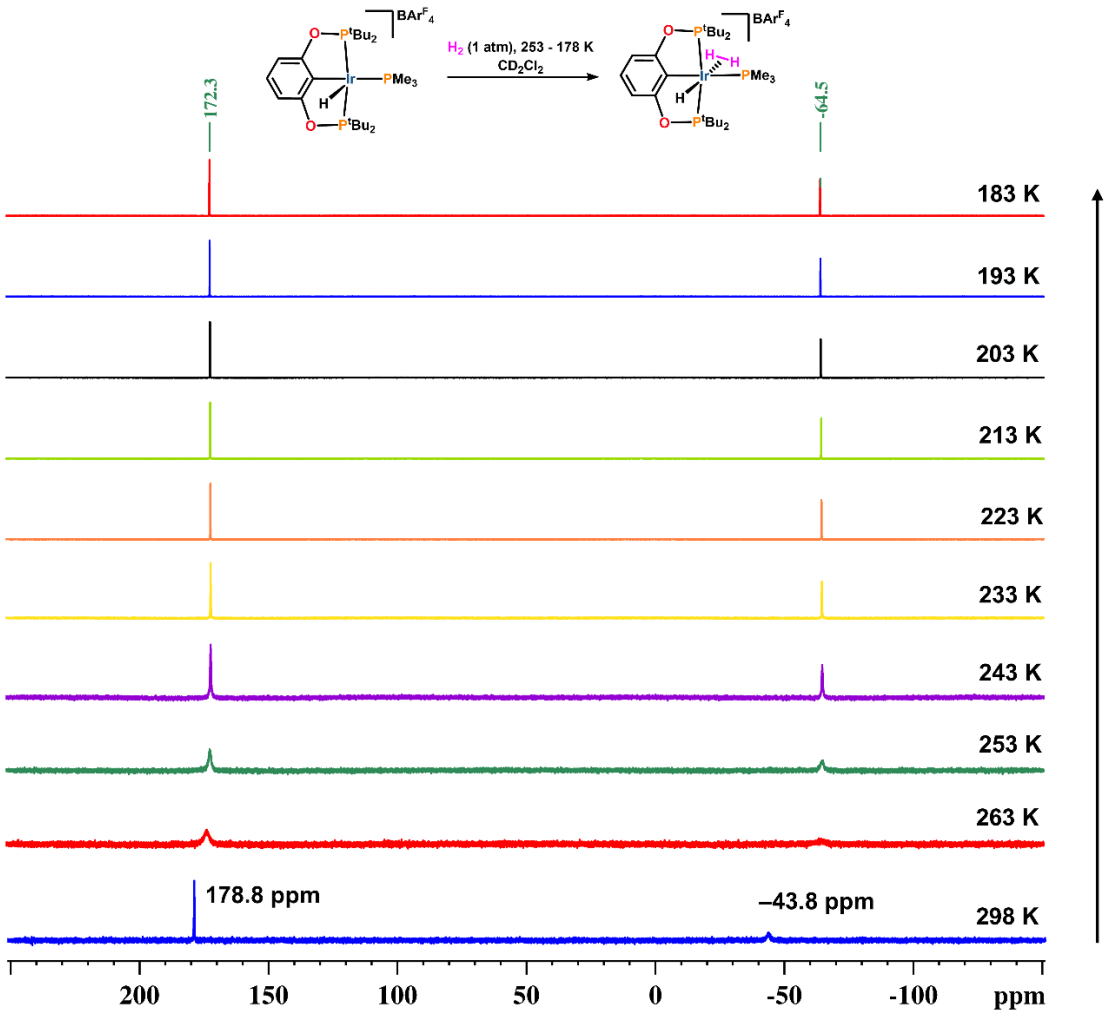


**Figure S41.** VT $^{31}P\{^{1}H\}$ NMR (202.4 MHz, $CD_2Cl_2$) spectral stack plot of the reaction of [Ir(H)(PMe$_3$)($^{tBu4}$POCOP)][BAr$^F_4$] (**3**) with $H_2$: formation of [Ir(H)($\eta^2$-$H_2$)(PMe$_3$)($^{tBu4}$POCOP)][BAr$^F_4$] (**5**).

The peaks of complex **5** resolved over a temperature range of 253-178 K.

**Table S1:** Spin-lattice relaxation time ($T_1$) values (500.0 MHz, $CD_2Cl_2$) of bound $H_2$ in [Ir(H)($\eta^2$-$H_2$)(PMe$_3$)($^{tBu4}$POCOP)][BAr$^F_4$] (**5**) at different temperatures.

| T in K | (1/T)10$^3$ in K$^{-1}$ | $T_1$ in ms | ln($T_1$) |
|---|---|---|---|
| 243 | 4.115 | 38.96 (±0.23) | 3.662 |
| 233 | 4.292 | 27.42 (±0.33) | 3.311 |
| 223 | 4.484 | 18.73 (±0.25) | 2.93 |
| 213 | 4.695 | 16.30 (±0.43) | 2.791 |
| 203 | 4.926 | 15.87 (±0.32) | 2.764 |
| 193 | 5.181 | 18.76 (±0.35) | 2.932 |
| 183 | 5.464 | 26.40 (±0.27) | 3.273 |
| 178 | 5.618 | 34.63 (±0.49) | 3.545 |

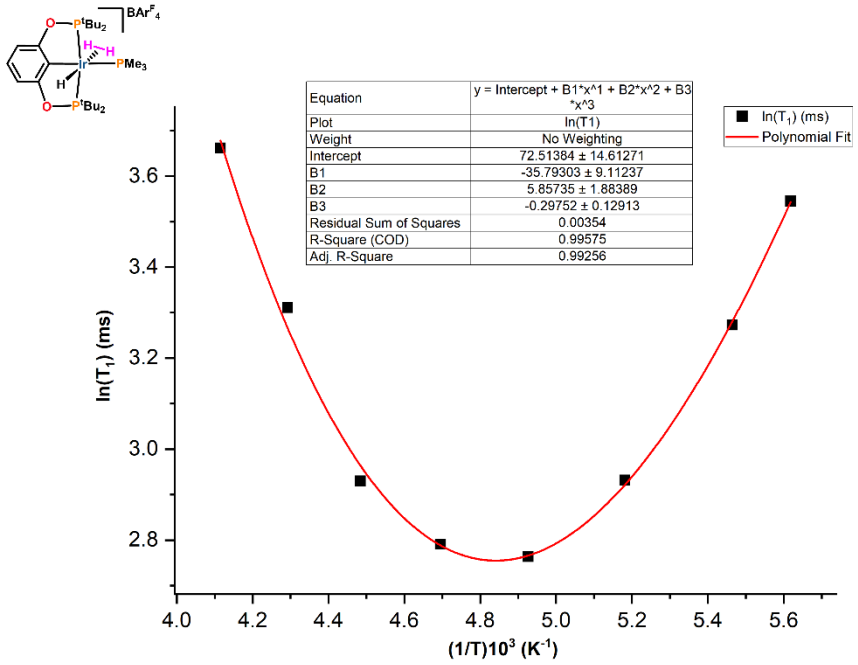


**Figure S42.** Plot of $T_1$ (500.0 MHz, $CD_2Cl_2$) of bound $H_2$ in [Ir(H)($\eta^2$-$H_2$)($PMe_3$)($^{tBu4}$POCOP)][$BAr^F_4$] (**5**) vs temperature. From the plot, $T_1$(min) was calculated to be 15.64 ms at 207 K.

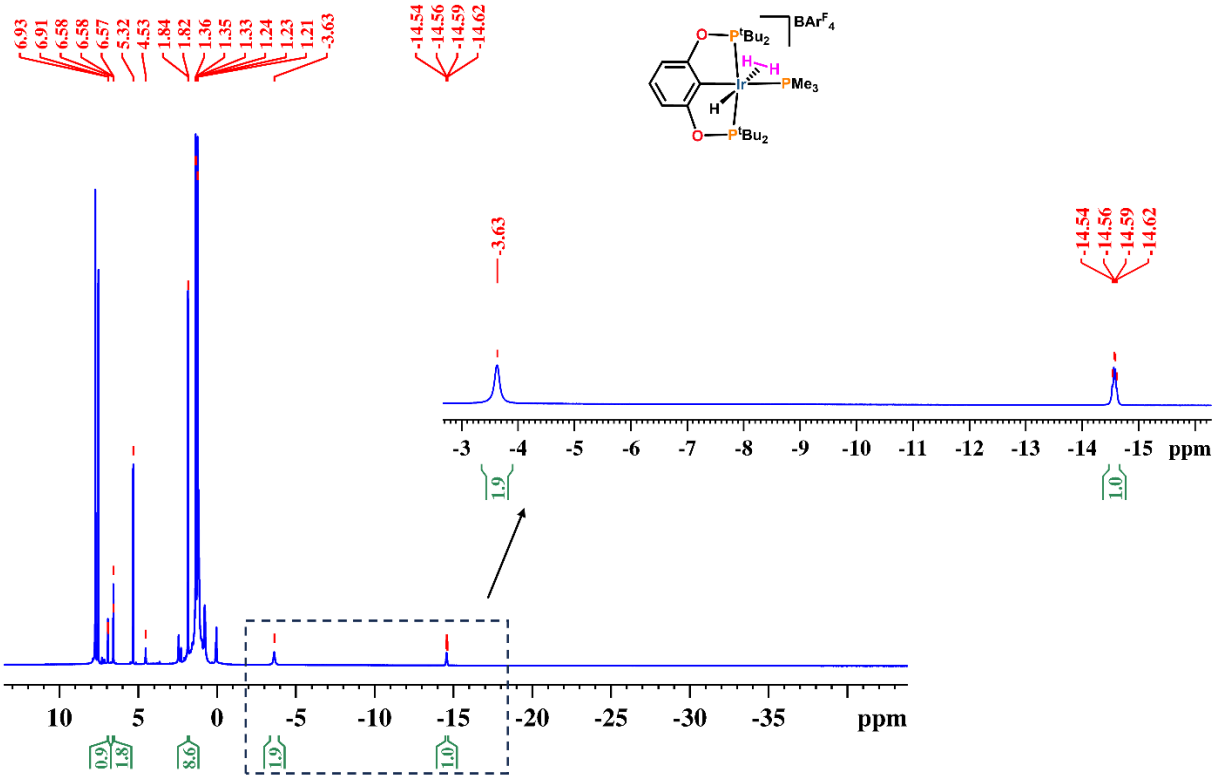


**Figure S43.** $^1$H NMR (500.0 MHz, $CD_2Cl_2$, 213 K) spectrum of [Ir(H)($\eta^2$-$H_2$)($PMe_3$)($^{tBu4}$POCOP)][$BAr^F_4$] (**5**).

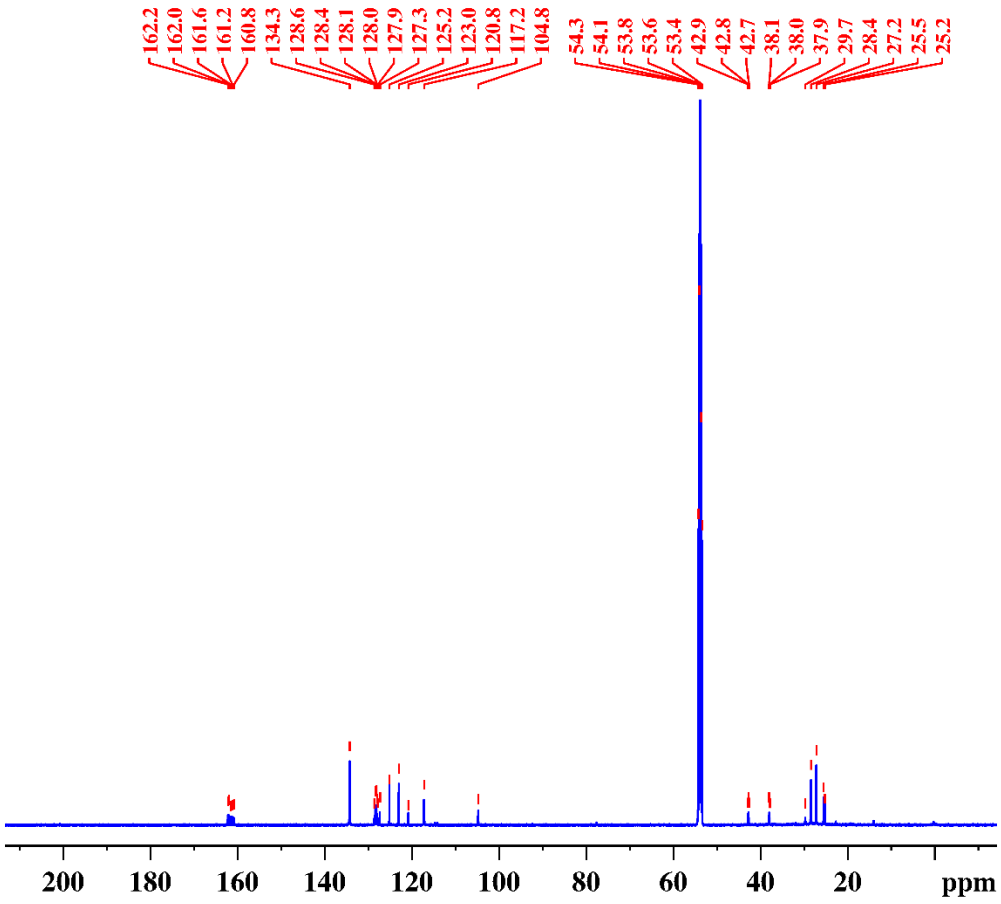


**Figure S44.** $^{13}C\{^{1}H\}$ NMR (125.0 MHz, $CD_2Cl_2$, 213 K) spectrum of [Ir(H)($\eta^2$-$H_2$)($PMe_3$)($^{tBu4}$POCOP)][$BAr^F_4$] (**5**).

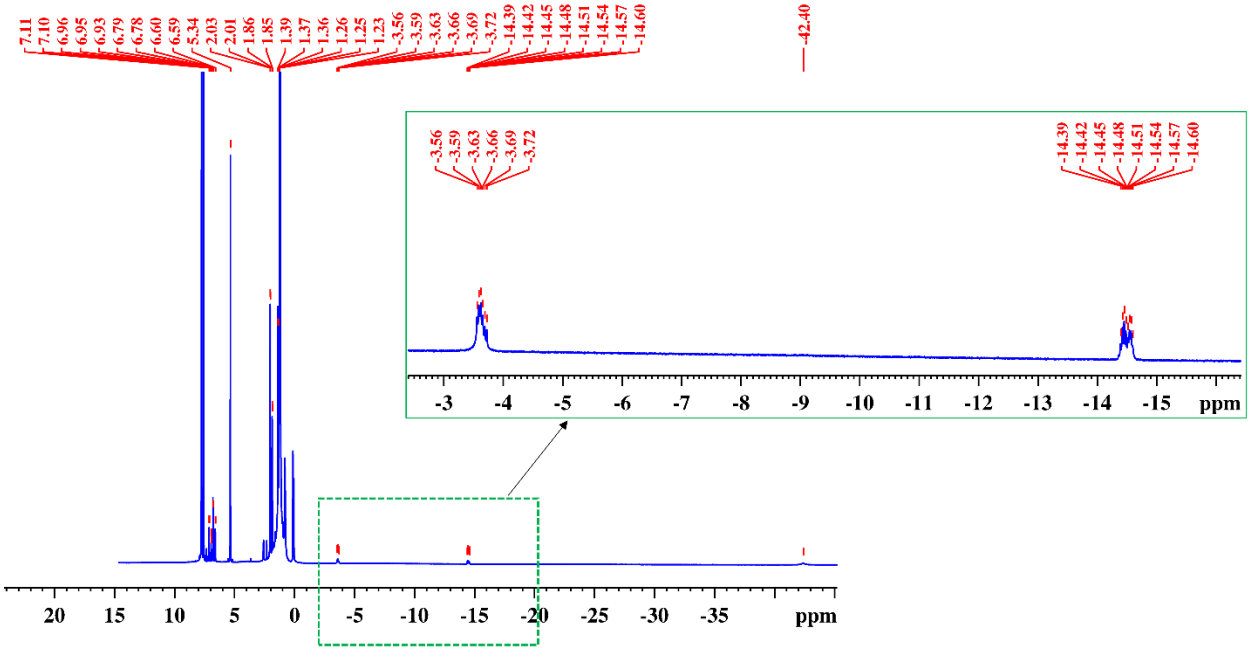


**Figure S45.** $^{1}H$ NMR (500.0 MHz, $CD_2Cl_2$, 213 K) spectrum of [Ir(H)($\eta^2$-HD)($PMe_3$)($^{tBu4}$POCOP)][$BAr^F_4$] (**5-HD**), formed upon purging HD gas through a solution of [Ir(H)($PMe_3$)($^{tBu4}$POCOP)][$BAr^F_4$] (**3**).

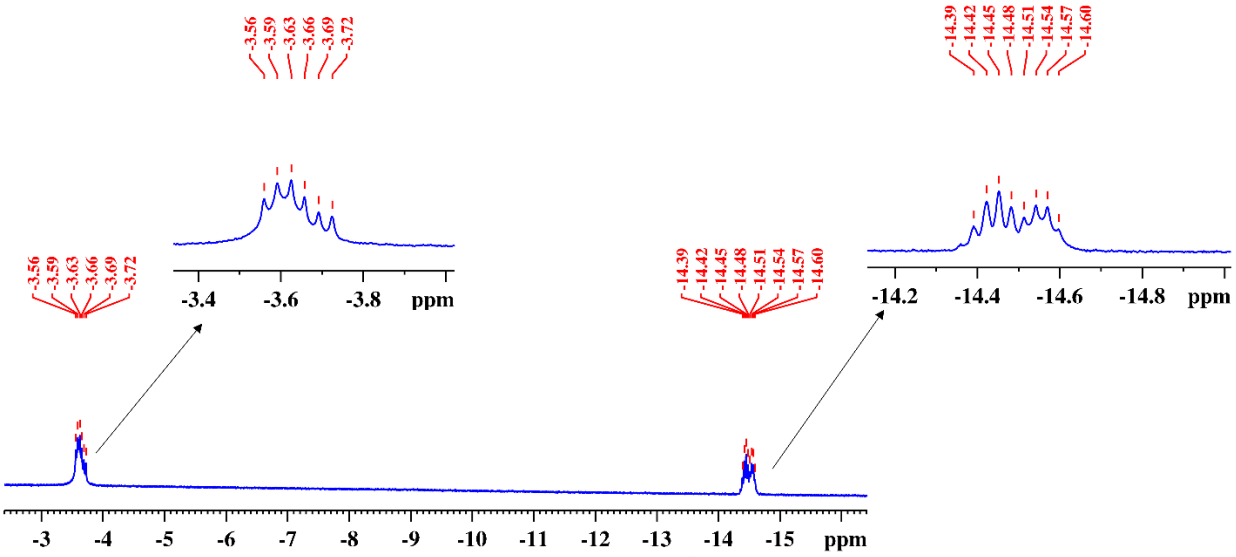


**Figure S46.** Partial $^{1}H$ NMR (500.0 MHz, $CD_2Cl_2$, 213 K) spectrum of [Ir(H)($\eta^2$-HD)($PMe_3$)($^{tBu4}$POCOP)][$BAr^F_4$] (**5-HD**), formed upon purging HD gas through a solution of [Ir(H)($PMe_3$)($^{tBu4}$POCOP)][$BAr^F_4$] (**3**).

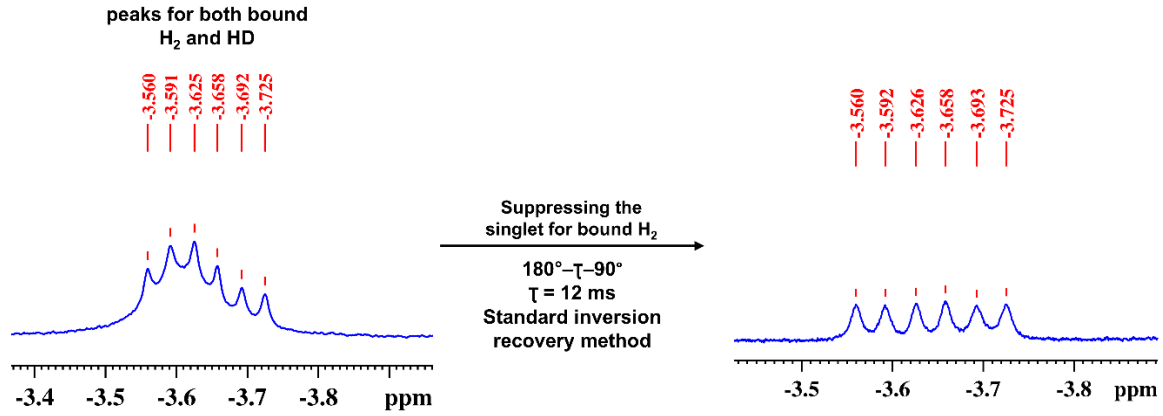


**Figure S47.** Partial $^{1}H$ NMR (500.0 MHz, $CD_2Cl_2$, 213 K) spectra of [Ir(H)($\eta^2$-HD)($PMe_3$)($^{tBu4}$POCOP)][$BAr^F_4$] (**5-HD**), formed upon purging HD gas through a solution of [Ir(H)($PMe_3$)($^{tBu4}$POCOP)][$BAr^F_4$] (**3**) (spectrum shown in left side) and **5-HD** after supressing the singlet for Ir($H_2$) (spectrum shown in right side).

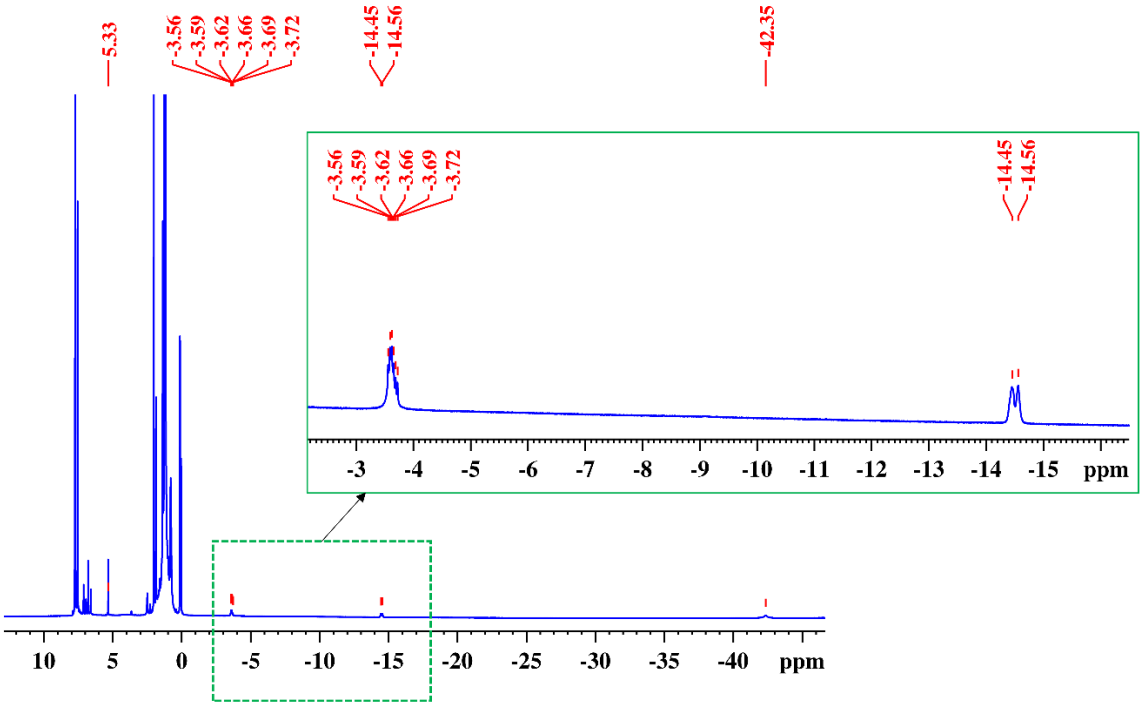


**Figure S48.** $^{1}H\{^{31}P\}$ NMR (500.0 MHz, $CD_2Cl_2$, 213 K) spectrum of [Ir(H)($\eta^2$-HD)($PMe_3$)($^{tBu4}$POCOP)][$BAr^F_4$] (**5-HD**), formed upon purging HD gas through a solution of [Ir(H)($PMe_3$)($^{tBu4}$POCOP)][$BAr^F_4$] (**3**).

Multiplet at –3.64 ppm, containing peaks for bound $H_2$ and HD, was unaffected after $^{31}P$ decoupling.

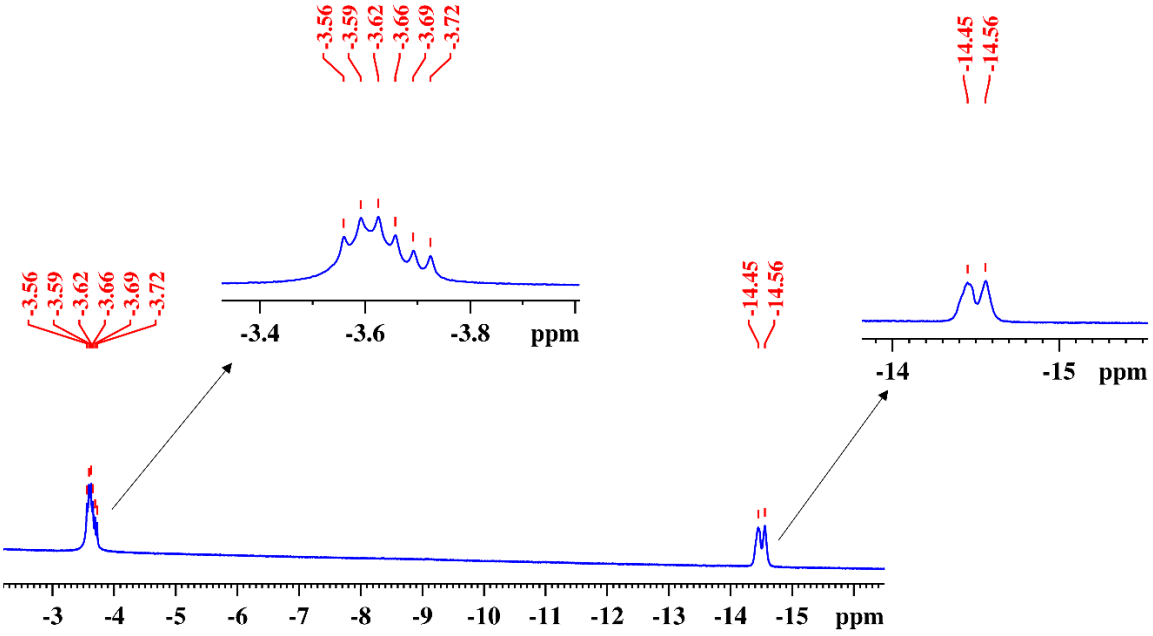


**Figure S49.** Partial $^{1}H\{^{31}P\}$ NMR (500.0 MHz, $CD_2Cl_2$, 213 K) spectrum of [Ir(H)($\eta^2$-HD)($PMe_3$)($^{tBu4}$POCOP)][$BAr^F_4$] (**5-HD**), formed upon purging HD gas through a solution of [Ir(H)($PMe_3$)($^{tBu4}$POCOP)][$BAr^F_4$] (**3**).

Multiplet at –3.64 ppm, containing peaks for bound $H_2$ and HD, was unaffected after $^{31}P$ decoupling.

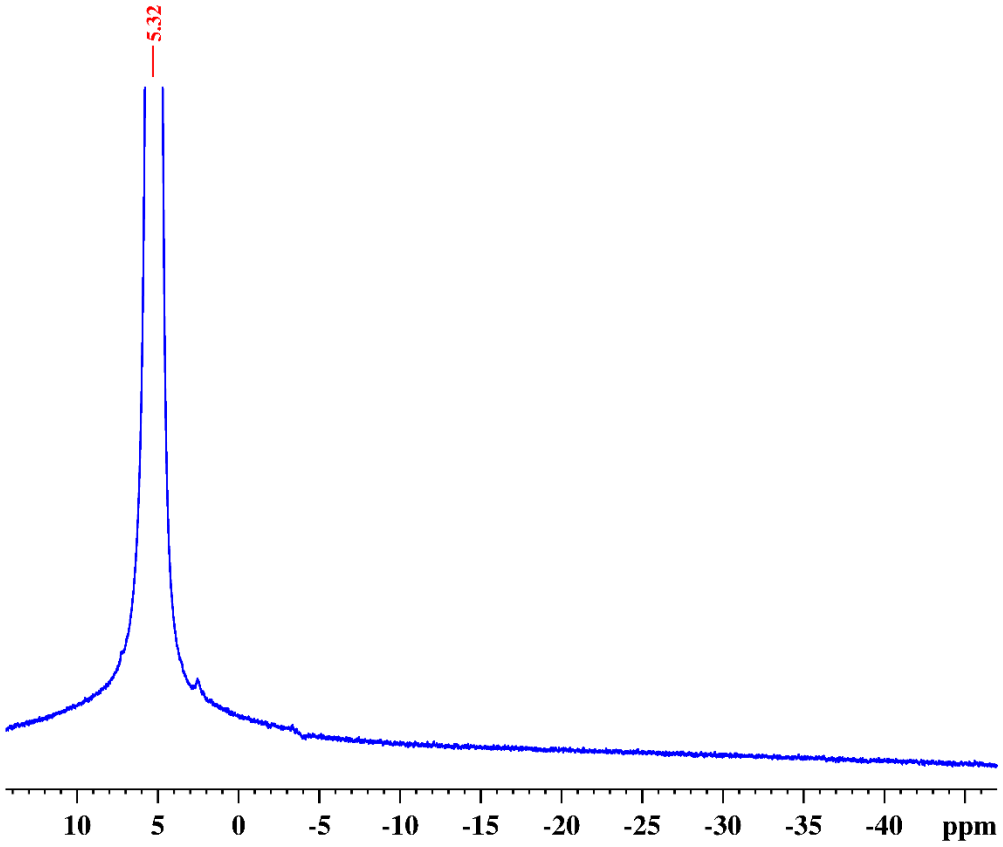


**Figure S50.** $^{2}H$ NMR (76.7 MHz, $CD_2Cl_2$, 213 K) spectrum of [Ir(H)($\eta^2$-HD)($PMe_3$)($^{tBu4}$POCOP)][$BAr^F_4$] (**5-HD**), formed upon purging HD gas through a solution of [Ir(H)($PMe_3$)($^{tBu4}$POCOP)][$BAr^F_4$] (**3**).

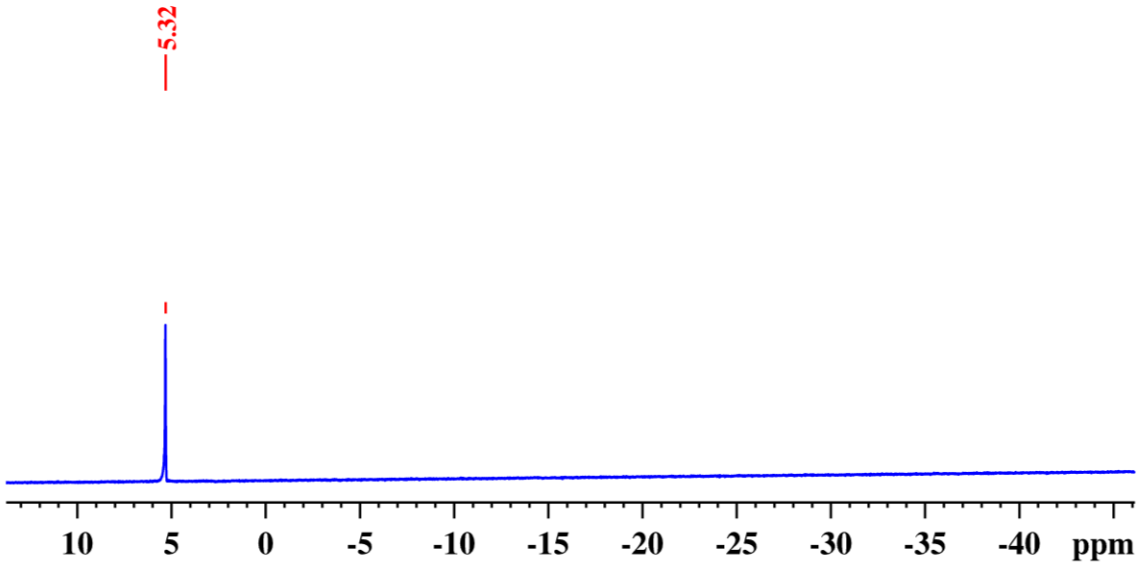


**Figure S51A.** $^{2}H$ NMR (76.7 MHz, $CH_2Cl_2$, 213 K) spectrum of [Ir(H)($\eta^2$-HD)($PMe_3$)($^{tBu4}$POCOP)][$BAr^F_4$] (**5-HD**), formed upon purging HD gas through a solution of [Ir(H)($PMe_3$)($^{tBu4}$POCOP)][$BAr^F_4$] (**3**). 10.0 µL of $CD_2Cl_2$ was added for reference.

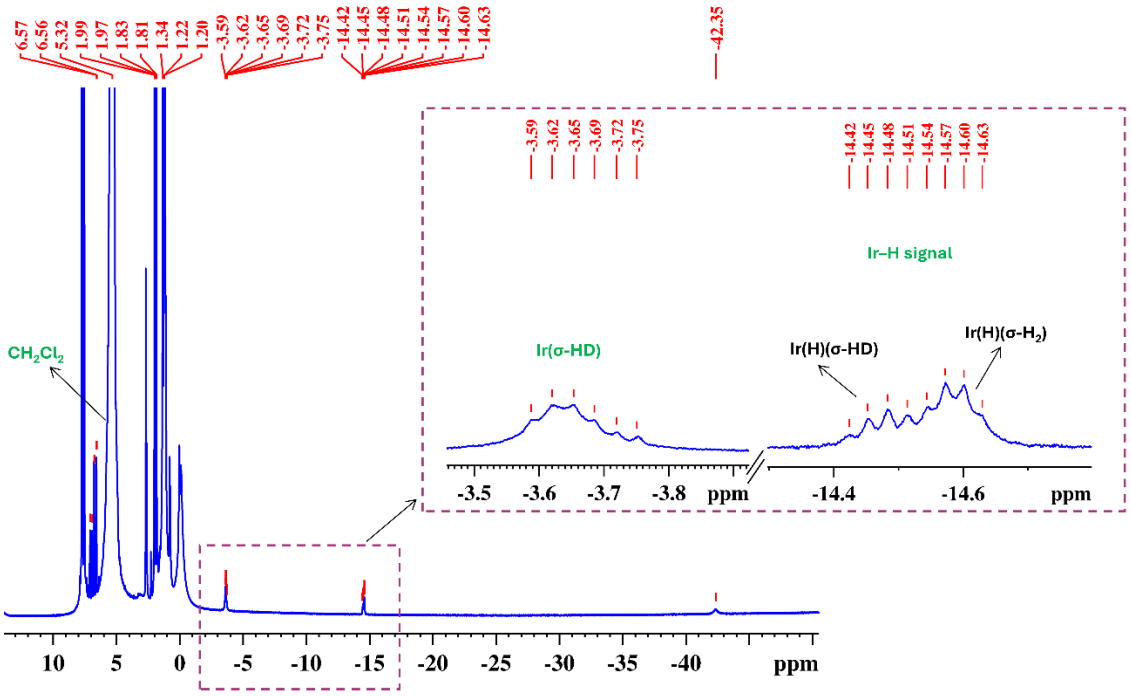


**Figure S51B.** $^{1}H$ NMR (500 MHz, $CH_2Cl_2$+$CD_2Cl_2$, 213 K) spectrum of [Ir(H)($\eta^2$-HD)($PMe_3$)($^{tBu4}$POCOP)][$BAr^F_4$] (**5-HD**), formed upon purging HD gas through a solution of [Ir(H)($PMe_3$)($^{tBu4}$POCOP)][$BAr^F_4$] (**3**). For acquiring $^{1}H$ and $^{31}P\{^{1}H\}$ NMR spectral data of complex **5-HD**, 0.2 mL of $CD_2Cl_2$ was added to the same sample under HD gas.

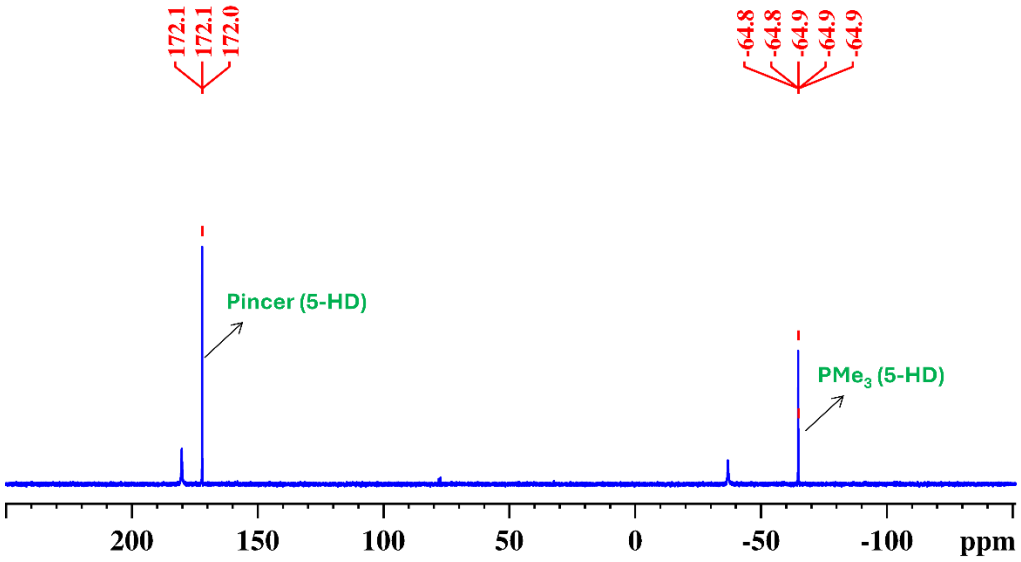


**Figure S51C**. $^{31}P\{^{1}H\}$ NMR (202.4 MHz, $CH_2Cl_2$+$CD_2Cl_2$, 213 K) spectrum of [Ir(H)($\eta^2$-HD)($PMe_3$)($^{tBu4}$POCOP)][$BAr^F_4$] (**5-HD**), formed upon purging HD gas through a solution of [Ir(H)($PMe_3$)($^{tBu4}$POCOP)][$BAr^F_4$] (**3**). For acquiring $^{1}H$ and $^{31}P\{^{1}H\}$ NMR spectral data of complex **5-HD**, 0.2 mL of $CD_2Cl_2$ was added to the same sample under HD gas.

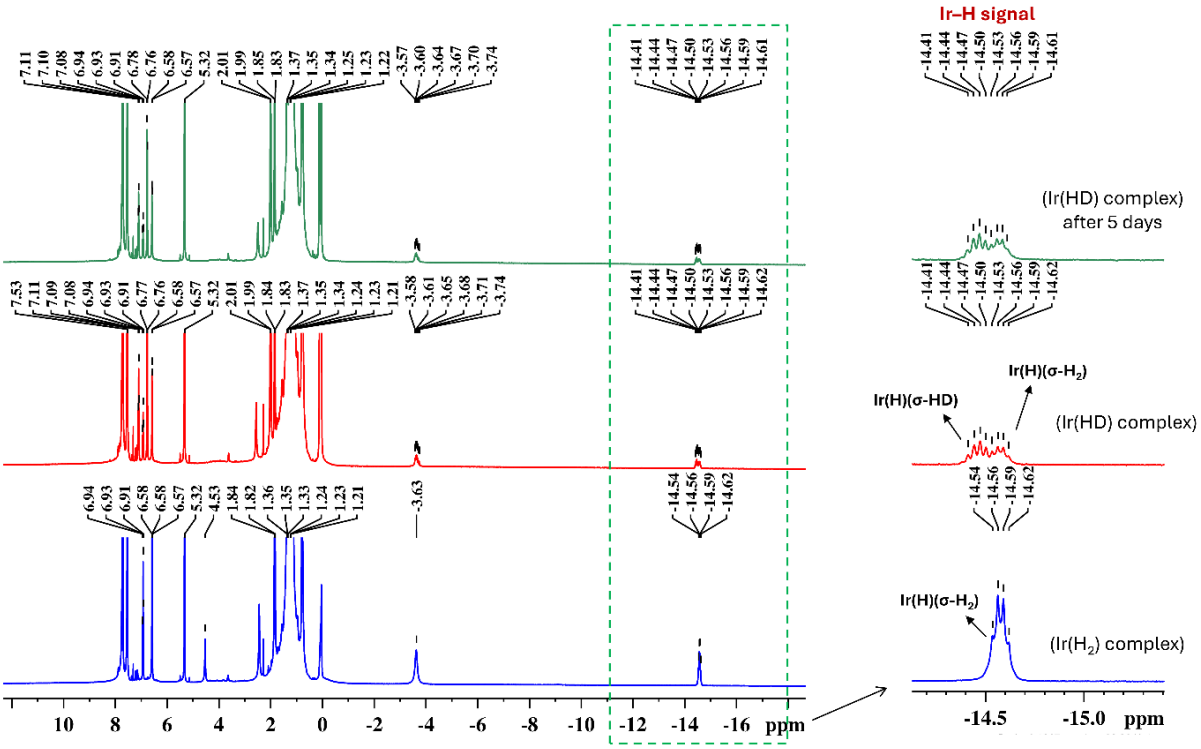


**Figure S52.** $^{1}$H NMR (500.0 MHz, $CD_2Cl_2$, 213 K) spectral stack plot of [Ir(H)($\eta^2$-$H_2$)($PMe_3$)($^{tBu4}$POCOP)][$BAr^F{}_4$] (**5**) (spectrum shown in blue color), [Ir(H)($\eta^2$-HD)($PMe_3$)($^{tBu4}$POCOP)][$BAr^F{}_4$] (**5-HD**) (spectrum shown in red color), formed upon purging HD gas through a solution of [Ir(H)($PMe_3$)($^{tBu4}$POCOP)][$BAr^F{}_4$] (**3**), and [Ir(H)($\eta^2$-HD)($PMe_3$)($^{tBu4}$POCOP)][$BAr^F{}_4$] (**5-HD**) after 5 days.

## 6. Reaction of [Ir(H)(PMe$_3$)($^{tBu4}$POCOP)][BAr$^F_4$] (**3**) with H$_3$B·THF at 298 K.

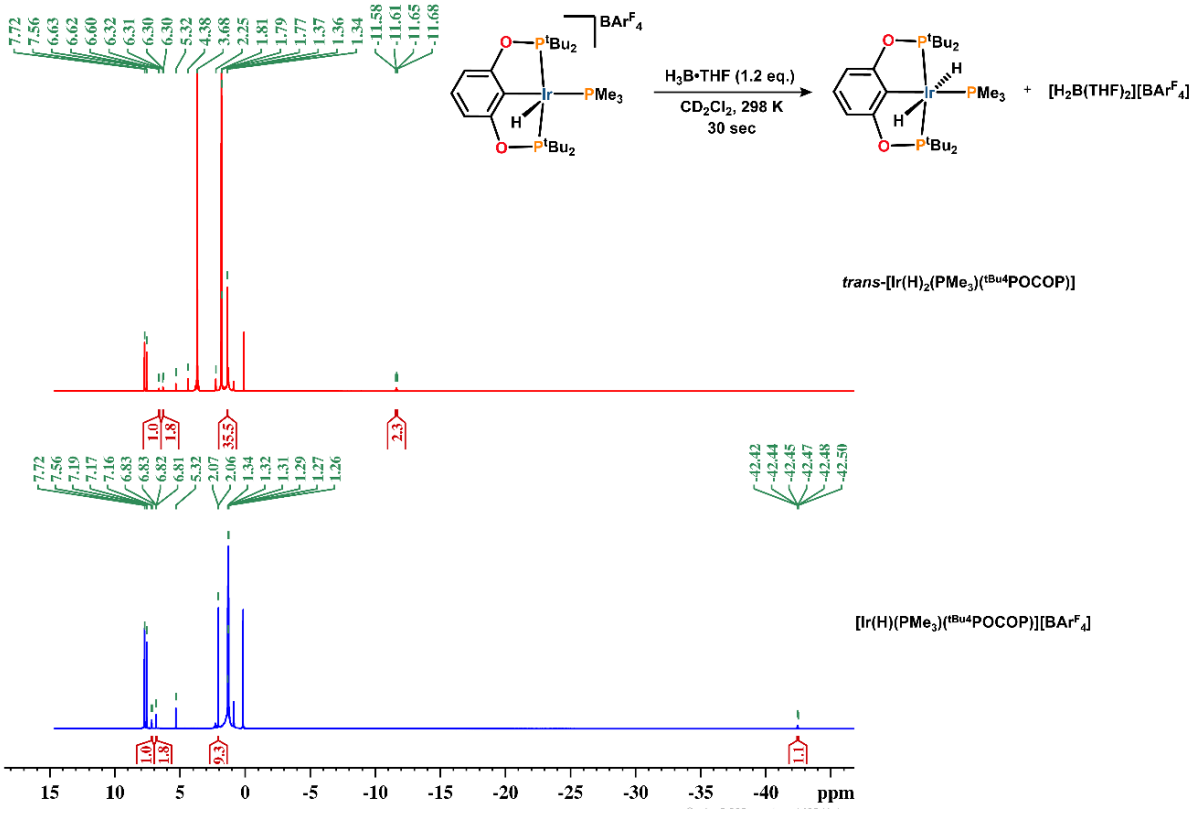


**Figure S53.** $^1$H NMR (500.0 MHz, $CD_2Cl_2$) spectral stack plot of reaction of [Ir(H)(PMe$_3$)($^{tBu}$POCOP)][BAr$^F_4$] (**3**) (spectrum shown in blue color) with H$_3$B·THF (1.2 equiv) at 298 K: formation of trans-[Ir(H)$_2$(PMe$_3$)($^{tBu}$POCOP)] (**6**) (spectrum shown in red color) and [H$_2$B(THF)$_2$][BAr$^F_4$].

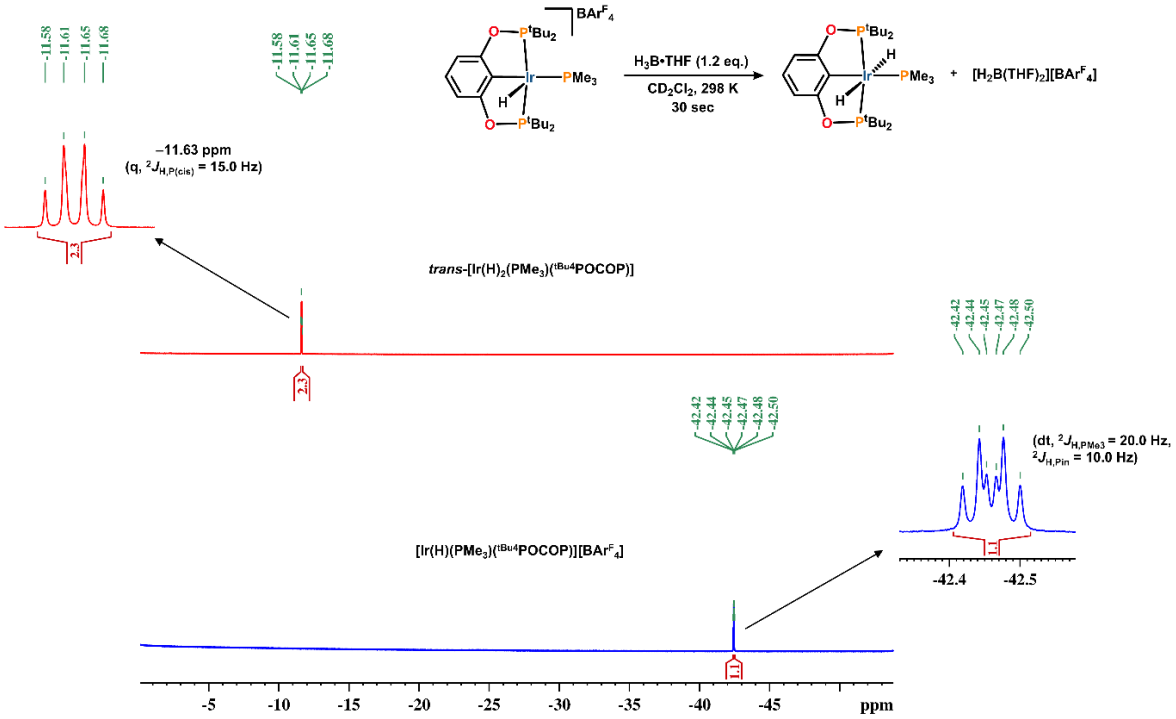


**Figure S54.** Partial $^1$H NMR (500.0 MHz, $CD_2Cl_2$) spectral stack plot (hydride region) of reaction of [Ir(H)(PMe$_3$)($^{tBu}$POCOP)][BAr$^F_4$] (**3**) (spectrum shown in blue color) with H$_3$B·THF (1.2 equiv) at 298 K: formation of trans-[Ir(H)$_2$(PMe$_3$)($^{tBu}$POCOP)] (**6**) (spectrum shown in red color) and [H$_2$B(THF)$_2$][BAr$^F_4$].

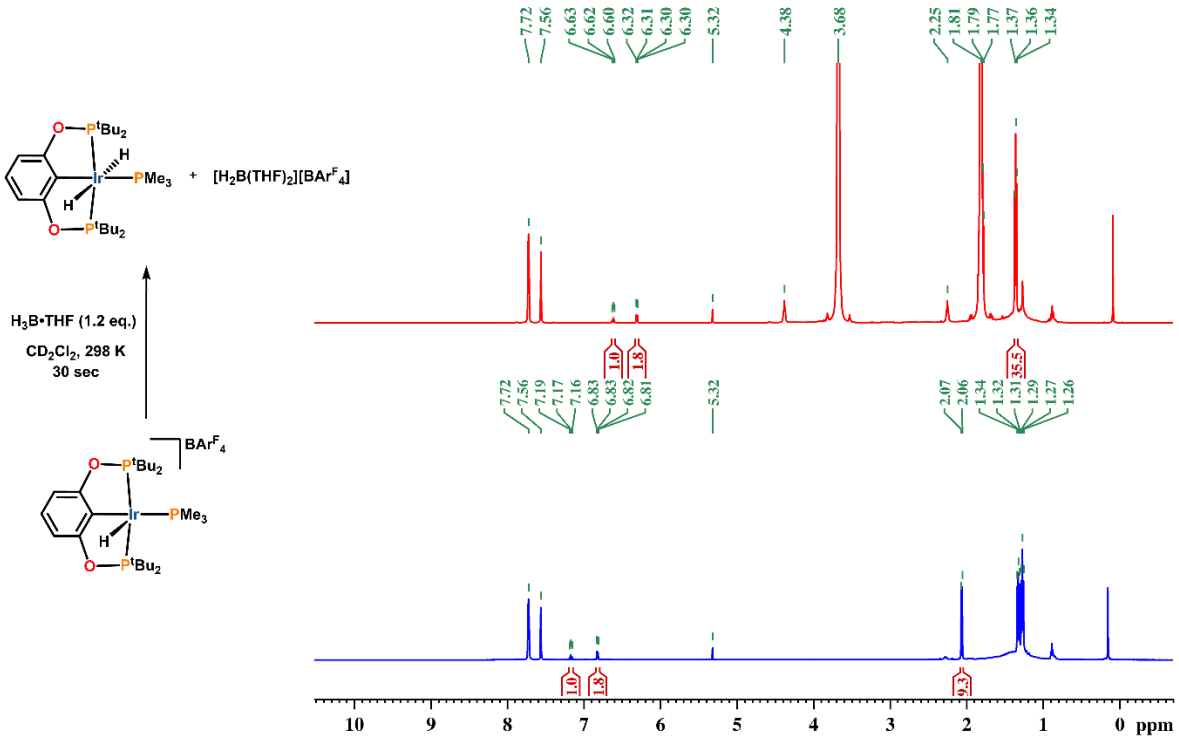


**Figure S55.** Partial $^{1}$H NMR (500.0 MHz, $CD_2Cl_2$) spectral stack plot (downfield region) of reaction of [Ir(H)(PMe$_3$)($^{tBu}$POCOP)][BAr$^F_4$] (**3**) (spectrum shown in blue color) with $H_3B{\cdot}THF$ (1.2 equiv) at 298 K: formation of trans-[Ir(H)$_2$(PMe$_3$)($^{tBu}$POCOP)] (**6**) (spectrum shown in red color) and [$H_2B(THF)_2$][BAr$^F_4$].

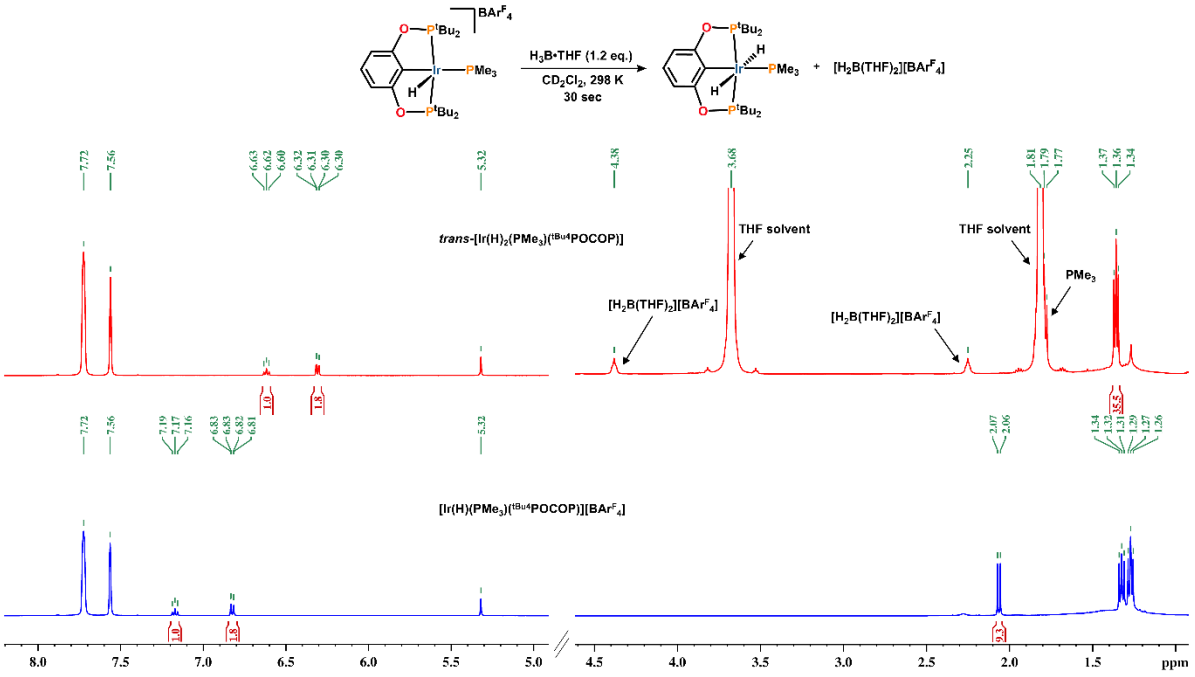


**Figure S56.** Partial $^{1}$H NMR (500.0 MHz, $CD_2Cl_2$) spectral stack plot (expanded downfield region) of reaction of [Ir(H)(PMe$_3$)($^{tBu}$POCOP)][BAr$^F_4$] (**3**) (spectrum shown in blue color) with $H_3B{\cdot}THF$ (1.2 equiv) at 298 K: formation of trans-[Ir(H)$_2$(PMe$_3$)($^{tBu}$POCOP)] (**6**) (spectrum shown in red color) and [$H_2B(THF)_2$][BAr$^F_4$].

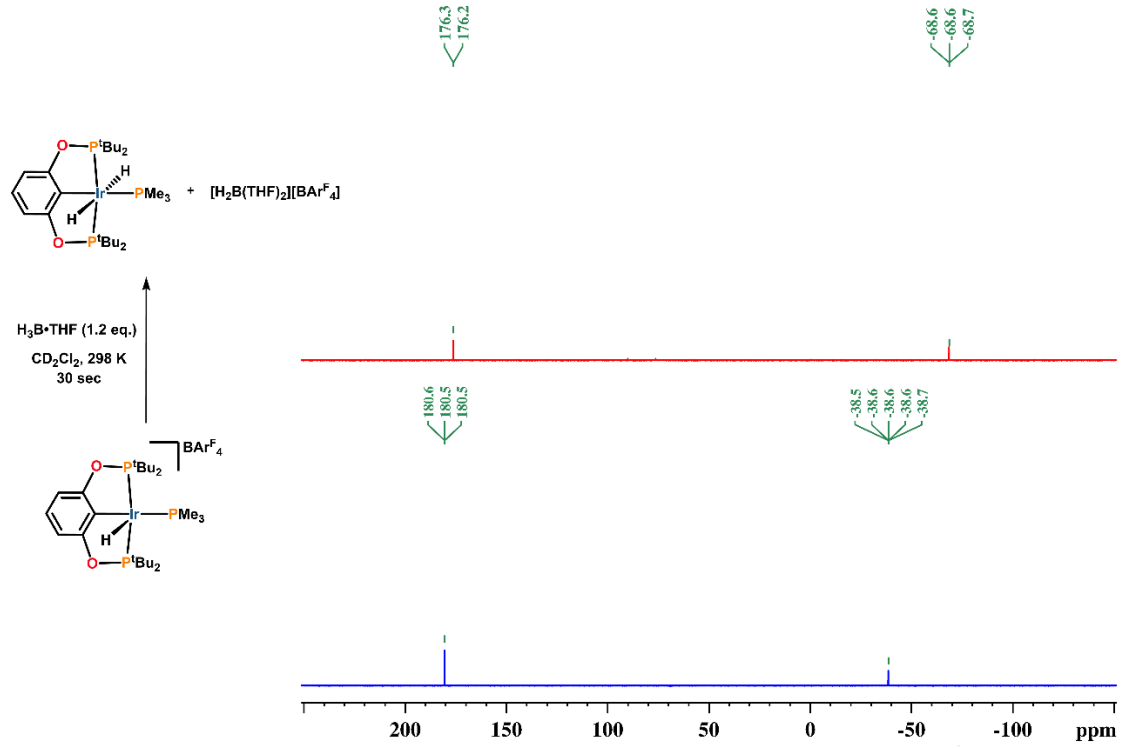


**Figure S57.** $^{31}P\{^{1}H\}$ NMR (161.9 MHz, $CD_2Cl_2$) spectral stack plot of reaction of [Ir(H)($PMe_3$)($^{tBu}$POCOP)][$BAr^F_4$] (**3**) (spectrum shown in blue color) with $H_3B{\cdot}THF$ (1.2 equiv) at 298 K: formation of trans-[Ir(H)$_2$($PMe_3$)($^{tBu}$POCOP)] (**6**) (spectrum shown in red color) and [$H_2B(THF)_2$][$BAr^F_4$].

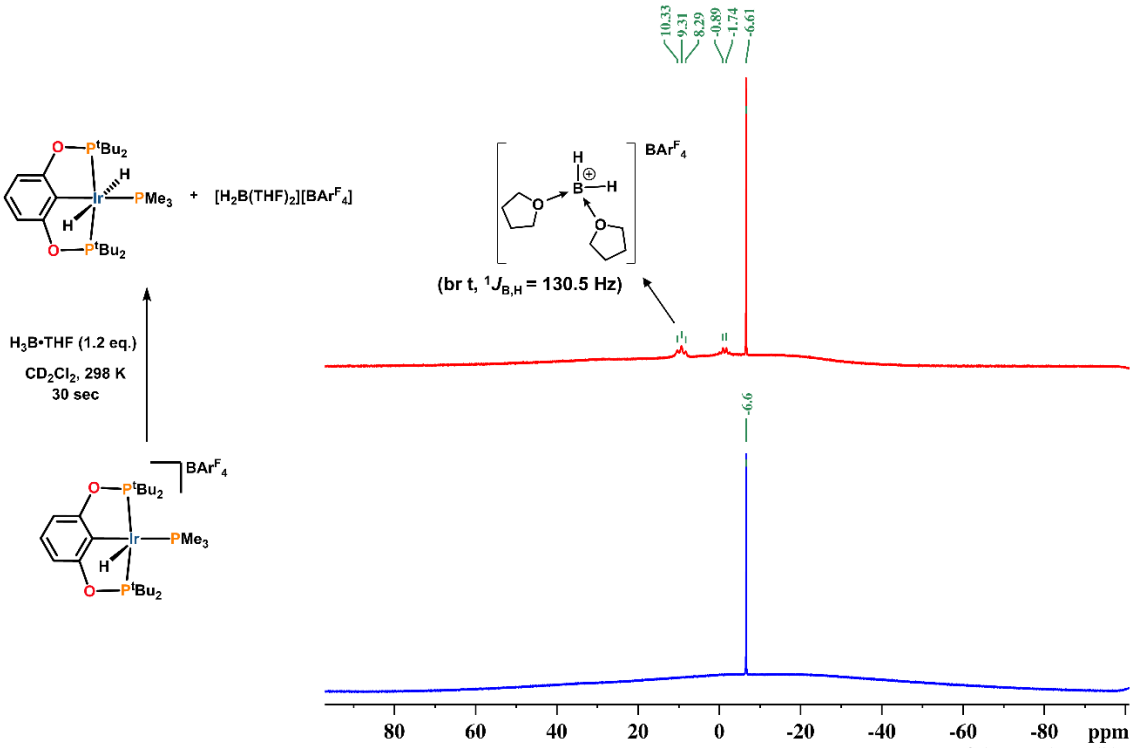


**Figure S58.** $^{11}B$ NMR (128.3 MHz, $CD_2Cl_2$) spectral stack plot of reaction of [Ir(H)($PMe_3$)($^{tBu}$POCOP)][$BAr^F_4$] (**3**) (spectrum shown in blue color) with $H_3B{\cdot}THF$ (1.2 equiv) at 298 K: formation of trans-[Ir(H)$_2$($PMe_3$)($^{tBu}$POCOP)] (**6**) (spectrum shown in red color) and [$H_2B(THF)_2$][$BAr^F_4$].

The quartet at –1.3 ppm corresponds to unreacted $H_3B{\cdot}THF$.

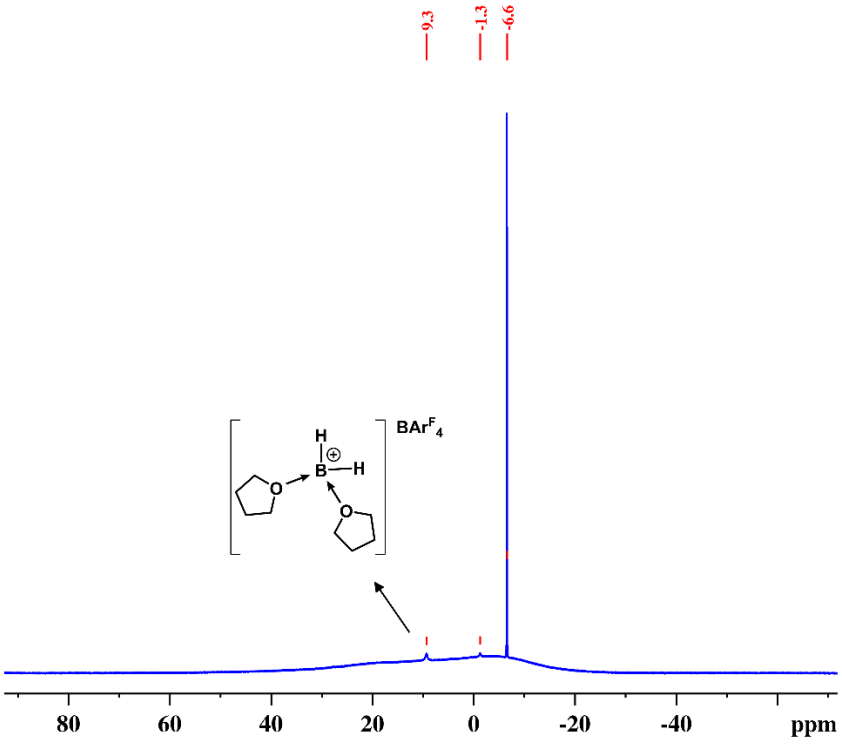


**Figure S59.** $^{11}B\{^1H\}$ NMR (160.4 MHz, $CD_2Cl_2$) spectrum of the reaction mixture of trans-[Ir(H)$_2$(PMe$_3$)($^{tBu}$POCOP)] (**6**) and [H$_2$B(THF)$_2$][BAr$^F_4$].

The broad singlet at –1.3 ppm corresponds to unreacted $H_3B$·THF.

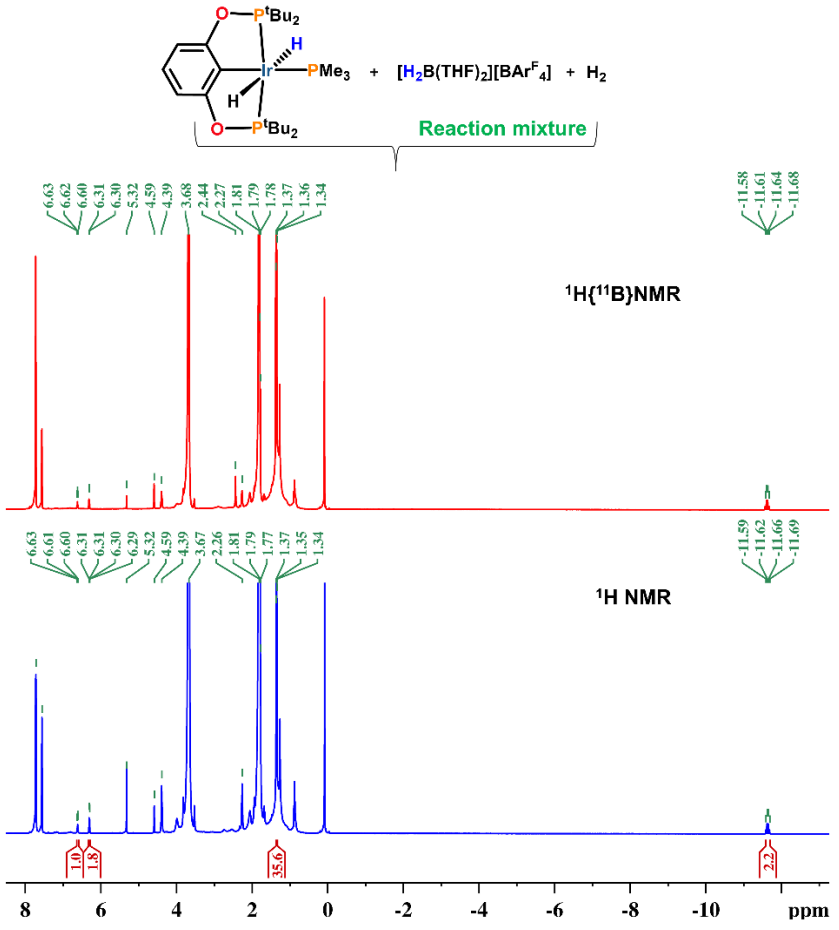

**Figure S60.** $^{1}H$ (spectrum shown in blue color) and $^{1}H\{^{11}B\}$ (spectrum shown in red color) NMR (500.0 MHz, $CD_2Cl_2$) spectral stack plot of the reaction mixture of *trans*-[Ir(H)$_2$(PMe$_3$)($^{tBu}$POCOP)] (**6**), [$H_2B(THF)_2$][$BAr^F_4$], and $H_2$.

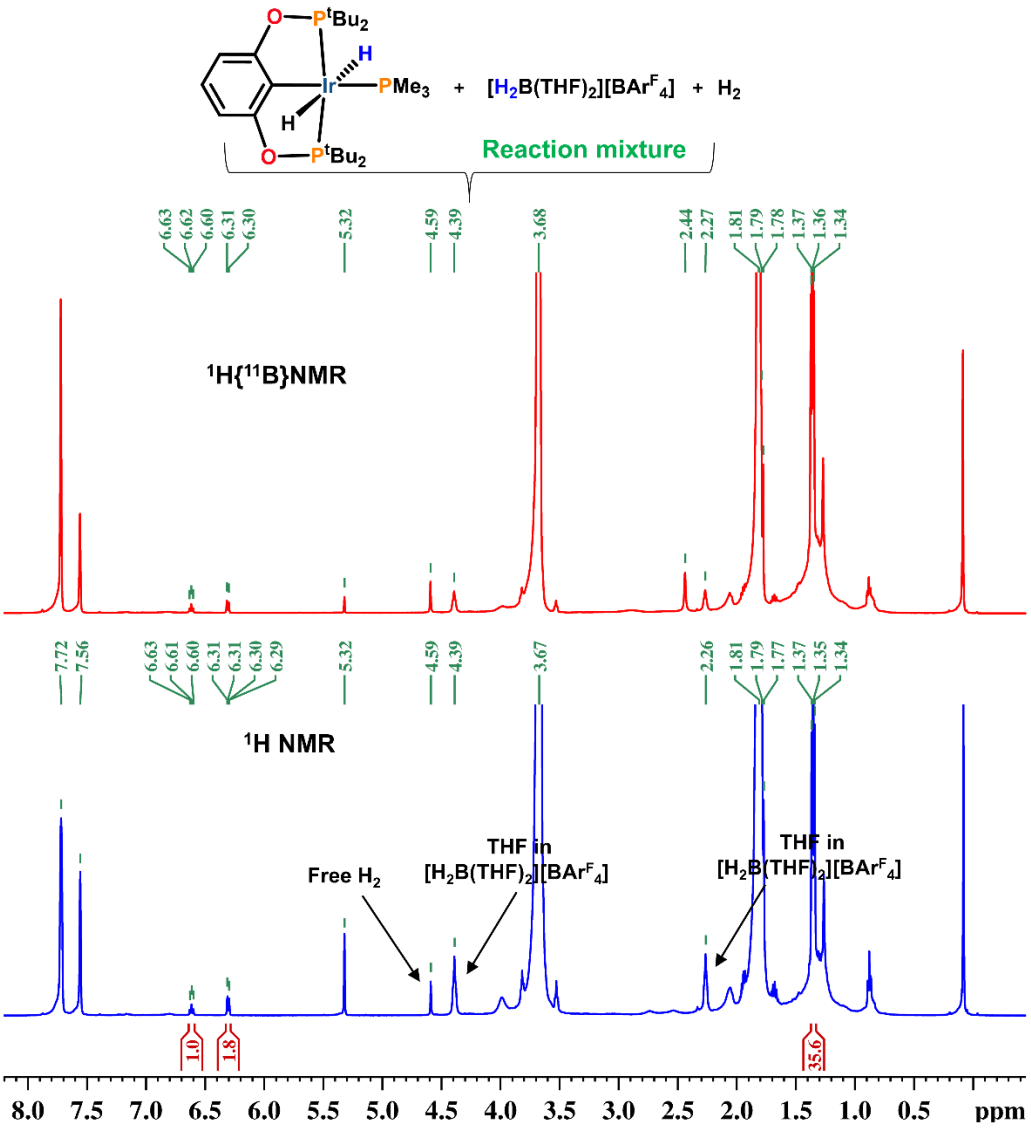


**Figure S61.** Partial $^{1}H$ (spectrum shown in blue color) and $^{1}H\{^{11}B\}$ (spectrum shown in red color) NMR (500.0 MHz, $CD_2Cl_2$) spectral stack plot (downfield region) of the reaction mixture of *trans*-[Ir(H)$_2$(PMe$_3$)($^{tBu}$POCOP)] (**6**), [$H_2B(THF)_2$][$BAr^F_4$], and $H_2$.

Signals corresponding to free $H_2$ and THF in [$H_2B(THF)_2$][$BAr^F_4$] adduct are shown in the $^{1}H$ NMR spectrum (spectrum shown in blue color).

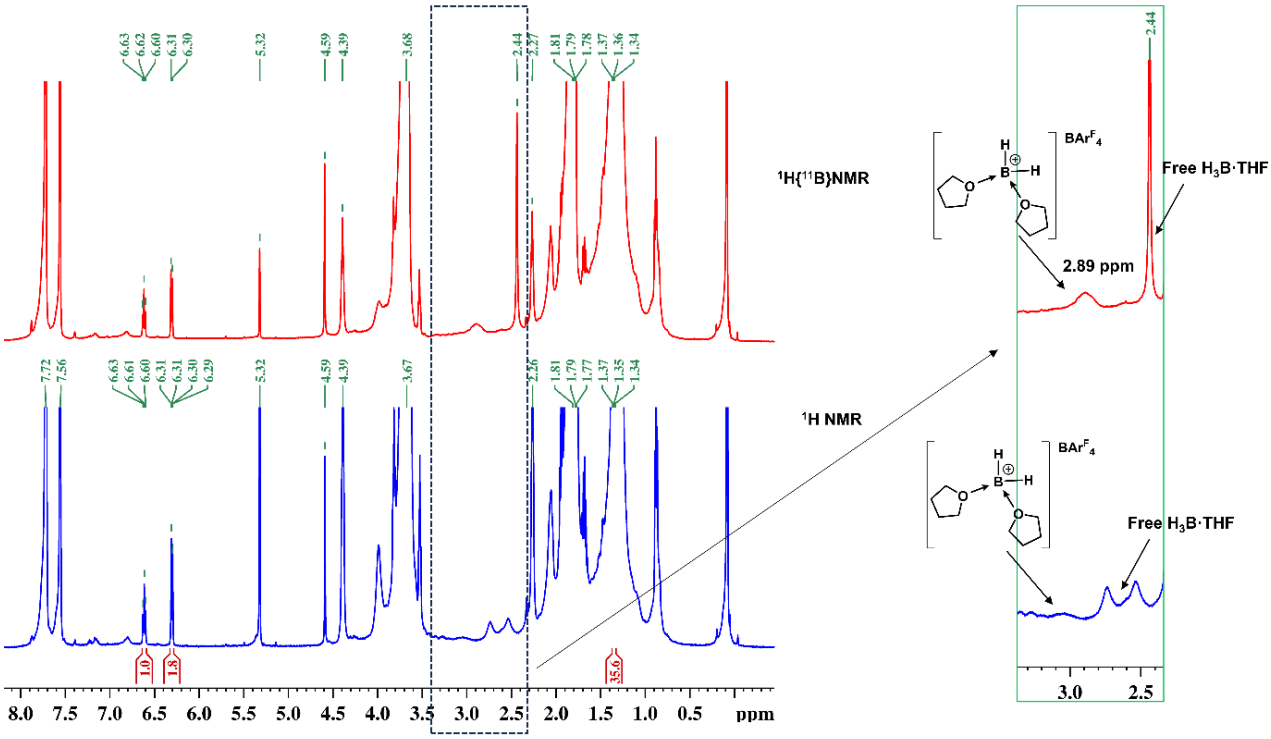


**Figure S62.** Partial $^1H$ (spectrum shown in blue color) and $^1H\{^{11}B\}$ (spectrum shown in red color) NMR (500.0 MHz, $CD_2Cl_2$) spectral stack plot (enlarged downfield region) of the reaction mixture of *trans*-[Ir(H)$_2$(PMe$_3$)($^{tBu}$POCOP)] (**6**), [$H_2B(THF)_2$][$BAr^F_4$], and $H_2$.

Unreacted $H_3B{\cdot}THF$ shows a quartet at 2.40 ppm in the $^1H$ NMR spectrum (spectrum shown in blue color). Half of the quartet overlaps with the solvent signal. Upon $^{11}B$ decoupling, it appears as a sharp signal at 2.44 ppm in the $^1H\{^{11}B\}$ NMR (spectrum shown in red color). The quartet of [$H_2B(THF)_2$][$BAr^F_4$] adduct overlaps with that of free $H_3B{\cdot}THF$, as seen in the $^1H$ NMR spectrum (spectrum in blue color). Upon $^{11}B$ decoupling, it appears as a sharp signal at 2.89 ppm in the $^1H\{^{11}B\}$ NMR spectrum (spectrum shown in red color).

## 7. Monitoring the reaction of [Ir(H)(PMe$_3$)($^{tBu4}$POCOP)][BAr$^F_4$] (**3**) with H$_3$B·THF from 178 to 298 K. (Pre-cooled probe experiment)

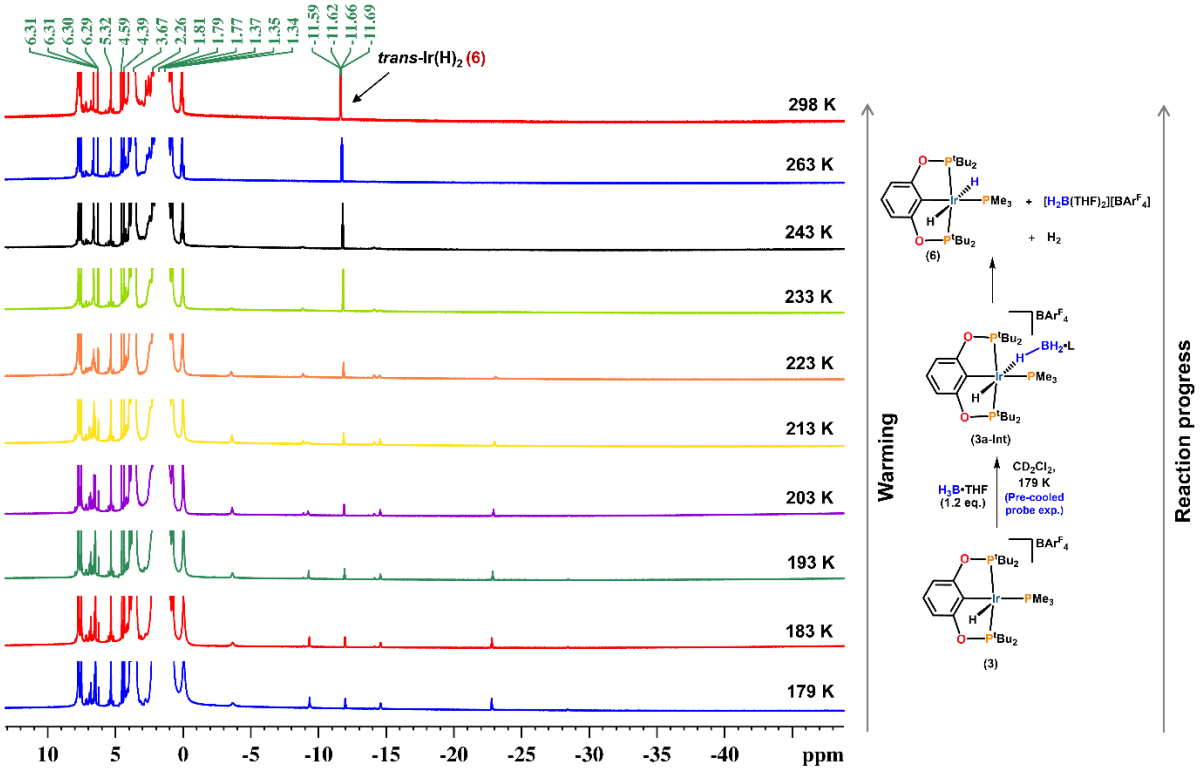


**Figure S63.** VT $^1$H NMR (500.0 MHz, $CD_2Cl_2$) spectral stack plot of monitoring of the reaction of [Ir(H)(PMe$_3$)($^{tBu}$POCOP)][BAr$^F_4$] (**3**) with H$_3$B·THF from 179 to 298 K.

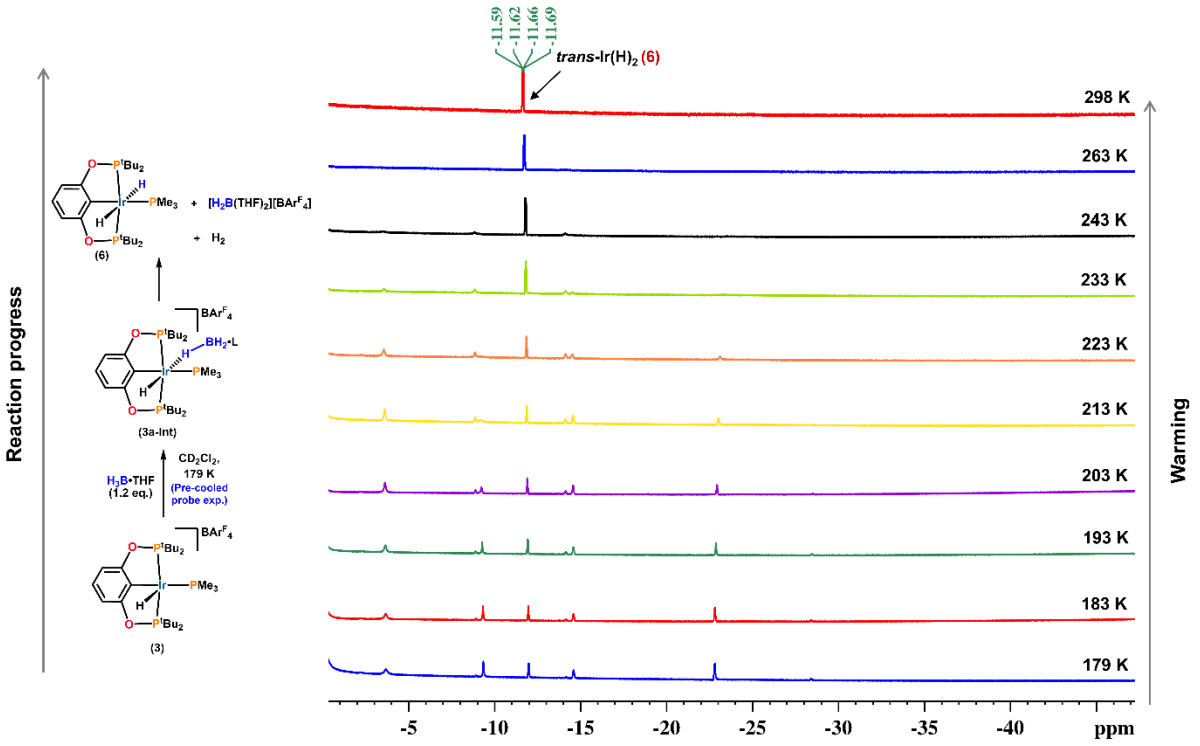


**Figure S64.** Partial VT $^1$H NMR (500.0 MHz, $CD_2Cl_2$) spectral stack plot (hydride region) of monitoring of the reaction of [Ir(H)(PMe$_3$)($^{tBu}$POCOP)][BAr$^F_4$] (**3**) with H$_3$B·THF from 179 to 298 K.

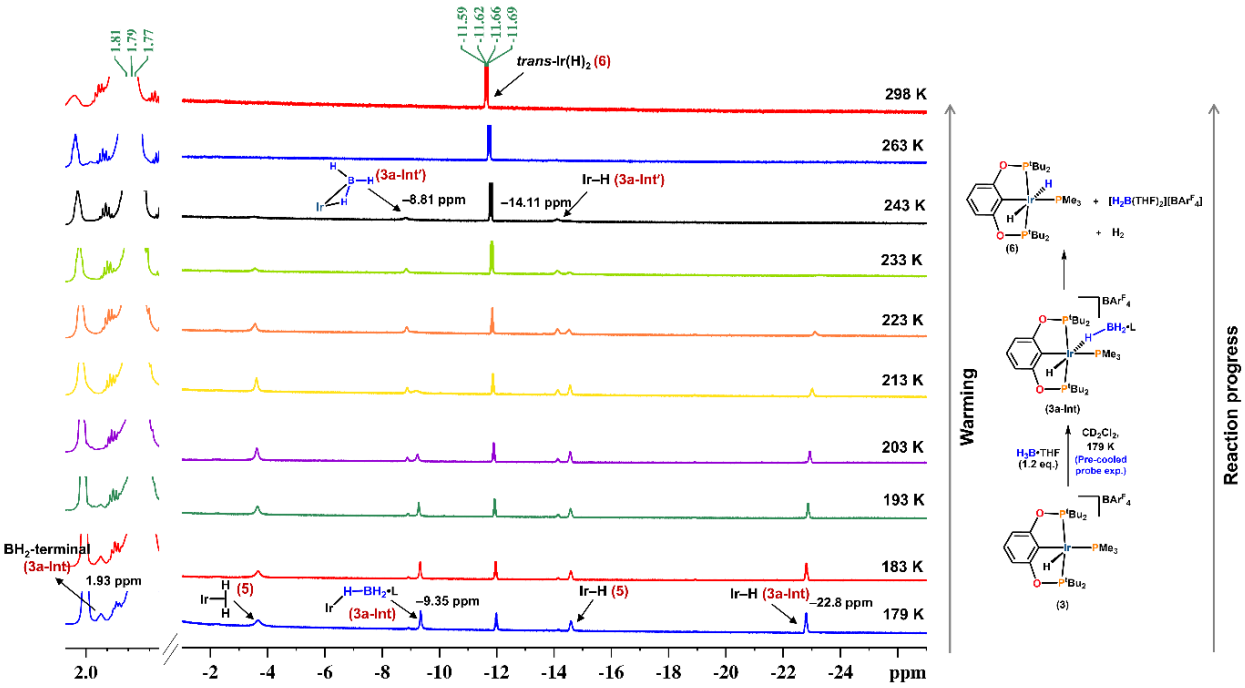


**Figure S65.** Partial VT $^{1}$H NMR (500.0 MHz, $CD_2Cl_2$) spectral stack plot of monitoring of the reaction of [Ir(H)($PMe_3$)($^{tBu}$POCOP)][$BAr^F_4$] (**3**) with $H_3B{\cdot}THF$ from 179 to 298 K.

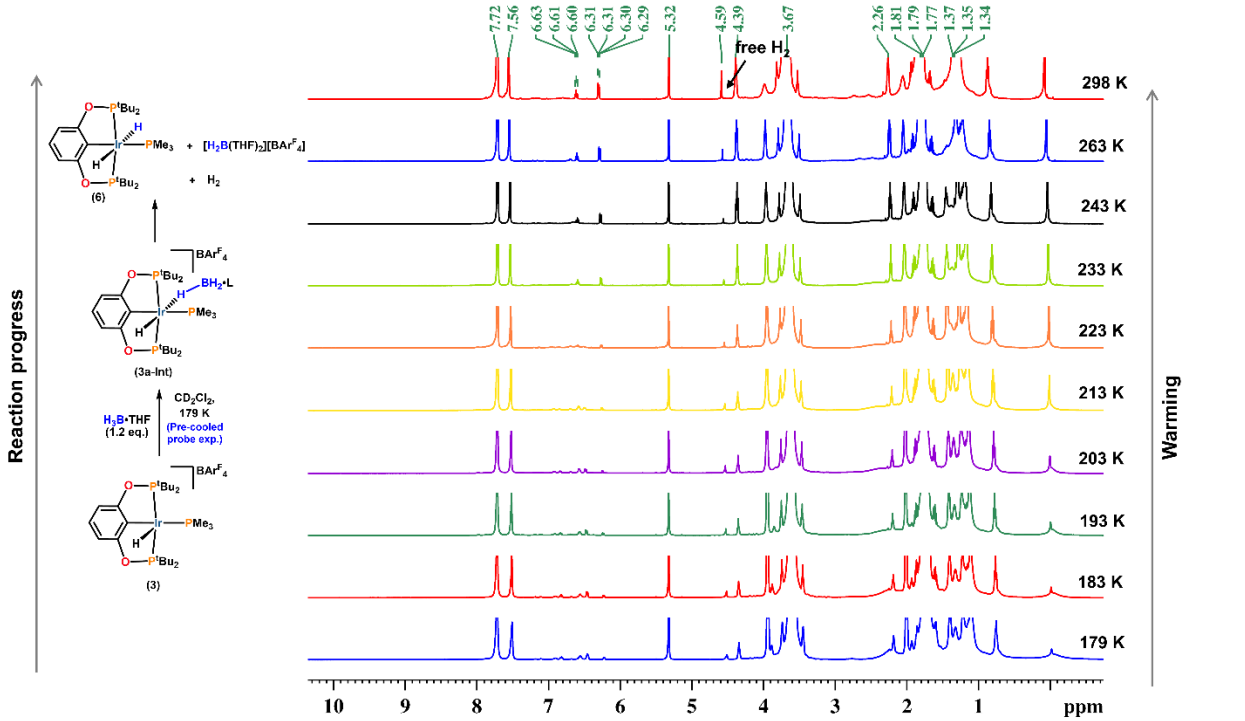


**Figure S66.** Partial VT $^{1}$H NMR (500.0 MHz, $CD_2Cl_2$) spectral stack plot (downfield region) of monitoring of the reaction of [Ir(H)($PMe_3$)($^{tBu}$POCOP)][$BAr^F_4$] (**3**) with $H_3B{\cdot}THF$ from 179 to 298 K.

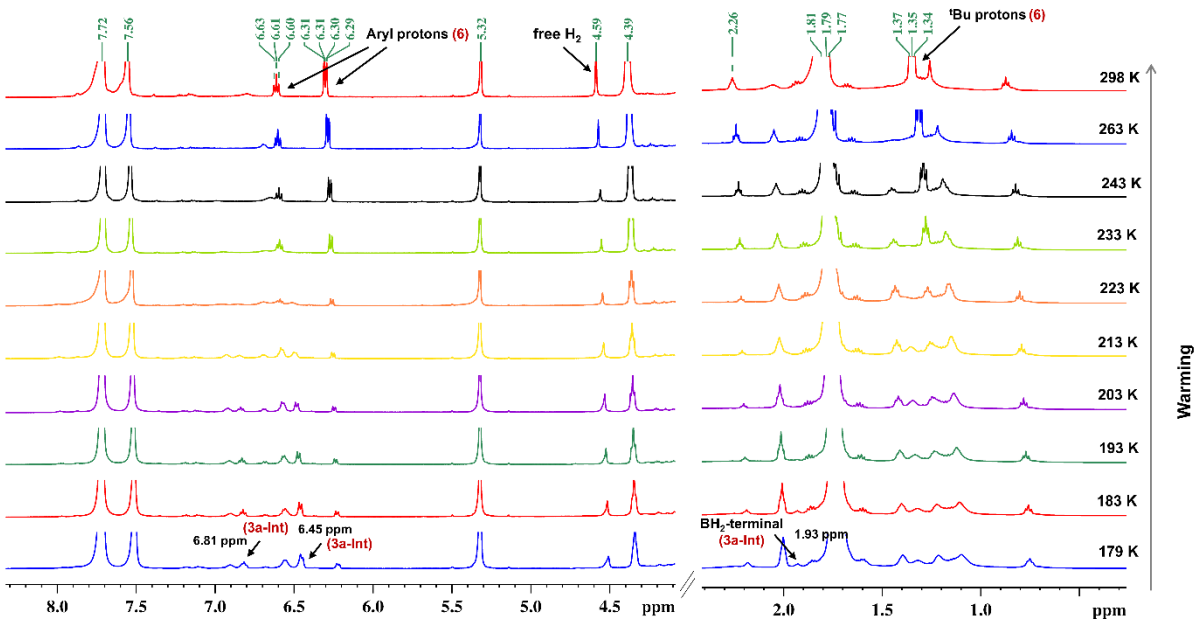


**Figure S67.** Partial VT $^{1}$H NMR (500.0 MHz, $CD_2Cl_2$) spectral stack plot (expanded downfield region) of monitoring of the reaction of [Ir(H)($PMe_3$)($^{tBu}$POCOP)][$BAr^F_4$] (**3**) with $H_3B{\cdot}THF$ from 179 to 298 K.

The protons corresponding to the $^{t}$Bu groups of the intermediate species could not be assigned due to signal broadening and overlap. However, the peak corresponding to complex **6** was clearly assigned.

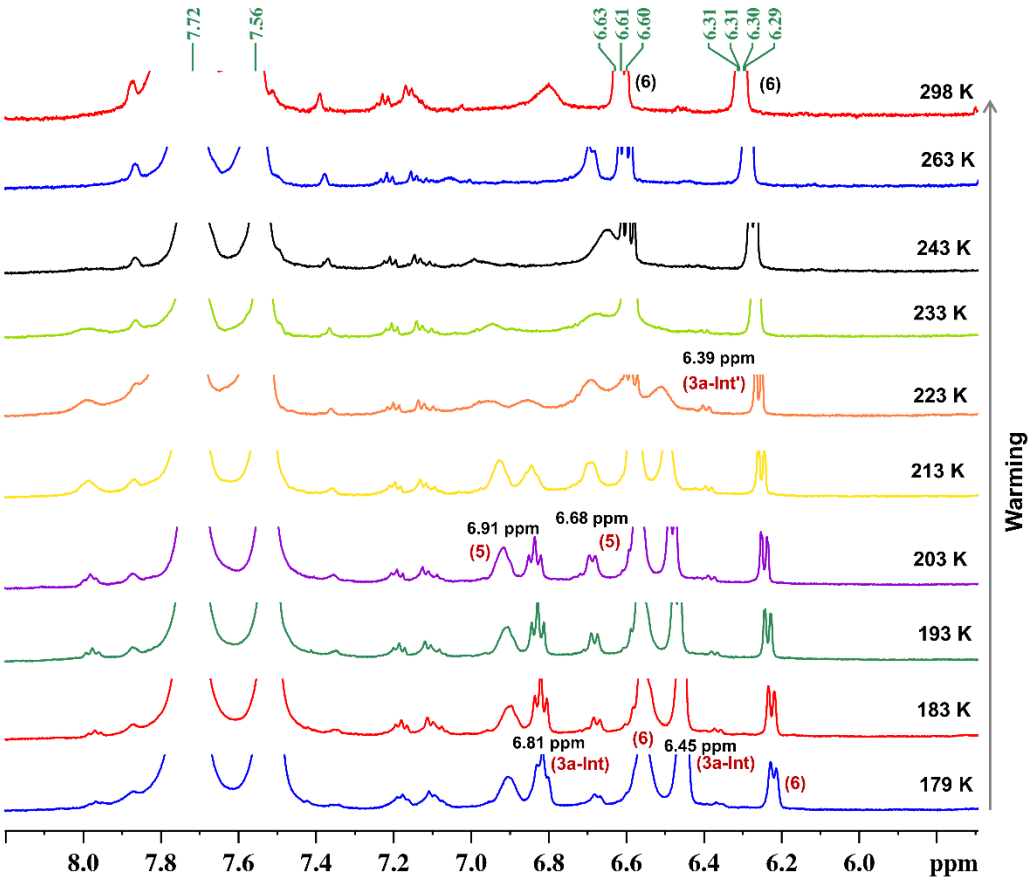


**Figure S68.** Partial VT $^{1}$H NMR (500.0 MHz, $CD_2Cl_2$) spectral stack plot (expanded aryl region) of monitoring of the reaction of [Ir(H)($PMe_3$)($^{tBu}$POCOP)][$BAr^F_4$] (**3**) with $H_3B{\cdot}THF$ from 179 to 298 K.

Only one of the aryl peaks corresponding to complex **3a-Int'** is shown**.** The other aryl peak could not be assigned due to overlapping with the aryl peaks of other intermediate complexes.

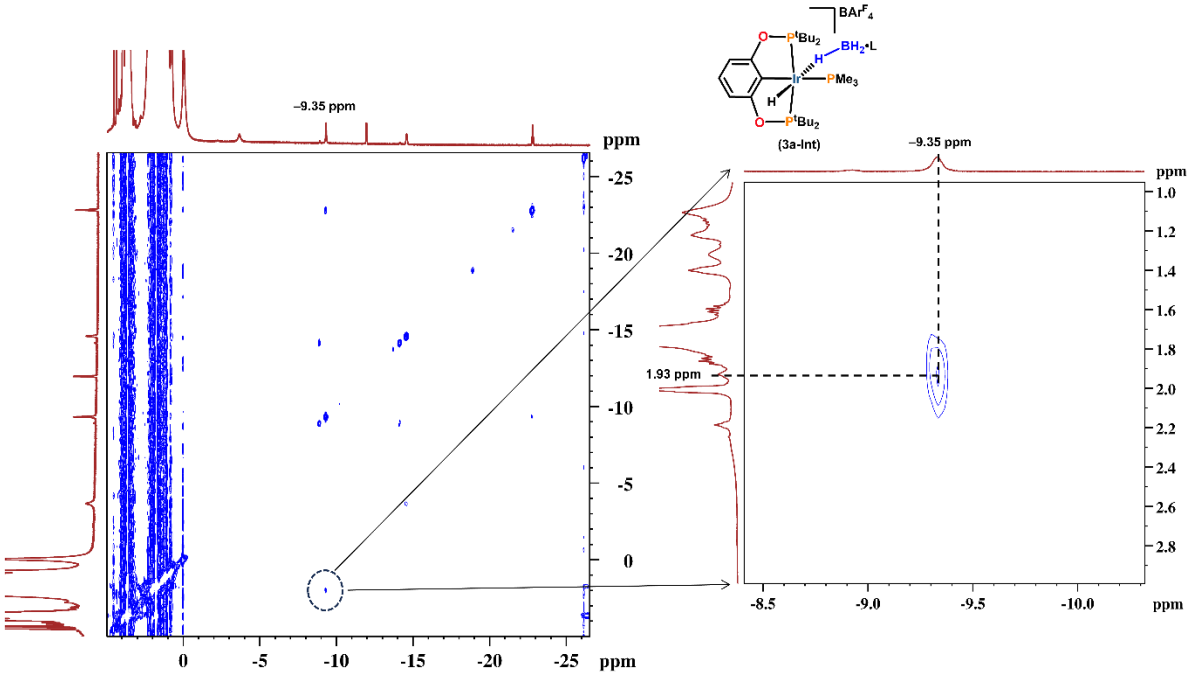


**Figure S69.** $^{1}$H-$^{1}$H COSY (500.0 MHz, $CD_2Cl_2$, 179 K) spectrum of *trans*-[Ir(H)($\eta^1$-$HBH_2$·THF)$PMe_3$($^{tBu4}$POCOP)][$BAr^F_4$] complex (**3a-Int**). The signal at −9.35 ppm correlated with an off-diagonal cross peak at 1.93 ppm.

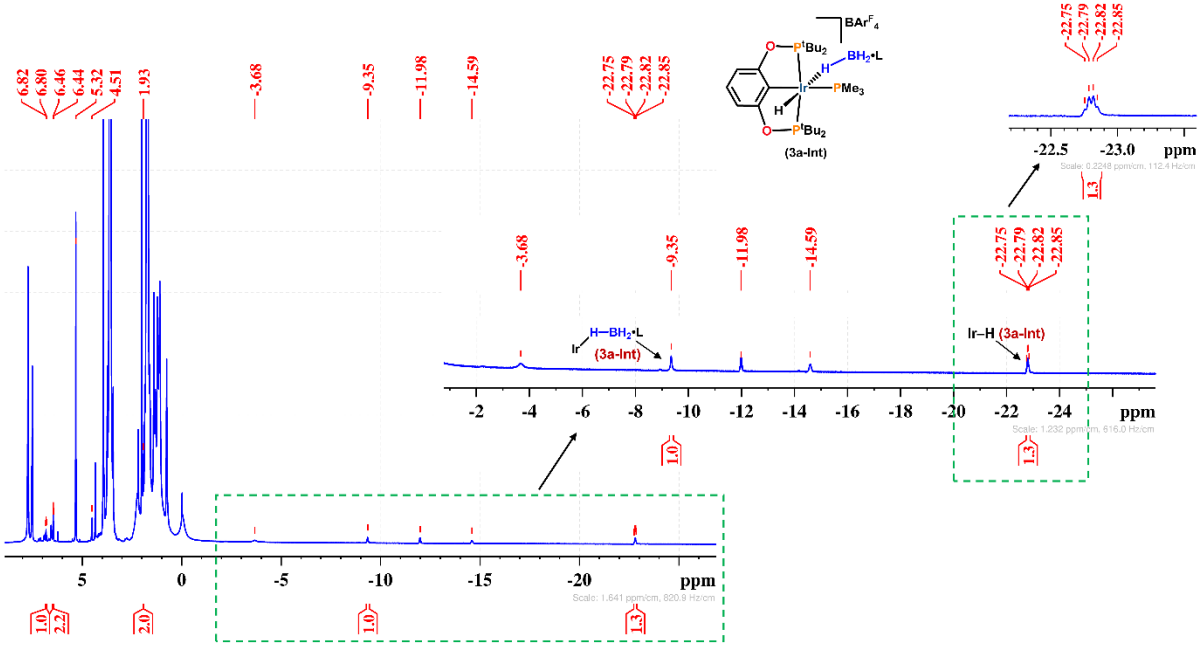


**Figure S70.** $^{1}$H NMR (500, $CD_2Cl_2$) spectrum of the reaction mixture after adding $H_3B$·THF to [Ir(H)($PMe_3$)($^{tBu}$POCOP)][$BAr^F_4$] (**3**) at 179 K: formation of mixture of products, *trans*-[Ir(H)($\eta^1$-$HBH_2$·THF)$PMe_3$($^{tBu4}$POCOP)][$BAr^F_4$] (**3a-Int**), *trans*-[Ir(H)$_2$($PMe_3$)($^{tBu}$POCOP)] (**6**), and [Ir(H)($\eta^2$-$H_2$)($PMe_3$)($^{tBu4}$POCOP)][$BAr^F_4$] (**5**). Only the peaks corresponding to complex **3a-Int** are highlighted here.

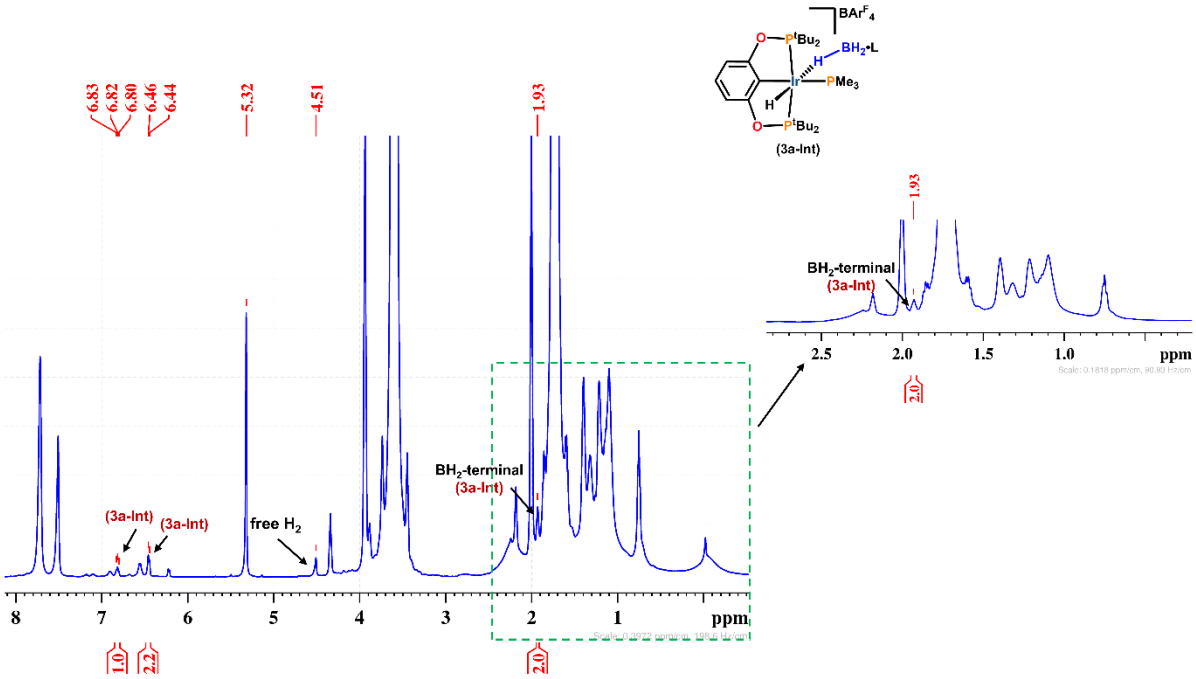


**Figure S71.** Partial $^{1}$H NMR (500, $CD_2Cl_2$) spectrum (downfield region) of the reaction mixture after adding $H_3B{\cdot}THF$ to [Ir(H)($PMe_3$)($^{tBu}$POCOP)][$BAr^F_4$] (**3**) at 179 K: formation of mixture of products, *trans*-[Ir(H)($\eta^1$-$HBH_2{\cdot}THF$)$PMe_3$($^{tBu4}$POCOP)][$BAr^F_4$] (**3a-Int**), *trans*-[Ir(H)$_2$($PMe_3$)($^{tBu}$POCOP)] (**6**), and [Ir(H)($\eta^2$-$H_2$)($PMe_3$)($^{tBu4}$POCOP)][$BAr^F_4$] (**5**). Only the peaks corresponding to complex **3a-Int** are highlighted here.

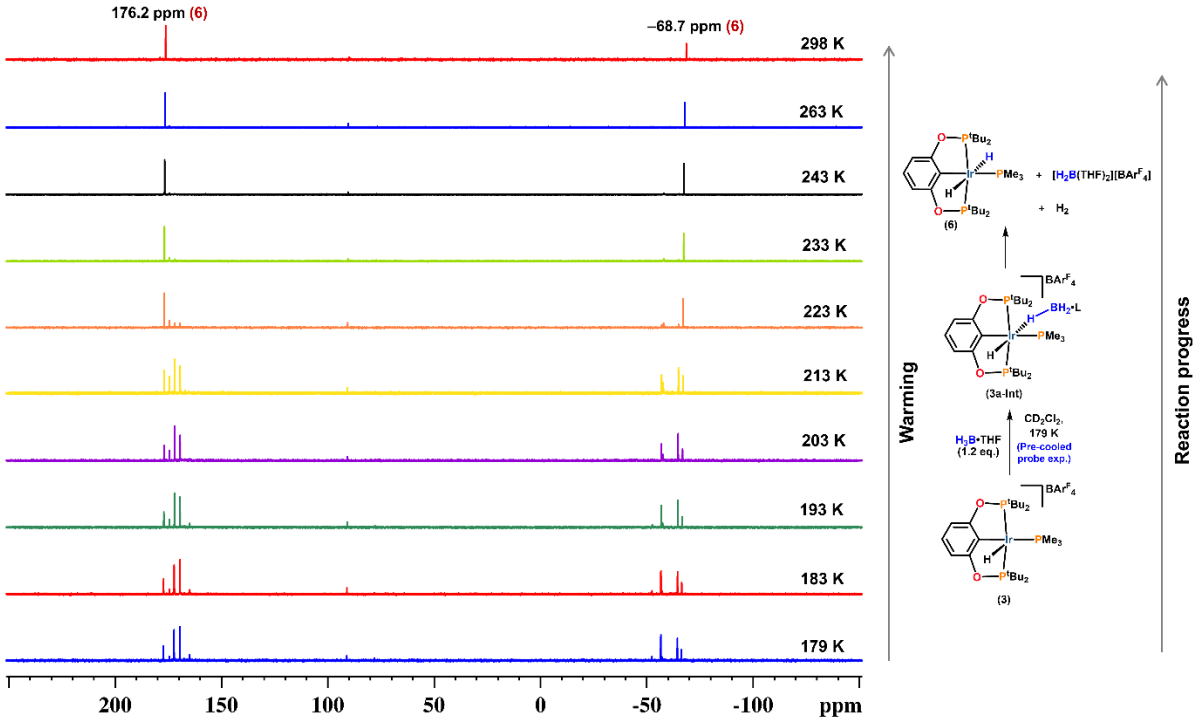


**Figure S72.** VT $^{31}P\{^{1}H\}$ NMR (202.4 MHz, $CD_2Cl_2$) spectral stack plot of the reaction of [Ir(H)($PMe_3$)($^{tBu}$POCOP)][$BAr^F_4$] (**3**) with $H_3B{\cdot}THF$ from 179 to 298 K.

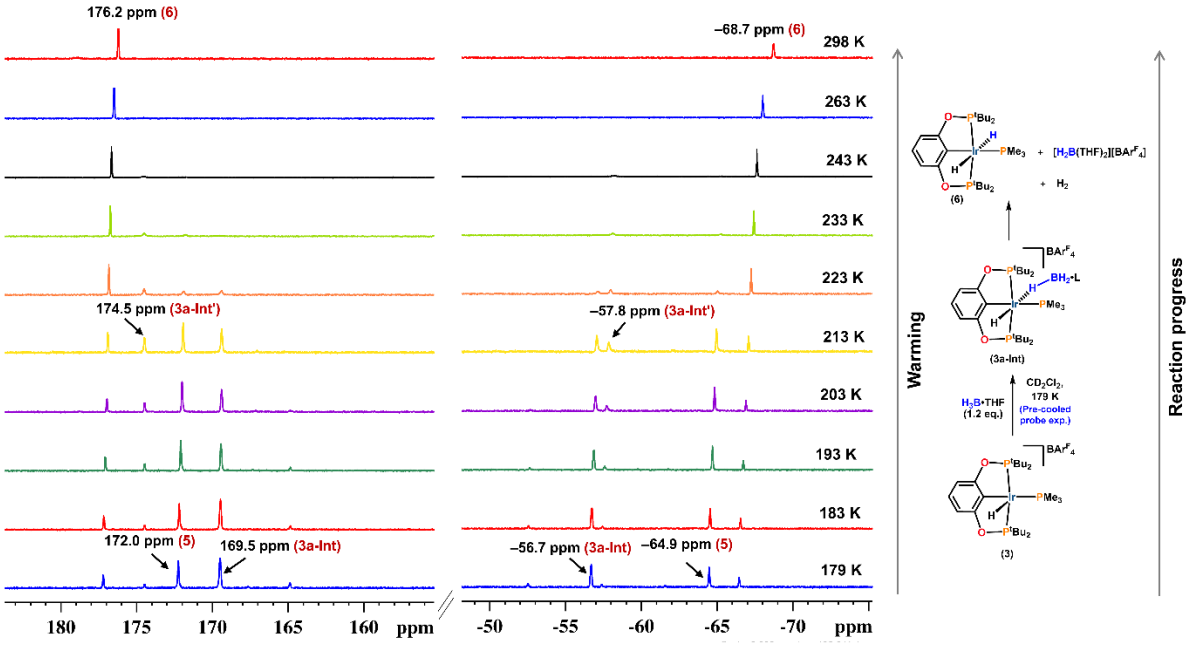


**Figure S73.** Partial VT $^{31}P\{^{1}H\}$ NMR (202.4 MHz, $CD_2Cl_2$) spectral stack plot of monitoring of the reaction of [Ir(H)($PMe_3$)($^{tBu}$POCOP)][$BAr^F_4$] (**3**) with $H_3B{\cdot}THF$ from 179 to 298 K.

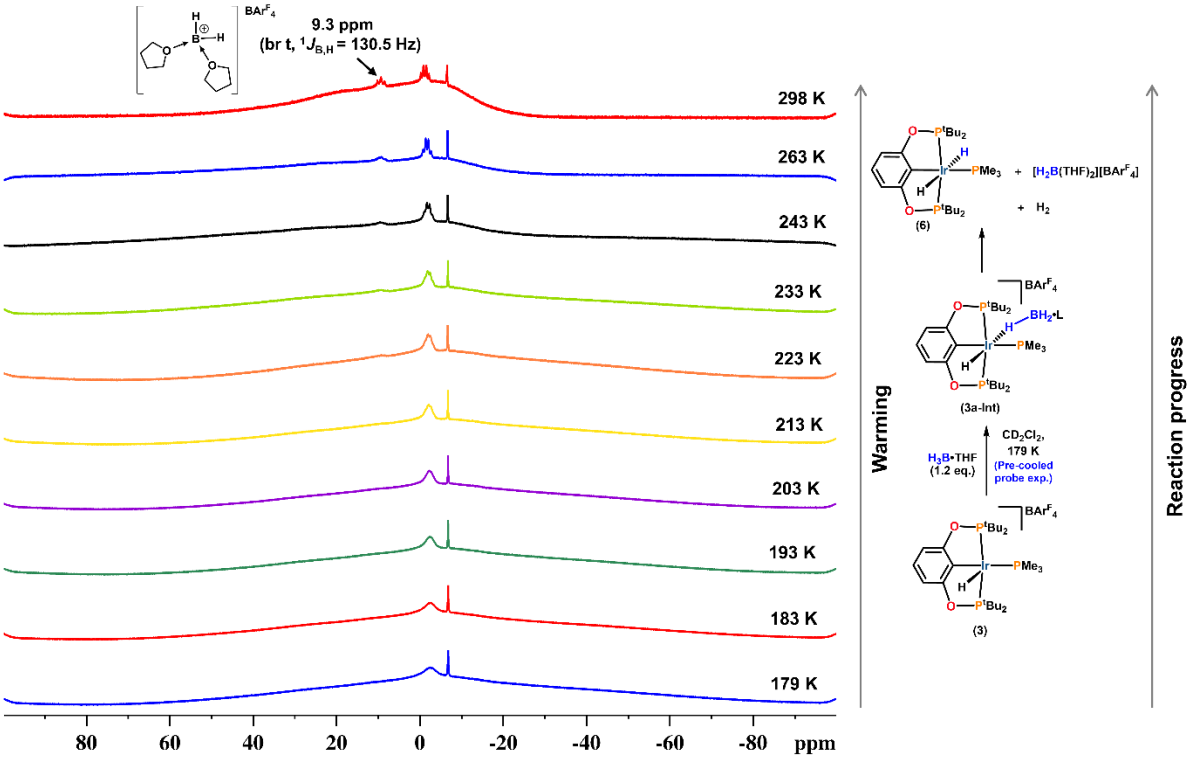


**Figure S74.** VT $^{11}B$ NMR (160.4 MHz, $CD_2Cl_2$) spectral stack plot of monitoring of the reaction of [Ir(H)($PMe_3$)($^{tBu}$POCOP)][$BAr^F_4$] (**3**) with $H_3B{\cdot}THF$ from 179 to 298 K.

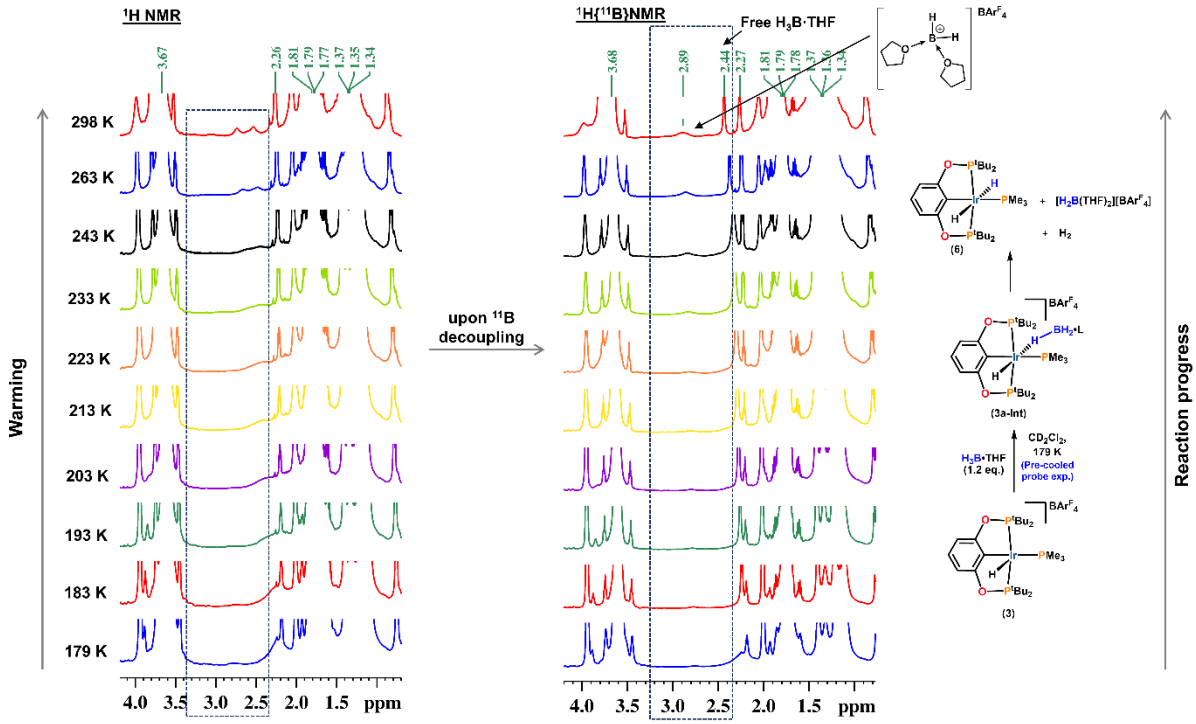


**Figure S75.** VT $^{1}H$ (left) and $^{1}H\{^{11}B\}$ (right) NMR (500, $CD_2Cl_2$) spectral stack plot of monitoring of the reaction of [Ir(H)($PMe_3$)($^{tBu}$POCOP)][$BAr^F_4$] (**3**) with $H_3B{\cdot}THF$ from 179 to 298 K.

Upon decoupling $^{11}B$ nucleus (right side spectral stack plot), a broad sharp signal appeared at 2.89 ppm for the [$H_2B(THF)_2$][$BAr^F_4$] adduct.

8. Characterization of *trans*-[Ir(H)$_2$(PMe$_3$)($^{tBu}$POCOP)] (**6**) synthesized by the reaction of [Ir(H)(PMe$_3$)($^{tBu4}$POCOP)][BAr$^F_4$] (**3**) with NaBH$_4$.

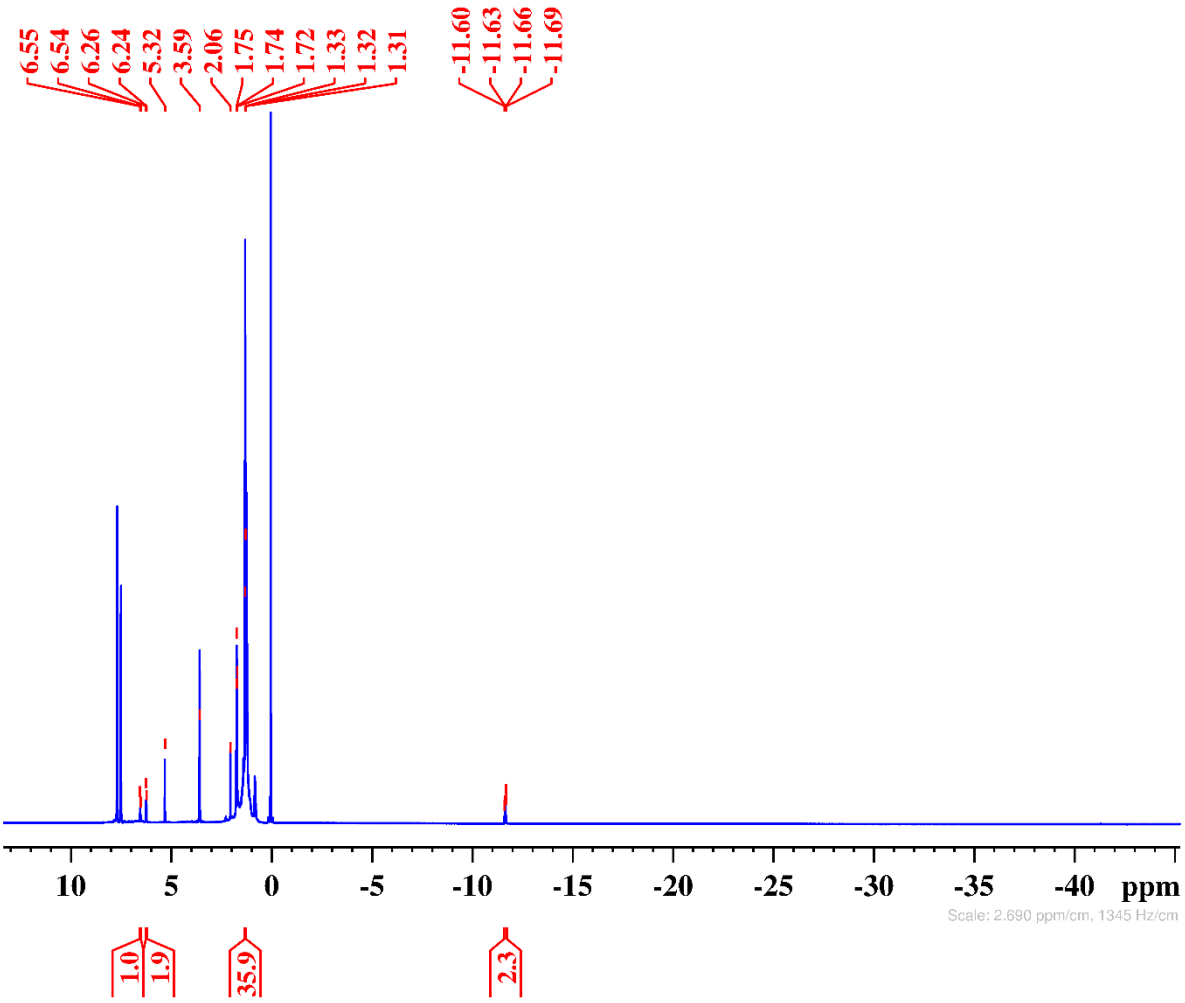


**Figure S76.** $^1$H NMR (500.0 MHz, $CD_2Cl_2$ + THF-$d_8$, 298 K) spectrum of *trans*-[Ir(H)$_2$PMe$_3$($^{tBu4}$POCOP)] (**6**) synthesized by the reaction of complex **3** with NaBH$_4$.

A signal at 2.06 ppm corresponds to the methyl protons of toluene, which was used as the solvent during the synthesis of complex **3**. Although the complex was subsequently washed with *n*-pentane and dried under vacuum, trace amounts of toluene remained in the sample.

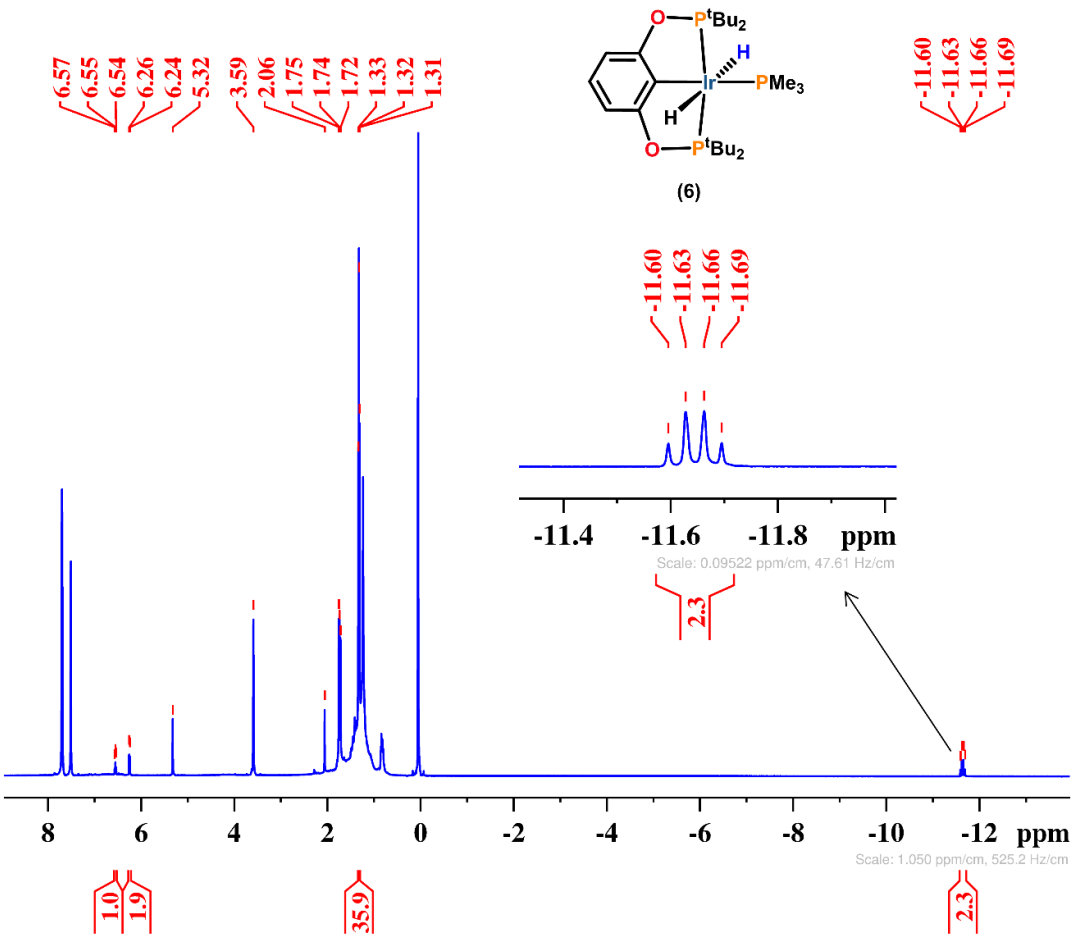


**Figure S77.** Partial $^{1}H$ NMR (500.0 MHz, $CD_2Cl_2$ + THF-$d_8$, 298 K) spectrum of *trans*-[Ir(H)$_2$PMe$_3$($^{tBu4}$POCOP)] (**6**) synthesized by the reaction of complex **3** with $NaBH_4$.

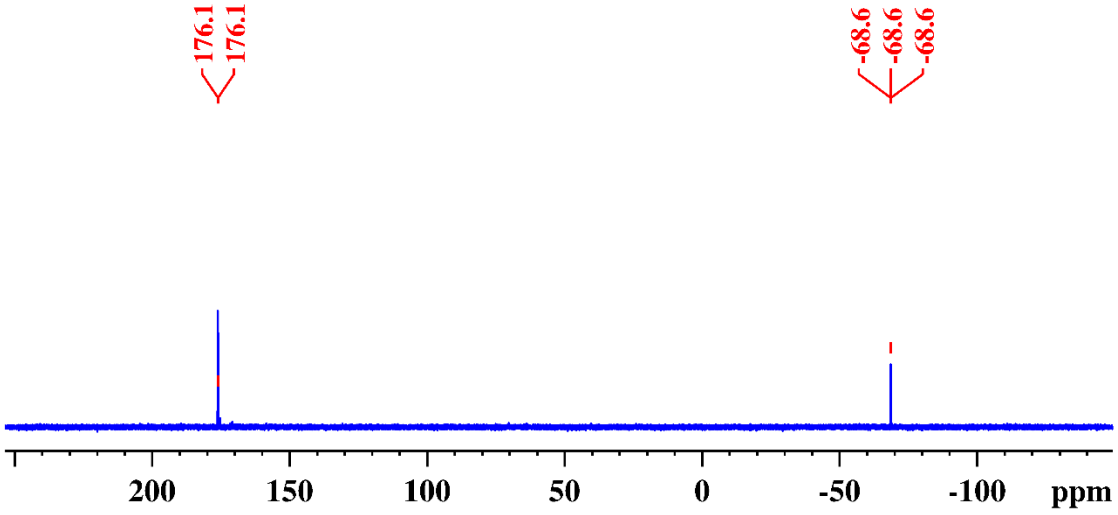


**Figure S78.** $^{31}P\{^{1}H\}$ NMR (202.4 MHz, $CD_2Cl_2$ + THF-$d_8$, 298 K) spectrum of *trans*-[Ir(H)$_2$PMe$_3$($^{tBu4}$POCOP)] (**6**) synthesized by the reaction of complex **3** with $NaBH_4$.

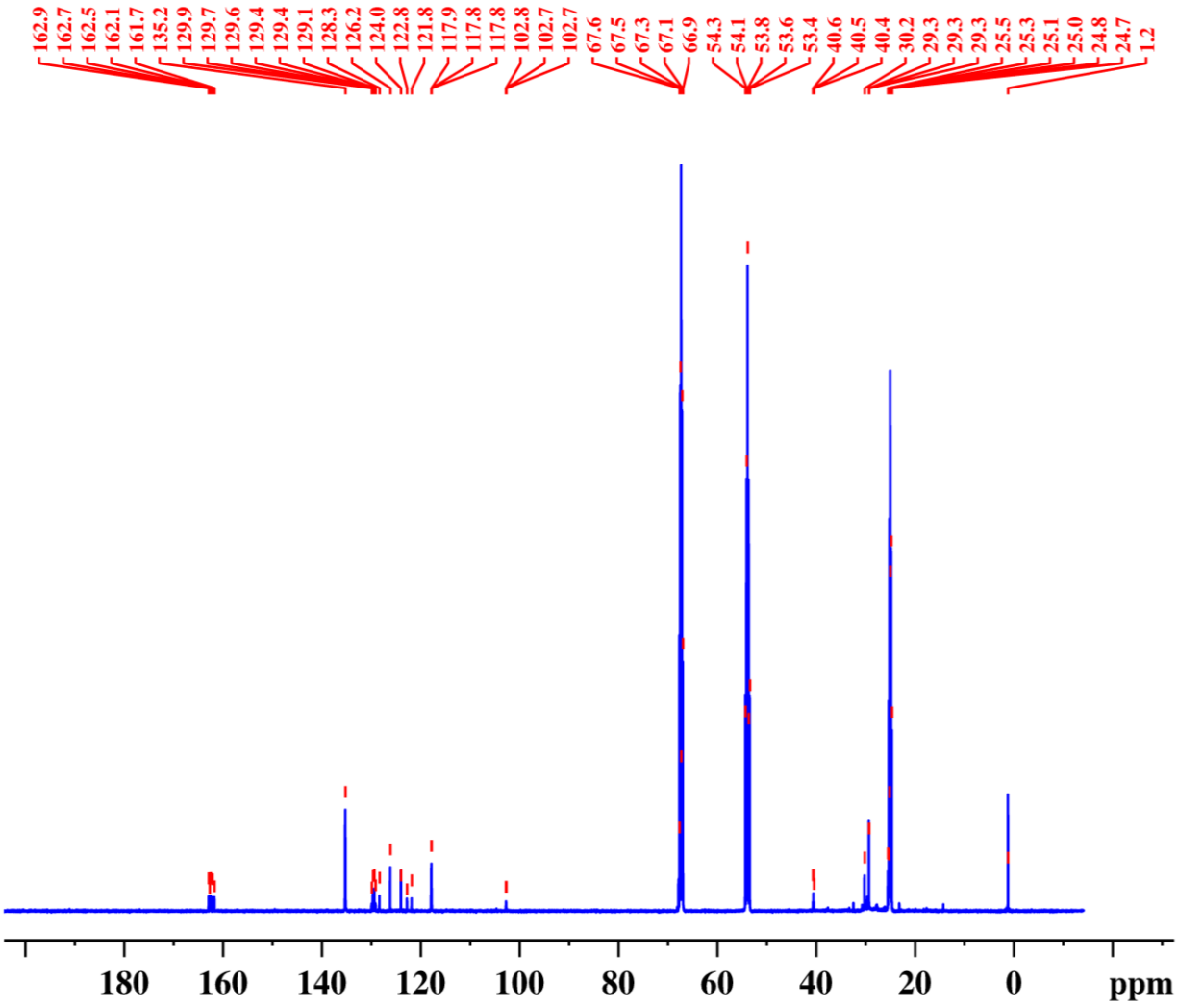


**Figure S79.** $^{13}C\{^{1}H\}$ NMR (125.7 MHz, $CD_2Cl_2$ + THF-$d_8$, 298 K) spectrum of *trans*-[Ir(H)$_2$PMe$_3$($^{tBu4}$POCOP)] (**6**) synthesized by the reaction of complex **3** with $NaBH_4$.

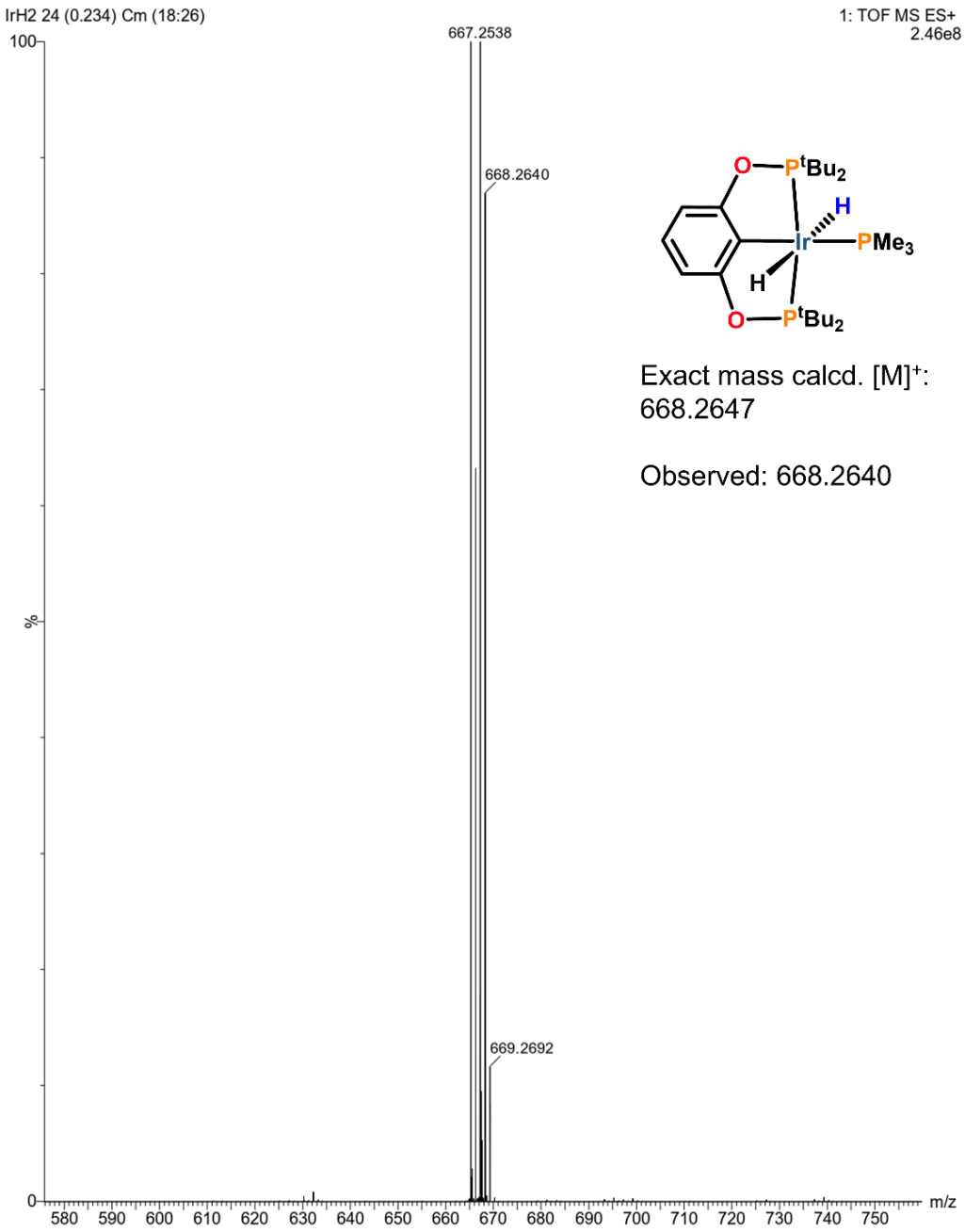


**Figure S80**. HRMS spectrograph of *trans*-[Ir(H)$_2$PMe$_3$($^{tBu4}$POCOP)] (**6**).

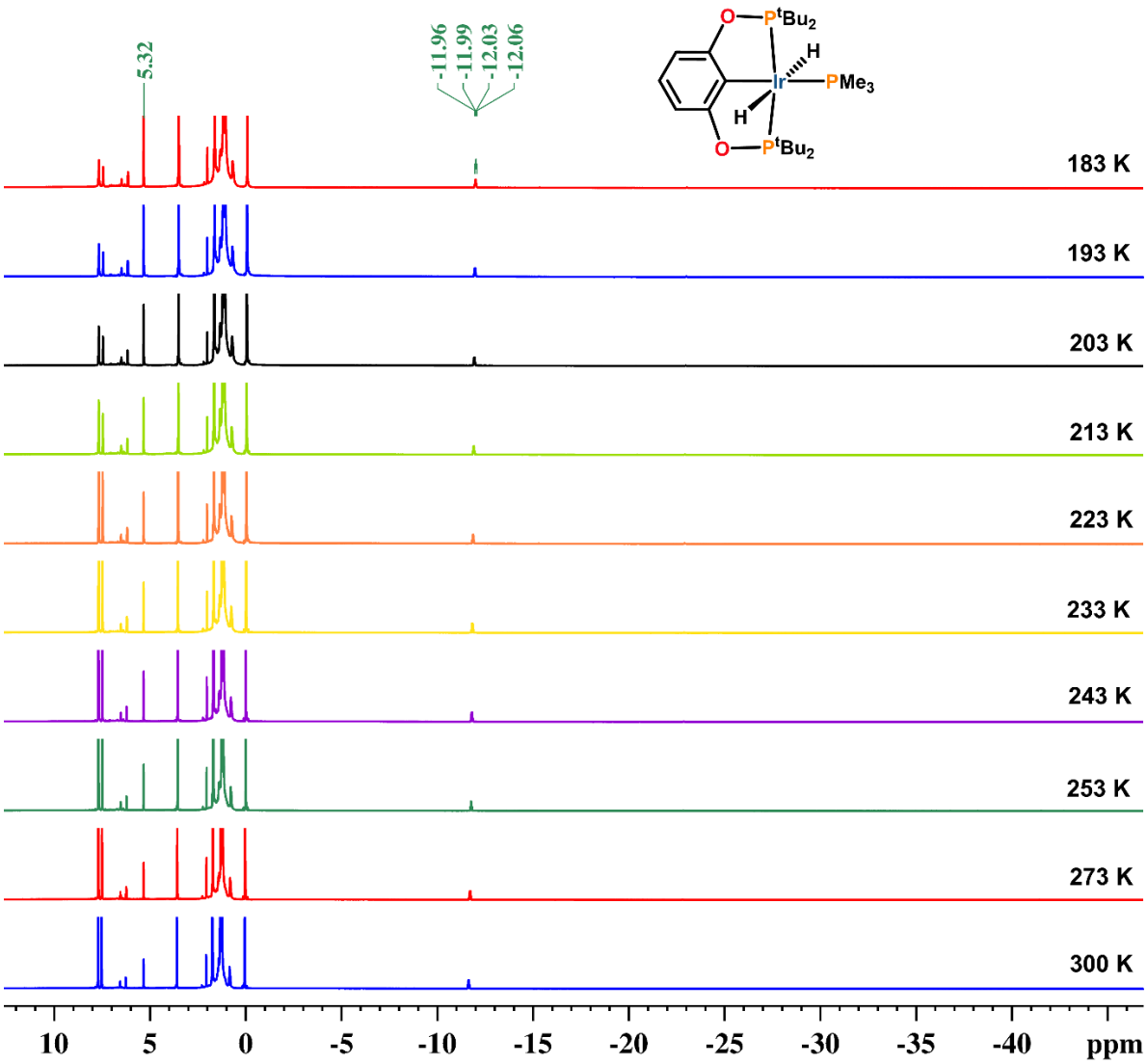


**Figure S81.** VT $^{1}$H NMR (500.0 MHz, $CD_2Cl_2$ + THF-$d_8$) spectral stack plot of *trans*-[Ir(H)$_2$PMe$_3$($^{tBu4}$POCOP)] (**6**).

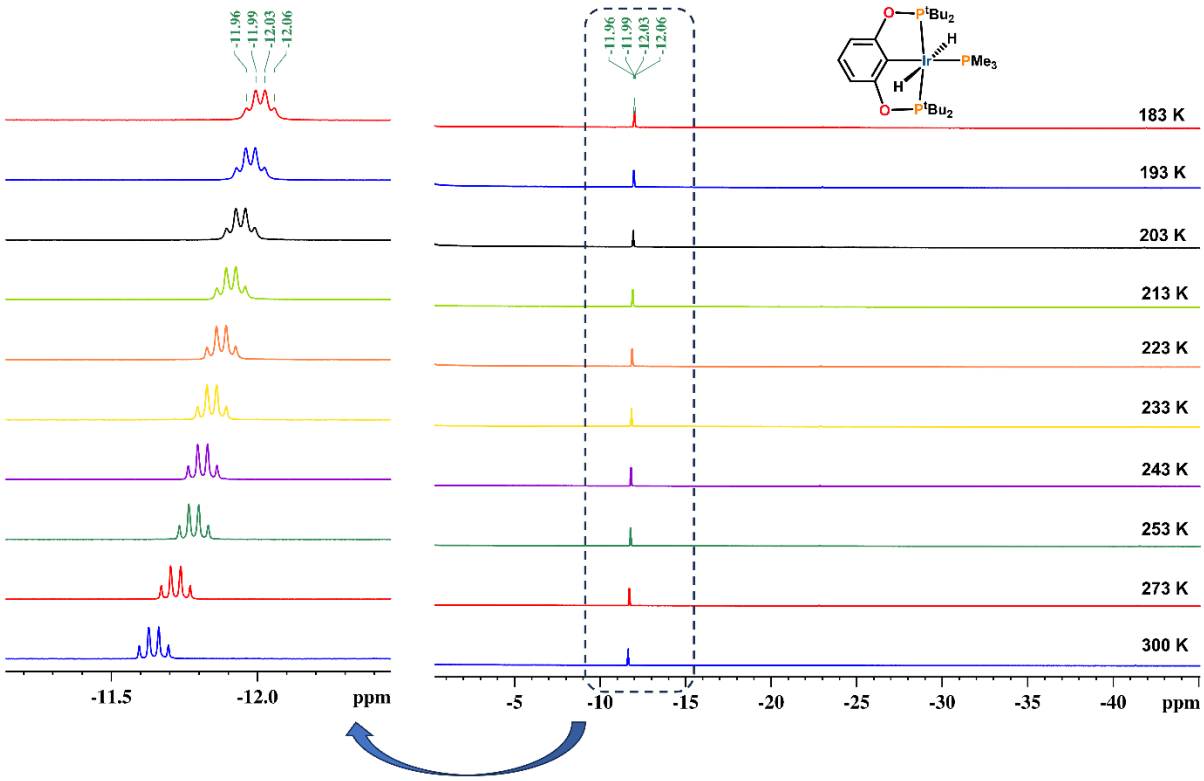


**Figure S82.** Partial VT $^{1}H$ NMR (500.0 MHz, $CD_2Cl_2$ + THF-$d_8$) spectral stack plot of *trans*-[Ir(H)$_2$PMe$_3$($^{tBu4}$POCOP)] (**6**).

## 9. Stability of *trans*-[Ir(H)$_2$(PMe$_3$)($^{tBu}$POCOP)] (**6**) under vacuum.

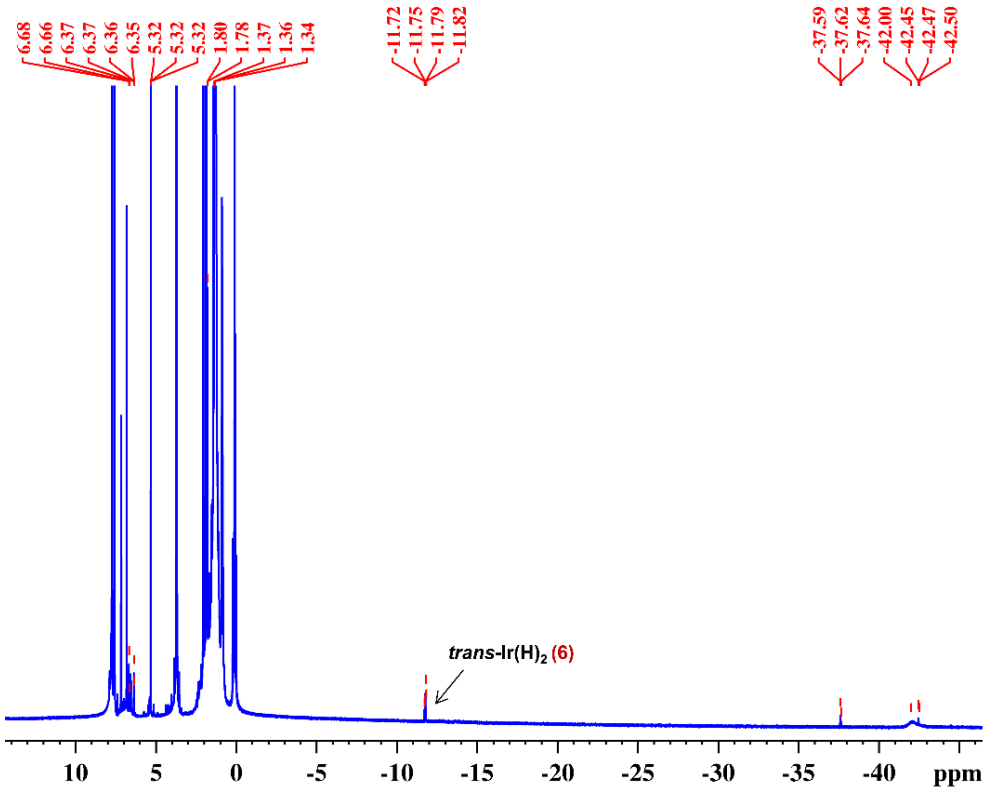

**Figure S83.** $^{1}H$ NMR (500 MHz, $CD_2Cl_2$, 298 K) spectrum of the reaction mixture obtained after applying vacuum to complex **6**.

Peaks at –37.62, –42, and –42.47 ppm could not be assigned.

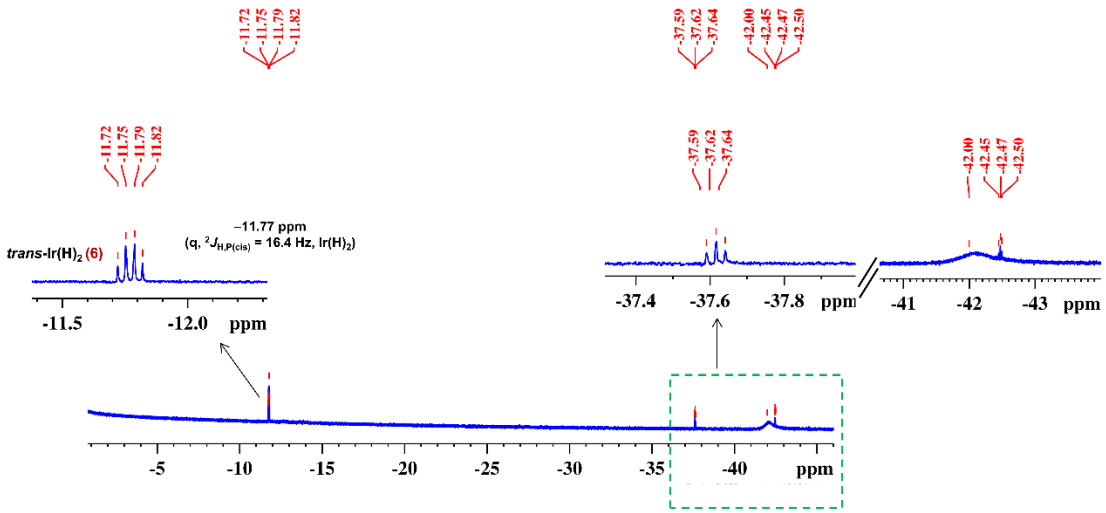


**Figure S84.** Partial $^{1}H$ NMR (500 MHz, $CD_2Cl_2$, 298 K) spectrum (hydride region) of the reaction mixture obtained after applying vacuum to complex **6**.

Peaks at –37.62, –42, and –42.47 ppm could not be assigned.

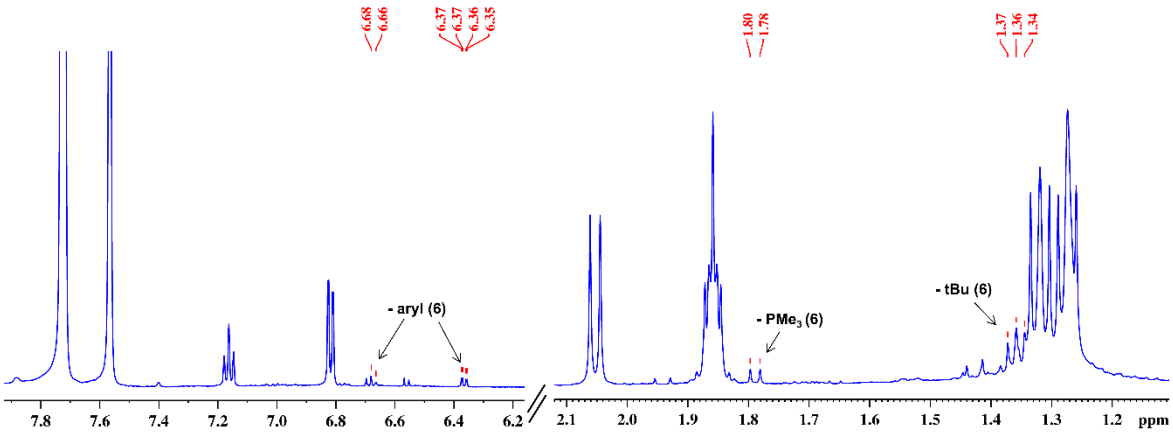


**Figure S85.** Partial $^{1}H$ NMR (500 MHz, $CD_2Cl_2$, 298 K) spectrum (downfield region) of the reaction mixture obtained after applying vacuum to complex **6**.

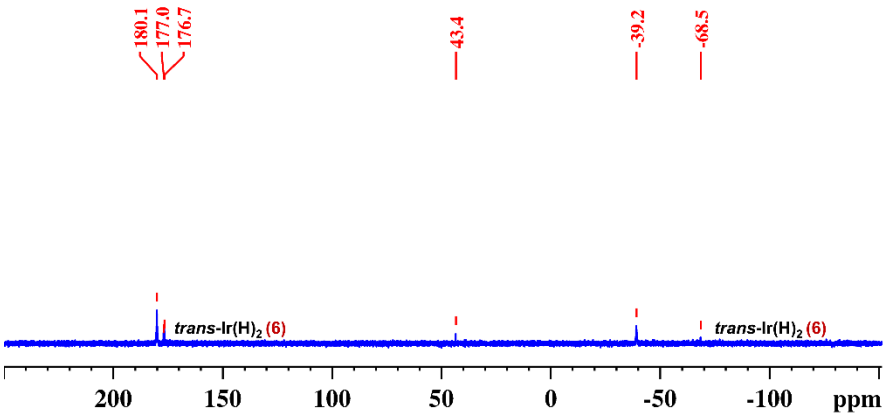


**Figure S86.** $^{31}P\{^{1}H\}$ NMR (202.4 MHz, $CD_2Cl_2$, 298 K) spectrum of the reaction mixture obtained after applying vacuum to complex **6**.

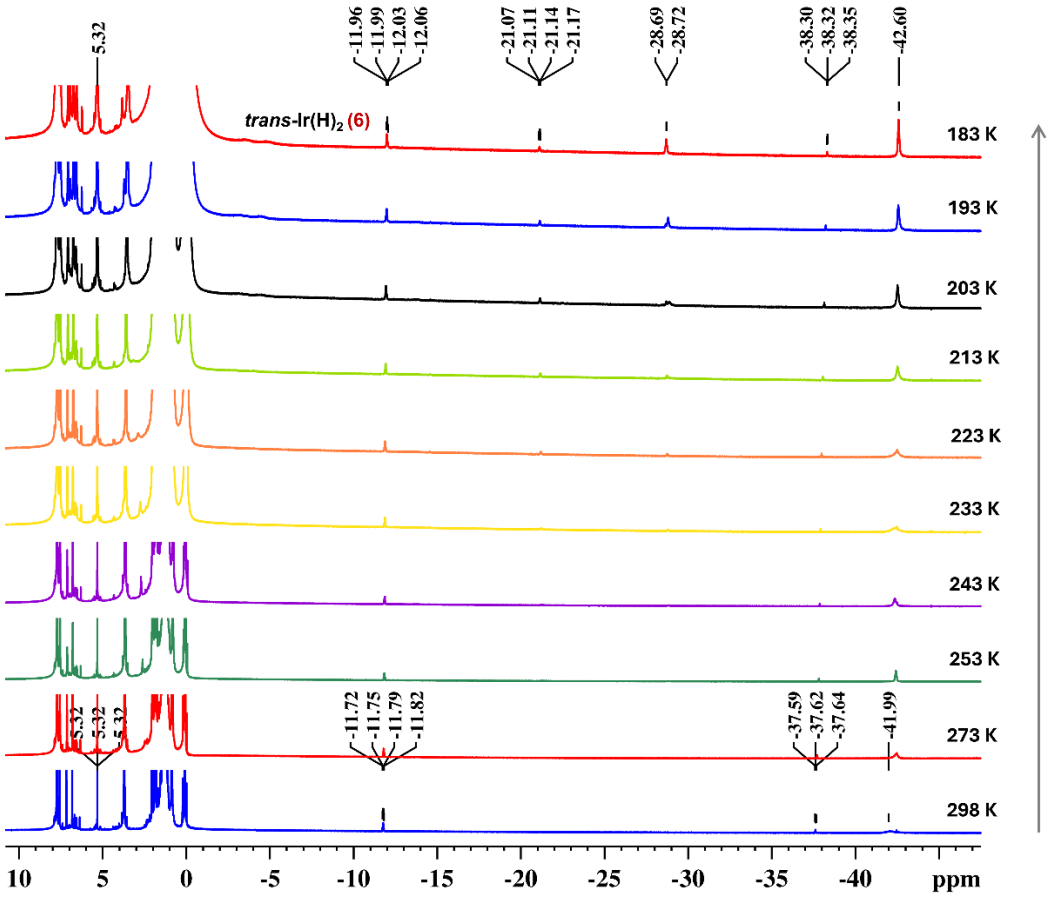


**Figure S87.** VT $^{1}H$ NMR (500 MHz, $CD_2Cl_2$) spectral stack plot of the reaction mixture obtained after applying vacuum to complex **6**.

Peaks at –21.12, –28.70, –38.32 and –42.60 ppm could not be assigned.

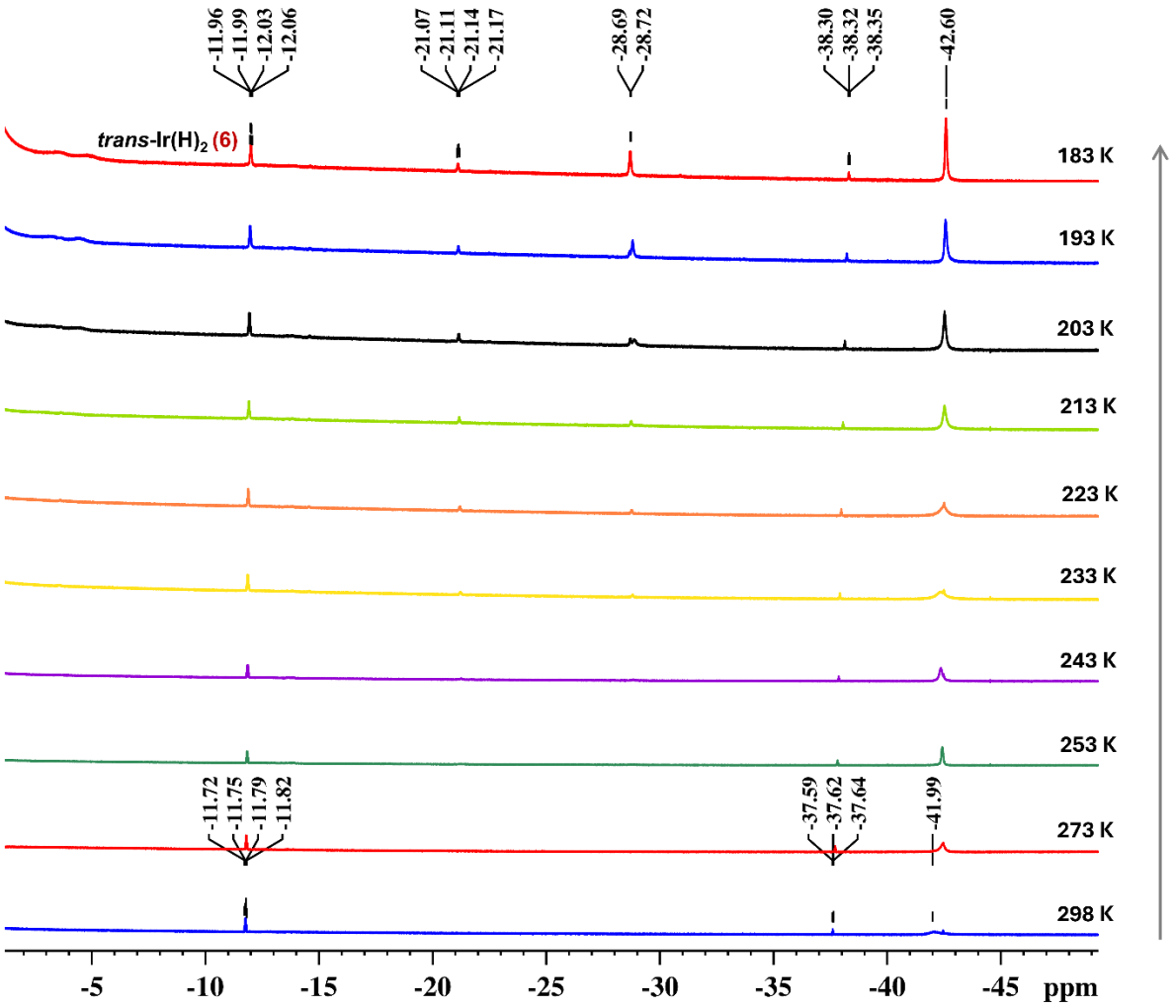


**Figure S88.** Partial VT $^{1}H$ NMR (500 MHz, $CD_2Cl_2$) spectral stack plot (hydride region) of the reaction mixture obtained after applying vacuum to complex **6**.

Peaks at –21.12, –28.70, –38.32 and –42.60 ppm could not be assigned.

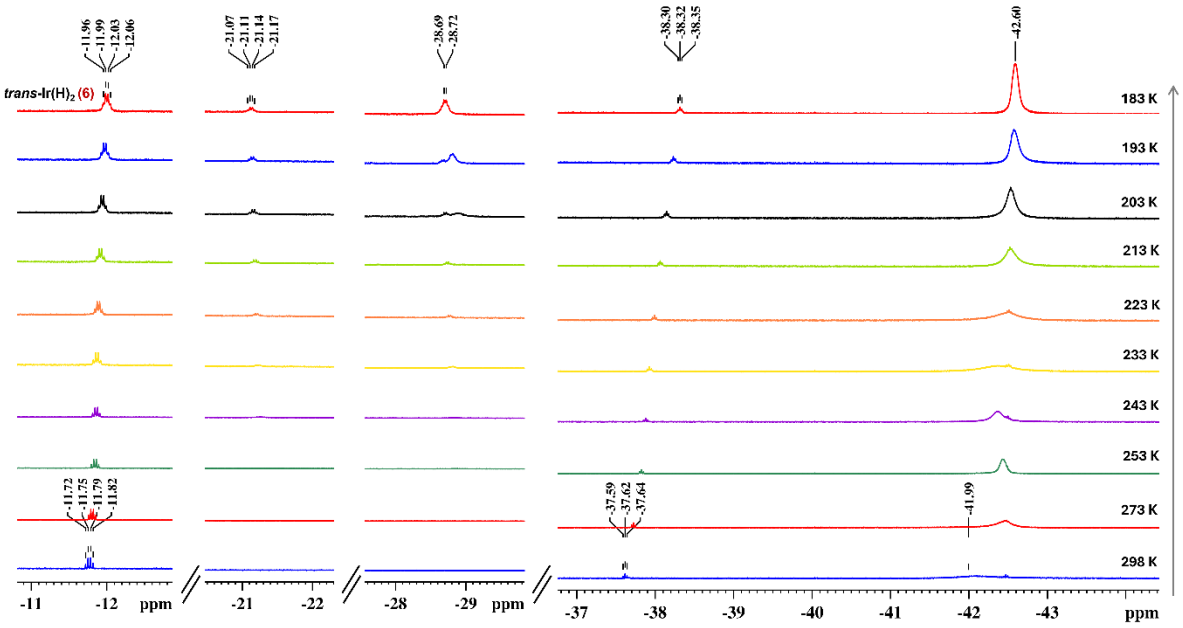


**Figure S89.** Partial VT $^{1}$H NMR (500 MHz, $CD_2Cl_2$) spectral stack plot (expanded hydride region) of the reaction mixture obtained after applying vacuum to complex **6**.

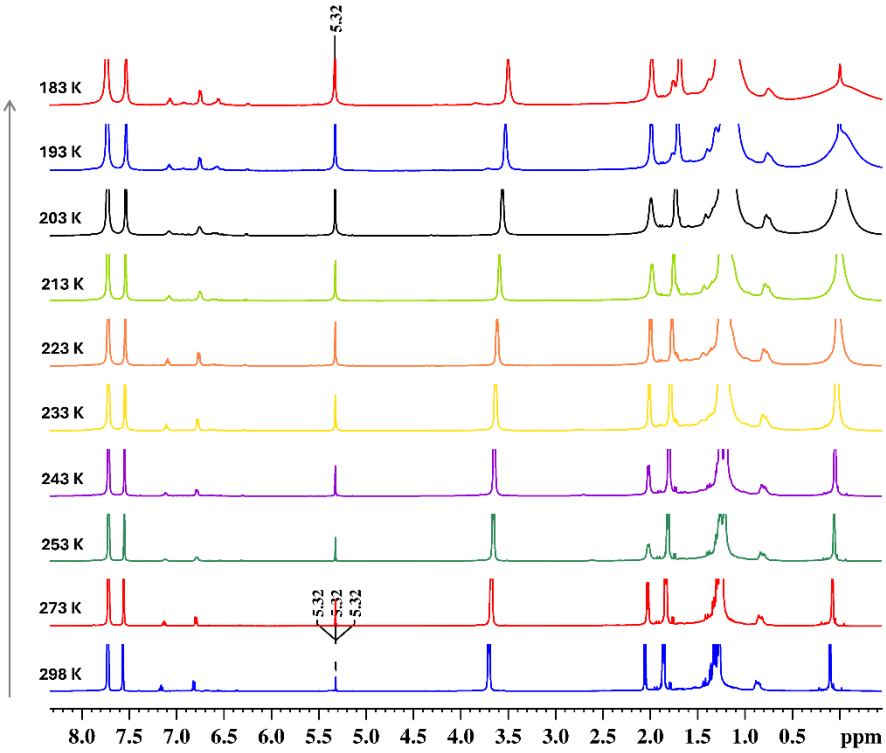


**Figure S90.** Partial VT $^{1}$H NMR (500 MHz, $CD_2Cl_2$) spectral stack plot (downfield region) of the reaction mixture obtained after applying vacuum to complex **6**.

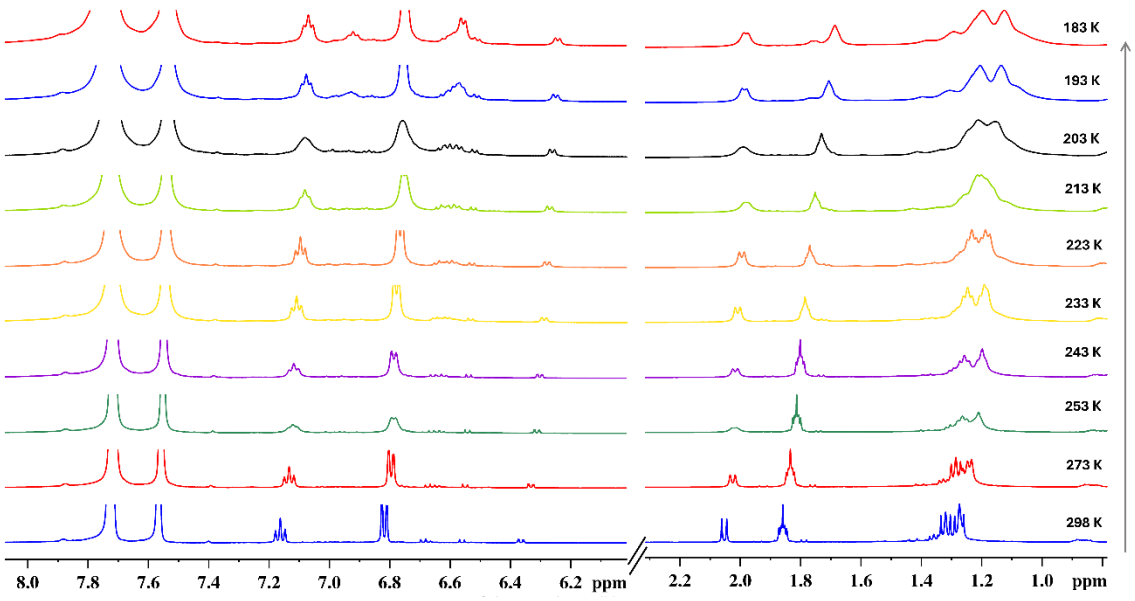


**Figure S91.** Partial VT $^{1}H$ NMR (500 MHz, $CD_2Cl_2$) spectral stack plot (expanded downfield region) of the reaction mixture obtained after applying vacuum to complex **6**.

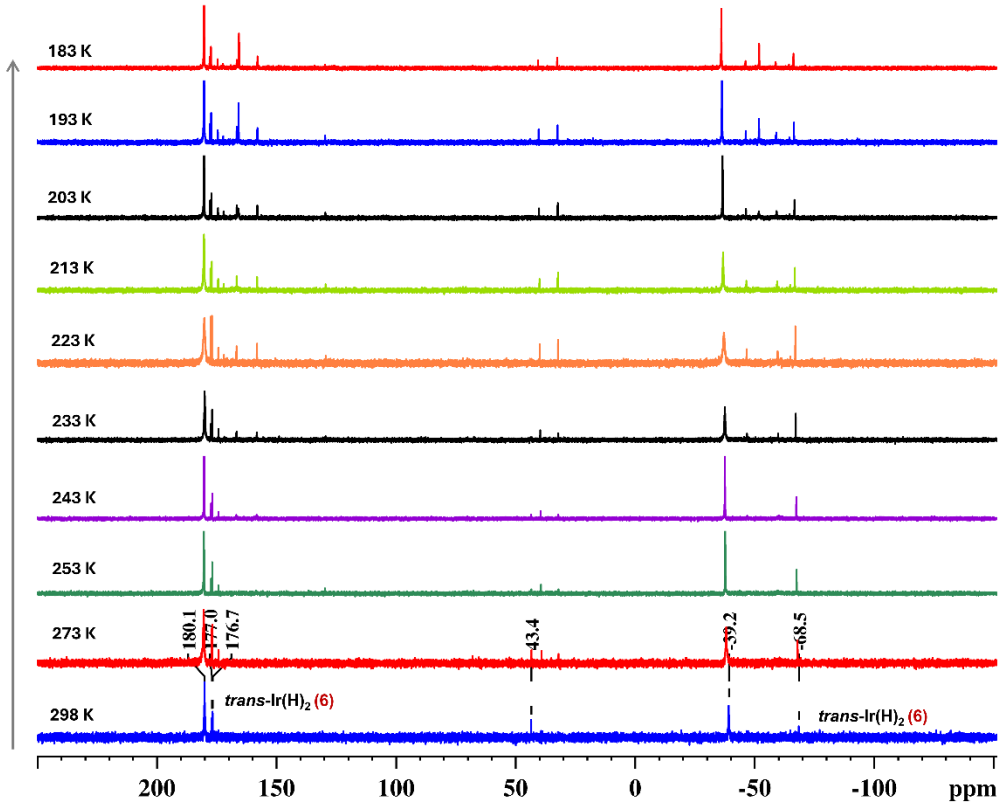


**Figure S92.** VT $^{31}P\{^{1}H\}$ NMR (202.4 MHz, $CD_2Cl_2$) spectral stack plot of the reaction mixture obtained after applying vacuum to complex **6**.

## 10. Reaction of [Ir(H)($PMe_3$)($^{tBu4}$POCOP)][$BAr^F_4$] (**3**) with $H_3B{\cdot}NMe_2H$ (DMAB).

**(A) Reaction of [Ir(H)($PMe_3$)($^{tBu4}$POCOP)][$BAr^F_4$] (3) with $H_3B{\cdot}NMe_2H$ after 30 min:**

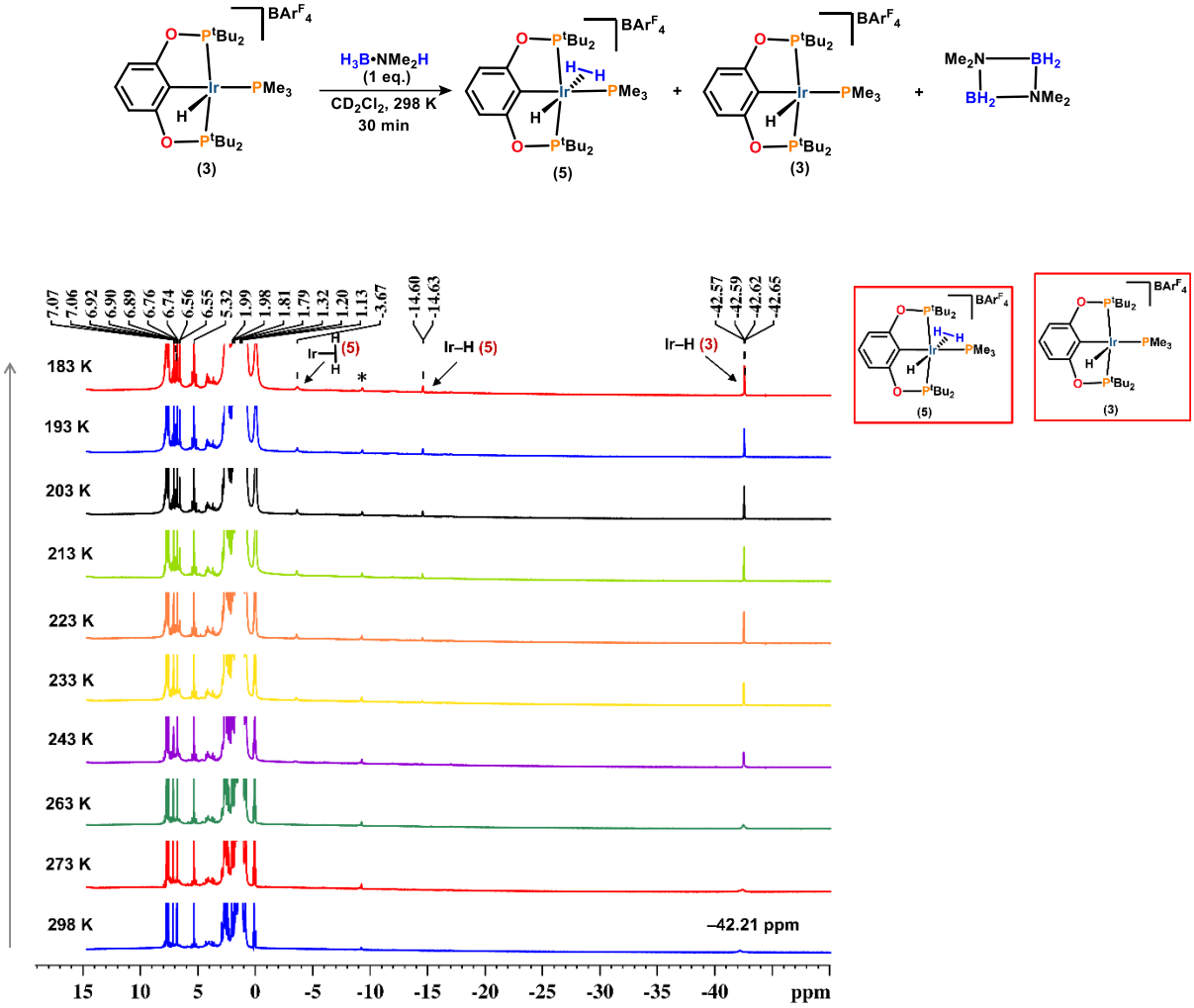


**Figure S93**. VT $^1$H NMR (500.0 MHz, $CD_2Cl_2$) spectral stack plot of reaction of [Ir(H)($PMe_3$)($^{tBu4}$POCOP)][$BAr^F_4$] (**3**) with $H_3B{\cdot}NMe_2H$ after 30 min.

The peaks of complexes **3** and **5** appeared upon cooling the sample to low temperature. *Unidentified impurity.

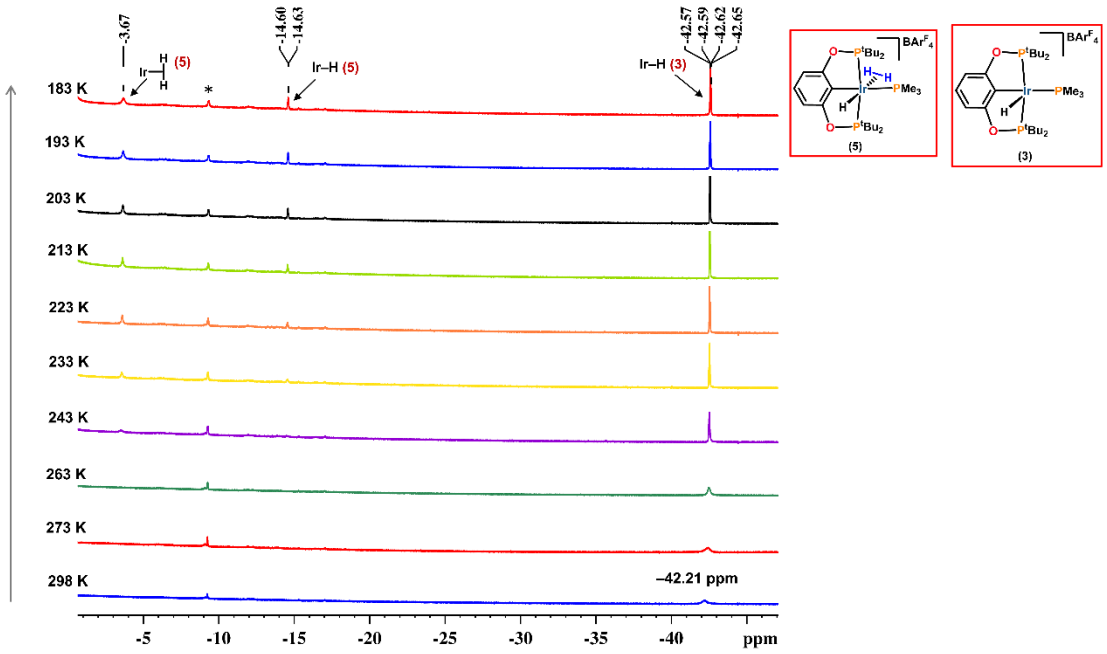


**Figure S94.** Partial VT $^1$H NMR (500.0 MHz, $CD_2Cl_2$) spectral stack plot (hydride region) of reaction of [Ir(H)(PMe$_3$)($^{tBu4}$POCOP)][BAr$^F_4$] (**3**) with $H_3B{\cdot}NMe_2H$ after 30 min.

The peaks of complexes **3** and **5** appeared upon cooling the sample to low temperature. *Unidentified impurity.

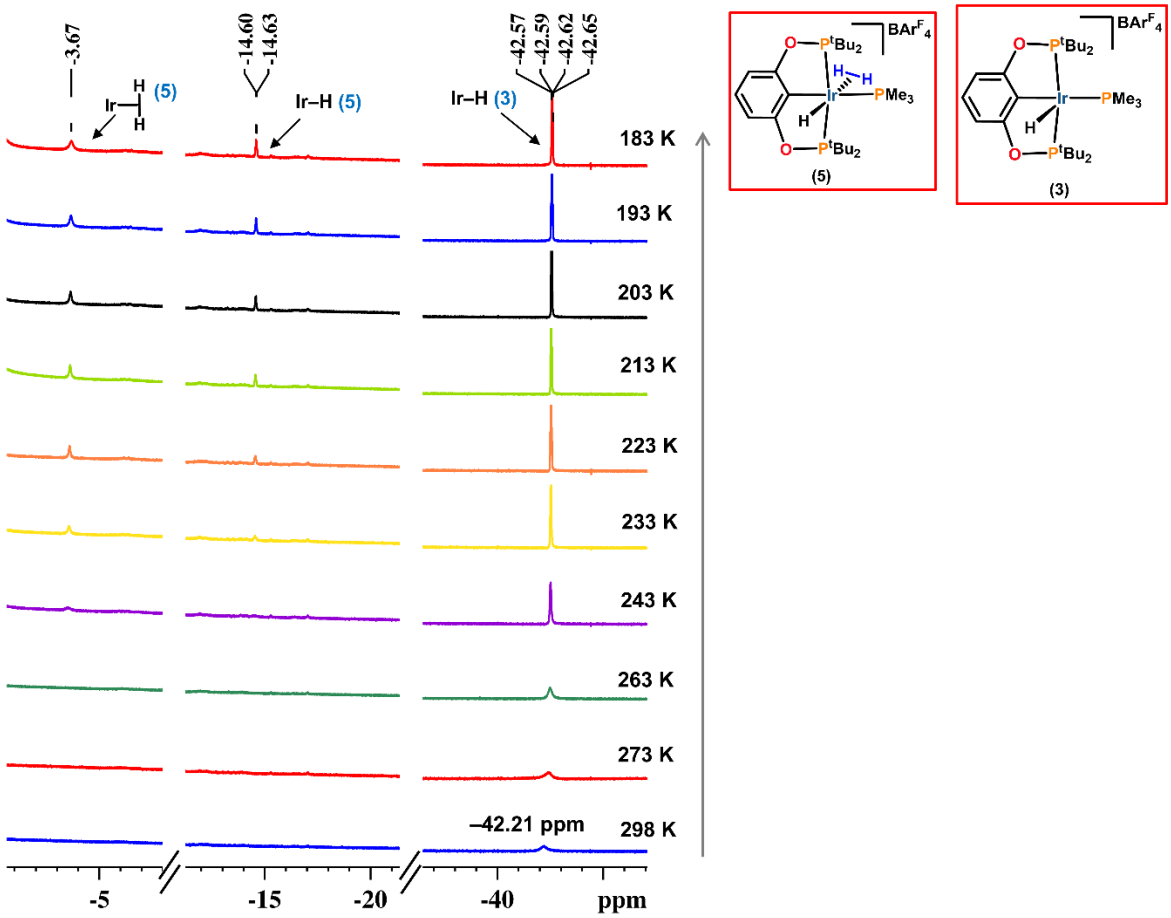


**Figure S95**. Partial VT $^{1}H$ NMR (500.0 MHz, $CD_2Cl_2$) spectral stack plot (expanded hydride region) of reaction of [Ir(H)($PMe_3$)($^{tBu4}$POCOP)][$BAr^F_4$] (**3**) with $H_3B{\cdot}NMe_2H$ after 30 min.

The peaks of complexes **3** and **5** appeared upon cooling the sample to low temperature.

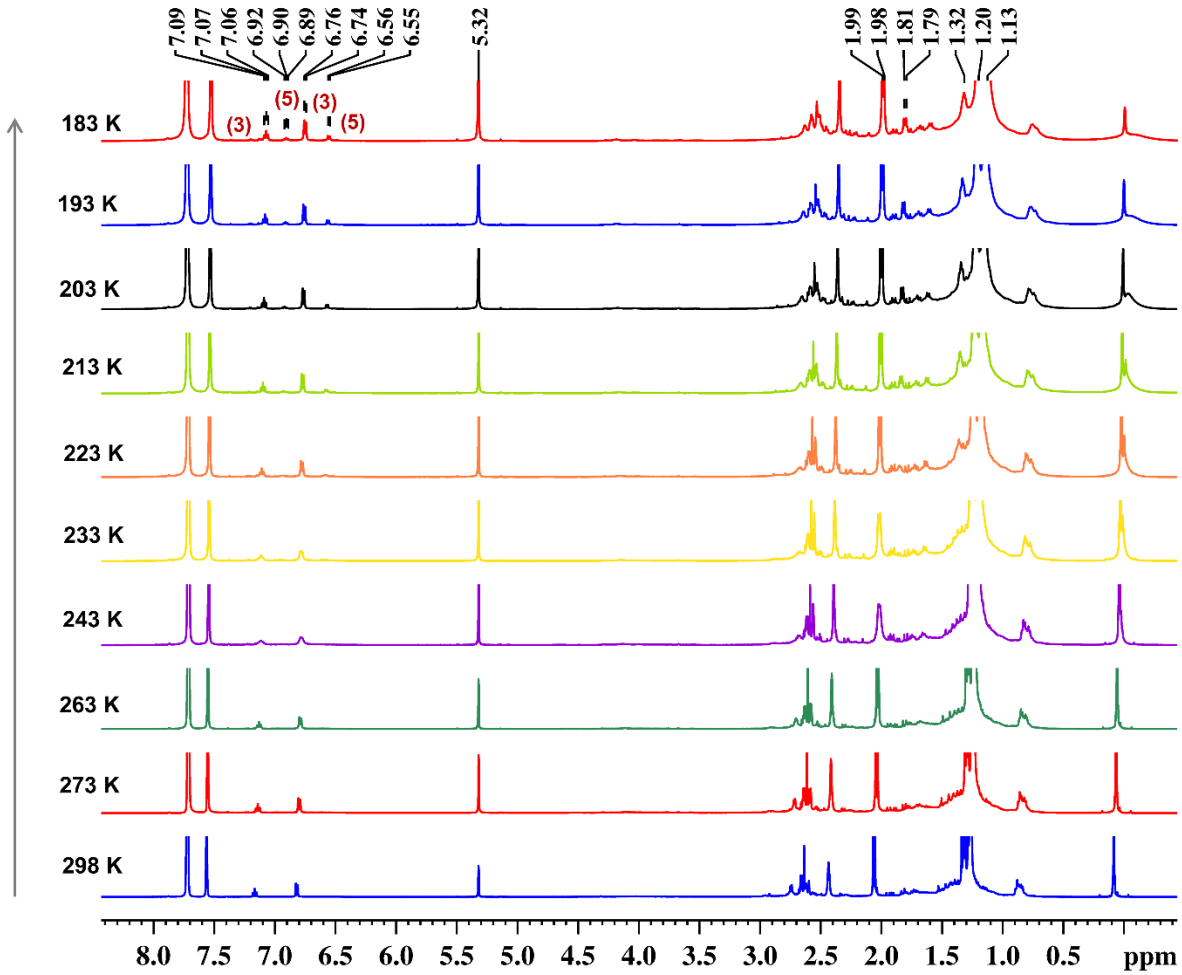


**Figure S96**. Partial VT $^{1}H$ NMR (500.0 MHz, $CD_2Cl_2$) spectral stack plot (downfield region) of reaction of [Ir(H)($PMe_3$)($^{tBu4}$POCOP)][$BAr^F_4$] (**3**) with $H_3B{\cdot}NMe_2H$ after 30 min.

The peaks of complexes **3** and **5** appeared upon cooling the sample to low temperature.

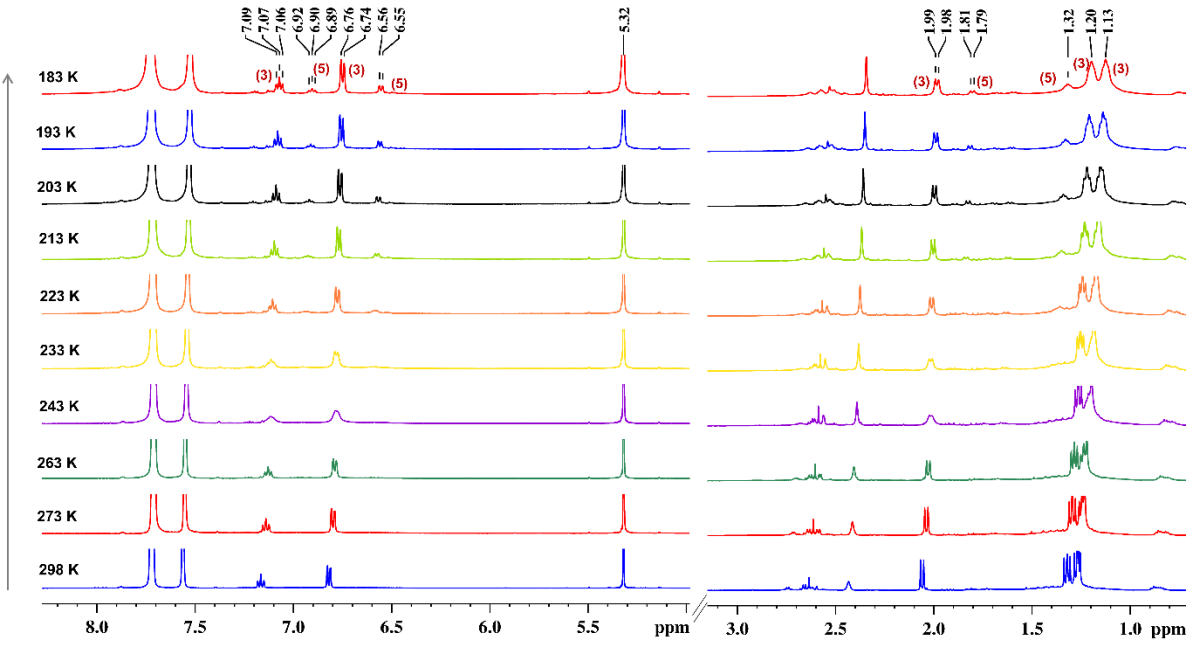

**Figure S97**. Partial VT $^{1}H$ NMR (500.0 MHz, $CD_2Cl_2$) spectral stack plot (expanded downfield region) of reaction of [Ir(H)($PMe_3$)($^{tBu4}$POCOP)][$BAr^F_4$] (**3**) with $H_3B{\cdot}NMe_2H$ after 30 min.

The peaks of complexes **3** and **5** appeared upon cooling the sample to low temperature.

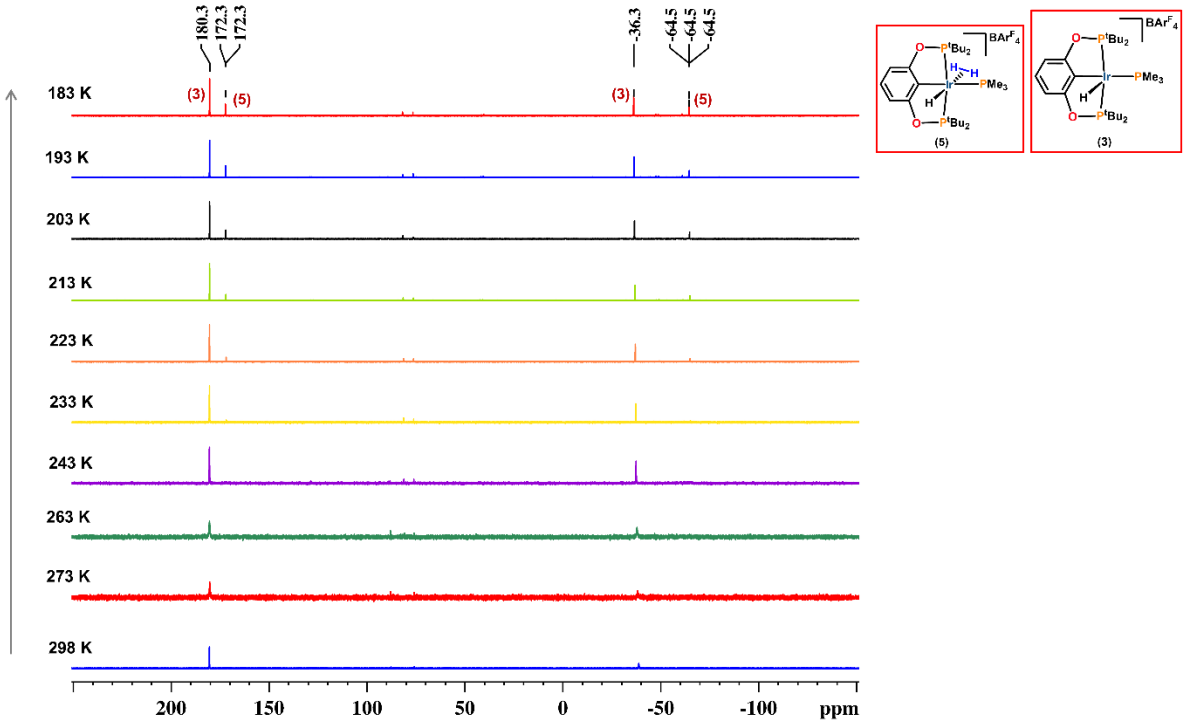


**Figure S98**. VT $^{31}P\{^{1}H\}$ NMR (202.4 MHz, $CD_2Cl_2$) spectral stack plot of reaction of [Ir(H)($PMe_3$)($^{tBu4}$POCOP)][$BAr^F_4$] (**3**) with $H_3B{\cdot}NMe_2H$ after 30 min.

The peaks of complexes **3** and **5** appeared upon cooling the sample to low temperature.

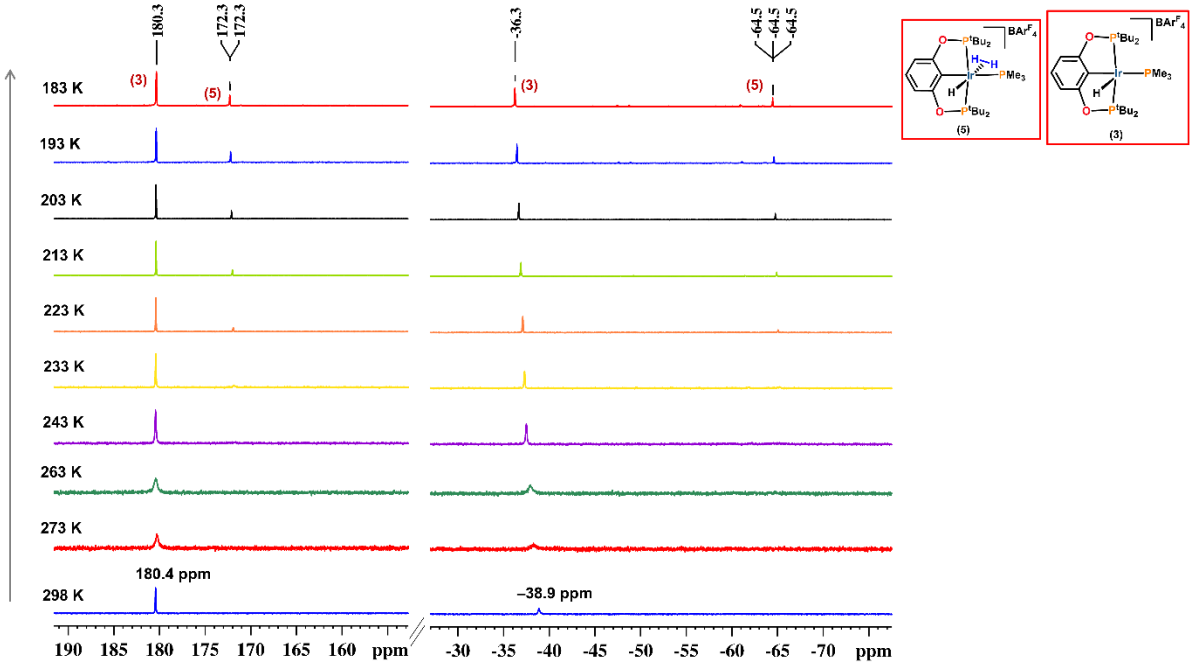


**Figure S99**. Partial VT $^{31}P\{^{1}H\}$ NMR (202.4 MHz, $CD_2Cl_2$) spectral stack plot of reaction of [Ir(H)($PMe_3$)($^{tBu4}$POCOP)][$BAr^F_4$] (**3**) with $H_3B{\cdot}NMe_2H$ after 30 min.

The peaks of complexes **3** and **5** appeared upon cooling the sample to low temperature.

**(B) Reaction of [Ir(H)(PMe$_3$)($^{tBu4}$POCOP)][BAr$^F_4$] (3) with H$_3$B·NMe$_2$H after 10 min:**

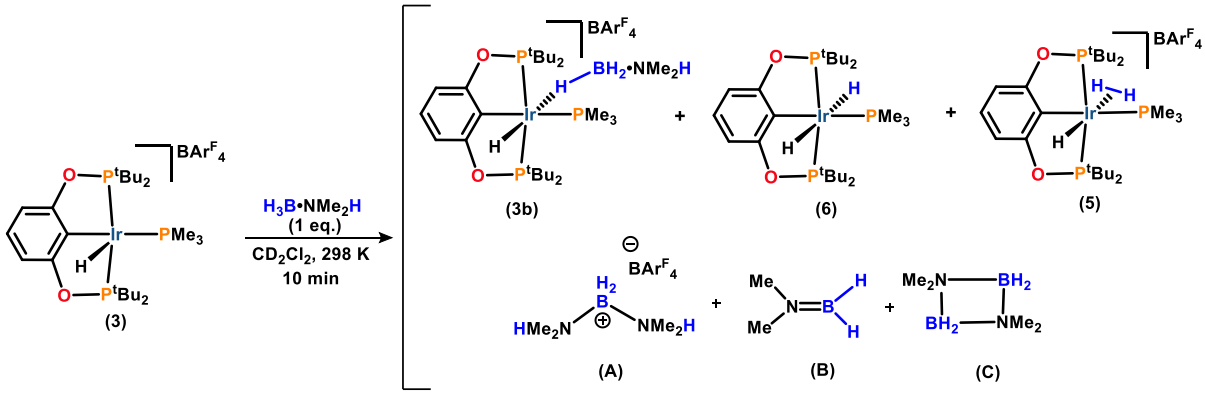


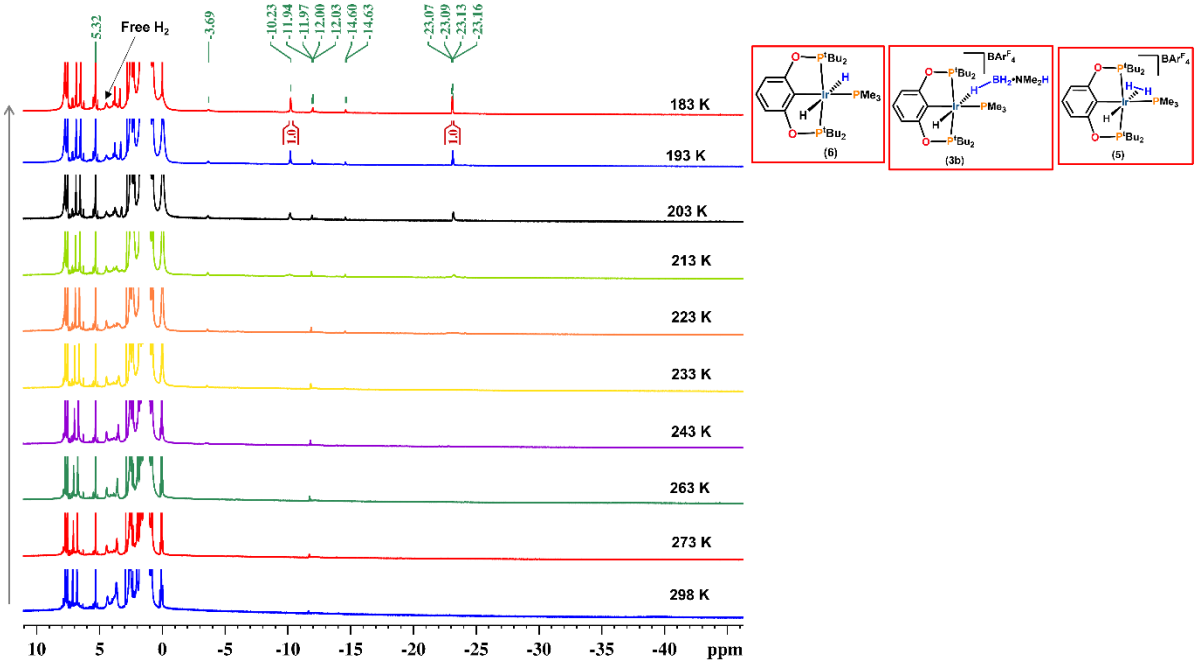


**Figure S100.** VT $^1$H NMR (500.0 MHz, CD$_2$Cl$_2$) spectral stack plot of reaction of [Ir(H)(PMe$_3$)($^{tBu4}$POCOP)][BAr$^F_4$] (**3**) with H$_3$B·NMe$_2$H after 10 min.

Complex **6** observed at 298 K, while complexes **3b** and **5** appeared upon cooling the sample to low temperature.

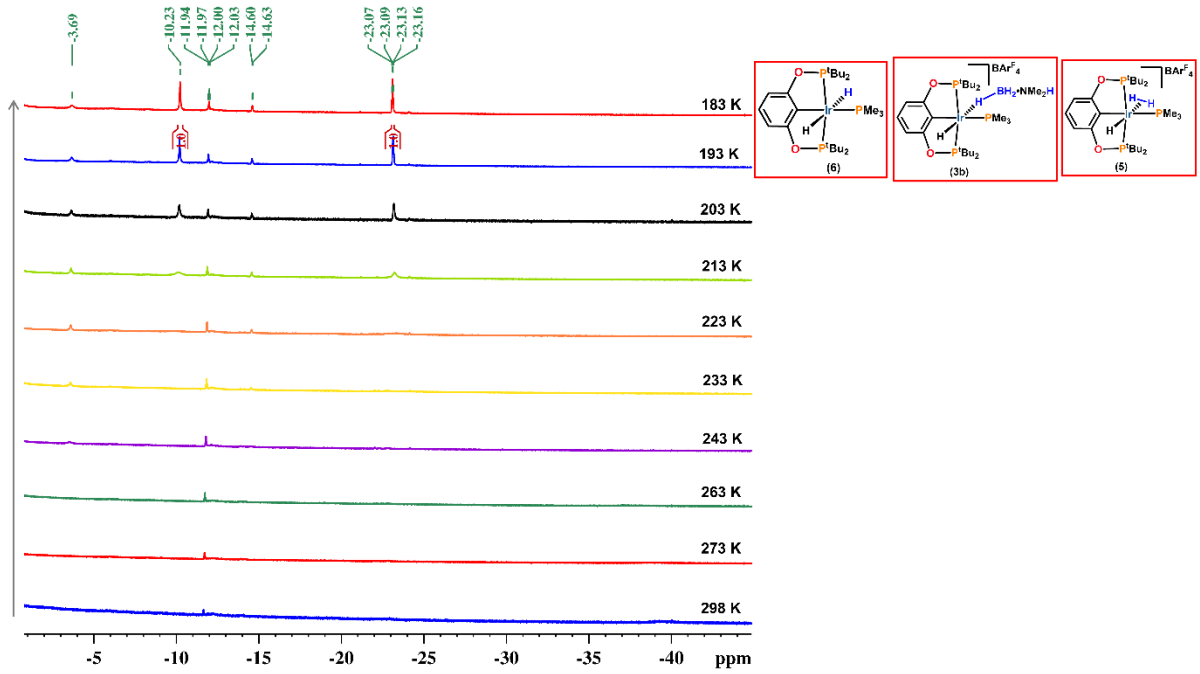


**Figure S101.** Partial VT $^{1}$H NMR (500.0 MHz, $CD_2Cl_2$) spectral stack plot (hydride region) of reaction of [Ir(H)($PMe_3$)($^{tBu4}$POCOP)][$BAr^F_4$] (**3**) with $H_3B{\cdot}NMe_2H$ after 10 min.

Complex **6** observed at 298 K, while complexes **3b** and **5** appeared upon cooling the sample to low temperature.

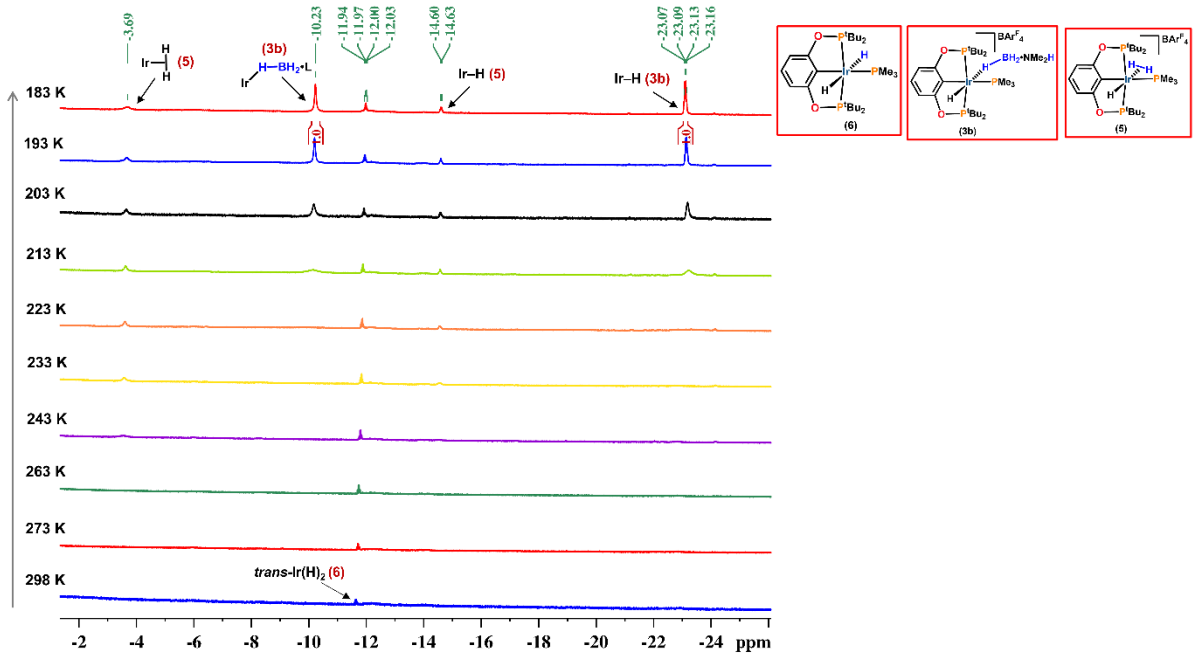


**Figure S102**. Partial VT $^{1}$H NMR (500.0 MHz, $CD_2Cl_2$) spectral stack plot (expanded hydride region) of reaction of [Ir(H)($PMe_3$)($^{tBu4}$POCOP)][$BAr^F_4$] (**3**) with $H_3B{\cdot}NMe_2H$ after 10 min.

Complex **6** observed at 298 K, while complexes **3b** and **5** appeared upon cooling the sample to low temperature.

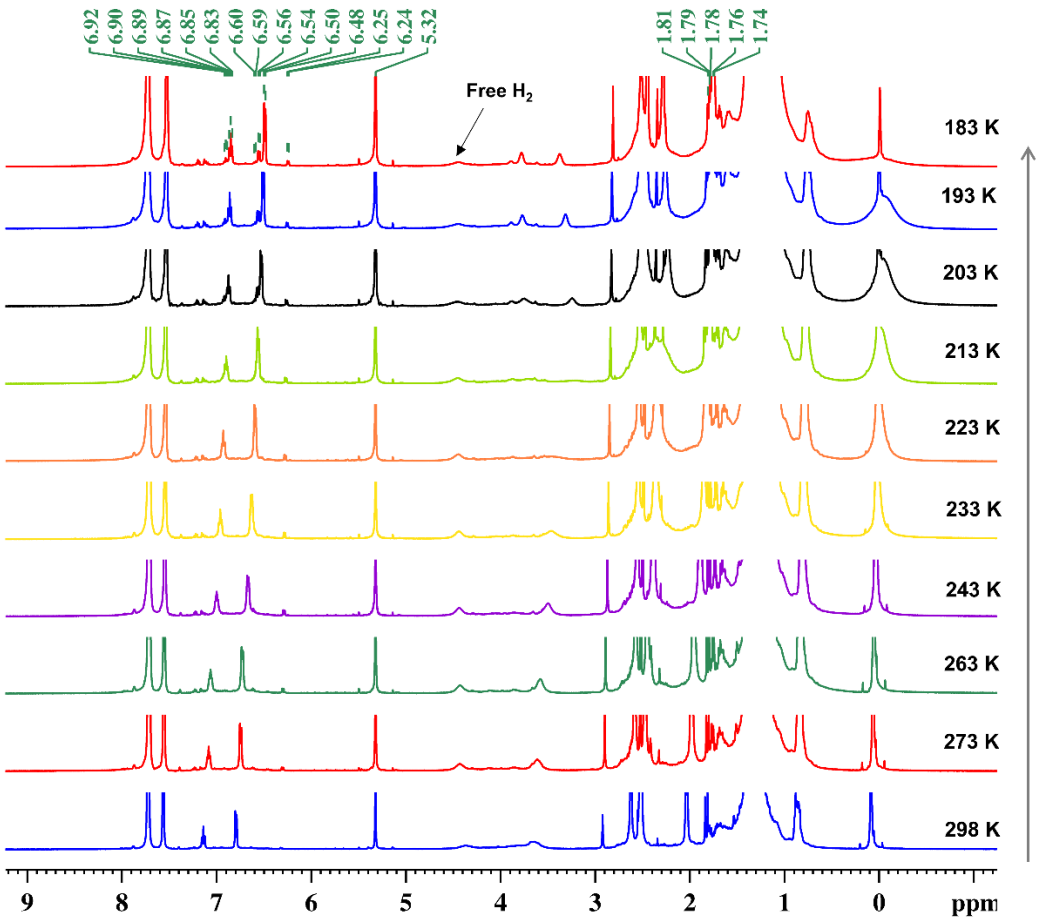


**Figure S103**. Partial VT $^{1}$H NMR (500.0 MHz, $CD_2Cl_2$) spectral stack plot (downfield region) of reaction of [Ir(H)($PMe_3$)($^{tBu4}$POCOP)][$BAr^F_4$] (**3**) with $H_3B{\cdot}NMe_2H$ after 10 min.

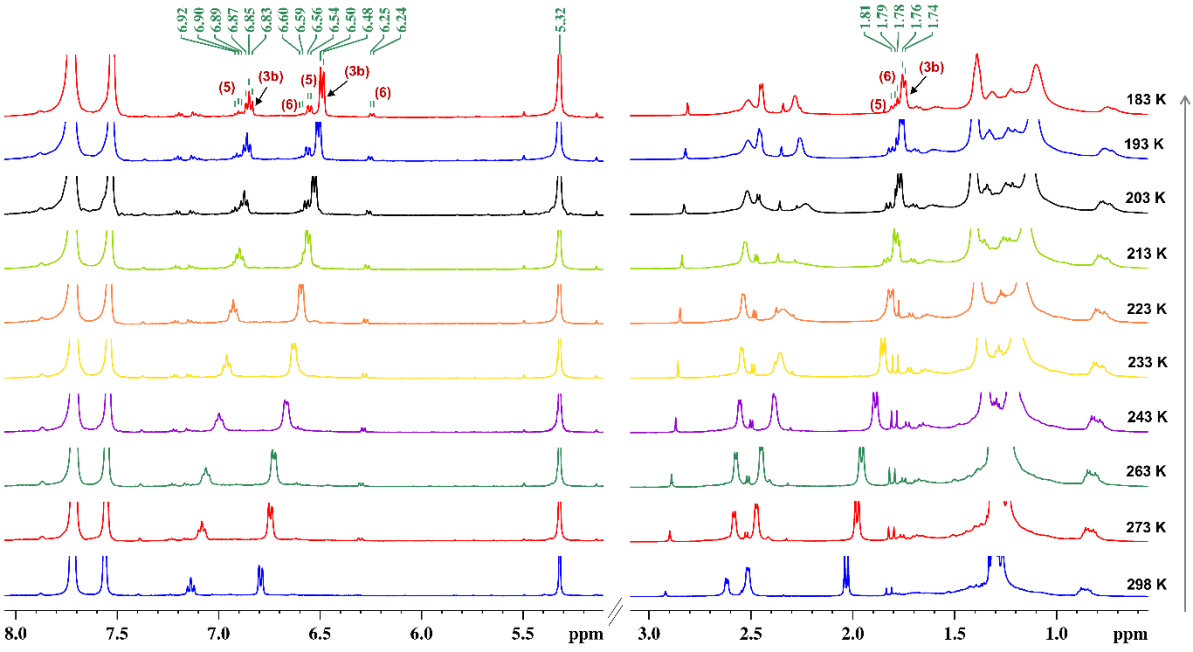


**Figure S104**. Partial VT $^{1}$H NMR (500.0 MHz, $CD_2Cl_2$) spectral stack plot (expanded downfield region) of reaction of [Ir(H)($PMe_3$)($^{tBu4}$POCOP)][$BAr^F_4$] (**3**) with $H_3B{\cdot}NMe_2H$ after 10 min.

The protons corresponding to the $^{t}$Bu groups of the intermediate species could not be assigned due to signal broadening and overlap.

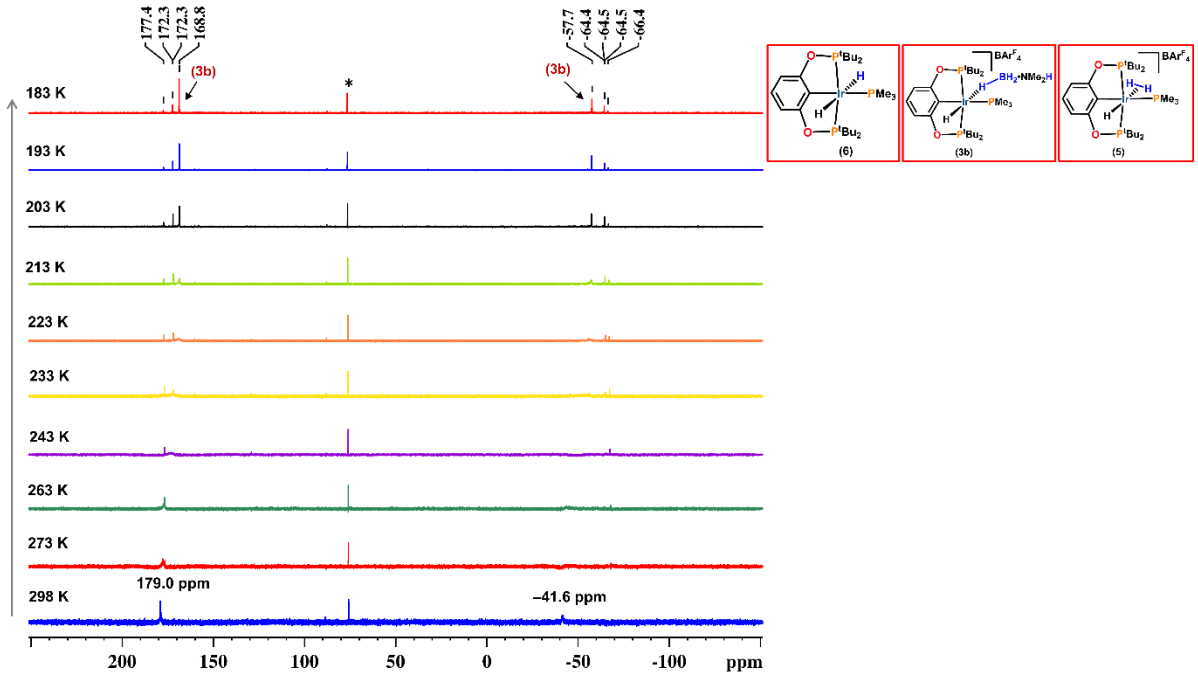


**Figure S105**. VT $^{31}P\{^{1}H\}$ NMR (202.4 MHz, $CD_2Cl_2$) spectral stack plot of reaction of [Ir(H)($PMe_3$)($^{tBu4}$POCOP)][$BAr^F_4$] (**3**) with $H_3B{\cdot}NMe_2H$ after 10 min.

*Unidentified impurity.

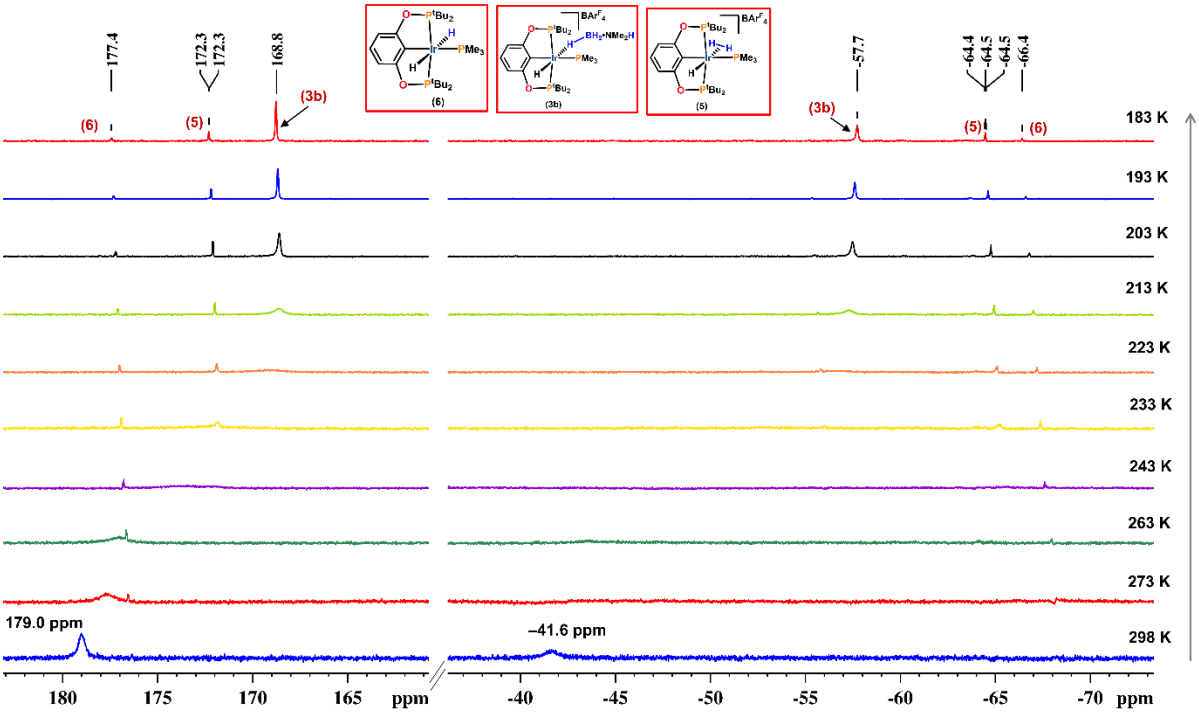


**Figure S106**. Partial VT $^{31}P\{^{1}H\}$ NMR (202.4 MHz, $CD_2Cl_2$) spectral stack plot of reaction of [Ir(H)($PMe_3$)($^{tBu4}$POCOP)][$BAr^F_4$] (**3**) with $H_3B{\cdot}NMe_2H$ after 10 min.

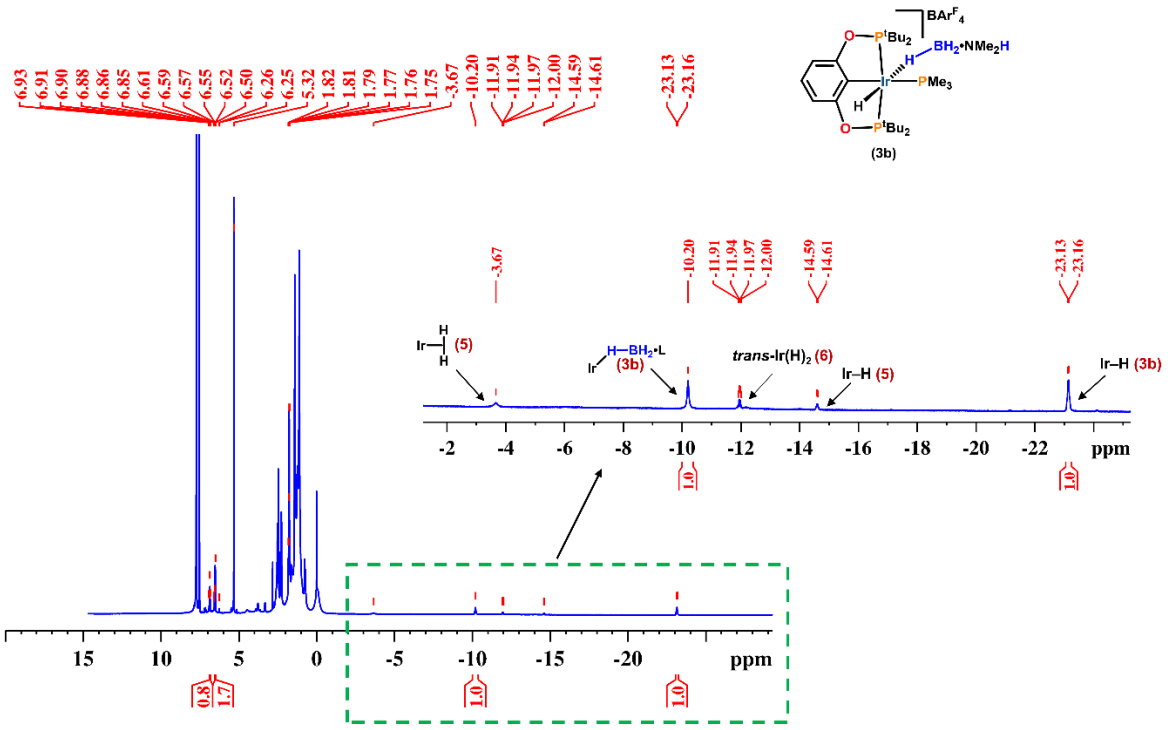


**Figure S107.** $^{1}$H NMR (500, $CD_2Cl_2$, 193 K) spectrum of the reaction mixture after 10 min of reaction of [Ir(H)($PMe_3$)($^{tBu4}$POCOP)][$BAr^F_4$] (**3**) with $H_3B{\cdot}NMe_2H$: formation of mixture of products, *trans*-[Ir(H)($\eta^1$-$HBH_2{\cdot}NMe_2H$)$PMe_3$($^{tBu4}$POCOP)][$BAr^F_4$] (**3b**), *trans*-[Ir(H)$_2$($PMe_3$)($^{tBu}$POCOP)] (**6**), and [Ir(H)($\eta^2$-$H_2$)($PMe_3$)($^{tBu4}$POCOP)][$BAr^F_4$] (**5**).

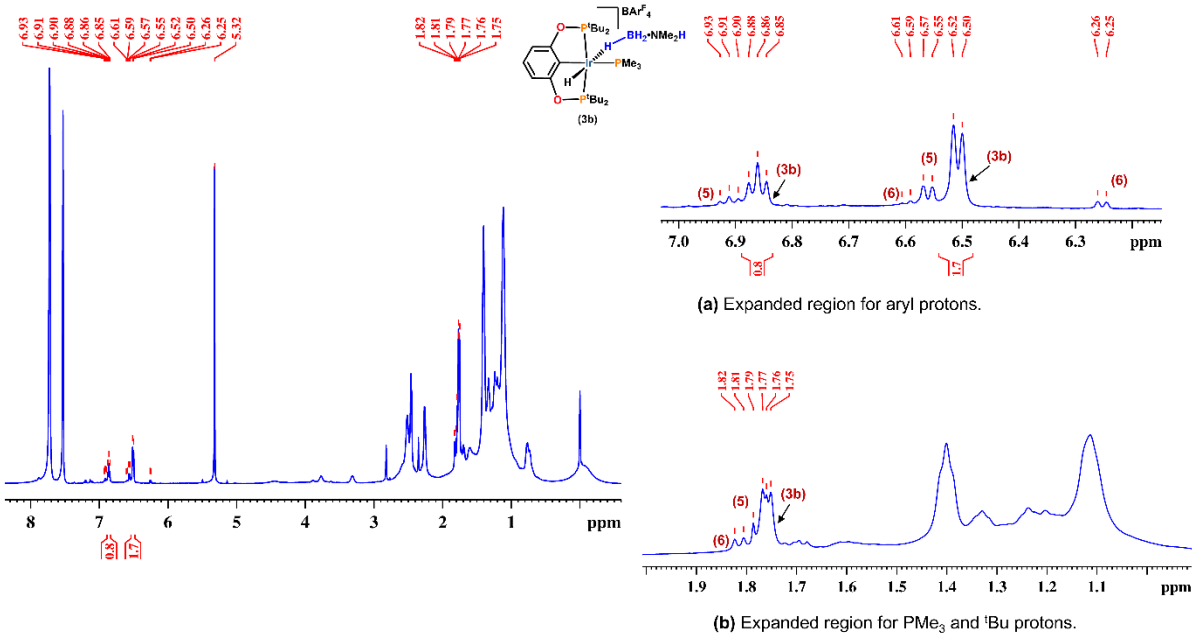


**Figure S108.** Partial $^{1}$H NMR (500, $CD_2Cl_2$, 193 K) spectrum (downfield region) of the reaction mixture after 10 min of reaction of [Ir(H)($PMe_3$)($^{tBu4}$POCOP)][$BAr^F_4$] (**3**) with $H_3B{\cdot}NMe_2H$: formation of mixture of products, *trans*-[Ir(H)($\eta^1$-$HBH_2{\cdot}NMe_2H$)$PMe_3$($^{tBu4}$POCOP)][$BAr^F_4$] (**3b**), *trans*-[Ir(H)$_2$($PMe_3$)($^{tBu}$POCOP)] (**6**), and [Ir(H)($\eta^2$-$H_2$)($PMe_3$)($^{tBu4}$POCOP)][$BAr^F_4$] (**5**).

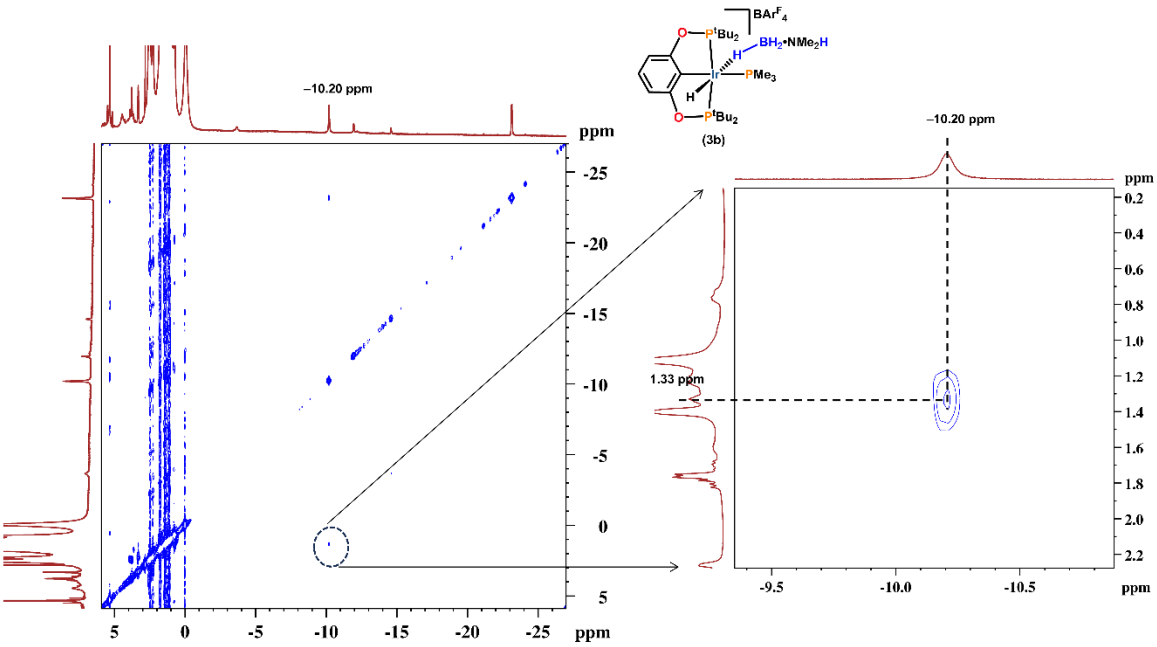


**Figure S109.** $^{1}$H-$^{1}$H COSY (500, $CD_2Cl_2$, 193 K) spectrum of *trans*-[Ir(H)($\eta^1$-$HBH_2{\cdot}NMe_2H$)$PMe_3$($^{tBu4}$POCOP)][$BAr^F_4$] complex (**3b**).

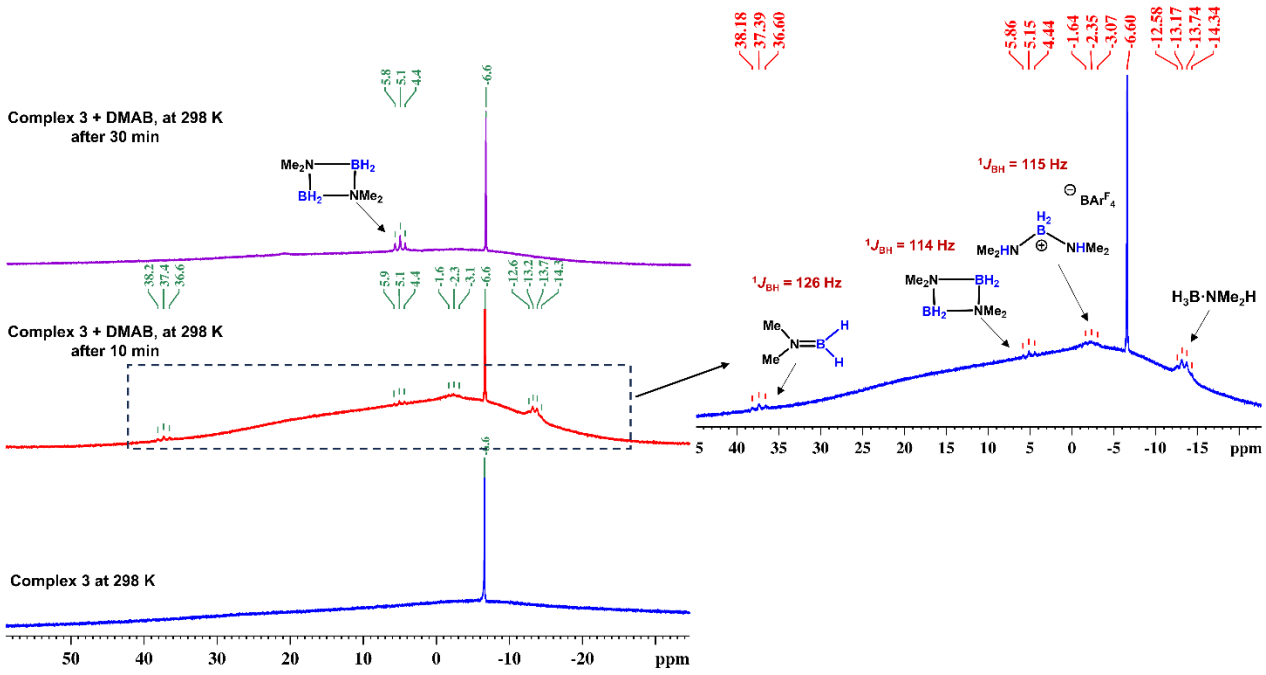


**Figure S110**. $^{11}$B NMR (160.4 MHz, $CD_2Cl_2$) spectral stack plot of monitoring of the reaction of [Ir(H)($PMe_3$)($^{tBu4}$POCOP)][$BAr^F_4$] (**3**) with $H_3B{\cdot}NMe_2H$.

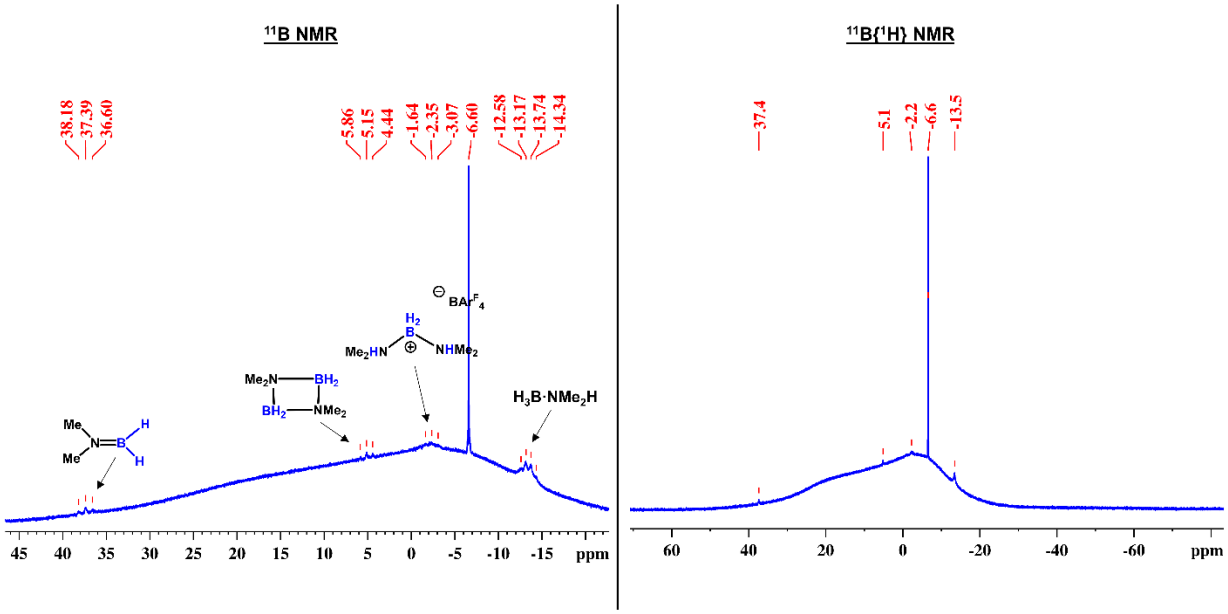


**Figure S111**. $^{11}B$ (left) and $^{11}B\{^1H\}$ (right) NMR (160.4 MHz, $CD_2Cl_2$) spectra of reaction of [Ir(H)($PMe_3$)($^{tBu4}$POCOP)][$BAr^F_4$] (**3**) with $H_3B{\cdot}NMe_2H$ after 10 min.

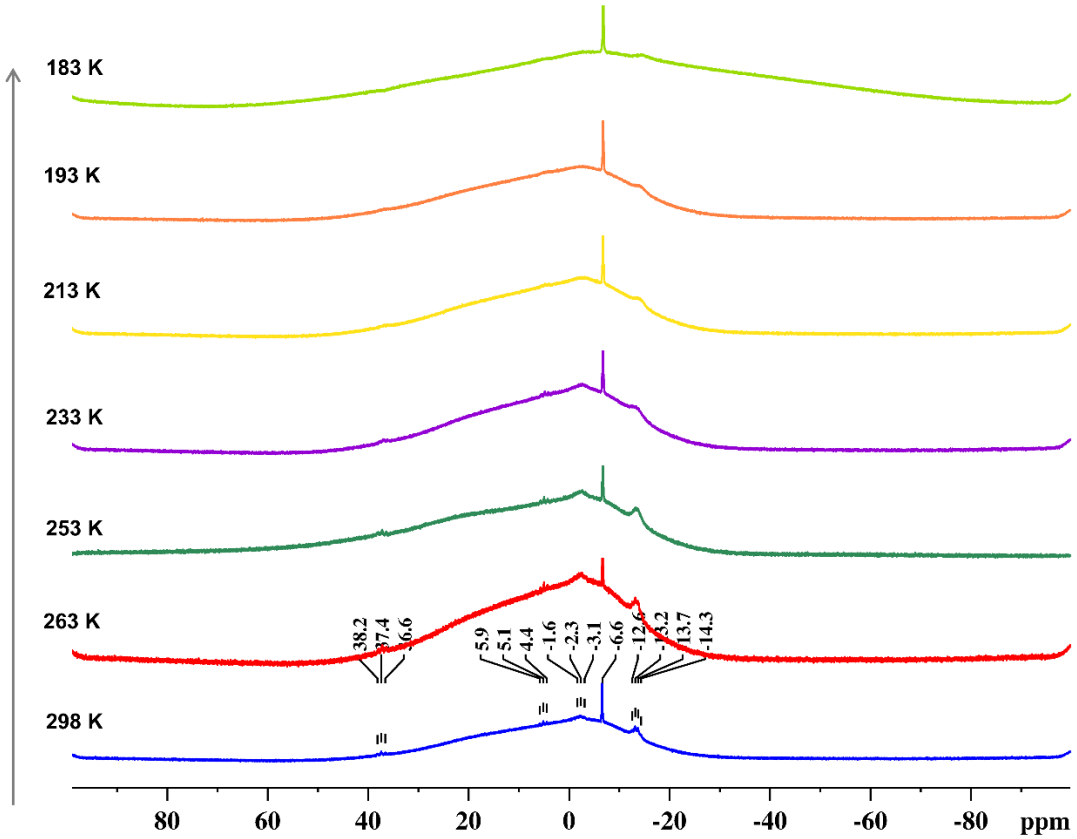


**Figure S112**. VT $^{11}B$ NMR (160.4 MHz, $CD_2Cl_2$) spectral stack plot of reaction of [Ir(H)($PMe_3$)($^{tBu4}$POCOP)][$BAr^F_4$] (**3**) with $H_3B{\cdot}NMe_2H$ after 10 min.

Spectral broadening occurs at low temperatures.

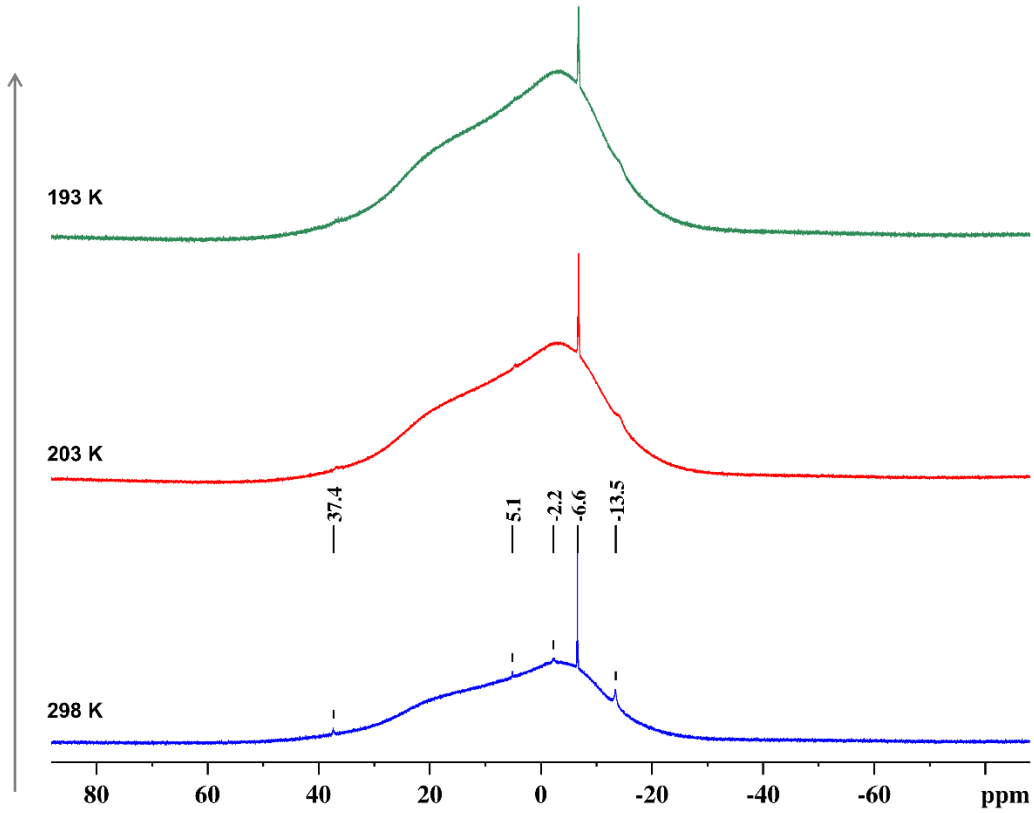


**Figure S113**. VT $^{11}B\{^{1}H\}$ NMR (160.4 MHz, $CD_2Cl_2$) spectral stack plot of reaction of [Ir(H)($PMe_3$)($^{tBu4}$POCOP)][$BAr^F_4$] (**3**) with $H_3B{\cdot}NMe_2H$ after 10 min.

Spectral broadening occurs at low temperatures.

## 11. Reaction of [Ir(H)(PMe$_3$)($^{tBu4}$POCOP)][BAr$^F_4$] (**3**) with H$_3$B·NMe$_3$.

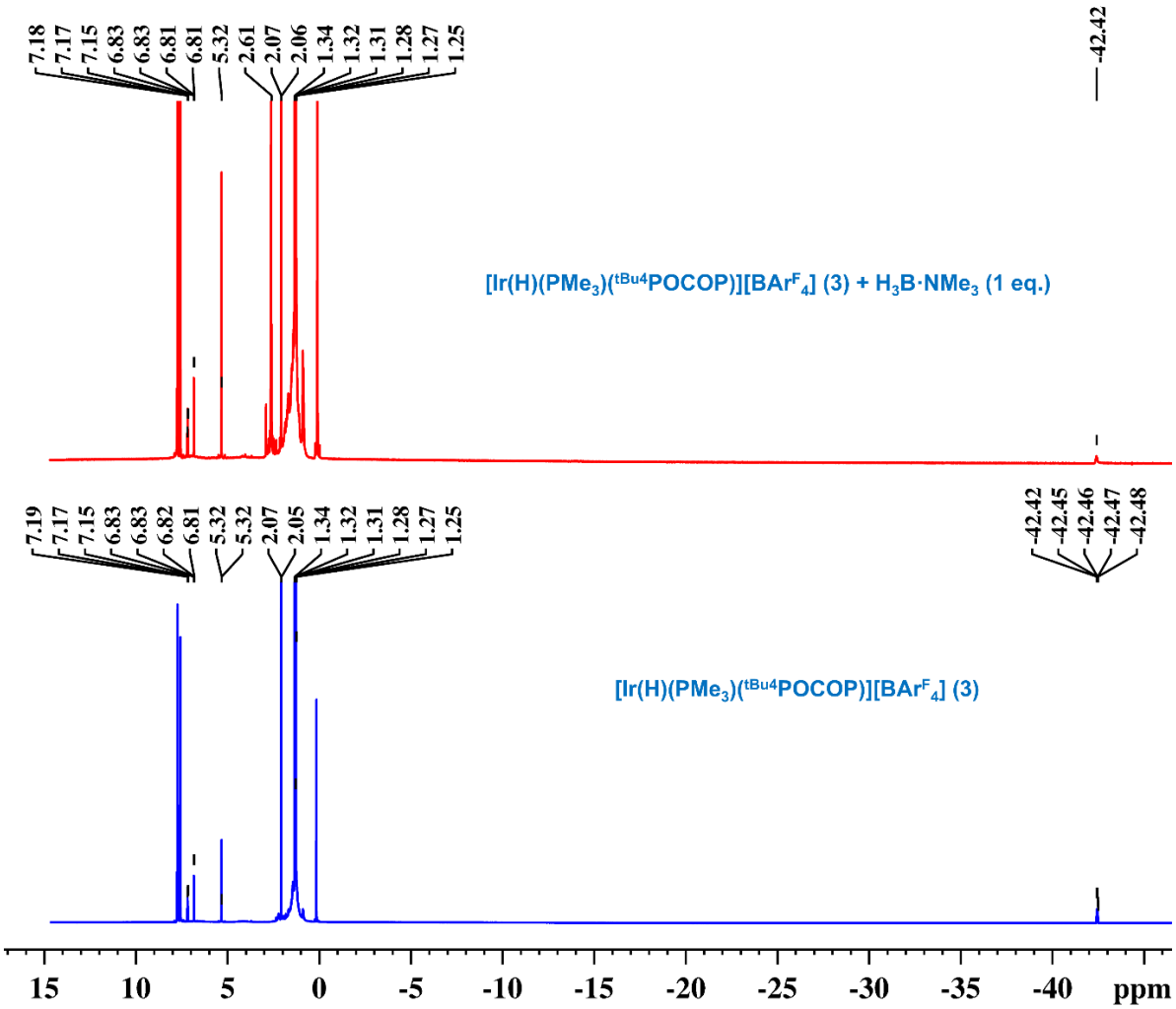


**Figure S114.** $^1$H NMR (500.0 MHz, $CD_2Cl_2$, 298 K) spectral stack plot of reaction of [Ir(H)(PMe$_3$)($^{tBu4}$POCOP)][BAr$^F_4$] (**3**) with H$_3$B·NMe$_3$.

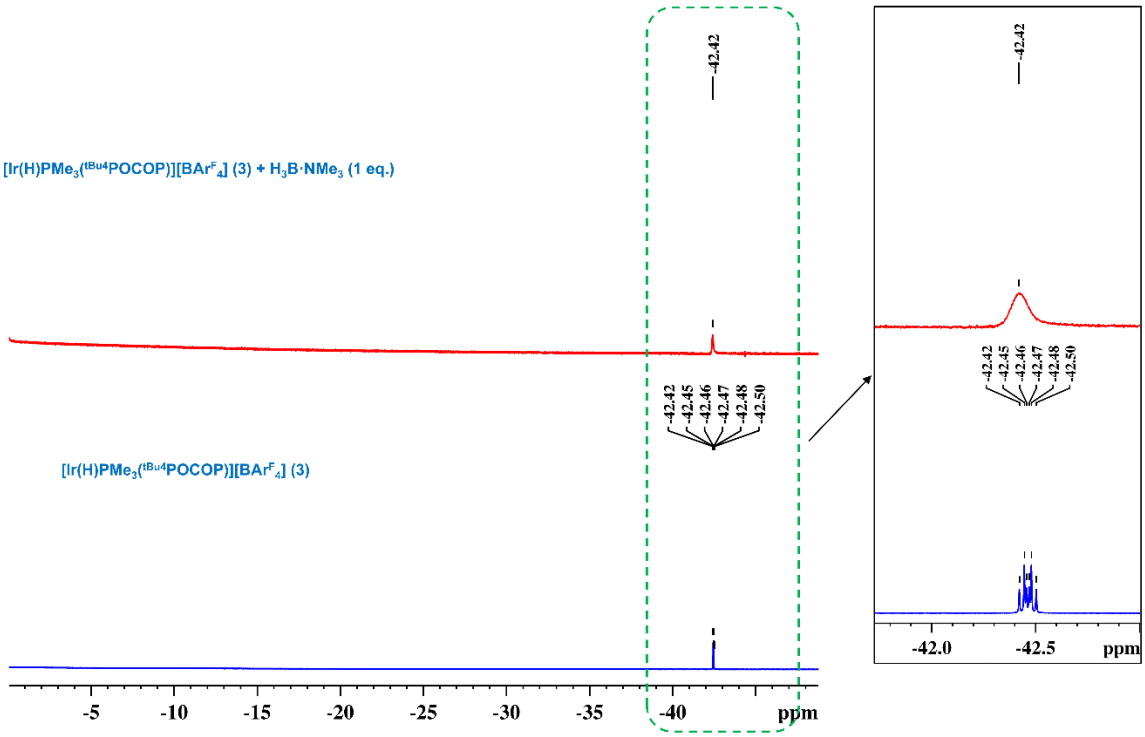


**Figure S115.** Partial $^{1}$H NMR (500.0 MHz, $CD_2Cl_2$, 298 K) spectral stack plot (hydride region) of reaction of [Ir(H)($PMe_3$)($^{tBu4}$POCOP)][$BAr^F_4$] (**3**) with $H_3B{\cdot}NMe_3$.

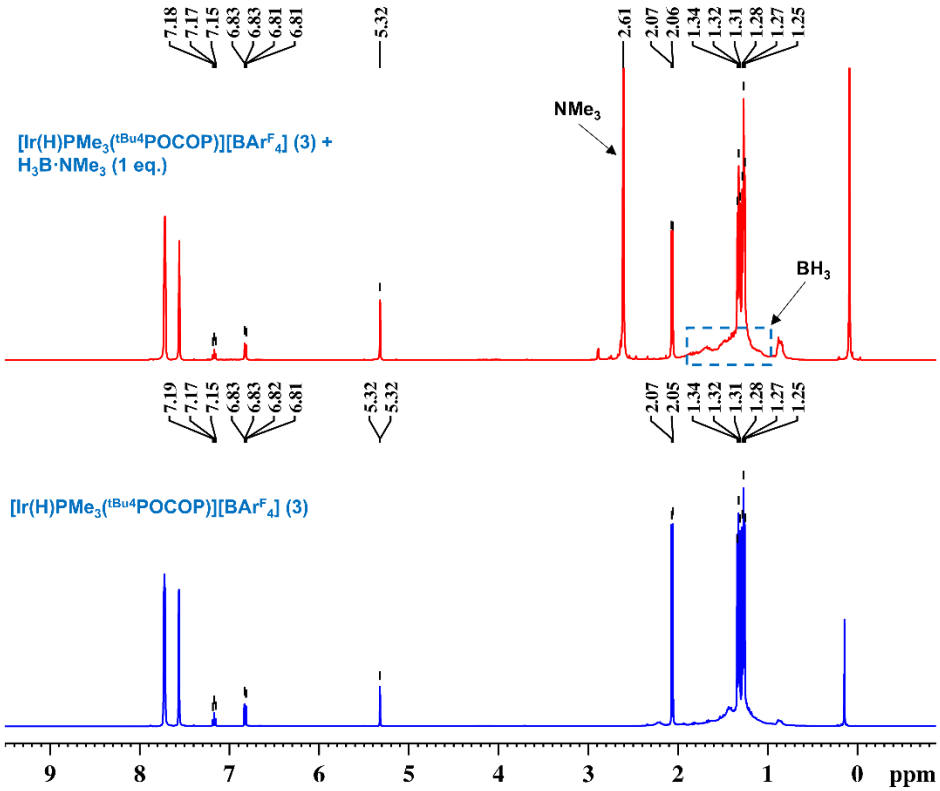


**Figure S116.** Partial $^{1}$H NMR (500.0 MHz, $CD_2Cl_2$, 298 K) spectral stack plot (downfield region) of reaction of [Ir(H)($PMe_3$)($^{tBu4}$POCOP)][$BAr^F_4$] (**3**) with $H_3B{\cdot}NMe_3$.

The quartet signal corresponding to $H_3B{\cdot}NMe_3$ at 1.70 ppm could not be assigned as it overlaps with $^{t}$Bu protons of complex **3**.

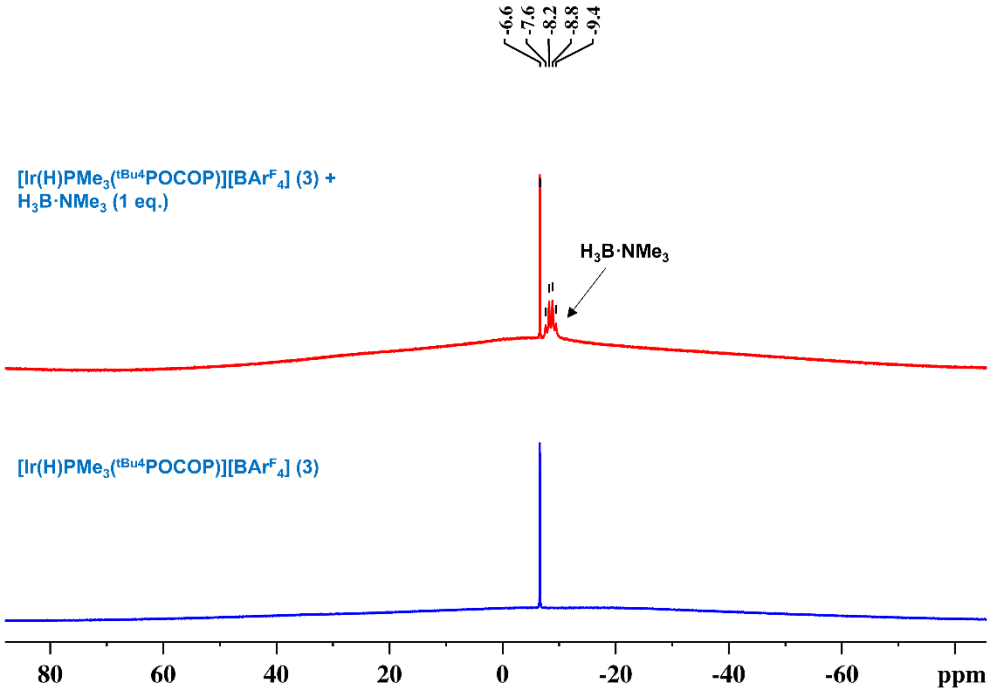


**Figure S117.** $^{11}$B NMR (160.4 MHz, $CD_2Cl_2$, 298 K) spectral stack plot of reaction of [Ir(H)($PMe_3$)($^{tBu4}$POCOP)][$BAr^F_4$] (**3**) with $H_3B{\cdot}NMe_3$.

## 12. Characterization of [Ir($PMe_3$)($^{tBu4}$POCOP)] (**7**) and its reaction with $H_2$ at 298 K.

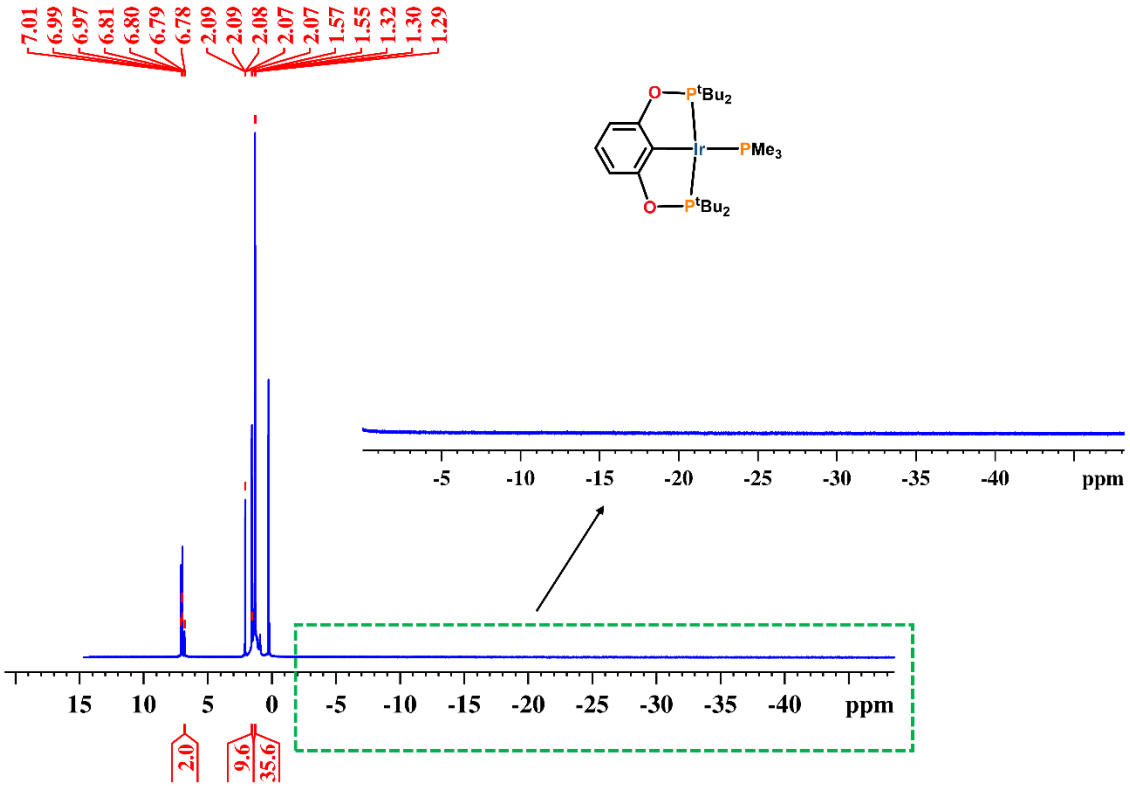


**Figure S118**. $^1$H NMR (400.0 MHz, Tol-$d_8$, 298 K) spectrum of [Ir($PMe_3$)($^{tBu4}$POCOP)] (**7**).

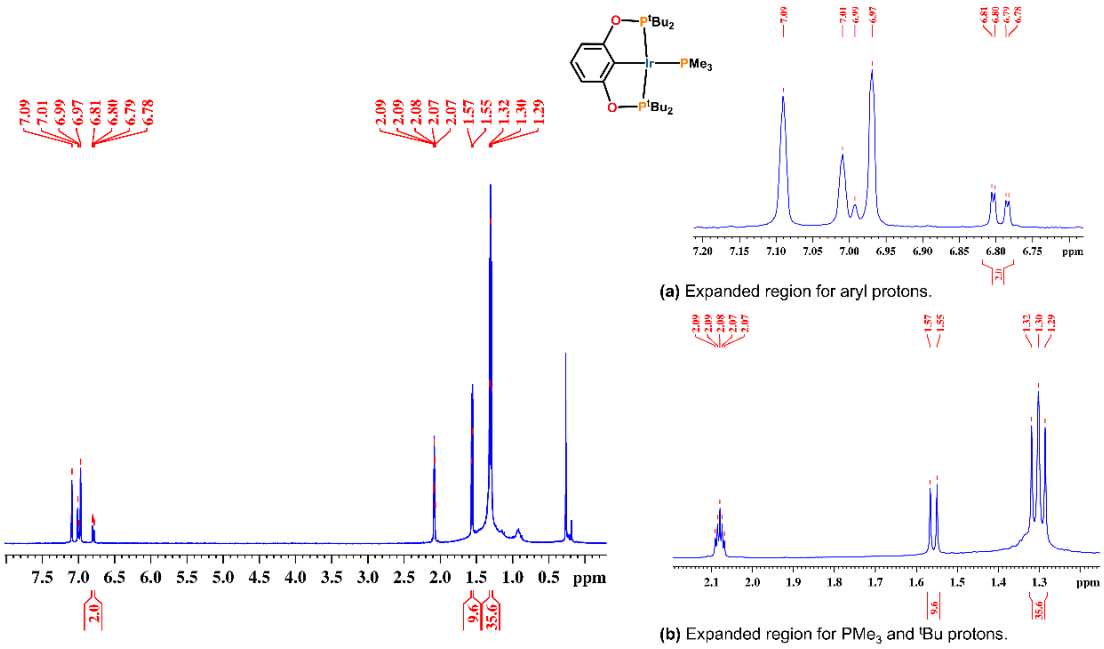


**Figure S119**. Partial $^{1}H$ NMR (400.0 MHz, Tol-$d_8$, 298 K) spectrum of [Ir($PMe_3$)($^{tBu4}$POCOP)] (**7**).

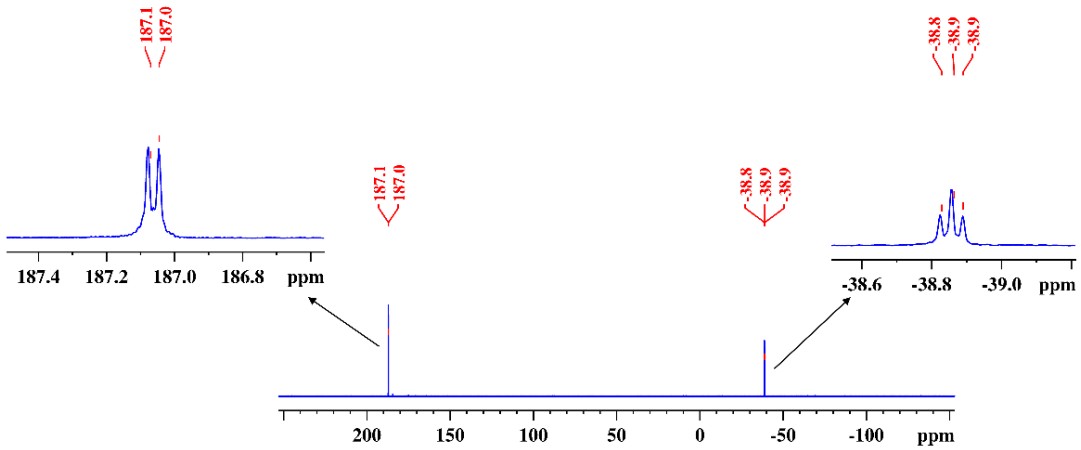

**Figure S120**. $^{31}P\{^{1}H\}$ NMR (161.9 MHz, Tol-$d_8$, 298 K) spectrum of [Ir($PMe_3$)($^{tBu4}$POCOP)] (**7**).

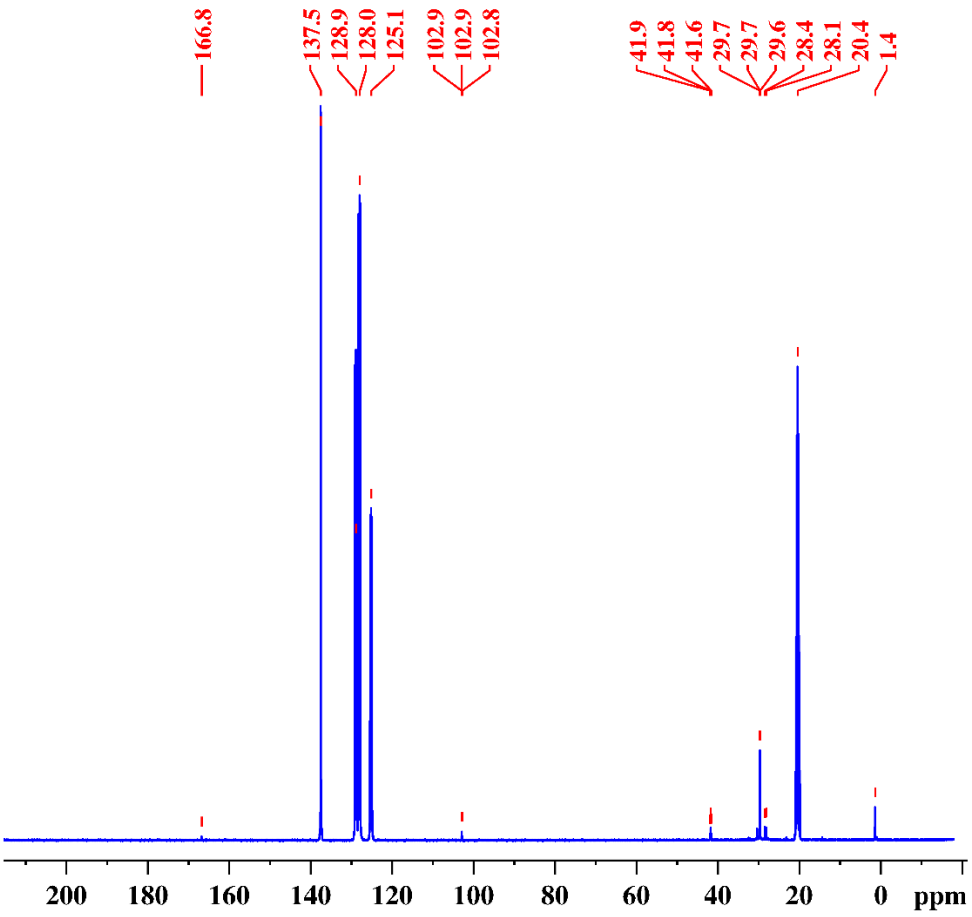


**Figure S121**. $^{13}C\{^{1}H\}$ NMR (100.6 MHz, Tol-$d_8$, 298 K) spectrum of [Ir($PMe_3$)($^{tBu4}$POCOP)] (**7**).

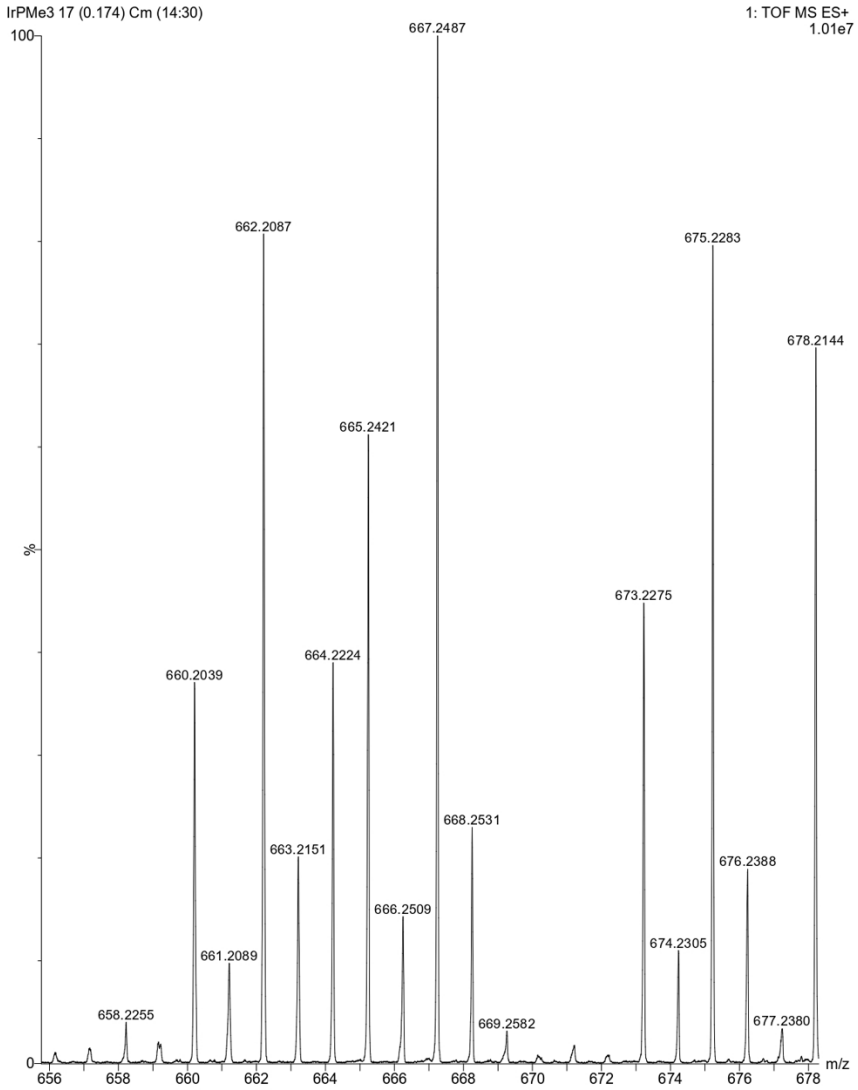


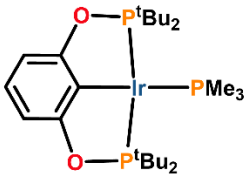


Exact mass calcd. $[M]^+$: 666.2491

Observed: 666.2509

**Figure S122**. HRMS spectrograph of [Ir(PMe$_3$)($^{tBu4}$POCOP)] (**7**).

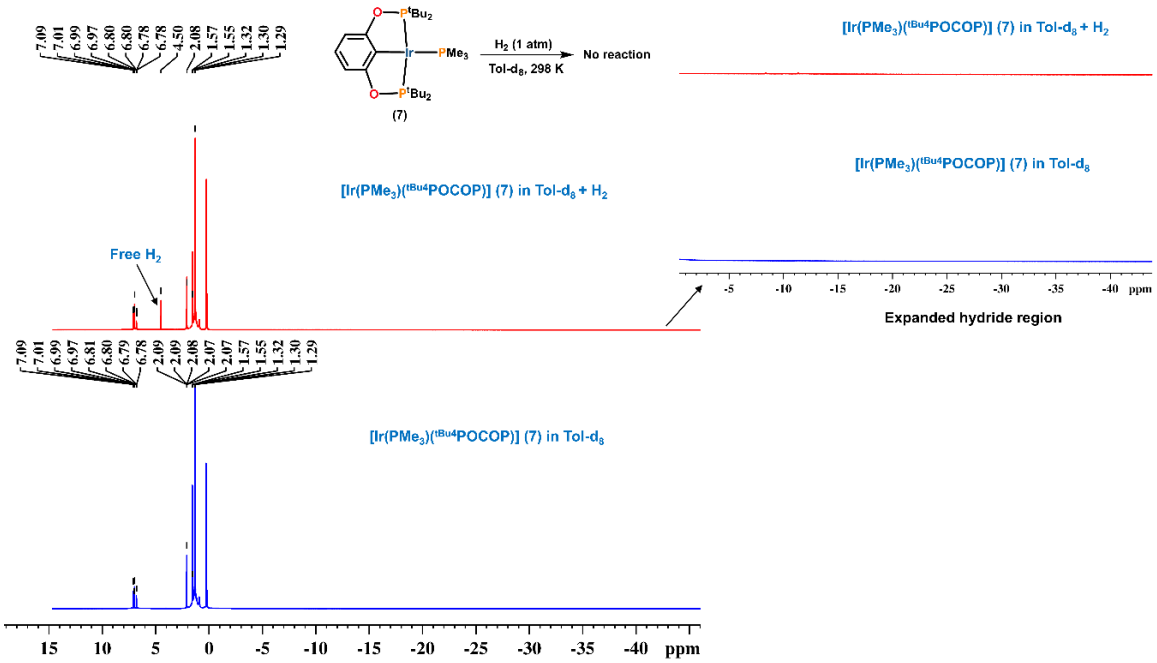


**Figure S123**. $^{1}$H NMR (400.0 MHz, Tol-$d_8$, 298 K) spectral stack plot of [Ir(PMe$_3$)($^{tBu4}$POCOP)] (**7**) (spectrum shown in blue color) and upon introducing $H_2$ to the reaction mixture (spectrum shown in red color).

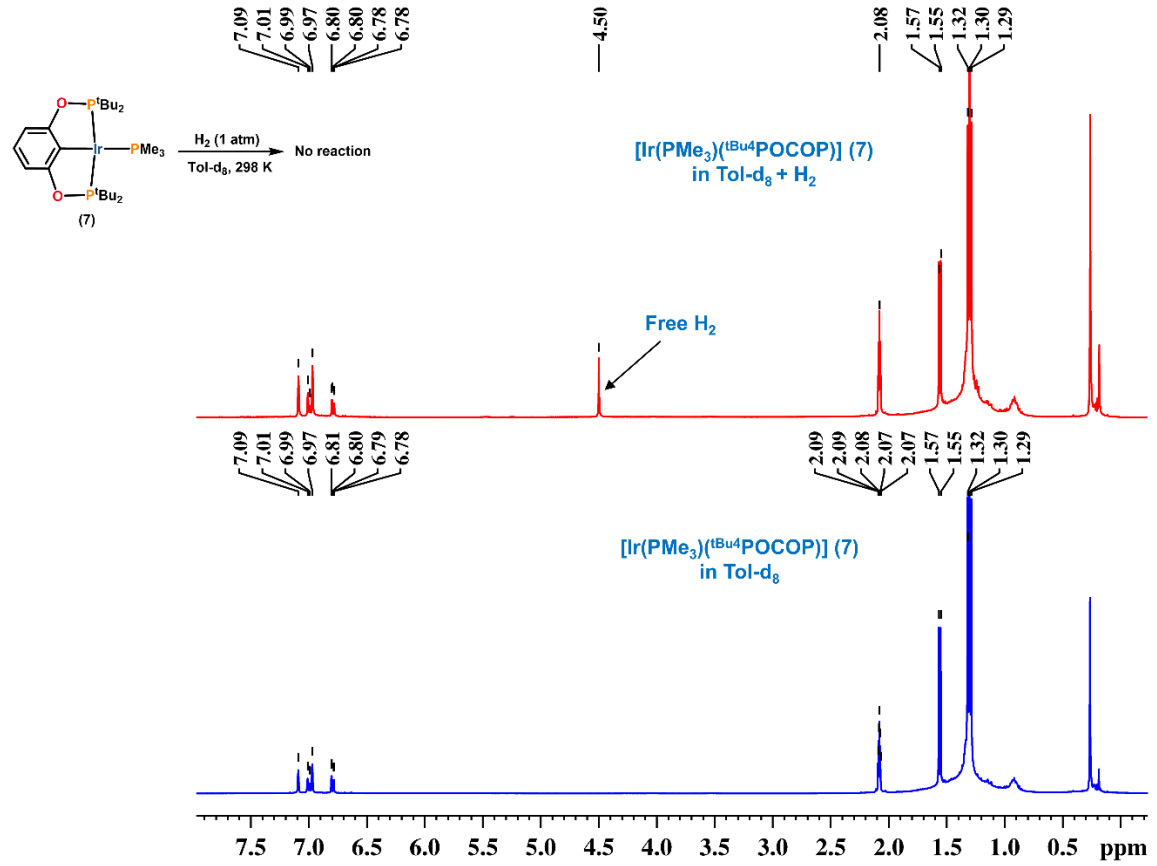


**Figure S124**. Partial $^{1}$H NMR (400.0 MHz, Tol-$d_8$, 298 K) spectral stack plot of [Ir(PMe$_3$)($^{tBu4}$POCOP)] (**7**) (spectrum shown in blue color) and upon introducing $H_2$ to the reaction mixture (spectrum shown in red color).

## 13. Crystallographic data for [Ir(H)($PMe_3$)($^{tBu4}$POCOP)][$BAr^F_4$] (**3**).

**Table S2.** Crystal data and structure refinement for [Ir(H)($PMe_3$)($^{tBu4}$POCOP)][$BAr^F_4$] (**3**).

| | |
|---|---|
| CCDC number | 2464181 |
| Identification code | [Ir(H)($PMe_3$)($^{tBu4}$POCOP)][$BAr^F_4$] (**3**) |
| Empirical formula | $C_{57}$ $H_{61}$ B $F_{24}$ Ir $O_2$ $P_3$ |
| Formula weight | 1529.97 |
| Temperature | 100(2) K |
| Wavelength | 0.71073 Å |
| Crystal system | Monoclinic |
| Space group | *P* $2_1$/n |
| Unit cell dimensions | a = 12.2359(5) Å<br>b = 39.5973(14) Å<br>c = 12.9688(4) Å<br>b = 93.8790(10)°. |
| Volume | 6269.1(4) Å$^3$ |
| Z | 4 |
| Density (calculated) | 1.621 mg/m$^3$ |
| Absorption coefficient | 2.318 mm$^{-1}$ |
| F(000) | 3048 |
| Crystal size | 0.390 x 0.220 x 0.140 mm$^3$ |
| Theta range for data collection | 2.442 to 30.530°. |
| Index ranges | -17<=h<=17,<br>-56<=k<=56,<br>-18<=l<=18 |
| Reflections collected | 200295 |
| Independent reflections | 19101 [R(int) = 0.0606] |
| Completeness to theta = 25.242° | 99.9 % |
| Absorption correction | Semi-empirical from equivalents |
| Max. and min. transmission | 0.7461 and 0.6420 |
| Refinement method | Full-matrix least-squares on $F^2$ |
| Data / restraints / parameters | 19101 / 597 / 912 |
| Goodness-of-fit on F2 | 1.139 |
| Final R indices [I>2sigma(I)] | R1 = 0.0436, wR2 = 0.0735 |
| R indices (all data) | R1 = 0.0529, wR2 = 0.0760 |
| Extinction coefficient | n/a |
| Largest diff. peak and hole | 1.123 and -3.151 e.Å$^{-3}$ |

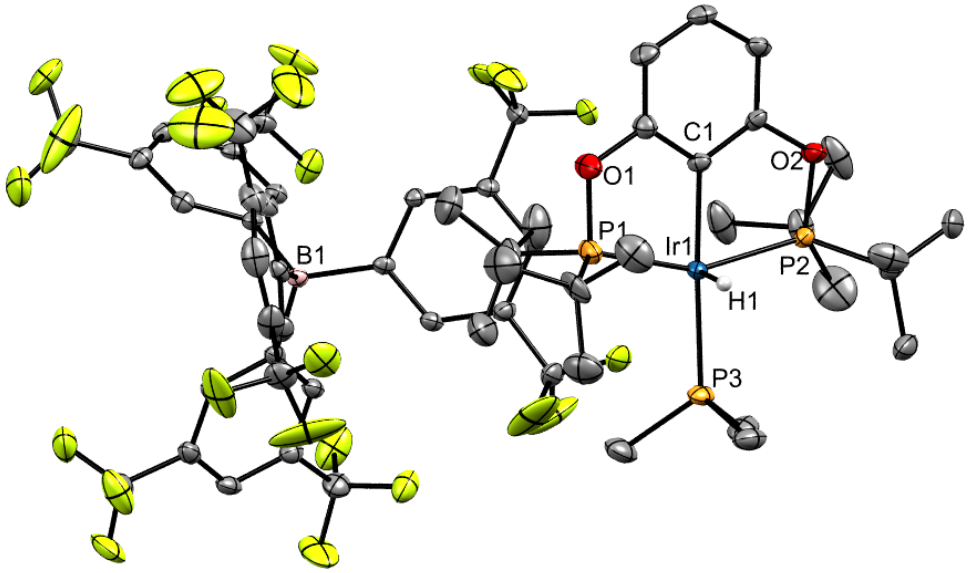


**Figure S125.** ORTEP view of complex [Ir(H)($PMe_3$)($^{tBu4}$POCOP)][$BAr^F_4$] (**3**) at 50% thermal ellipsoidal probability.

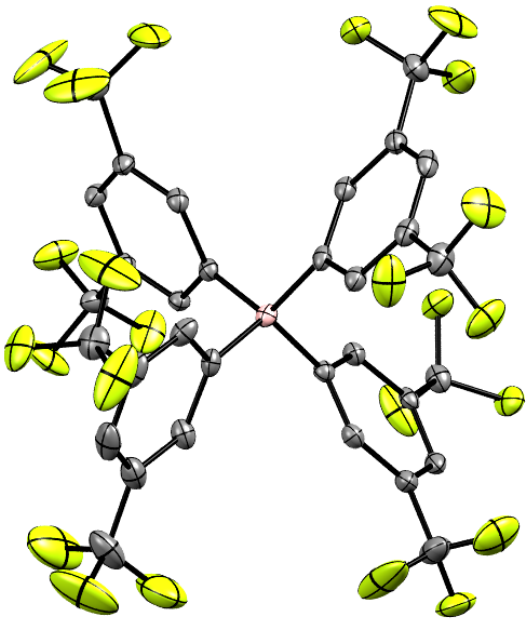

**Figure S126.** ORTEP view of complex [Ir(H)($PMe_3$)($^{tBu4}$POCOP)][$BAr^F_4$] (**3**) at 50% thermal ellipsoidal probability. Only $BAr^F_4$ counter anion has shown.

## 14. Computational Details.

**Optimized Cartesian Coordinates of all Stationary Points at PBE-D3/def2-TZVP level of theory**

Reactant (**3**)**:**

FINAL HEAT OF FORMATION = -2259.672814

| | | | | |
|---|---|---|---|---|
| Ir | 0.055694 | -0.605545 | -0.046124 | 0.000000 |
| P | -2.242920 | -0.171676 | -0.278029 | 0.000000 |
| P | 2.349367 | -0.093737 | 0.009859 | 0.000000 |

| | | | | |
|---|---|---|---|---|
| C | -3.086988 | -0.549630 | -1.924524 | 0.000000 |
| C | -2.252986 | 0.186643 | -2.993021 | 0.000000 |
| H | -1.204270 | -0.141684 | -2.998425 | 0.000000 |
| H | -2.276420 | 1.275296 | -2.858390 | 0.000000 |
| H | -2.683049 | -0.045444 | -3.979358 | 0.000000 |
| C | -3.067833 | -2.050310 | -2.230401 | 0.000000 |
| H | -3.542297 | -2.211330 | -3.210756 | 0.000000 |
| H | -3.627916 | -2.641680 | -1.494184 | 0.000000 |
| H | -2.042062 | -2.434370 | -2.290679 | 0.000000 |
| C | -4.530129 | -0.024883 | -1.962026 | 0.000000 |
| H | -4.898651 | -0.108943 | -2.996770 | 0.000000 |
| H | -4.596939 | 1.030207 | -1.666475 | 0.000000 |
| H | -5.199758 | -0.618387 | -1.326839 | 0.000000 |
| C | -3.306029 | -0.410732 | 1.272199 | 0.000000 |
| C | -3.733895 | -1.870861 | 1.451367 | 0.000000 |
| H | -0.957667 | -2.823565 | 2.656742 | 0.000000 |
| H | -4.382571 | -2.219592 | 0.635989 | 0.000000 |
| H | -4.306471 | -1.957344 | 2.387560 | 0.000000 |
| C | -4.548389 | 0.496135 | 1.305812 | 0.000000 |
| H | -4.975575 | 0.441180 | 2.319764 | 0.000000 |
| H | -5.324383 | 0.170588 | 0.604832 | 0.000000 |
| H | -4.301039 | 1.544337 | 1.099294 | 0.000000 |
| C | -2.367633 | 0.010203 | 2.423711 | 0.000000 |
| H | -2.894173 | -0.124608 | 3.381467 | 0.000000 |
| H | -2.071878 | 1.065810 | 2.346932 | 0.000000 |
| H | -1.453938 | -0.603591 | 2.459649 | 0.000000 |
| O | -2.356423 | 1.500955 | -0.346326 | 0.000000 |
| C | -1.169519 | 2.188914 | -0.282210 | 0.000000 |
| C | -1.216460 | 3.583741 | -0.323654 | 0.000000 |
| H | -2.176055 | 4.095287 | -0.400410 | 0.000000 |
| C | -0.012584 | 4.291587 | -0.267913 | 0.000000 |
| H | -0.029065 | 5.382109 | -0.299792 | 0.000000 |
| C | 1.212067 | 3.624882 | -0.172549 | 0.000000 |
| H | 2.156133 | 4.168356 | -0.131145 | 0.000000 |

| | | | | |
|---|---|---|---|---|
| C | 1.207180 | 2.229208 | -0.133958 | 0.000000 |
| O | 2.415166 | 1.581707 | -0.047550 | 0.000000 |
| C | 3.216746 | -0.301302 | 1.681759 | 0.000000 |
| C | 2.126368 | 0.076028 | 2.707810 | 0.000000 |
| H | 2.535115 | -0.042292 | 3.723390 | 0.000000 |
| H | 1.240129 | -0.573444 | 2.631232 | 0.000000 |
| H | 1.800859 | 1.119511 | 2.594394 | 0.000000 |
| C | 4.408630 | 0.652344 | 1.872117 | 0.000000 |
| H | 4.714482 | 0.599225 | 2.928960 | 0.000000 |
| H | 4.145148 | 1.692738 | 1.647364 | 0.000000 |
| H | 5.275096 | 0.368464 | 1.265220 | 0.000000 |
| C | 3.675515 | -1.745314 | 1.908818 | 0.000000 |
| H | 4.437821 | -2.060163 | 1.183354 | 0.000000 |
| H | 4.123805 | -1.818104 | 2.911818 | 0.000000 |
| C | 3.406367 | -0.441305 | -1.516519 | 0.000000 |
| C | 4.826425 | 0.127242 | -1.373456 | 0.000000 |
| H | 4.822947 | 1.183901 | -1.076029 | 0.000000 |
| H | 5.325564 | 0.053710 | -2.352267 | 0.000000 |
| H | 5.427321 | -0.445510 | -0.655648 | 0.000000 |
| C | 3.471247 | -1.941163 | -1.820220 | 0.000000 |
| H | 4.065785 | -2.084607 | -2.735474 | 0.000000 |
| H | 2.472682 | -2.356621 | -2.003787 | 0.000000 |
| H | 3.956129 | -2.516171 | -1.020640 | 0.000000 |
| C | 2.690687 | 0.271232 | -2.682748 | 0.000000 |
| H | 2.664646 | 1.359934 | -2.549212 | 0.000000 |
| H | 1.660784 | -0.088506 | -2.818342 | 0.000000 |
| H | 3.247114 | 0.053039 | -3.607225 | 0.000000 |
| C | 0.029869 | 1.458113 | -0.180496 | 0.000000 |
| H | 2.843116 | -2.457918 | 1.877933 | 0.000000 |
| H | 0.154754 | -1.036273 | -1.526569 | 0.000000 |
| P | 0.064409 | -2.950494 | 0.432286 | 0.000000 |
| C | -0.039910 | -3.258345 | 2.242718 | 0.000000 |
| H | 0.817269 | -2.809363 | 2.759055 | 0.000000 |
| H | -2.877016 | -2.549399 | 1.536749 | 0.000000 |

| | | | | |
|---|---|---|---|---|
| H | -0.042000 | -4.341359 | 2.429347 | 0.000000 |
| C | 1.483141 | -4.014020 | -0.045913 | 0.000000 |
| H | 1.340462 | -5.008068 | 0.400741 | 0.000000 |
| H | 1.500733 | -4.119468 | -1.137905 | 0.000000 |
| H | 2.441573 | -3.607094 | 0.284275 | 0.000000 |
| C | -1.251258 | -4.056871 | -0.213674 | 0.000000 |
| H | -1.133612 | -5.047061 | 0.248419 | 0.000000 |
| H | -2.255023 | -3.680437 | -0.003452 | 0.000000 |
| H | -1.132248 | -4.160106 | -1.299627 | 0.000000 |

Product (**6**):

FINAL HEAT OF FORMATION = -2260.408723

| | | | | |
|---|---|---|---|---|
| Ir | 0.046429 | -0.611599 | 0.090105 | 0.000000 |
| P | -2.220359 | -0.174244 | -0.188121 | 0.000000 |
| P | 2.314956 | -0.099914 | 0.098579 | 0.000000 |
| C | -2.962637 | -0.528892 | -1.914777 | 0.000000 |
| C | -2.171614 | 0.359747 | -2.895931 | 0.000000 |
| H | -1.089025 | 0.200286 | -2.796336 | 0.000000 |
| H | -2.387654 | 1.425209 | -2.742288 | 0.000000 |
| H | -2.471930 | 0.092064 | -3.921633 | 0.000000 |
| C | -2.741715 | -1.996596 | -2.295307 | 0.000000 |
| H | -3.085638 | -2.152665 | -3.330628 | 0.000000 |
| H | -3.306890 | -2.685691 | -1.653115 | 0.000000 |
| H | -1.675893 | -2.252587 | -2.243447 | 0.000000 |
| C | -4.451533 | -0.183465 | -2.048659 | 0.000000 |
| H | -4.733448 | -0.281764 | -3.109830 | 0.000000 |
| H | -4.667424 | 0.848249 | -1.740978 | 0.000000 |
| H | -5.091327 | -0.868946 | -1.477574 | 0.000000 |
| C | -3.493132 | -0.443527 | 1.215022 | 0.000000 |
| C | -3.909151 | -1.915532 | 1.320629 | 0.000000 |
| H | -0.973372 | -2.831527 | 2.805777 | 0.000000 |
| H | -4.368695 | -2.294695 | 0.396640 | 0.000000 |
| H | -4.654362 | -2.019624 | 2.125669 | 0.000000 |
| C | -4.750808 | 0.437800 | 1.078760 | 0.000000 |

| | | | | |
|---|---|---|---|---|
| H | -5.289061 | 0.405601 | 2.039551 | 0.000000 |
| H | -5.440531 | 0.082298 | 0.307200 | 0.000000 |
| H | -4.496603 | 1.484470 | 0.870140 | 0.000000 |
| C | -2.781522 | -0.027195 | 2.515263 | 0.000000 |
| H | -3.477723 | -0.175615 | 3.356478 | 0.000000 |
| H | -2.491663 | 1.033134 | 2.492706 | 0.000000 |
| H | -1.872372 | -0.613454 | 2.691666 | 0.000000 |
| O | -2.357160 | 1.502147 | -0.215724 | 0.000000 |
| C | -1.163471 | 2.194258 | -0.236834 | 0.000000 |
| C | -1.210611 | 3.588976 | -0.340816 | 0.000000 |
| H | -2.172996 | 4.095191 | -0.430746 | 0.000000 |
| C | -0.007685 | 4.302620 | -0.319058 | 0.000000 |
| H | -0.020466 | 5.391011 | -0.400421 | 0.000000 |
| C | 1.211124 | 3.628766 | -0.186653 | 0.000000 |
| H | 2.160062 | 4.166334 | -0.155324 | 0.000000 |
| C | 1.196873 | 2.233029 | -0.086148 | 0.000000 |
| O | 2.399883 | 1.580011 | 0.088447 | 0.000000 |
| C | 3.412566 | -0.334170 | 1.649929 | 0.000000 |
| C | 2.530984 | 0.046950 | 2.853534 | 0.000000 |
| H | 3.124355 | -0.080565 | 3.773420 | 0.000000 |
| H | 1.630088 | -0.574177 | 2.916200 | 0.000000 |
| H | 2.205889 | 1.095718 | 2.797913 | 0.000000 |
| C | 4.644350 | 0.593423 | 1.673017 | 0.000000 |
| H | 5.060141 | 0.575124 | 2.693413 | 0.000000 |
| H | 4.379386 | 1.631120 | 1.435371 | 0.000000 |
| H | 5.437016 | 0.267303 | 0.992939 | 0.000000 |
| C | 3.866302 | -1.790703 | 1.801941 | 0.000000 |
| H | 4.450093 | -2.145949 | 0.940493 | 0.000000 |
| H | 4.509735 | -1.873927 | 2.692317 | 0.000000 |
| C | 3.278576 | -0.423560 | -1.521445 | 0.000000 |
| C | 4.758382 | -0.020905 | -1.469465 | 0.000000 |
| H | 4.893036 | 1.016817 | -1.137043 | 0.000000 |
| H | 5.174531 | -0.103139 | -2.487094 | 0.000000 |
| H | 5.348210 | -0.683885 | -0.822956 | 0.000000 |

| | | | | |
|---|---|---|---|---|
| C | 3.162156 | -1.897311 | -1.923873 | 0.000000 |
| H | 3.638828 | -2.036072 | -2.907773 | 0.000000 |
| H | 2.108946 | -2.194846 | -2.005861 | 0.000000 |
| H | 3.668171 | -2.566956 | -1.215096 | 0.000000 |
| C | 2.581999 | 0.437357 | -2.594694 | 0.000000 |
| H | 2.737513 | 1.509630 | -2.417639 | 0.000000 |
| H | 1.502214 | 0.236843 | -2.629043 | 0.000000 |
| H | 3.016050 | 0.183661 | -3.575103 | 0.000000 |
| C | 0.026976 | 1.464225 | -0.129536 | 0.000000 |
| H | 3.015492 | -2.466059 | 1.956813 | 0.000000 |
| H | 0.149479 | -0.974744 | -1.550293 | 0.000000 |
| P | 0.051642 | -2.917747 | 0.600325 | 0.000000 |
| C | -0.054171 | -3.275185 | 2.402244 | 0.000000 |
| H | 0.796299 | -2.806574 | 2.914013 | 0.000000 |
| H | -3.060381 | -2.558785 | 1.583778 | 0.000000 |
| H | -0.050657 | -4.357362 | 2.596288 | 0.000000 |
| C | 1.465479 | -3.996494 | 0.112849 | 0.000000 |
| H | 1.327819 | -4.993928 | 0.554930 | 0.000000 |
| H | 1.478349 | -4.091766 | -0.980022 | 0.000000 |
| H | 2.426335 | -3.589320 | 0.436157 | 0.000000 |
| C | -1.253567 | -4.043010 | -0.055723 | 0.000000 |
| H | -1.136220 | -5.036205 | 0.401315 | 0.000000 |
| H | -2.260369 | -3.670597 | 0.147881 | 0.000000 |
| H | -1.129883 | -4.135088 | -1.141878 | 0.000000 |
| H | -0.050862 | -0.302263 | 1.717840 | 0.000000 |

$H_3B{\cdot}THF$:

FINAL HEAT OF FORMATION = -258.847807

| | | | | |
|---|---|---|---|---|
| B | 2.254992 | 0.005220 | 0.236851 | 0.000000 |
| H | 2.722703 | -1.076570 | -0.072604 | 0.000000 |
| H | 2.768622 | 0.939185 | -0.353487 | 0.000000 |
| H | 2.201786 | 0.175837 | 1.448624 | 0.000000 |
| C | -0.050333 | 1.204936 | -0.137664 | 0.000000 |
| O | 0.751670 | -0.036704 | -0.282959 | 0.000000 |

| | | | | |
|---|---|---|---|---|
| C | -0.066911 | -1.190740 | 0.123219 | 0.000000 |
| C | -1.477115 | -0.738749 | -0.190329 | 0.000000 |
| C | -1.450400 | 0.735443 | 0.247095 | 0.000000 |
| H | 0.436966 | 1.824705 | 0.625050 | 0.000000 |
| H | -0.003254 | 1.702759 | -1.113811 | 0.000000 |
| H | 0.298664 | -2.046167 | -0.455647 | 0.000000 |
| H | 0.095031 | -1.362446 | 1.199125 | 0.000000 |
| H | -1.677012 | -0.828590 | -1.267831 | 0.000000 |
| H | -2.225423 | -1.328136 | 0.354036 | 0.000000 |
| H | -2.225981 | 1.336606 | -0.243203 | 0.000000 |
| H | -1.593058 | 0.810447 | 1.334228 | 0.000000 |

**3a-Int**:

FINAL HEAT OF FORMATION = -2518.545100

| | | | | |
|---|---|---|---|---|
| Ir | 0.050490 | 0.368485 | 0.321712 | 0.000000 |
| P | 2.157730 | 0.185477 | 1.404300 | 0.000000 |
| P | -1.418353 | -0.304049 | -1.407652 | 0.000000 |
| C | 3.624484 | 0.700466 | 0.303100 | 0.000000 |
| C | 3.511854 | -0.045556 | -1.037904 | 0.000000 |
| H | 2.666672 | 0.312782 | -1.636222 | 0.000000 |
| H | 3.419143 | -1.132467 | -0.910307 | 0.000000 |
| H | 4.427571 | 0.149574 | -1.616665 | 0.000000 |
| C | 3.570481 | 2.211114 | 0.026828 | 0.000000 |
| H | 4.371587 | 2.469200 | -0.683102 | 0.000000 |
| H | 3.721482 | 2.817141 | 0.928425 | 0.000000 |
| H | 2.615103 | 2.497704 | -0.435829 | 0.000000 |
| C | 4.976429 | 0.310139 | 0.924632 | 0.000000 |
| H | 5.768402 | 0.550301 | 0.198351 | 0.000000 |
| H | 5.028988 | -0.767919 | 1.129445 | 0.000000 |
| H | 5.205057 | 0.858068 | 1.844970 | 0.000000 |
| C | 2.584407 | 0.575515 | 3.235251 | 0.000000 |
| C | 3.195718 | 1.970304 | 3.438518 | 0.000000 |
| H | -2.319188 | 2.431037 | 2.265033 | 0.000000 |
| H | 4.206892 | 2.058661 | 3.025085 | 0.000000 |

| | | | | |
|---|---|---|---|---|
| H | 3.271498 | 2.149686 | 4.522647 | 0.000000 |
| C | 3.531640 | -0.481701 | 3.838083 | 0.000000 |
| H | 3.687675 | -0.215438 | 4.896095 | 0.000000 |
| H | 4.513816 | -0.512492 | 3.355954 | 0.000000 |
| H | 3.096359 | -1.486999 | 3.801394 | 0.000000 |
| C | 1.258355 | 0.492307 | 3.998421 | 0.000000 |
| H | 1.448129 | 0.670860 | 5.068643 | 0.000000 |
| H | 0.810600 | -0.502870 | 3.890829 | 0.000000 |
| H | 0.524827 | 1.228190 | 3.650887 | 0.000000 |
| O | 2.411112 | -1.472546 | 1.486798 | 0.000000 |
| C | 1.522631 | -2.270942 | 0.794411 | 0.000000 |
| C | 1.731370 | -3.654293 | 0.799898 | 0.000000 |
| H | 2.582183 | -4.076669 | 1.335432 | 0.000000 |
| C | 0.826601 | -4.467119 | 0.109838 | 0.000000 |
| H | 0.969137 | -5.548883 | 0.108129 | 0.000000 |
| C | -0.253515 | -3.912729 | -0.585894 | 0.000000 |
| H | -0.955649 | -4.536736 | -1.139648 | 0.000000 |
| C | -0.417325 | -2.525582 | -0.560740 | 0.000000 |
| O | -1.485435 | -1.972603 | -1.247386 | 0.000000 |
| C | -3.284830 | 0.017572 | -1.476558 | 0.000000 |
| C | -3.780231 | -0.093162 | -0.029160 | 0.000000 |
| H | -4.855998 | 0.141207 | -0.002237 | 0.000000 |
| H | -3.261738 | 0.592066 | 0.646400 | 0.000000 |
| H | -3.643684 | -1.110426 | 0.361260 | 0.000000 |
| C | -4.068199 | -1.021983 | -2.302005 | 0.000000 |
| H | -5.138622 | -0.872838 | -2.088076 | 0.000000 |
| H | -3.808524 | -2.048217 | -2.013885 | 0.000000 |
| H | -3.933146 | -0.913275 | -3.381361 | 0.000000 |
| C | -3.545270 | 1.431209 | -2.015900 | 0.000000 |
| H | -3.288935 | 1.530036 | -3.078563 | 0.000000 |
| H | -4.617348 | 1.658524 | -1.911227 | 0.000000 |
| C | -0.649076 | -0.138192 | -3.149683 | 0.000000 |
| C | -1.589975 | -0.582693 | -4.280652 | 0.000000 |
| H | -1.961193 | -1.604609 | -4.129221 | 0.000000 |

| | | | | |
|---|---|---|---|---|
| H | -1.012048 | -0.575917 | -5.218538 | 0.000000 |
| H | -2.440888 | 0.094511 | -4.420320 | 0.000000 |
| C | -0.210825 | 1.310890 | -3.403783 | 0.000000 |
| H | 0.263623 | 1.364797 | -4.395900 | 0.000000 |
| H | 0.521677 | 1.656894 | -2.663494 | 0.000000 |
| H | -1.058242 | 2.009923 | -3.407570 | 0.000000 |
| C | 0.579305 | -1.066940 | -3.199396 | 0.000000 |
| H | 0.283563 | -2.124052 | -3.190615 | 0.000000 |
| H | 1.272200 | -0.901878 | -2.369520 | 0.000000 |
| H | 1.117039 | -0.872501 | -4.140455 | 0.000000 |
| C | 0.442989 | -1.667750 | 0.139076 | 0.000000 |
| H | -2.993879 | 2.200359 | -1.459253 | 0.000000 |
| H | 0.951856 | 0.810538 | -0.880038 | 0.000000 |
| P | -0.528493 | 2.654685 | 0.638866 | 0.000000 |
| C | -2.196571 | 2.988877 | 1.327175 | 0.000000 |
| H | -2.982783 | 2.680804 | 0.629662 | 0.000000 |
| H | 2.580195 | 2.774341 | 3.023256 | 0.000000 |
| H | -2.301903 | 4.064624 | 1.526858 | 0.000000 |
| C | -0.480689 | 3.737772 | -0.839764 | 0.000000 |
| H | -0.756078 | 4.763420 | -0.557515 | 0.000000 |
| H | 0.534438 | 3.740496 | -1.258824 | 0.000000 |
| H | -1.171216 | 3.378596 | -1.610341 | 0.000000 |
| C | 0.478875 | 3.666557 | 1.787713 | 0.000000 |
| H | 0.081132 | 4.690640 | 1.819292 | 0.000000 |
| H | 0.441150 | 3.240769 | 2.797216 | 0.000000 |
| H | 1.518513 | 3.699623 | 1.442226 | 0.000000 |
| B | -1.794942 | -0.349745 | 2.814831 | 0.000000 |
| H | -2.936251 | -0.587681 | 2.500705 | 0.000000 |
| H | -1.105690 | -0.187250 | 1.739770 | 0.000000 |
| H | -1.628406 | 0.585065 | 3.557008 | 0.000000 |
| C | -1.409212 | -2.930389 | 2.864716 | 0.000000 |
| C | -1.445270 | -3.264242 | 5.227824 | 0.000000 |
| C | -0.893179 | -3.874943 | 3.923834 | 0.000000 |
| H | -0.840315 | -2.904144 | 1.931434 | 0.000000 |

| | | | | |
|---|---|---|---|---|
| H | -2.485366 | -3.046327 | 2.662822 | 0.000000 |
| H | -0.806273 | -3.488584 | 6.090198 | 0.000000 |
| H | -2.450297 | -3.654046 | 5.434894 | 0.000000 |
| H | 0.206197 | -3.879578 | 3.917334 | 0.000000 |
| H | -1.245480 | -4.900583 | 3.760052 | 0.000000 |
| C | -1.511262 | -1.758859 | 4.960349 | 0.000000 |
| H | -2.503832 | -1.324605 | 5.135495 | 0.000000 |
| H | -0.746888 | -1.167083 | 5.475492 | 0.000000 |
| O | -1.208983 | -1.612067 | 3.505803 | 0.000000 |

**3a-Int'**:

FINAL HEAT OF FORMATION = -2286.249433

| | | | | |
|---|---|---|---|---|
| Ir | -0.007540 | 0.354917 | 0.354678 | 0.000000 |
| P | 2.141840 | 0.170457 | 1.450921 | 0.000000 |
| P | -1.386820 | -0.318864 | -1.482744 | 0.000000 |
| C | 3.587426 | 0.657175 | 0.299401 | 0.000000 |
| C | 3.458288 | -0.120435 | -1.021870 | 0.000000 |
| H | 2.620056 | 0.237314 | -1.628617 | 0.000000 |
| H | 3.354113 | -1.202927 | -0.871123 | 0.000000 |
| H | 4.376422 | 0.050713 | -1.603598 | 0.000000 |
| C | 3.544950 | 2.161282 | -0.009948 | 0.000000 |
| H | 4.340791 | 2.390596 | -0.734897 | 0.000000 |
| H | 3.713332 | 2.788989 | 0.872838 | 0.000000 |
| H | 2.590190 | 2.449259 | -0.473074 | 0.000000 |
| C | 4.943373 | 0.260447 | 0.911871 | 0.000000 |
| H | 5.722452 | 0.485877 | 0.167807 | 0.000000 |
| H | 4.989660 | -0.816345 | 1.123910 | 0.000000 |
| H | 5.196950 | 0.814816 | 1.820425 | 0.000000 |
| C | 2.612918 | 0.625743 | 3.262190 | 0.000000 |
| C | 3.273616 | 2.008819 | 3.388368 | 0.000000 |
| H | -2.391260 | 2.495532 | 2.249793 | 0.000000 |
| H | 4.256453 | 2.066387 | 2.909692 | 0.000000 |
| H | 3.424837 | 2.205255 | 4.461048 | 0.000000 |
| C | 3.552975 | -0.448174 | 3.852586 | 0.000000 |

| | | | | |
|---|---|---|---|---|
| H | 3.784043 | -0.139512 | 4.884318 | 0.000000 |
| H | 4.500620 | -0.546570 | 3.315515 | 0.000000 |
| H | 3.071331 | -1.431682 | 3.891622 | 0.000000 |
| C | 1.338765 | 0.625137 | 4.112176 | 0.000000 |
| H | 1.610414 | 0.855334 | 5.154790 | 0.000000 |
| H | 0.851518 | -0.358642 | 4.117520 | 0.000000 |
| H | 0.618054 | 1.386364 | 3.791100 | 0.000000 |
| O | 2.352212 | -1.472701 | 1.570120 | 0.000000 |
| C | 1.514639 | -2.272906 | 0.809976 | 0.000000 |
| C | 1.771622 | -3.645455 | 0.765801 | 0.000000 |
| H | 2.619721 | -4.060693 | 1.310677 | 0.000000 |
| C | 0.919391 | -4.456001 | 0.010946 | 0.000000 |
| H | 1.101069 | -5.530622 | -0.035743 | 0.000000 |
| C | -0.156977 | -3.907564 | -0.694332 | 0.000000 |
| H | -0.818772 | -4.528053 | -1.299068 | 0.000000 |
| C | -0.363324 | -2.529993 | -0.617630 | 0.000000 |
| O | -1.424972 | -1.975043 | -1.323152 | 0.000000 |
| C | -3.253795 | -0.005072 | -1.448195 | 0.000000 |
| C | -3.730522 | -0.137957 | 0.008784 | 0.000000 |
| H | -4.824327 | -0.016894 | 0.023654 | 0.000000 |
| H | -3.307579 | 0.625025 | 0.670530 | 0.000000 |
| H | -3.501355 | -1.131132 | 0.421915 | 0.000000 |
| C | -4.028347 | -1.055608 | -2.271128 | 0.000000 |
| H | -5.101452 | -0.883055 | -2.094848 | 0.000000 |
| H | -3.793668 | -2.077520 | -1.949518 | 0.000000 |
| H | -3.856978 | -0.975219 | -3.347639 | 0.000000 |
| C | -3.546299 | 1.406120 | -1.978054 | 0.000000 |
| H | -3.324760 | 1.505838 | -3.048350 | 0.000000 |
| H | -4.616749 | 1.620929 | -1.840574 | 0.000000 |
| C | -0.634058 | -0.101688 | -3.212485 | 0.000000 |
| C | -1.582683 | -0.515008 | -4.348848 | 0.000000 |
| H | -1.940825 | -1.545914 | -4.231712 | 0.000000 |
| H | -1.010507 | -0.469086 | -5.288761 | 0.000000 |
| H | -2.441228 | 0.158498 | -4.457657 | 0.000000 |

| | | | | |
|---|---|---|---|---|
| C | -0.191326 | 1.352552 | -3.414972 | 0.000000 |
| H | 0.294206 | 1.435096 | -4.399208 | 0.000000 |
| H | 0.533917 | 1.668241 | -2.654490 | 0.000000 |
| H | -1.038173 | 2.052079 | -3.407332 | 0.000000 |
| C | 0.590032 | -1.035713 | -3.270870 | 0.000000 |
| H | 0.289601 | -2.090574 | -3.303808 | 0.000000 |
| H | 1.266960 | -0.901696 | -2.421692 | 0.000000 |
| H | 1.147192 | -0.809055 | -4.192593 | 0.000000 |
| C | 0.447693 | -1.676572 | 0.135737 | 0.000000 |
| H | -2.986503 | 2.181892 | -1.440286 | 0.000000 |
| H | 1.047313 | 0.871791 | -0.736653 | 0.000000 |
| P | -0.574159 | 2.672627 | 0.644007 | 0.000000 |
| C | -2.239892 | 3.043604 | 1.310853 | 0.000000 |
| H | -3.024693 | 2.757070 | 0.602357 | 0.000000 |
| H | 2.648427 | 2.819971 | 3.001469 | 0.000000 |
| H | -2.317881 | 4.122285 | 1.505429 | 0.000000 |
| C | -0.483694 | 3.732877 | -0.844809 | 0.000000 |
| H | -0.721785 | 4.769870 | -0.570849 | 0.000000 |
| H | 0.530892 | 3.695113 | -1.262697 | 0.000000 |
| H | -1.187784 | 3.393925 | -1.612161 | 0.000000 |
| C | 0.462840 | 3.646831 | 1.793086 | 0.000000 |
| H | 0.098412 | 4.683052 | 1.822483 | 0.000000 |
| H | 0.411097 | 3.225447 | 2.803461 | 0.000000 |
| H | 1.502134 | 3.647328 | 1.445282 | 0.000000 |
| B | -0.850647 | -0.164301 | 2.389729 | 0.000000 |
| H | -1.429195 | -0.182825 | 1.201987 | 0.000000 |
| H | -0.607145 | -1.253359 | 2.831991 | 0.000000 |
| H | -1.353190 | 0.656143 | 3.107062 | 0.000000 |

THF:

FINAL HEAT OF FORMATION = -232.247176

| | | | | |
|---|---|---|---|---|
| C | 0.386378 | -1.170173 | 0.142531 | 0.000000 |
| O | 1.221246 | 0.003370 | -0.000085 | 0.000000 |
| C | 0.379919 | 1.172413 | -0.142271 | 0.000000 |

| | | | | |
|---|---|---|---|---|
| C | -1.034123 | 0.729416 | 0.228673 | 0.000000 |
| C | -1.030030 | -0.735149 | -0.228823 | 0.000000 |
| H | 0.784888 | -1.962872 | -0.509363 | 0.000000 |
| H | 0.433277 | -1.522005 | 1.189637 | 0.000000 |
| H | 0.773882 | 1.966959 | 0.510271 | 0.000000 |
| H | 0.425223 | 1.525072 | -1.189077 | 0.000000 |
| H | -1.183962 | 0.789874 | 1.317713 | 0.000000 |
| H | -1.807328 | 1.336761 | -0.260774 | 0.000000 |
| H | -1.799938 | -1.346723 | 0.260382 | 0.000000 |
| H | -1.179168 | -0.796487 | -1.317978 | 0.000000 |

$H_2B(THF)_2$:

FINAL HEAT OF FORMATION = -490.372902

| | | | | |
|---|---|---|---|---|
| B | 0.014697 | 1.402573 | 0.063059 | 0.000000 |
| H | 0.094689 | 1.970225 | 1.122423 | 0.000000 |
| C | 1.928022 | 0.112159 | -1.230549 | 0.000000 |
| C | 1.889510 | -0.122458 | 1.206901 | 0.000000 |
| C | 3.015801 | -0.838057 | -0.779032 | 0.000000 |
| H | 2.308748 | 1.095632 | -1.534146 | 0.000000 |
| H | 1.245417 | -0.285264 | -1.989602 | 0.000000 |
| C | 3.280586 | -0.393633 | 0.668285 | 0.000000 |
| H | 1.387839 | -1.025887 | 1.576882 | 0.000000 |
| H | 1.822405 | 0.686112 | 1.942226 | 0.000000 |
| H | 2.660224 | -1.877686 | -0.810144 | 0.000000 |
| H | 3.905033 | -0.752824 | -1.415700 | 0.000000 |
| H | 3.793249 | -1.162753 | 1.258820 | 0.000000 |
| H | 3.885520 | 0.523654 | 0.686524 | 0.000000 |
| C | -1.948717 | 0.062412 | 1.244412 | 0.000000 |
| C | -1.908484 | 0.096956 | -1.201200 | 0.000000 |
| C | -2.907216 | -0.973390 | 0.678562 | 0.000000 |
| H | -2.442858 | 0.879813 | 1.782455 | 0.000000 |
| H | -1.136809 | -0.355038 | 1.850496 | 0.000000 |
| C | -3.239841 | -0.439523 | -0.725097 | 0.000000 |
| H | -1.227572 | -0.697061 | -1.540160 | 0.000000 |

| | | | | |
|---|---|---|---|---|
| H | -1.954936 | 0.907851 | -1.935550 | 0.000000 |
| H | -2.416983 | -1.954515 | 0.608463 | 0.000000 |
| H | -3.797362 | -1.075782 | 1.310774 | 0.000000 |
| H | -3.619927 | -1.222146 | -1.392920 | 0.000000 |
| H | -3.981131 | 0.370490 | -0.673547 | 0.000000 |
| H | 0.095572 | 2.055278 | -0.946524 | 0.000000 |
| O | -1.336763 | 0.690358 | 0.034152 | 0.000000 |
| O | 1.118332 | 0.321917 | 0.005355 | 0.000000 |

TS:

FINAL HEAT OF FORMATION = -2750.777012

| | | | | |
|---|---|---|---|---|
| Ir | 0.615875 | 0.841375 | -0.505282 | 0.000000 |
| P | 2.428015 | 0.404941 | 0.922827 | 0.000000 |
| P | -0.458101 | 0.587871 | -2.570479 | 0.000000 |
| C | 4.111897 | 1.087962 | 0.330984 | 0.000000 |
| C | 4.339254 | 0.602352 | -1.111294 | 0.000000 |
| H | 3.583535 | 1.006806 | -1.792687 | 0.000000 |
| H | 4.334617 | -0.493258 | -1.187555 | 0.000000 |
| H | 5.326388 | 0.961476 | -1.442427 | 0.000000 |
| C | 4.078820 | 2.624203 | 0.328094 | 0.000000 |
| H | 5.016766 | 3.000403 | -0.110494 | 0.000000 |
| H | 3.993452 | 3.051496 | 1.335612 | 0.000000 |
| H | 3.246949 | 2.995335 | -0.287645 | 0.000000 |
| C | 5.293656 | 0.567209 | 1.166275 | 0.000000 |
| H | 6.226719 | 0.917223 | 0.696634 | 0.000000 |
| H | 5.321654 | -0.530893 | 1.179682 | 0.000000 |
| H | 5.295565 | 0.934327 | 2.197940 | 0.000000 |
| C | 2.420545 | 0.411035 | 2.849136 | 0.000000 |
| C | 2.948935 | 1.722614 | 3.454130 | 0.000000 |
| H | -2.107018 | 2.265048 | 1.484407 | 0.000000 |
| H | 4.026229 | 1.857674 | 3.305524 | 0.000000 |
| H | 2.772636 | 1.689869 | 4.541180 | 0.000000 |
| C | 3.226757 | -0.764871 | 3.436668 | 0.000000 |
| H | 3.117952 | -0.728133 | 4.533009 | 0.000000 |

| | | | | |
|---|---|---|---|---|
| H | 4.296265 | -0.713588 | 3.207870 | 0.000000 |
| H | 2.847720 | -1.733504 | 3.089937 | 0.000000 |
| C | 0.960205 | 0.219877 | 3.275104 | 0.000000 |
| H | 0.893365 | 0.272252 | 4.373666 | 0.000000 |
| H | 0.587693 | -0.762142 | 2.963347 | 0.000000 |
| H | 0.290110 | 0.972919 | 2.843177 | 0.000000 |
| O | 2.718867 | -1.245182 | 0.727795 | 0.000000 |
| C | 2.087091 | -1.841690 | -0.347819 | 0.000000 |
| C | 2.430928 | -3.158390 | -0.674597 | 0.000000 |
| H | 3.193402 | -3.682909 | -0.097276 | 0.000000 |
| C | 1.778660 | -3.772360 | -1.750031 | 0.000000 |
| H | 2.032618 | -4.798429 | -2.021474 | 0.000000 |
| C | 0.806860 | -3.081191 | -2.482712 | 0.000000 |
| H | 0.299753 | -3.541329 | -3.331785 | 0.000000 |
| C | 0.507699 | -1.764571 | -2.117017 | 0.000000 |
| O | -0.446125 | -1.075113 | -2.848541 | 0.000000 |
| C | -2.312554 | 0.865504 | -2.909447 | 0.000000 |
| C | -3.040128 | 0.396480 | -1.643845 | 0.000000 |
| H | -4.109605 | 0.647340 | -1.727815 | 0.000000 |
| H | -2.634023 | 0.856172 | -0.738977 | 0.000000 |
| H | -2.956100 | -0.691802 | -1.529243 | 0.000000 |
| C | -2.875735 | 0.040471 | -4.083330 | 0.000000 |
| H | -3.975350 | 0.074481 | -4.017873 | 0.000000 |
| H | -2.568135 | -1.011163 | -4.024426 | 0.000000 |
| H | -2.595785 | 0.434281 | -5.063968 | 0.000000 |
| C | -2.585862 | 2.358905 | -3.137392 | 0.000000 |
| H | -2.127947 | 2.734877 | -4.061649 | 0.000000 |
| H | -3.673173 | 2.513153 | -3.220385 | 0.000000 |
| C | 0.561307 | 1.180894 | -4.080823 | 0.000000 |
| C | -0.140543 | 0.968897 | -5.430744 | 0.000000 |
| H | -0.462837 | -0.071664 | -5.568624 | 0.000000 |
| H | 0.583355 | 1.200399 | -6.228617 | 0.000000 |
| H | -1.000765 | 1.634507 | -5.572480 | 0.000000 |
| C | 0.927248 | 2.663580 | -3.929866 | 0.000000 |

| | | | | |
|---|---|---|---|---|
| H | 1.574760 | 2.953862 | -4.772245 | 0.000000 |
| H | 1.476064 | 2.846830 | -2.997253 | 0.000000 |
| H | 0.044438 | 3.316848 | -3.953577 | 0.000000 |
| C | 1.850779 | 0.338488 | -4.103239 | 0.000000 |
| H | 1.646322 | -0.704153 | -4.379933 | 0.000000 |
| H | 2.364371 | 0.343888 | -3.136634 | 0.000000 |
| H | 2.529168 | 0.764866 | -4.859002 | 0.000000 |
| C | 1.126339 | -1.102867 | -1.047955 | 0.000000 |
| H | -2.233306 | 2.978318 | -2.302428 | 0.000000 |
| H | 1.758161 | 1.608155 | -1.392527 | 0.000000 |
| P | -0.161586 | 2.948318 | 0.209532 | 0.000000 |
| C | -1.922651 | 3.040597 | 0.729094 | 0.000000 |
| H | -2.592816 | 2.861230 | -0.118917 | 0.000000 |
| H | 2.437777 | 2.610689 | 3.070819 | 0.000000 |
| H | -2.143067 | 4.030551 | 1.153118 | 0.000000 |
| C | -0.019613 | 4.356878 | -0.962785 | 0.000000 |
| H | -0.437524 | 5.269290 | -0.514276 | 0.000000 |
| H | 1.042555 | 4.519001 | -1.191012 | 0.000000 |
| H | -0.540512 | 4.144225 | -1.901951 | 0.000000 |
| C | 0.609443 | 3.746886 | 1.672295 | 0.000000 |
| H | 0.152798 | 4.733446 | 1.836924 | 0.000000 |
| H | 0.452100 | 3.132414 | 2.565875 | 0.000000 |
| H | 1.684779 | 3.875465 | 1.501653 | 0.000000 |
| B | -1.940390 | -1.010850 | 1.463508 | 0.000000 |
| H | -2.799876 | -0.481951 | 0.840572 | 0.000000 |
| H | -0.621193 | 0.110219 | 0.457050 | 0.000000 |
| H | -1.389450 | -0.614878 | 2.434067 | 0.000000 |
| C | -2.166540 | -3.064597 | -0.116577 | 0.000000 |
| C | -0.600999 | -4.483787 | 0.992832 | 0.000000 |
| C | -2.005656 | -4.487428 | 0.368900 | 0.000000 |
| H | -1.653465 | -2.866867 | -1.065719 | 0.000000 |
| H | -3.192022 | -2.684870 | -0.134464 | 0.000000 |
| H | 0.169456 | -4.529857 | 0.210893 | 0.000000 |
| H | -0.448462 | -5.316369 | 1.690139 | 0.000000 |

| | | | | |
|---|---|---|---|---|
| H | -2.091587 | -5.199264 | -0.461601 | 0.000000 |
| H | -2.770531 | -4.726596 | 1.120910 | 0.000000 |
| C | -0.531585 | -3.153604 | 1.715593 | 0.000000 |
| H | -0.953969 | -3.179147 | 2.726888 | 0.000000 |
| H | 0.453444 | -2.675402 | 1.702138 | 0.000000 |
| O | -1.431621 | -2.266292 | 0.913671 | 0.000000 |
| C | -4.763667 | -2.046863 | 2.222382 | 0.000000 |
| O | -3.375783 | -2.007875 | 2.685814 | 0.000000 |
| C | -3.351353 | -1.595324 | 4.084475 | 0.000000 |
| C | -4.750458 | -1.882470 | 4.603595 | 0.000000 |
| C | -5.613176 | -1.534712 | 3.382522 | 0.000000 |
| H | -4.843114 | -1.427246 | 1.317592 | 0.000000 |
| H | -4.995087 | -3.093261 | 1.967240 | 0.000000 |
| H | -2.555454 | -2.166482 | 4.581507 | 0.000000 |
| H | -3.109569 | -0.520467 | 4.136840 | 0.000000 |
| H | -4.853701 | -2.946823 | 4.862870 | 0.000000 |
| H | -4.995380 | -1.282259 | 5.489490 | 0.000000 |
| H | -6.604711 | -2.004290 | 3.404802 | 0.000000 |
| H | -5.748448 | -0.445381 | 3.308937 | 0.000000 |